

NASA CR-174,907

DOE/NASA/0312-1
NASA CR-174907

NASA-CR-174907
19860006695

Ceramic Automotive Stirling Engine Study

S. Musikant, W. Chiu, D. Darooka,
D.M. Mullings, and C.A. Johnson
General Electric Company

January 1985

LIBRARY COPY

JAN 20 1985

LEWIS RESEARCH CENTER
LIBRARY, NASA
HAMPTON, VIRGINIA

Prepared for
NATIONAL AERONAUTICS AND SPACE ADMINISTRATION
Lewis Research Center
Under Contract DEN 3-312

for
U.S. DEPARTMENT OF ENERGY
Conservation and Renewable Energy
Office of Vehicle and Engine R&D



NF01215

DISCLAIMER

This report was prepared as an account of work sponsored by an agency of the United States Government. Neither the United States Government nor any agency thereof, nor any of their employees, makes any warranty, express or implied, or assumes any legal liability or responsibility for the accuracy, completeness, or usefulness of any information, apparatus, product, or process disclosed, or represents that its use would not infringe privately owned rights. Reference herein to any specific commercial product, process, or service by trade name, trademark, manufacturer, or otherwise, does not necessarily constitute or imply its endorsement, recommendation, or favoring by the United States Government or any agency thereof. The views and opinions of authors expressed herein do not necessarily state or reflect those of the United States Government or any agency thereof.

Printed in the United States of America

Available from

National Technical Information Service
U.S. Department of Commerce
5285 Port Royal Road
Springfield, VA 22161

NTIS price codes¹

Printed copy A16
Microfiche copy A01

¹Codes are used for pricing all publications. The code is determined by the number of pages in the publication. Information pertaining to the pricing codes can be found in the current issues of the following publications, which are generally available in most libraries: *Energy Research Abstracts (ERA)*, *Government Reports Announcements and Index (GRA and I)*, *Scientific and Technical Abstract Reports (STAR)*, and publication, NTIS-PR-360 available from NTIS at the above address.

Ceramic Automotive Stirling Engine Study

S. Musikant, W. Chiu, D. Darooka,
D.M. Mullings, and C.A. Johnson
General Electric Company
Space Systems Division
Valley Forge Space Center
Philadelphia, Pennsylvania 19101

January 1985

Prepared for
National Aeronautics and Space Administration
Lewis Research Center
Cleveland, Ohio 44135
Under Contract DEN 3-312

for
U.S. DEPARTMENT OF ENERGY
Conservation and Renewable Energy
Office of Vehicle and Engine R&D
Washington, D.C. 20545
Under Interagency Agreement DE-A101-85CE50112

A96-16165 #

TABLE OF CONTENTS

<u>SECTION</u>	<u>TITLE</u>	<u>PAGE</u>
1.0	INTRODUCTION AND SUMMARY.	1-1
1.1	Background.	1-1
1.2	Concept Evolution	1-1
1.3	Primary Design Description.	1-3
1.4	External Heating System	1-8
1.5	Heater Head Design.	1-12
	1.5.1 Heater Tube Stress	1-13
	1.5.2 Engine Cylinder Structural Analysis.	1-15
1.6	Material Selections	1-17
1.7	Thermodynamic and Performance Analysis.	1-19
1.8	Manufacturing and Cost Analysis	1-23
1.9	Long Range Ceramic Standard Engine (Case II).	1-24
1.10	Federal Driving Cycle	1-27
1.11	Critical Development Areas.	1-30
	1.11.1 Critical Materials Problems.	1-30
	1.11.2 Critical Design Issues	1-31
	REFERENCES.	1-34
2.0	REQUIREMENTS.	2-1
2.1	Design.	2-1
2.2	Performance Evaluation.	2-3
2.3	Production, Cost Evaluation	2-3
3.0	OVERVIEW OF DESIGN PROCESS AND TRADE OFFS	3-1
3.1	Configuration Trade Off	3-1
3.2	Materials Considerations.	3-10
	3.2.1 Introduction	3-10
	3.2.2 Operating Conditions For Structural Components.	3-10
	3.2.3 Material Selection	3-12
4.0	EXTERNAL HEAT SYSTEM.	4-1
4.1	Preliminary Considerations.	4-1
4.2	Analytical Representation of the External Heat System (EHS)	4-1
4.3	Results of The EHS Model.	4-5
4.4	Summary and Conclusions	4-12

TABLE OF CONTENTS (CONTINUED)

<u>SECTION</u>	<u>TITLE</u>	<u>PAGE</u>
5.0	HOT SIDE.	5-1
5.1	General	5-1
5.2	Thermal Performance Analysis of Proposed Ceramic Stirling Engine.	5-3
5.2.1	Introduction	5-3
5.2.2	Heater Head Thermal Analysis	5-3
5.2.3	Heat Transfer At The Dome.	5-6
5.2.4	Heat Transfer At The Heater Head Tubes	5-6
5.3	Performance Analysis.	5-12
5.3.1	Case Design Features and Thermodynamic Analysis.	5-12
5.3.2	Thermodynamic Analysis	5-12
5.3.3	Case Design Optimization	5-18
5.4	Summary and Conclusions	5-29
	REFERENCES.	5-31
6.0	COLD SIDE	6-1
6.1	Configuration	6-1
6.2	Advanced Concepts For Seals and Bearings For Ceramic Automotive Stirling Engine	6-2
6.2.1	Shuttle/Pumping Losses	6-2
6.2.2	Piston Rod Seal.	6-4
6.2.3	Crank Shaft Bearings	6-6
7.0	STRUCTURAL ANALYSIS	7-1
7.1	General	7-1
7.2	Stress Levels In Ceramic Heater Head Pressure Vessel	7-4
7.2.1	Introduction	7-4
7.2.2	Summary of Results	7-4
7.2.3	Recommendations For Future Work.	7-7
7.2.4	Discussion of Analysis of Cylinder Stresses and Choice of Ceramics	7-8
7.3	Stress Analysis For Heater Head Tubes.	7-18
7.3.1	Summary and Conclusions	7-18
7.3.2	Introduction.	7-19
7.3.3	Structural Analysis Program	7-19
7.3.4	Heater Head Tube Configuration.	7-19
7.3.5	Load Conditions Analyzed.	7-25
7.3.6	Stress Analysis Results	7-25

TABLE OF CONTENTS (CONTINUED)

<u>SECTION</u>	<u>TITLE</u>	<u>PAGE</u>
8.0	PERFORMANCE MAPPING OF THE PROPOSED CERAMIC AUTOMOTIVE STIRLING ENGINE DESIGN.	8-1
8.1	Introduction	8-1
8.2	Parasitic Power Requirements	8-1
	8.2.1 EHS Blower.	8-3
	8.2.2 Water Pump.	8-5
	8.2.3 Alternator.	8-5
	8.2.4 Lubricating Oil Pump.	8-5
	8.2.5 Hydrogen Gas Compressor	8-9
8.3	Friction Power	8-9
8.4	External Heating System Efficiency	8-9
8.5	Performance Map For Case	8-9
8.6	Summary and Conclusions.	8-16
9.0	CERAMIC PROCESSES.	9-1
9.1	Materials Selections	9-1
9.2	Production and Process Evaluation (Case)	9-3
9.3	Glossary of Terms.	9-3
9.4	Manufacturing Process and Cost Analysis.	9-5
10.0	MANUFACTURING PROCESSES.	10-1
10.1	Introduction	10-1
10.2	Detailed Parts Analysis.	10-9
	10.2.1 Manufacturing Procedures For Piece Parts.	10-9
11.0	COST ANALYSIS.	11-1
11.1	Introduction To Cost Analysis.	11-1
12.0	LONG RANGE CERAMIC STANDARD ENGINE (CASE II)	12-1
12.1	Introduction	12-1
12.2	Description of Concept For Case II	12-1
12.3	Design of Case II.	12-5
	12.3.1 Review of Case I Design	12-5
	12.3.2 Potential Design Improvement.	12-12
	12.3.3 Candidate Long-Range Ceramic Standard Design Concepts.	12-12
	12.3.4 Long Range Standard Reference Conceptual Design	12-15
12.4	Application of Heat Pipes to Ceramic Automotive Stirling Engine	12-16
	12.4.1 Introduction.	12-16
	12.4.2 Some Basis Design Considerations.	12-16
	12.4.3 Selection of Heat Pipe Working Fluid.	12-22
	12.4.4 Sizing of Heat Pipes.	12-22

TABLE OF CONTENTS (CONTINUED)

<u>SECTION</u>	<u>TITLE</u>	<u>PAGE</u>
12.0	12.4.5 Baseline Conceptual Design.	12-24
	12.5 Approach For Reduction In Various Losses	12-30
	12.6 External Heating System.	12-42
	12.7 Performance.	12-47
	12.8 Cold Start Penalty	12-53
	12.9 Federal Driving Cycle.	12-58
	REFERENCES	12-61
13.0	CRITICAL DEVELOPMENT AREAS	13-1
	13.1 Critical Materials Problems.	13-1
	13.2 Critical Design Issues	13-2
APPENDIX I	COMPUTER PROGRAM LISTINGS.	I-1
APPENDIX II	ESTIMATE OF DISPLACER PISTON RING FRICTION POWER LOSSES.	II-1
APPENDIX III	SAPV.2 STRUCTURAL ANALYSIS DATA OUTPUT	III-1
APPENDIX IV	MANUFACTURING AND COST DATA	IV-1

FOREWORD

A conceptual design study for a Ceramic Automotive Stirling Engine (CASE) was performed. Year 1990 structural ceramic technology was assumed. Structural and performance analyses of the conceptual design were performed as well as a manufacturing and cost analysis. The general conclusions from this study are that such an engine would be 10-26% more efficient over its performance map than the current metal Automotive Stirling Reference Engine (ASRE). Cost of such a ceramic engine is likely to be somewhat higher than that of the ASRE but engine cost is very sensitive to the ultimate cost of the high purity, ceramic powder raw materials required to fabricate high performance parts.

When the design study was projected to the year 2000 technology, substantial net efficiency improvements, on the order of 25 to 46% over the ASRE, were computed. A schematic of the overall investigation is shown on Figure 1.

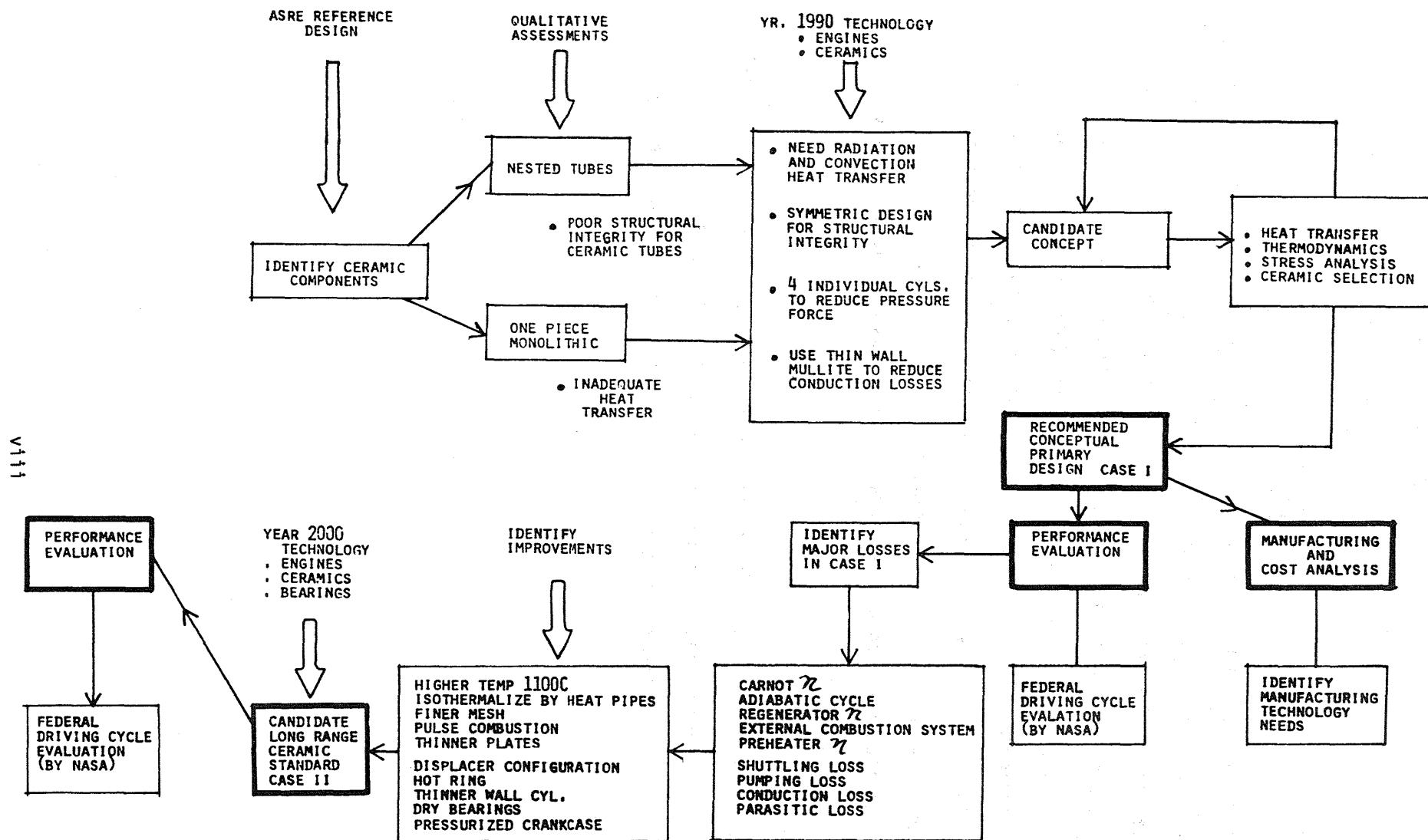


FIGURE 1 CERAMIC AUTOMOTIVE STIRLING ENGINE STUDY

SECTION 1

INTRODUCTION AND SUMMARY

1.1 BACKGROUND

This report describes the conceptual ceramic engine "primary design", the related trade-off analysis, and the performance predictions for the ceramic engine. The analysis of fabrication techniques and cost estimation for this "primary design" are included. The design concepts and preliminary performance analysis for the "Long Range Ceramic Standard" are also described.

1.2 CONCEPT EVOLUTION

Initially, both a nested tube heater head concept and a monolithic type heater head concept were considered. The first concept consists of external heater head tubes analogous to the ASRE configuration. The concept suffers from the fact that, in this case, joints and seals for the tube assembly are located in the hot combustion zone and are vulnerable to damage from shock and vibration. In addition, this concept does not provide sufficient heat input density at higher temperatures and lacks temperature uniformity across the length of the tubes.

The monolithic heater head concept on the other hand, eliminates the need for external heater tubes. The working gas heat transfer occurs in passages integrally formed in the ceramic cylinder head structure. It offers the potential advantage of being relatively simple and rugged in construction, thus offering better shock and vibration resistance and reduced joint and seal requirements. However, there exists a limitation imposed by the required heat input density that must be achieved for a particular application. The heater head for automotive application requires large heat input density in order to meet the power and size requirements. The stress and thermal analyses reveal

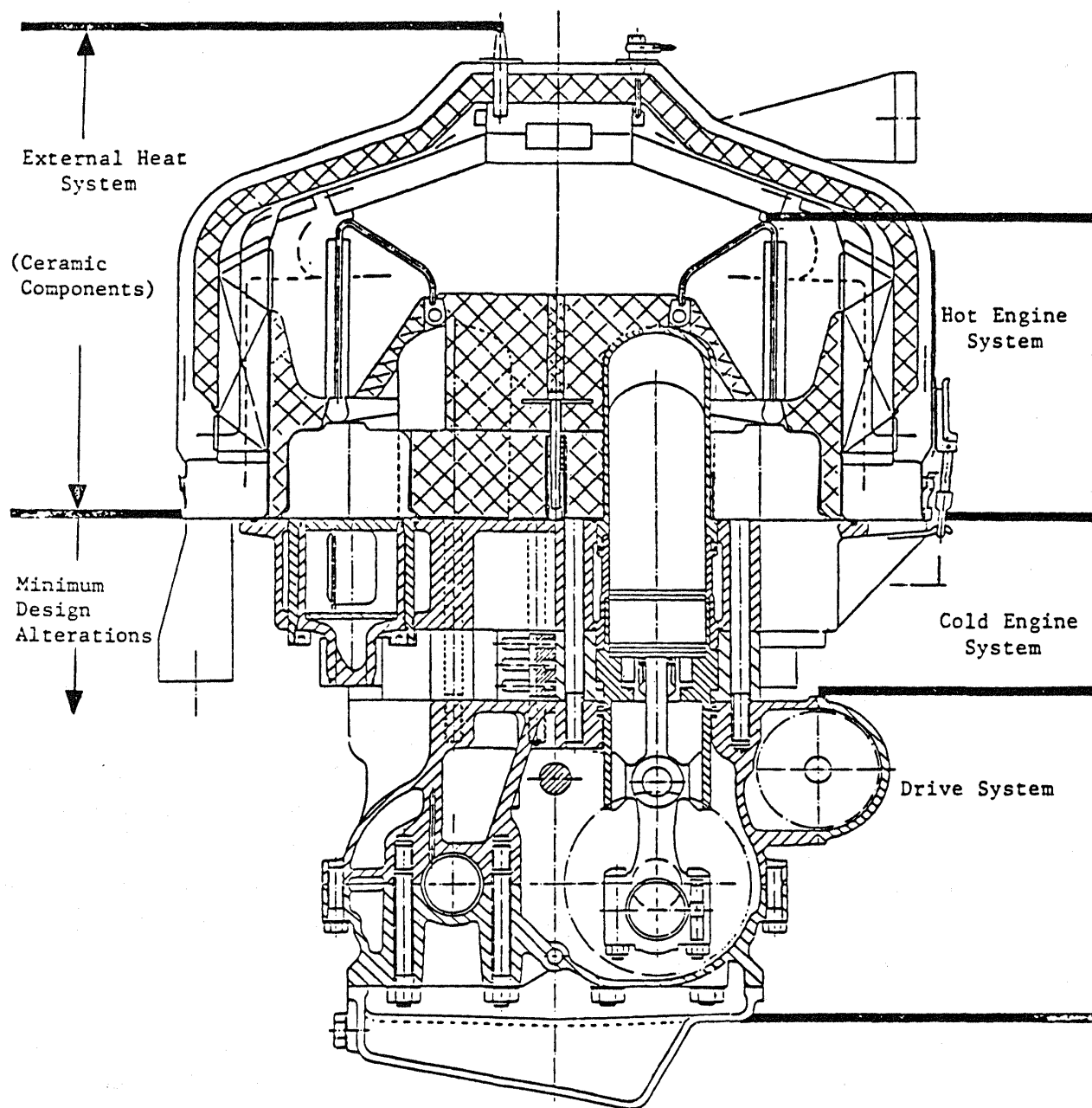


FIGURE 1.1 REFERENCE ENGINE DESIGN

that at heat flux density exceeding about 25 w/cm^2 , the temperature gradient and stress level become unacceptable. The size of the heater head pressure vessel would become exceptionally large for automotive application at a lower heat flux density. It is concluded that the ceramic monolithic type heater head where heat is transferred through the walls of the pressure vessel would be infeasible in meeting the requirements of an automotive Stirling engine.

The preliminary assessment revealed that the following general approaches are preferred for the CASE design:

1. Ceramic components should avoid complex contour to avoid potential stress concentration.
2. Joints and seals should be minimized.
3. Radiation heat transfer and other means to enhance heat transfer should be incorporated to take full advantage of the higher temperature capability of ceramic materials.

1.3 PRIMARY DESIGN DESCRIPTION

Figure 1.2 shows a layout of the final concept selected for detailed evaluation. The engine hot section comprises all ceramic components, except the outer combustor housing and engine retainer rings and bolts. The cold section below the engine cylinder and the drive system are all metal parts just as in the ASRE design. The gas cooler and regenerator are annular in cross-section.

The concept has the following key features:

1. Four separate cylinders having symmetric heater head/regenerator/cooler assembly provide good structural integrity and producibility of the ceramic components and ensure uniform heat distribution.
2. Combination of jet impingement and radiation heat transfer offers high heat flux density at the heater head, thereby allowing the use of a structurally sound ceramic heater at moderate lengths and curvatures.
3. The overall engine envelope remains similar to ASRE.

Since the cooler and regenerator assembly are of annular type, a V-type cylinder configuration was selected to maintain the overall dimensions close to ASRE design. The V-configuration also reduces the length of interconnect passage of working gas between cylinders.

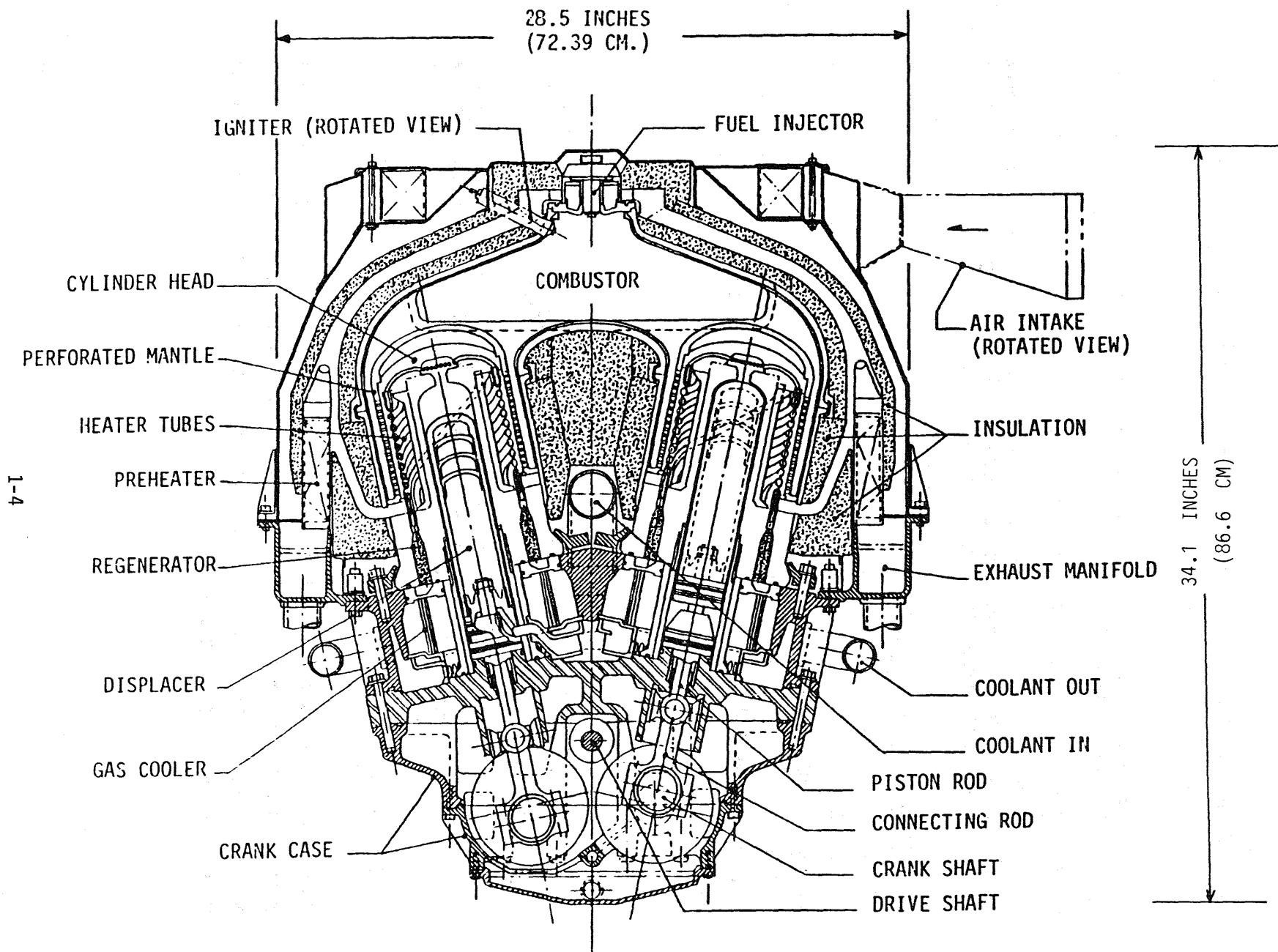


FIGURE 1.2 CERAMIC AUTOMOTIVE STIRLING ENGINE

The basic combustor design concept is similar to the ASRE design but utilizes ceramics. The air-preheater can be constructed with staggered, finned heat exchanger plates which are extruded from Si_3N_4 or SiC material as illustrated in Figure 1.3.

Figure 1.4 is an enlarged view of one engine cylinder. This engine cylinder, including the annular regenerator housing, is made of mullite ($3\text{Al}_2\text{O}_3 \cdot 2\text{SiO}_2$) and has internal flow passages in its dome for connection with the external heater tubes. Twenty-four spiral heater tubes evenly surround the engine cylinder at 135° offset and connect the cylinder head and the regenerator housing. A cylindrical bell-shaped mantle covers the engine cylinder pressure vessel including the spiral heater tubes.

The combustion gases, after heating the mantle dome which radiates heat to the cylinder head, are directed to the perforated portion of the mantle and create jet streams impinging against the heater tubes. The perforated mantle transfers heat to the heater tubes by radiation. The combination of radiative and jet impingement convective heat transfer not only results in very effective heat transfer, but also ensures a uniform heater tube temperature distribution. The enhanced heat transfer also allows the use of a shorter heater tube, and thus reduces the engine void volume for greater efficiency.

To reduce the stress level in the ceramic cylinder structure during initial heat up, porous ceramic insulation is placed at the O.D. of the engine cylinder. This insulation reduces the outer surface temperature of the structural ceramic cylinder so that the radial thermal gradient in the ceramic wall is minimized as are the stresses due to such a thermal gradient.

The cylinder is attached to the engine mounting block using a circular retaining ring which is bolted to the colder metal plate. The design of the retaining ring and its ceramic interface represents one of the critical design areas for the ceramic engine since maximum stress of the ceramic vessel occurs at this interface.

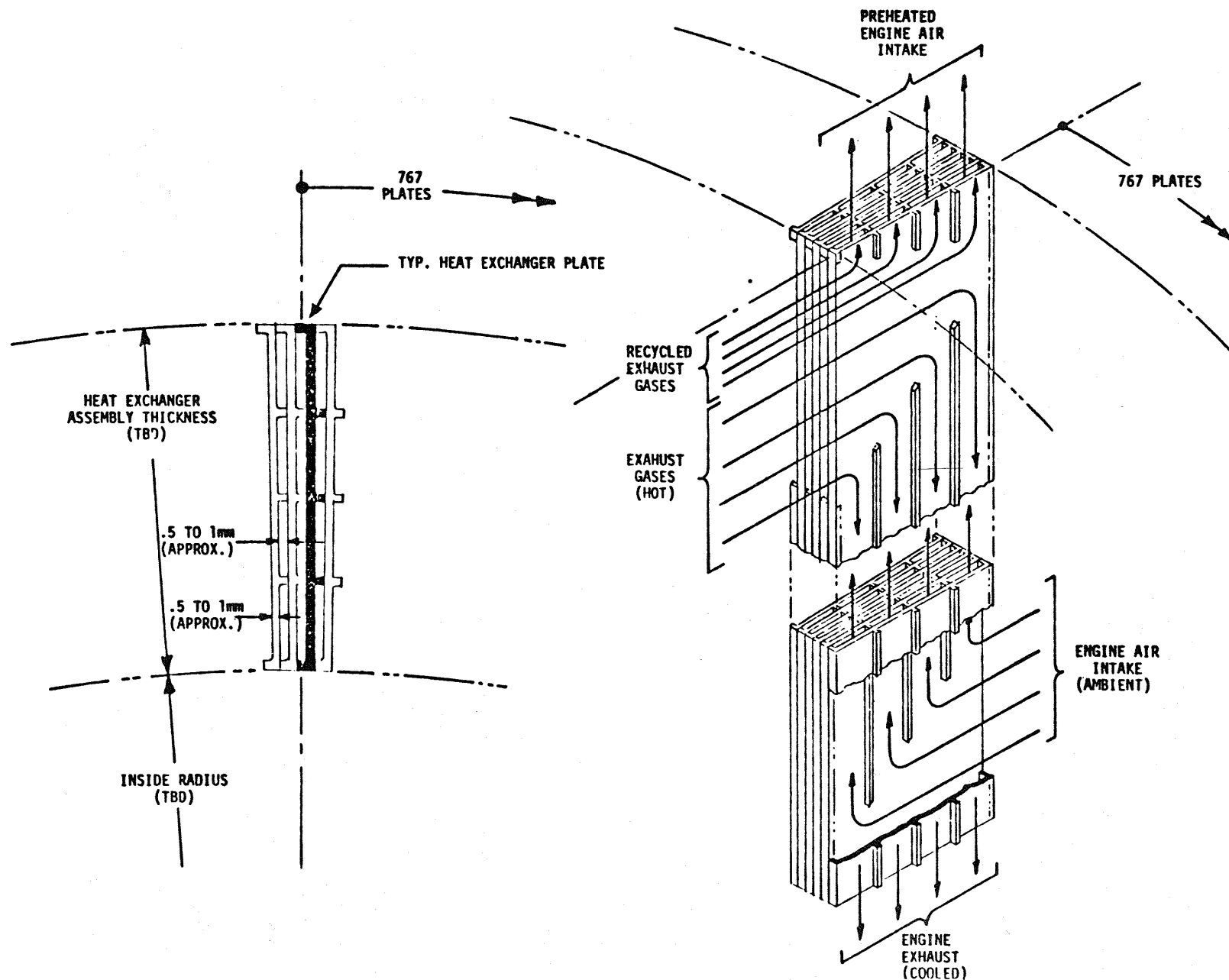


FIGURE 1.3 CERAMIC AIR-PREHEATER CONCEPT

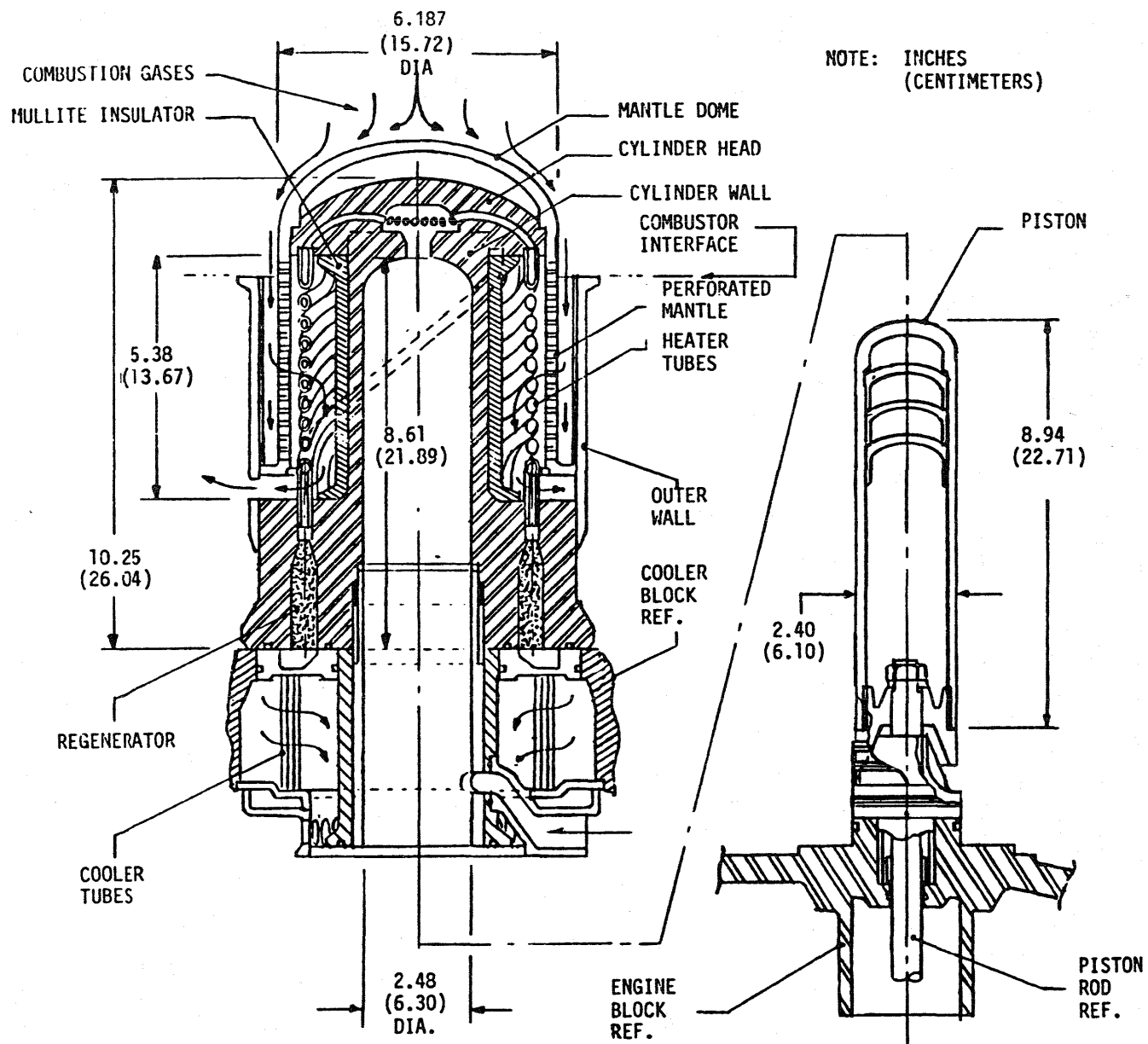
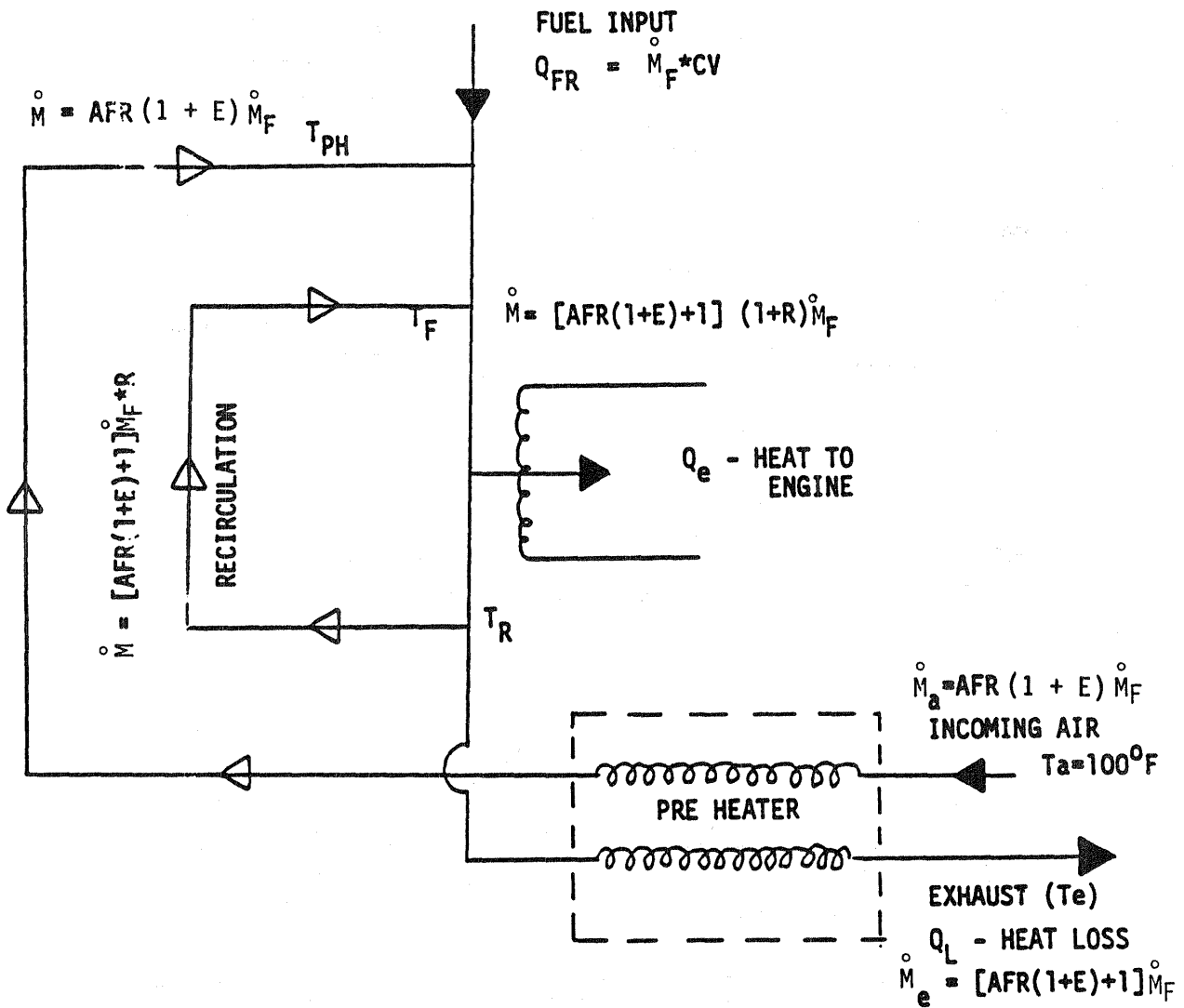


FIGURE 1.4 EXPLODED VIEW OF THE ENGINE HOT SECTION

1.4 EXTERNAL HEATING SYSTEM

A computer simulation program was developed to analyze the effect of increased heater head tube temperature on the performance of the external heating system (EHS). The efficiency of the external heating system was estimated as a function of the flame temperature, recirculation level, preheater effectiveness, heater head tube temperature and the number of heat transfer units. Figure 1.5 is the schematic representation of the external heating system analyzed here. The definitions and the nomenclatures used are also denoted. In this analysis of the effect of recirculation on combustion flame temperature, an idealized case is considered in which mixing of the gases is considered to be instantaneous, and the flame process is regarded as taking place in a homogenous reactor flow system in which fully reacted combustion products are recirculated back to the flame front, which is assumed to be at or above ignition temperature.

A result of this simulation is plotted in Figure 1.6 which represents the heater head tube temperature as a function of external heating system efficiency. The curves are drawn at a fixed Number of Transfer Units; (NTU) equal to 4, giving the maximum achievable tube temperature. Any further increase in NTU does not improve the heat transfer effectiveness as seen from Figure 1.7. An important result is that the tube temperature decreases with increase in EHS efficiency. Thus, for a recirculation level of 50% and the preheater effectiveness of 90% and for the desirable heater tube temperature of 980°C (1800°F), the maximum achievable EHS efficiency is 89%. Another important result is that the heater tube temperature can be raised by increasing the mass flow rate (increased recirculation), despite the fact that increased recirculation incurs a lower flame temperature. One can achieve higher heater tube temperature at the expense of reduced EHS efficiency by maintaining the recirculation level and increasing the preheater effectiveness. However, after a certain limit, the size of the preheater becomes unacceptable for a given application.



- o COMBUSTION EFFICIENCY = 100%
 (CONVERSION OF FUEL TO HEAT)
- o EXTERNAL HEATING SYSTEM EFFICIENCY = $\frac{Q_e}{Q_{FR}} = 1 - \frac{Q_L}{Q_{FR}}$

FIGURE 1.5 A SCHEMATIC REPRESENTATION OF EXTERNAL HEATING SYSTEM

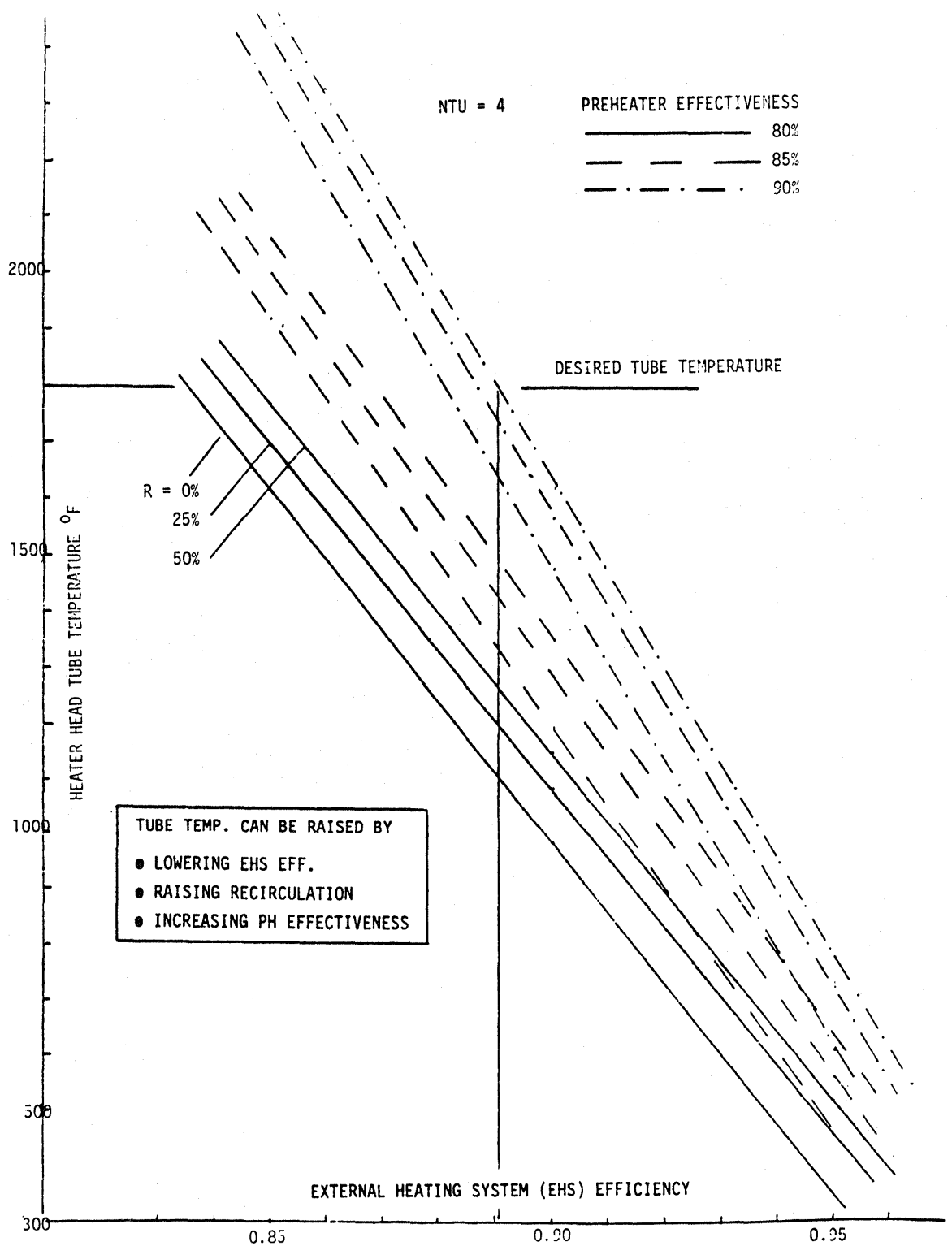


FIGURE 1.6 HEATER HEAD TUBE TEMPERATURE AS A FUNCTION OF EXTERNAL HEAT SYSTEM EFFICIENCY

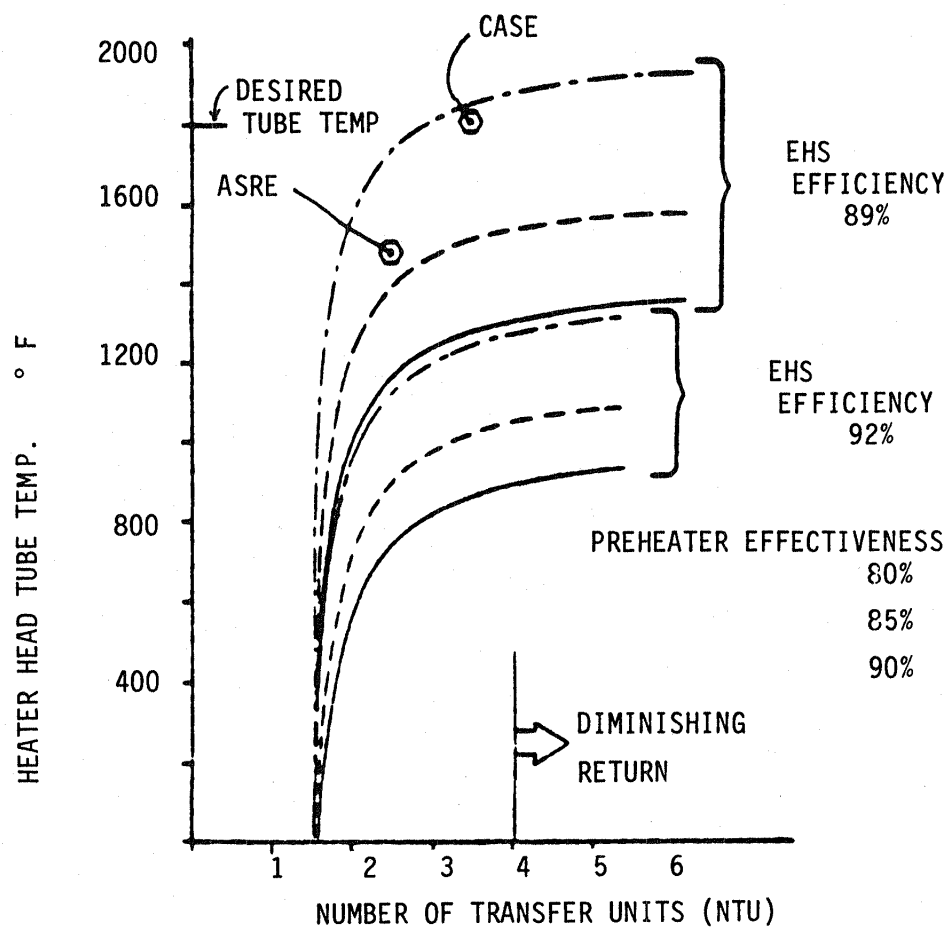


FIGURE 1.7 EFFECT OF NTU ON TUBE TEMPERATURE

The selected design point for CASE therefore is at 89% EHS efficiency with 980°C (1800°F) heater tube temperature. This requires 90% preheater effectiveness and 50% recirculation. At this point, the adiabatic flame temperature is expected to be 2260°C (4100°F) with a preheat air temperature of 1024°C (1875°F).

1.5 HEATER HEAD DESIGN

A single combustor unit supplies heat to all four engine cylinders which are symmetrically located around a central point. The heat is transferred to the engine cylinder first at the dome. The hot combustion gases, after transferring some of the heat at the dome, pass through an annular passage surrounding the engine cylinder and transfer the heat, mostly by convection, to a perforated mantle which in turn radiates heat to the engine fin-tube assembly. The combustion gases which may still be sufficiently hot, especially at full load condition, transfer the remaining heat by impinging on the fin-tube assembly. Thus, the heater tubes and the cylinder are maintained at a uniform temperature by properly distributing the heat around the engine cylinder. The advantage of being able to transfer heat at the dome lies in the fact that at maximum load conditions, one need not provide as much heat transfer surface area at the tubes (reduced void volume) and that there is some merit in being able to transfer heat closest to the expansion space. Moreover, during start-up condition, the temperature difference between the tube assembly and the engine cylinder is reduced, thereby relieving the thermal stresses generated at the interconnections.

The CASE heater head heat exchanger consists of a single row of twenty-four closely spaced spiral tubes in a swirling cross flow. The amount of heat that is not transferred by radiation at the dome and at the fin-tube assembly must be transferred by convection at the fin-tube assembly, and this amount of heat determines the heat transfer area required at the tubes. The relative magnitude of the heat transfer by radiation and convection at three different

load conditions is shown in Figure 1.8. While most of the heat at part load condition is transferred by radiation at the dome, a large amount of heat must be transferred by convection to the tubes at full load conditions.

1.5.1 HEATER TUBE STRESS

The heater tube is a modified helix, each tube wrapping around the cylinder at 135° offset. The tube dimensions are:

OD = 0.243 in. (6.17 mm)
ID = 0.118 in. (3.0 mm)
Total exposed length = 8.1 in. (205.7 mm)

Fins, if needed, will be integrally molded.

The stress condition considered is at the anticipated maximum ΔT between the two ends of the tube of 500°F (260°C) at start-up, and peak internal pressure of 3000 psi (20.1 MPa).

The SAPV2 stress analysis program was used to compute the maximum stresses in the tubes. For silicon carbide, the tube material properties used in the analysis were modulus of elasticity = 54×10^6 psi (3.72×10^5 MPa), and coefficient of thermal expansion = $2.67 \times 10^{-6}/^\circ\text{F}$ ($4.8 \times 10^{-6}/^\circ\text{C}$). For these conditions, the maximum stresses were computed to be:

Maximum Tensile Stress = 19740 psi (136 MPa)
Maximum Shear Stress = 11130 psi (77 MPa)

These stresses are considered to be within the range of acceptable working stresses for the proposed ceramic heater head tubulars.

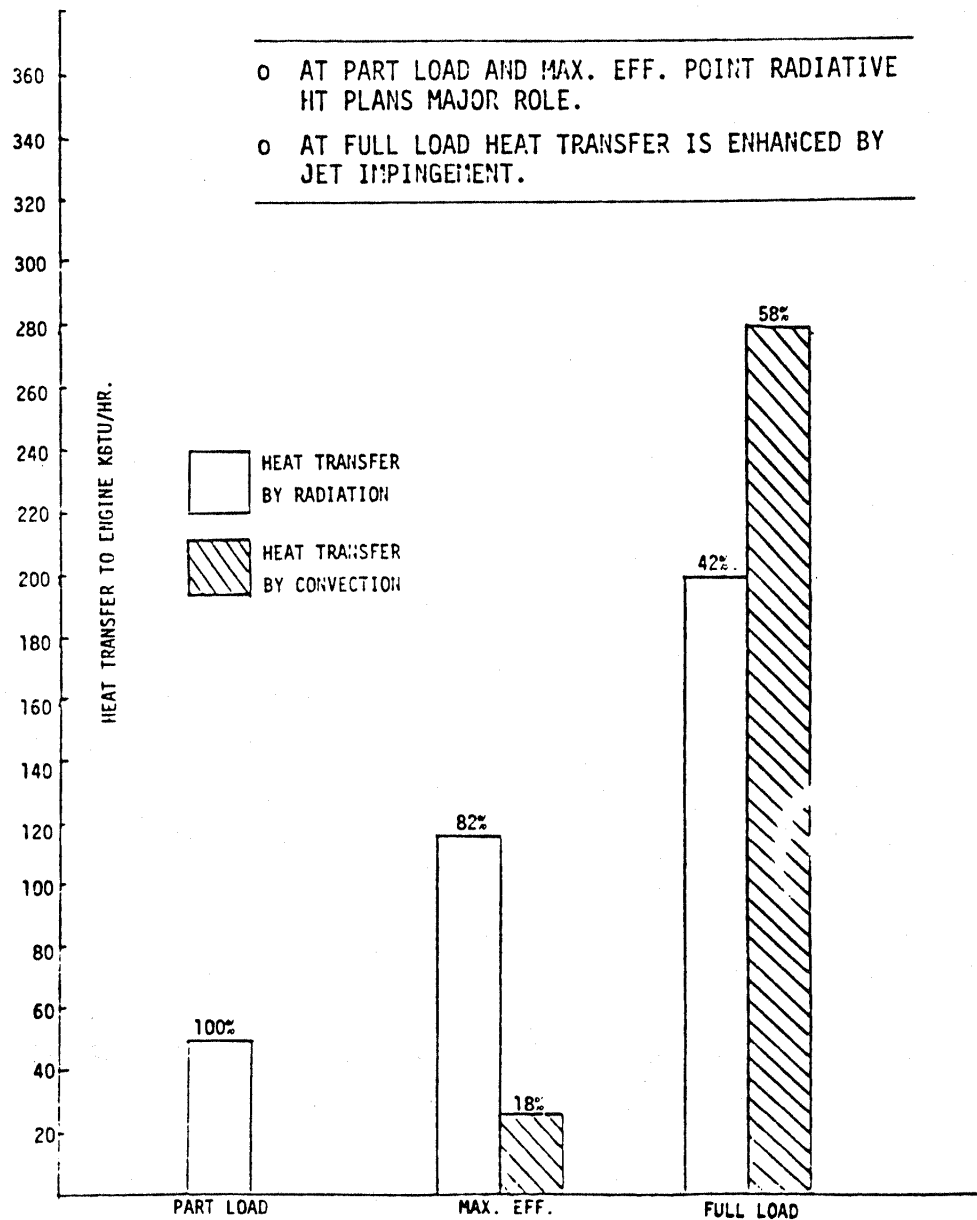


FIGURE 1.8 RADIATIVE VS CONVECTIVE CONTRIBUTION TO TOTAL HEATER HEAD HEAT TRANSFER

1.5.2 ENGINE CYLINDER STRUCTURAL ANALYSIS

The critical stress problem in the cylinder occurs in the vicinity of the hold down flange. The stresses in this region are primarily due to the thermal gradient in this region. Finite Element Method (FEM) models of the ceramic (mullite) cylinder and the steel retaining ring were used to determine stresses.

The NASTRAN (NASA STRUCTURAL ANALYSIS) code using isoparametric axisymmetric elements was used to evaluate stresses due to internal pressure and equilibrium (operating) thermal gradients.

The FEM analysis showed that stresses resulting from the thermal gradient are dominant. The stresses are sensitive to geometry and influence the number of start/stop cycles the structure can withstand. The maximum tensile stress predicted was 23049 psi near the retaining ring.

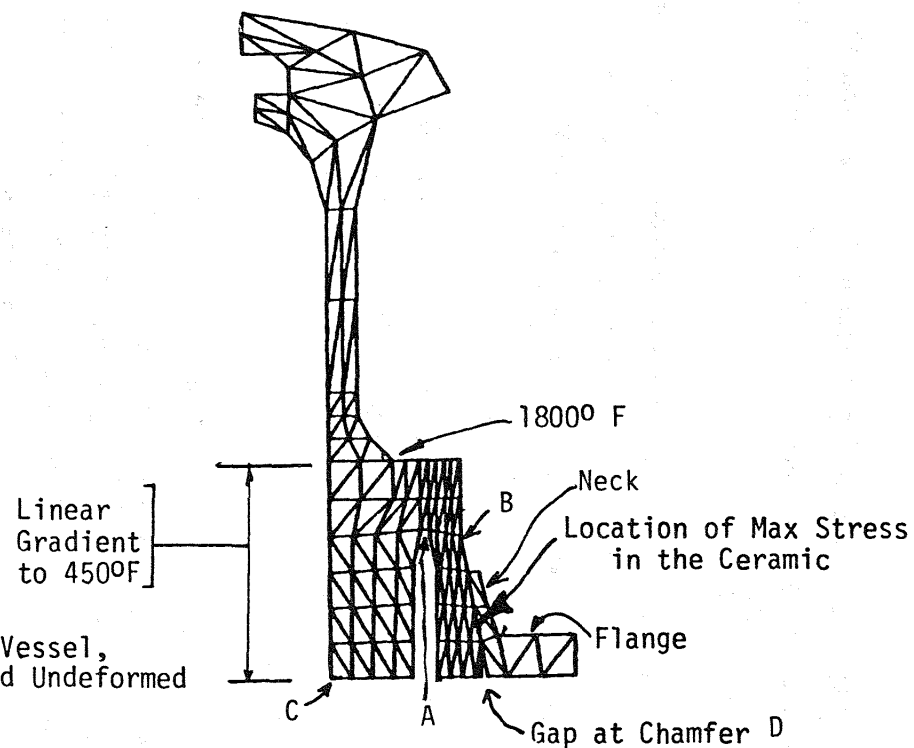
High cycle fatigue stress levels due to the internal pressure of 2000 ± 1000 psi were predicted to be about one-third of the thermal gradient stresses. Locations of maximum stress from internal pressure do not coincide with locations of maximum thermal stresses.

To maintain maximum combined stresses below 25000 psi, the steel retainer has to be cooled to 300°F at the neck, and 200°F at the flange, as indicated in Figure 1.9. In addition, a chamfer at the outer base of the ceramic structure is required. Under these conditions, the maximum principal stress was calculated to vary between 19.9 and 23.0 kpsi (137 and 159 MPa).

For a wall thickness of 0.41 inch, the maximum range of high cycle fatigue principal stress at the wall I.D. is 4.3 to 12.9 kpsi (30-89 MPa).

The maximum stresses occur in relatively local areas; hence, the quality of the ceramic components will have to be especially carefully controlled in these regions. Figure 1.9 also summarizes the calculated stress conditions for the proposed mullite cylinder.

LOCATION	TEMP °F
A	1369
B	1000
C	450
D	400
Neck	300
Flange	200
Model ID#	.14



1-16

Ceramic Heater Head Pressure Vessel,
Thin Wall, 0.41 Inch Chamfered Undeformed
Shape

3000°F Retaining Ring Chamfer; 4500°F to 4000°F @ Z=0.	Comment
6300 psi (at top of ring)	1000 psi Internal Pressure
18258 psi	Thermal Equilibrium
19855 psi (at location shown above)	1000 psi & Thermal Equilibrium
23049 psi	3000 psi & Thermal Equilibrium

1.6 MATERIALS SELECTIONS

Materials selections for the key elements of the Ceramic Automotive Stirling Engine are summarized in Table 1.1. Heat transfer considerations led to the choice of mullite for the cylinder and regenerator housing and the displacer where, in addition to structural strength, low thermal conductivity is needed to minimize heat losses. The cylinder head, the heater tubes, and the mantle require high thermal conductivity as well as structural strength and, therefore, SiC was chosen for those components. In addition, a low thermal conductivity ceramic fiber core for the regenerator will reduce thermal losses. A commercially available aluminum borosilicate fibrous material was chosen for this element.

From the point of view of material integrity at high temperatures, the most critical component is the combustion housing where temperatures up to 3800°F (2093°C) must be sustained. A ZrO₂ coated Si₃N₄ is proposed for this element. In an oxidizing environment, ZrO₂ is chemically stable up to 4800°F. A thin coating on the order of 20-30 mils is anticipated to reduce the temperature at the Si₃N₄ /ZrO₂ interface to approximately 2500°F (1371°C), which the Si₃N₄ can tolerate. Due to a large difference in the expansion coefficients, a gradient bond will be required.

The air preheater choice was Si₃N₄ although SiC would also serve. Manufacturing problems and manufacturing costs will ultimately be decisive in this choice. The high thermal conductivity of these materials is needed for an efficient air preheater heat exchanger design.

From the point of view of mechanical strength, the high temperature developmental structural ceramics are already approaching the 700 MPa modulus of rupture strength level. Advances in fracture toughness by composite technology and transformation toughening, as well as improvements in Weibull modulus, are anticipated in the 1990 technology base. In this conceptual design, stress levels below 25 kpsi (172 MPa) have been maintained. Not every component has been analyzed; hence, much design effort remains to be performed if the ceramic Stirling concept is pursued further.

TABLE 1.1 CERAMIC AUTOMOTIVE STIRLING ENGINE

MAJOR CERAMIC COMPONENTS

1-18	<u>External Heat System</u>	<u>Material</u>	<u>Operating Temp °F</u>	<u>Key Property</u>
	Air Preheater Matrix	Si ₃ N ₄	1500-1800	HIGH THERMAL CONDUCTIVITY
	Air Preheater Housing			
	Insulation Outer	Alumina-Silicate Fiber	2000	HIGH TEMPERATURE DURABILITY
	Insulation Inner	ZrO ₂ Fiber	3000	HIGH TEMPERATURE DURABILITY
	Combustor	Si ₃ N ₄	3600-3800	HIGH TEMPERATURE DURABILITY, THERMAL SHOCK CAPABILITY (ZrO ₂ MELTS AT 4800F, Si ₃ N ₄ SUBLIMES AT 3360F, 1 atm)
		ZrO ₂ Coated		
	Ejectors	Si ₃ N ₄	2000	THERMAL SHOCK CAPABILITY
	EGR - Valve	Si ₃ N ₄	2000	THERMAL SHOCK CAPABILITY
	Fuel Nozzles	SIS 2361 (Water Cool)		
<u>Hot Engine System</u>				
Cylinders & Regenerator Housings	Mullite	1800	LOW THERMAL CONDUCTIVITY, HIGH STRENGTH & FRACTURE TOUGHNESS	
Cylinder Head	SiC	1800	HIGH THERMAL CONDUCTIVITY	
Heater Tubes	SiC	1800	HIGH THERMAL CONDUCTIVITY	
Regenerator Matrix	Alumina-Boro-Silicate Fiber	1800	LOW THERMAL CONDUCTIVITY (NEXTEL), HIGH SPECIFIC HEAT	
Mantel	SiC	2200-2400	HIGH THERMAL CONDUCTIVITY	
Displacer	Mullite	1800	LOW THERMAL CONDUCTIVITY	
Cylinder Liner	SiC	600	WEAR RESISTANT	

The relatively low stress level allowed in this design may be too modest as the ceramic fabrication technology advances and performance of the structural ceramics becomes less susceptible to statistical variation.

1.7 THERMODYNAMIC AND PERFORMANCE ANALYSIS

In order to analyze the performance of the CASE primary design, an updated version of Martini's second order code(2) was utilized. In order to gain confidence in the ability of the code to predict the performance of the proposed CASE design, it was first checked out against the published performance predictions of ASRE at four operating points of loads and speeds. The predictions of the Martini code were within 5% of published results in all the cases except for very low load conditions.

The code was utilized to optimize the performance of the proposed CASE design. Based on this optimization process, the performance of the CASE design at four operating points was compared with that of the ASRE design. The effect of average heater head temperature on indicated efficiency at maximum efficiency point is compared in Figure 1.10 for two cases. It is seen that for the CASE design, 81% of the Carnot efficiency can be achieved compared to 75% for the ASRE design.

Utilizing the aforementioned results, performance maps for the CASE design were prepared. The results are based on the auxiliary power requirements and friction losses characteristic of the ASRE design. Some savings in blower and coolant pump power requirements are realized because of the improved overall efficiency level which results in reduced air flow and heat rejection requirements. The performance map is presented in Figure 1.11 and the results are tabulated for four load conditions in Table 1.2. The results indicate that a net gain of 10 to 26% over the ASRE design can be expected depending on the load condition. The most significant gain occurs at full load condition. It is noticed that because of overall improved performance, the maximum rated power of the engine (60 kW) can be obtained at a lower speed of 3300 rpm compared to 4000 rpm for ASRE design. This has the added benefit of reduced wear and longer life, especially for the piston rings and seals.

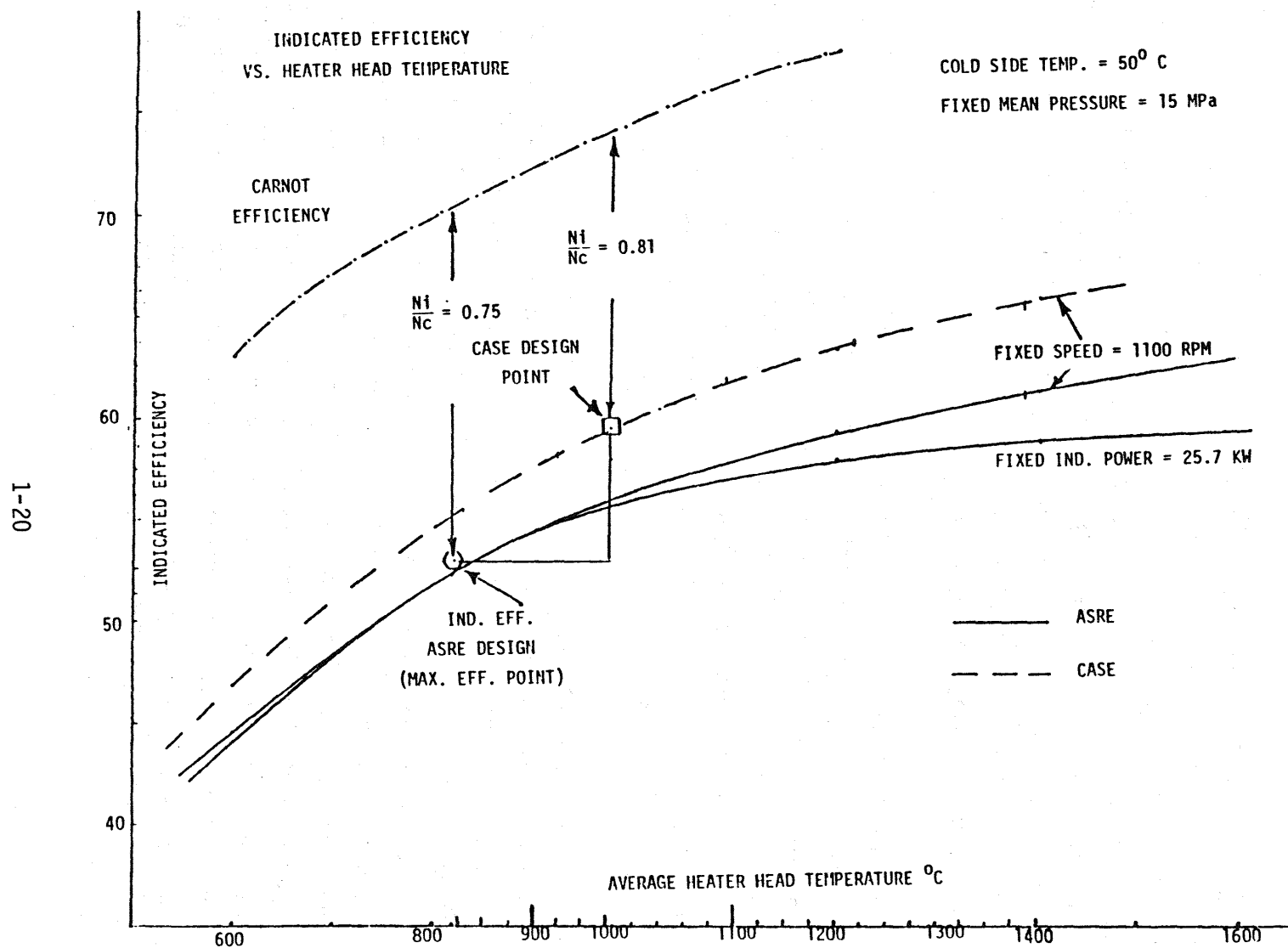


FIGURE 1.10 RATIO OF INDICATED EFFICIENCY TO CARNOT EFFICIENCY

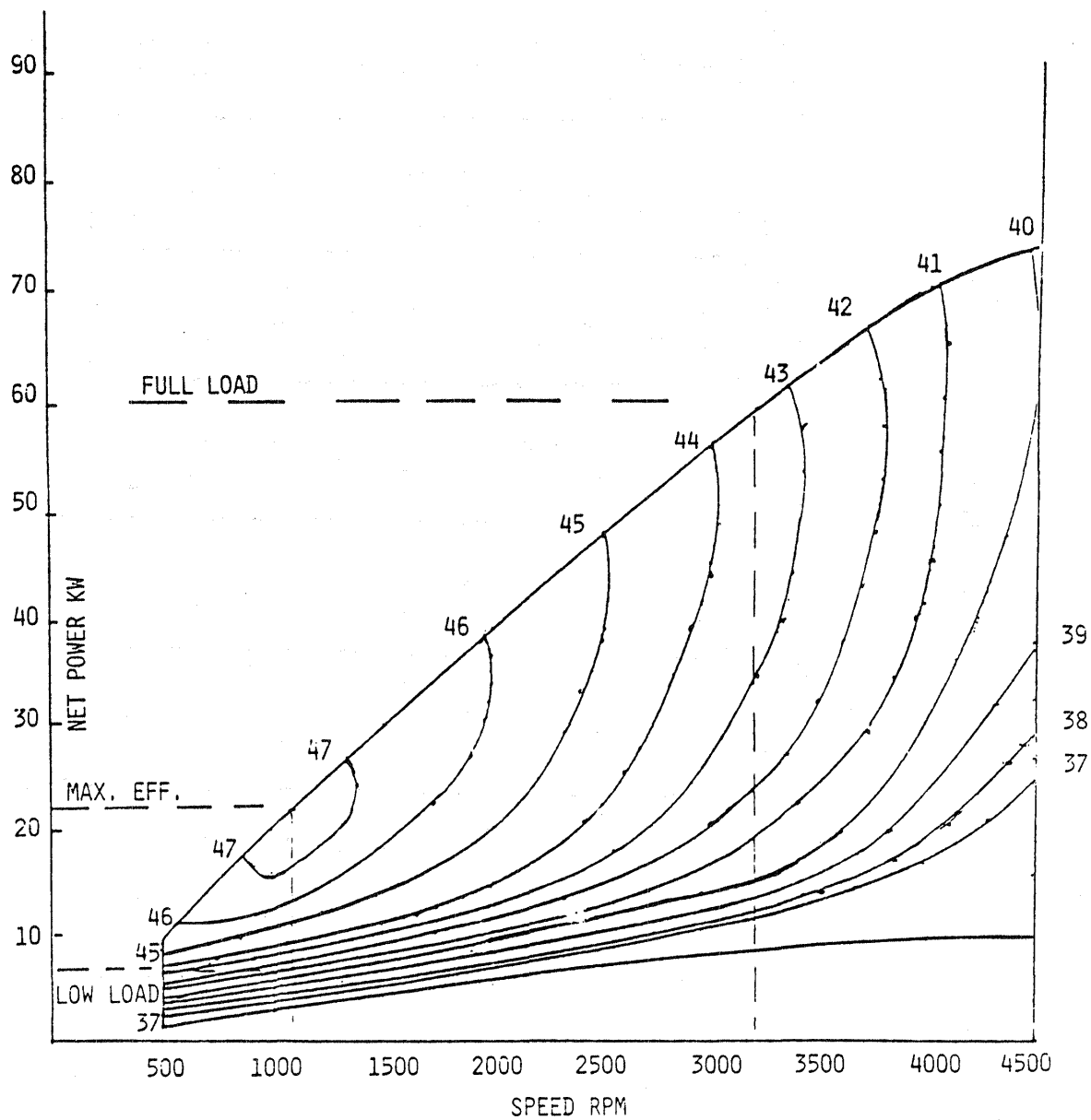


FIGURE 1.11 PERFORMANCE MAP OF CASE: CURVES OF CONSTANT NET EFFICIENCY (%)

TABLE 1.2 PERFORMANCE COMPARISON OF CASE AND ASRE DESIGN

		FULL LOAD (60 kW)		MAX. EFFICIENCY		PART LOAD		LOW LOAD	
		CASE	ASRE	CASE	ASRE	CASE	ASRE	CASE	ASRE
ENGINE SPEED	(RPM)	3300	4000	1100	1100	2000	2000	1000	1000
CHARGE PRESSURE	(MPa)	15	15	15	15	5	5	5	5
INDICATED POWER	(KW)	69.2	73.3	25.0	24.8	14.8	15.0	7.2	7.9
1-22 FRICTION	(KW)	6.9	9.6	2.2	2.2	2.0	2.0	0.9	0.9
AUXILIARIES	(KW)	1.8	3.6	0.3	0.5	0.7	0.8	0.3	0.4
NET POWER	(KW)	60.5	60.1	22.5	22.1	12.1	12.2	6.0	6.6
EXTERNAL HEATING SYSTEM EFFICIENCY	(%)	89	90.5	89	92.4	89	91.7	89	89.8
INDICATED EFF.	(%)	55.57	46.1	60.0	52.8	58.17	50.9	55.3	48.5
NET EFFICIENCY	(%)	43.2	34.2	48.1	43.5	42.4	37.7	41.0	36.4
PERCENTAGE GAIN OVER ASRE		26.3%		10.6%		12.5%		12.6%	

1.8 MANUFACTURING AND COST ANALYSIS

An estimate was made of the manufacturing cost for the primary design (CASE I) assuming anticipated 1990's structural ceramic production technology. All dollar values stated are in 1984 dollars.

The metal component costs were assumed to be the same as those projected for the Mod 1 engine by Mechanical Technology, Inc. (MTI) as reported in "Manufacturing Cost Analysis" - Report December 9, 1981 under contract DEN-3-32.

A sizeable portion of the cost in producing the component parts lies in the raw material powder cost. The engine cost analysis was conducted at three levels, I, II and III, for various assumed raw material costs. Currently, high quality powders required for high performance ceramic parts are expensive: for example, SiC or Si₃N₄ powder of high quality costs in the neighborhood of \$80./lb., mullite is \$30./lb. while zirconia (used for coatings) is approximately \$10./lb. Since we are contemplating 1990's production, we arbitrarily set the three levels at considerably reduced costs anticipating a significant "learning curve" reduction for powder as follows:

	Powder Cost \$/lb.		
	<u>Level I</u>	<u>Level II</u>	<u>Level III</u>
Si ₃ N ₄	5	10	20
SiC	5	10	20
Mullite	1	3	5
Zirconia	2	5	10

Cost estimating was based on 300,000 units per year, therefore, highly automated production techniques were visualized for each major ceramic component upon which as realistic as possible a cost analysis was made.

Although much of the automated manufacturing equipment is not yet in existence, based on present knowledge, we know it is feasible to achieve when the demand arises for a large-scale ceramics processing industry.

The summary of the CASE cost analysis is provided in Table 1.3. The MTI Mod 1 estimated cost is \$1498 compared to the CASE estimates of \$1942, \$2634, and \$4017 at the three levels of the raw powder costs assumed above. The sensitivity of the ceramic engine cost to powder cost is evident and much effort will be made in the future to reduce powder costs so that ceramic structural parts can be competitive with the older materials technologies.

1.9 LONG RANGE CERAMIC STANDARD ENGINE (CASE II)

At the conclusion of the effort on the "primary design", CASE I, an additional investigation was carried out to assess the potential for a ceramic automotive Stirling engine based on the year 2000 ceramic technology and somewhat more radical departures from conventional design approaches.

Based on the evaluation of various candidate component concepts, a reference design for the Long Range Ceramic Standard engine concept was developed and is illustrated in Figure 1.12.

A pulse combustor which enhances heat transfer is located at the top center of the engine. Another advantage of the pulse combustor is its compactness, higher efficiency of burning and lower CO and NO_x in the exhaust products. There is a noise penalty which will need to be treated with muffling devices.

The engine consists of four double acting cylinder/displacer assemblies. Heat pipes with lithium as the transfer medium carry energy from the pulse combustor to the cylinder wall and hence to the working fluid. One of the most important characteristics of the heat pipe is its capability of nearly isothermal operation thus effecting an efficient thermodynamic cycle for the engine. The hot side temperature for this design was raised to 1100°C (improved to 980°C for the primary design CASE I and 800°C for the ASRE). The high temperature imposes a need for ceramic heat pipes in the CASE II design.

TABLE 1.3 CASES ENGINE COST (1984) EXTRAPOLATED FROM MOD-1 ENGINE COST DATA

	(1)	(2)	(3)	(4)			(5)		
	Est. Basic Engine Cost (Mod 1 Design)	Est. Cost ¹ Equivalent Top Side Components	Est. Cost ¹ Lower Engine Block Components	Cost Equivalent ² Ceramic Engine Top Side Components			CASES Est. Basic Cost (Col 3 + Col 4)		
				4					
				Level I	Level II	Level III	Level I	Level II	Level III
Matl.	887.91			629.54	1,339.78	2,609.20			
Labor	155.50			114.87	114.87	114.87			
Burden ⁵	445.34			328.98	328.98	328.98			
Scrap ³	8.98			36.05	66.99	130.46			
	<u>1,497.73</u>	<u>664.82</u>	<u>832.91</u>	<u>1,109.44</u>	<u>1,850.62</u>	<u>3,183.51</u>	<u>1,942.35</u>	<u>2,683.53</u>	<u>4,016.92</u>

NOTES:

1. From Report dated 12/9/81, by Mechanical Technology, Inc. Under Contract DEN3-32
2. Equivalent parts exchange where clear identification is possible.
3. For ceramic parts, 5 percent of material is considered normal loss factor.
4. Level refers to material cost projections
5. Burden is 28% of labor

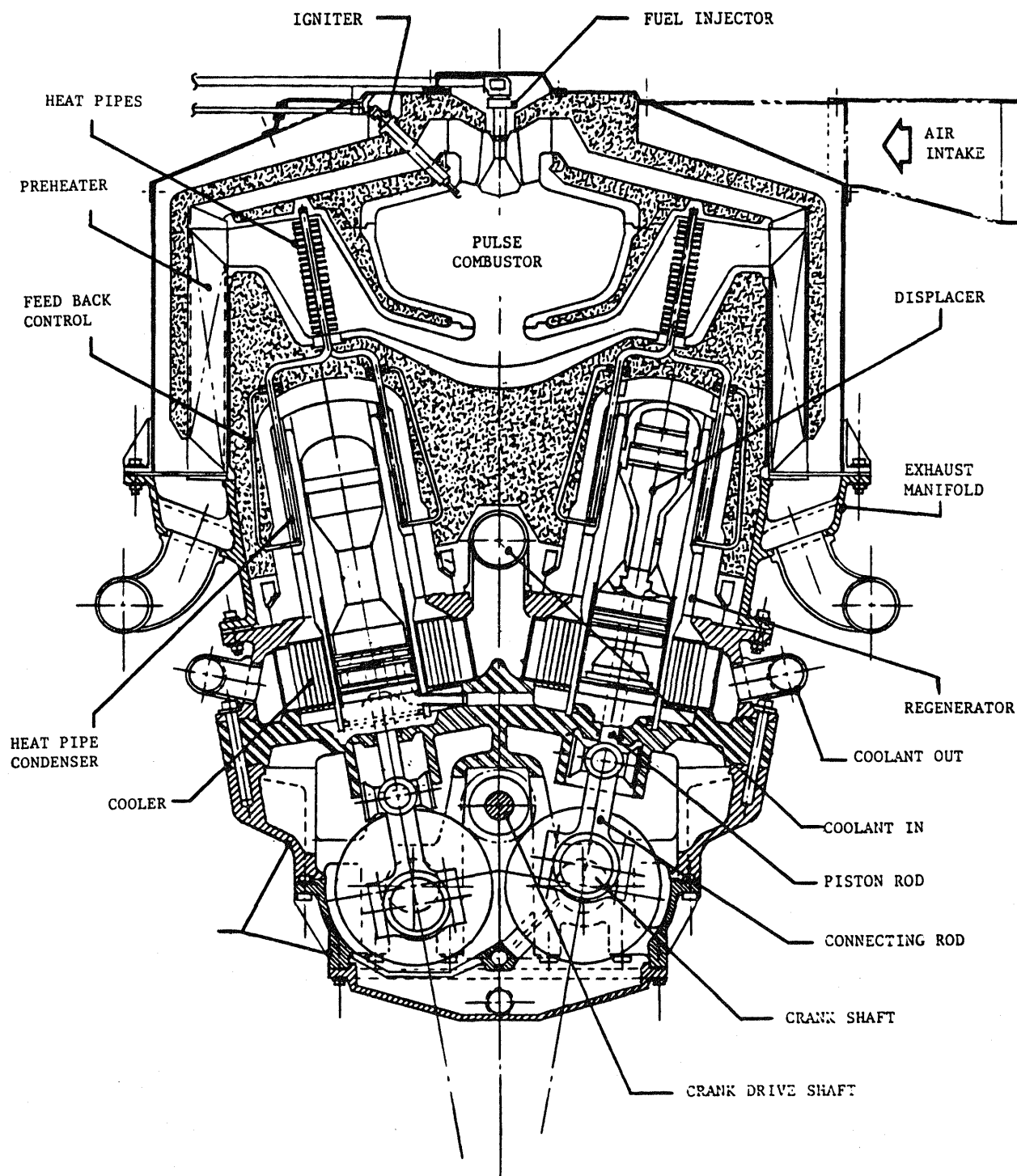


FIGURE 1.12 LONG RANGE AUTOMOTIVE STIRLING ENGINE CONCEPT
UTILIZING HEAT PIPES AND PULSE COMBUSTION

At the maximum efficiency point the net efficiency gain is 25% on the ASRE design (54.2% vs 43.5%). Although the concept was aimed to automobile application, these design concepts can be applied, as well, to other future Stirling engine applications. The performance comparison of the CASE I, CASE II, and the ASRE designs is provided in Table 1.4.

Another feature of this design is a seal ring on the hot side of the displacer as well as a ring on the cold side to minimize gas shuttling losses.

By raising the hot side temperature to 1100°C (2012°F), the flame temperature increases over the earlier designs to 4300°F (2371°C) thus improving a severe condition for the wall of combustion chamber. In fact, the combustion chamber design in both CASE I and CASE II will be a critical issue.

Other novel features of the CASE II design concept include pressurized crankcase to minimize problems associated with the piston rod seals and a dry lubrication system which will involve ceramic bearings.

1.10 FEDERAL DRIVING CYCLE

Based on the performance estimates derived in this study, NASA Lewis has made estimates of overall fuel consumption based on the Federal Driving Cycle codes. Table 1.5 compares the CASE I, CASE II and ASRE performance. It appears that a ceramic Stirling engine will enjoy a decided advantage over a metal engine in terms of fuel consumption where the duty cycle is relatively steady.

TABLE 1.4 PERFORMANCE COMPARISON OF CASE AND ASRE DESIGN

		FULL LOAD			MAX EFFICIENCY			PART LOAD			LOW LOAD		
		CASE 2	CASE 1	ASRE	CASE 2	CASE 1	ASRE	CASE 2	CASE 1	ASRE	CASE 2	CASE 1	ASRE
ENGINE SPEED	(RPM)	3400	3300	4000	1100	1100	1100	2000	2000	2000	1000	1000	1000
CHARGE PRESSURE	(MPa)	15	15	15	15	15	15	6	5	5	6	5	5
INDICATED POWER	(KW)	68.5	69.2	73.3	24.6	25.0	24.8	16.2	14.8	15.0	8.5	7.2	7.9
FRICTION	(KW)	7.2	6.9	9.6	2.2	2.2	2.2	2.1	2.0	2.0	1.0	0.9	0.9
AUXILIARIES	(KW)	1.3	1.8	3.6	0.3	0.3	0.5	0.6	0.7	0.8	0.3	0.3	0.4
NET POWER	(KW)	60.0	60.5	60.1	22.1	22.5	22.1	13.5	12.1	12.2	7.2	6.0	6.6
EXTERNAL HEATING SYSTEM EFFICIENCY	(%)	90	89	90.5	90	89	92.4	90	89	91.7	90	89	89.8
INDICATED EFF.	(%)	63.38	55.57	46.1	67.1	60.0	52.8	62.48	58.17	50.9	63.8	55.3	48.5
NET EFFICIENCY	(%)	50.0	43.2	34.2	54.2	48.1	43.5	47.1	42.4	37.7	48.6	41.0	36.4
PERCENTAGE GAIN OVER ASRE		46.2	26.3		24.6	10.6		24.9	12.5		33.5	12.6	

TABLE 1.5 COMPARISON BETWEEN CERAMIC AND METAL STIRLING ENGINES

	ASRE	CASE I	CASE II	
PERFORMANCE				
BSFC (BEST)	.32 lb/BHP-HR	.287 lb/BHP-HR	0.255 lb/BHP-HR	
BRAKE η	43%	48%	54%	
METRO-HWY	34.6 MPG (CITY)	34.9 MPG (CITY)	42.8 (CITY)	48.1 (CITY)
DRIVING CYCLE	66.0 MPG (HWY)	68.5 MPG (HWY)	76.8 (HWY)	86.1 (HWY)
	44.0 MPG (COMB.)	44.8 MPG (COMB.)	53.4 (COMB.)	60.0 (COMB.)
	PHOENIX WITH AUTOMATIC	PHOENIX WITH AUTOMATIC	PHOENIX WITH AUTOMATIC	PHOENIX WITH CVT
RATED POWER	80 BHP @ 4000 rpm	80 BHP @ 3300 rpm	80 BHP @ 3400 rpm	
CONFIGURATION	U-4 CYL.	V-4 CYL.	V-4 CYL.	
WEIGHT	145 LB. HOT SIDE	184 LB. HOT SIDE		
	585 LB. TOTAL	625 LB. TOTAL	400 LB. TOTAL	
SIZE	22" x 22" x 26"	30" x 30" x 33"	24" x 24" x 33"	
	163 gm FUEL (CSP)	184 gm FUEL (CSP)	131 gm FUEL (CSP)	

1.11 CRITICAL DEVELOPMENT AREAS

1.11.1 CRITICAL MATERIALS PROBLEMS

In order to realize the design presented, certain critical materials development tasks will be required:

1. The continued development of structural ceramics is needed to provide ceramics which are strong, have a high fracture toughness, and a high Weibull modulus. Fiber and whisker reinforcement and transformation toughening technology will be advanced to meet these needs. The reaction of any of these ceramics with H_2 at the temperature of operation must be investigated and possible dopants to H_2 be defined to reduce deleterious reactions, if any.

Although much R&D work has been done on SiC, Si_3N_4 and ZrO_2 , very little has been conducted on mullite. Mullite should be further developed because of its unique combination of favorable properties for heat engine application, in particular its low thermal conductivity coupled with excellent mechanical properties.

2. In a number of places, the gas tight joining of SiC to mullite is required:
 - a. SiC head to mullite cylinder
 - b. SiC heater head tubes to the mullite regenerator housing

These joints not only have to be gas tight but have to withstand substantial stresses due to pressure and thermal strain loads. The development of process technology to provide such joints is a critically important task.

3. The effect of high temperature, high pressure hydrogen on the SiC and mullite, and on the joints, needs to be evaluated for long time exposure.
4. The highest temperature exposure of the ceramic components will be directly beneath the burner where the surface temperature is anticipated to reach 3800°F (2093°C). Zirconia coated Si_3N_4 is proposed for this area. A relatively thin layer of zirconia will substantially reduce the maximum temperature that the substrate will reach. (Also, an active cooling loop can be incorporated in this area, if necessary, to reduce the surface temperature). The development of this coating process and thermal durability tests of the composite will need to be conducted.

5. In this design, a ceramic fiber regenerator core is proposed. The fabrication techniques and the ability of the core to tolerate cyclic high temperature hydrogen gas flow will have to be evaluated.
6. Development of the fabrication for a complete cylinder assembly would follow the successful solution of the above problems. These development needs are summarized in Table 1.6.

1.11.2 CRITICAL DESIGN ISSUES

In the area of thermal and structural designs, the following critical issues will have to be resolved.

1. The emissions level, especially the NO_x emission, from the combustion exhaust may increase as the flame temperature is increased. The influence of the combustion gas recirculation level and other means to reduce NO_x emissions needs to be investigated.
2. The present study does not allow a rigorous transient analysis. More in-depth transient analysis is needed to investigate the effect of thermal shock on key ceramic components and identify means to reduce the thermal shock. Start-up stresses are severe for ceramics.
3. Potential for the performance advantage of a ceramic engine over a metal engine is shown to be feasible in this study, but has not been fully explored as indicated in Figure 1.10. Additional design iteration will allow the reduction of localized stress level and permit even higher engine operating temperature.
4. A more rigorous structural analysis should include the engine cylinder and heater head as a whole so that the stress concentration at the tube-cylinder head interface can also be evaluated. The natural frequency of the tubes and their dynamic response need to be analyzed to assess potential failure modes of the engine.
5. The cumulative probability of failure as a function of the volumetric distribution of stress and flaw population needs to be analyzed. Such an analysis will require extensive statistical data on the materials selected.

TABLE 1.6 CRITICAL MATERIALS PROBLEMS

1. JOINING

DEVELOP JOINING PROCEDURES FOR (A) SiC TO SiC
(B) SiC TO MULLITE

- JOINTS MUST BE IMPERMEABLE TO H₂ AND CHEMICALLY STABLE AT 1800°F, CYCLIC LOADING CONDITIONS
- HEATER HEAD-CYLINDER ASSEMBLY IS VERY COMPLEX, ASSEMBLY PROCESS DEVELOPMENT IS NEEDED

2. HEATER HEAD TUBE FABRICATION

- TUBES ARE THIN WALL, MUST BE IMPERMEABLE TO H₂ AND WITHSTAND CYCLIC STRESSES
- FABRICATION TECHNIQUES NEED TO BE VERIFIED
- DURABILITY TESTING IN CYCLIC STRESS IS REQUIRED

TABLE 1.6 CRITICAL MATERIALS PROBLEMS (CONT'D)

3. COMBUSTOR HOUSING

DEVELOP A ZrO_2 COATED Si_3N_4 (OR SiC) TO WITHSTAND TEMPERATURES UP TO $3800^\circ F$ AND BE RESISTANT TO THERMAL SHOCK STRESSES

4. TRANSFORMATION TOUGHENED MULLITE

DEVELOP A HIGH STRENGTH MULLITE (1000,000 PSI MOR) AND HIGH FRACTURE TOUGHNESS ($K_{IC} \geq 5$), HIGH WEIBULL MODULES (TBD) AT ELEVATED TEMPERATURES ($> 1800^\circ F$)

5. REGENERATOR CORE

DEVELOP DURABLE CERAMIC FIBER FOR REGENERATOR CORE WHICH CAN TAKE $1800^\circ F$ AND CYCLIC H_2 GAS FLOW WITHOUT DEGENERATION

6. CHEMICAL RESISTANCE

VERIFY DURABILITY OF MULLITE AND SiC IN $1800^\circ F$ H_2 GAS

REFERENCES

1. "Automotive Stirling Reference Engine Design Report", Doc. No. DOE/NASA/0013-12, NASA CR-65381, MTI 81 ASE 164DR2.
2. W. R. Martini, "Stirling Engine Design Manual" Second Edition, DOE/NASA/3194-1, NASA CR-68088, January 1983.

SECTION 2

REQUIREMENTS

2.1 DESIGN

The General Electric conceptual ceramic automotive Stirling engine primary design is based on the Automotive Stirling Reference Engine (ASRE) and incorporates the following requirements and goals:

1. The design reflects the most advanced design and ceramic fabrication practice that can be reasonably projected to exist circa 1990.
2. The design is for the same power level, working gas, operating pressures, and fuels as the ASRE and targeted for the same overall envelope and weight.
3. Design goals include optimization of fuel consumption over the combined Federal Driving Cycle, and the highest feasible overall engine efficiency.
4. Engine life goal is 4000 hours over the combined Federal Driving Cycle. Stress analysis considered the combination of pressure and thermal stresses for maximum power, steady state points, and transients.
5. The effect of higher heater head operating temperatures on engine cold end components, in particular, the rod seal was considered.
6. Feasibility of using high thermal conductivity ceramic (e.g., SiC) for the heat exchange portion of the heater head and low thermal conductivity ceramic (for example, oxide ceramics) in the cylinder, regenerator housings, and manifolds and the problem of joining dissimilar materials were investigated.

The general design guidelines are summarized in Table 2.1. The ASRE was shown in Figure 1.1

A "Long Range Ceramic Standard" Stirling engine preliminary conceptual design is also to be established based on the same requirements as are listed above except that the technology base is that anticipated to exist circa year 2000.

TABLE 2.1 DESIGN GUIDELINES

- REFLECT MOST ADVANCED PRACTICE THAT WILL EXIST IN 1990
- DESIGN FOR SAME POWER LEVEL, WORKING GAS, OPERATING PRESSURE AND FUELS AS AUTOMOTIVE STIRLING REFERENCE ENGINE (ASRE)
- TARGET FOR SAME OVERALL ENVELOPE AND WEIGHT AS ASRE
- OPTIMIZE FOR LOWEST FUEL CONSUMPTION AND HIGHEST FEASIBLE OVERALL ENGINE EFFICIENCY
- AIM FOR ENGINE LIFE GOAL OF 4000 HOURS
- USE HIGH THERMAL CONDUCTIVITY CERAMIC FOR HEAT EXCHANGE PORTION AND LOW CONDUCTIVITY CERAMIC FOR CYLINDER, REGENERATOR HOUSINGS AND MANIFOLDS
- INVESTIGATE PROBLEMS OF JOINING DISSIMILAR MATERIALS, HOT-TO-COLD INTERFACES AND EFFECT OF HIGHER OPERATING TEMPERATURE ON ENGINE COLD END COMPONENTS

2.2 PERFORMANCE EVALUATION

The overall performance attainable with the engine primary design arrived at based on the design requirements of paragraph 2.1 above were predicted. Engine maps showing power, torque and thermal efficiency over the anticipated operating regime were generated.

1. Part load point performance for candidate design configurations from Task I were calculated to provide guidance for design iterations required to optimize performance. Engine design and performance information which is presented in NASA CR 165381 for the ASRE was the starting point for estimating ceramic engine performance.
2. Predicted engine performance maps for the engine primary design were developed showing power, torque, and thermal efficiency for a range of engine speeds up to the maximum design speed, a range of working fluid pressures from three to fifteen MPa, and heater head temperatures from approximately 800°C to the maximum operating temperature for the subject ceramic engine design.

A preliminary performance evaluation of the long range ceramic standard was also projected.

2.3 PRODUCTION, COST EVALUATION

The feasibility of mass production for the ceramic engine primary design was evaluated, including an estimate of production costs for automotive volume levels (300,000 units/year).

1. The materials, processes, and fabrication techniques required to achieve the specified design characteristics were determined.
2. The feasibility of manufacturing ceramic Stirling engines in mass production (300,000/year) was evaluated and impediments to this level of production identified.
3. A rough estimate of the ceramic Stirling engine manufacturing cost was made by comparison with internal combustion engines and all-metal Stirling engines.

SECTION 3

OVERVIEW OF DESIGN PROCESS AND TRADE OFFS

3.1 CONFIGURATION TRADE OFF

A flow sheet is shown in Figure 3.1 which schematically describes the trade-off analysis and evolution of the concept adopted for the CASE primary design. A fundamental premise of the designs considered was that SiC would be used where high thermal conductivity was advantageous. Since the two materials have very nearly equal coefficients of expansion, sound joints between SiC and mullite are expected to be achievable.

The initial effort was toward establishing a baseline concept which can be shown by supporting calculations to achieve an acceptably high efficiency which in principle is fabricable, and in which the anticipated stress levels are within acceptable limits.

Two concepts were considered. The first is a monolithic design wherein the working fluid heat transfer occurs in passages integrally formed in the ceramic head structure. A radiant surface is positioned close to the head and the combustion gases flow through the intervening passageway heating the radiant surface which radiates to the head. The combustion energy is thus transferred to the monolithic head structure via radiation and convection and thence to the working fluid.

The second concept considered external heater tubes analogous to the ASRE configuration but modified to take advantage of a radiant heat transfer surface positioned close to the tubes as in the case of the monolithic head described above. These tubes were conceived as being fabricated from SiC which has a very high thermal conductivity. Figure 3.2 lists some of the pros and cons of the two concepts.

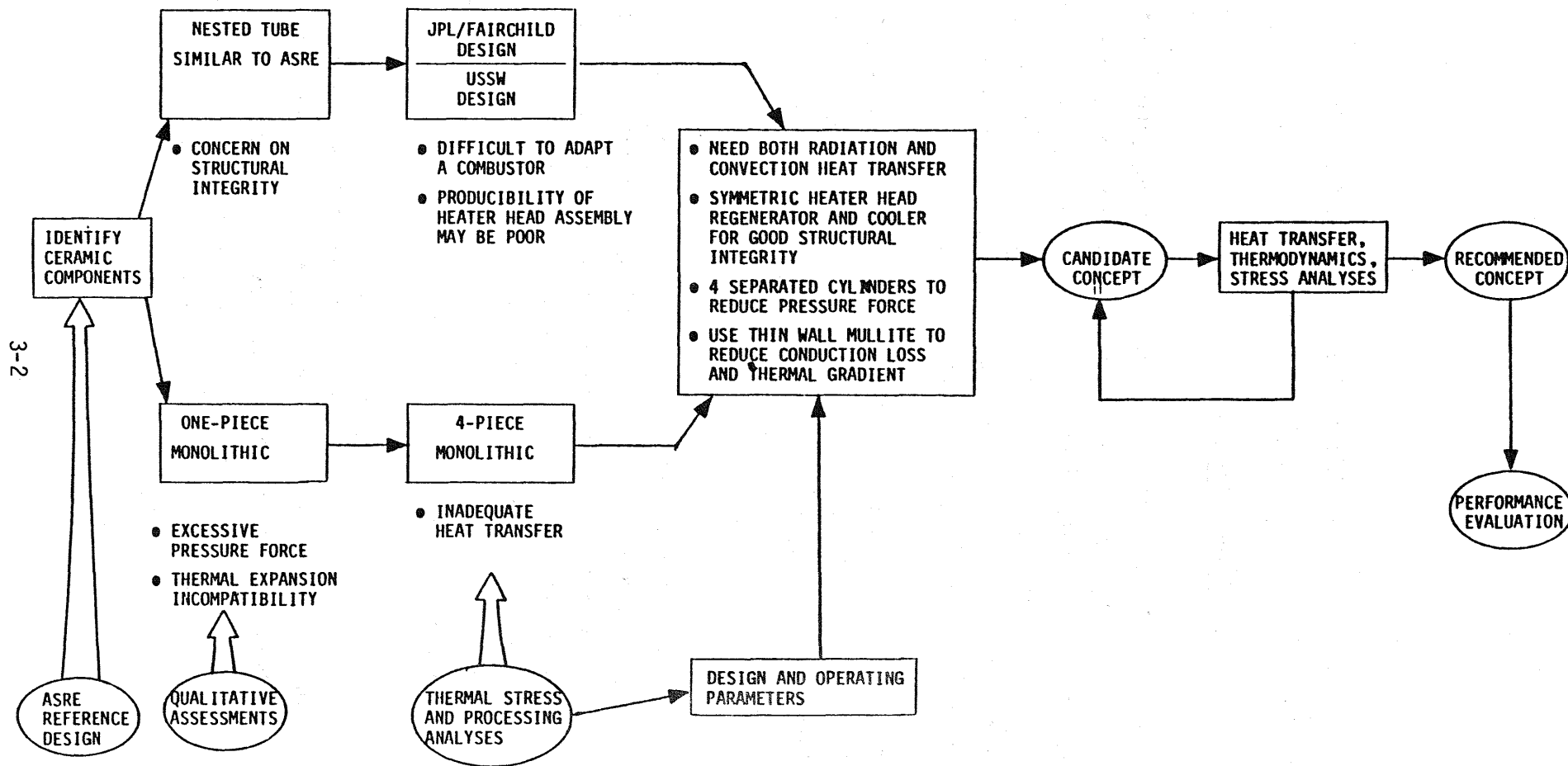


FIGURE 3.1 EVOLUTION OF DESIGN

HEATER HEAD CONCEPT

PROS

CONS

COMMENTS

NESTED-TUBE SIMILAR TO ASRE

- SEPARATED CYL. HEADS & REG. HOUSING
SUBJECTED TO LESS LATERAL THERMAL
STRESS
- CLOSER TO METAL ASRE DESIGN - LESS
RISK IN PERFORMANCE PENALTY
- TUBE ASSEMBLY PROVIDES SOME FLEX-
IBILITY FOR THERMAL EXPANSION
- MORE SUITABLE FOR CONVECTIVE HEAT
TRANSFER

- TUBE ASSEMBLY, JOINTS & SEALS
CUMBERSOME AND LESS RELIABLE
- SHOCK & VIBRATION RESISTANCE
FOR CERAMIC TUBE ASSEMBLY YET
TO BE PROVEN

- NEED A TUBE ASSEMBLY
WITH GOOD STRUCTURAL
INTEGRITY
- INVESTIGATE MEANS TO
PROMOTE RADIATION
HEAT TRANSFER

MONOLITHIC (ONE-PIECE OR MULTIPLE PIECES)

- BETTER SHOCK & VIBRATION RESISTANCE
- REDUCED JOINT AND SEAL REQUIREMENTS
- POSSIBILITY TO IMPLEMENT RADIATION
HEAT TRANSFER:
 - UNIFORM HEAT DISTRIBUTION
 - HIGHER TEMP. CAPABILITY
 - SMALLER VOID VOL. AT HEATER HEAD

- LESS HEAT TRANSFER SURFACE
AVAILABLE
- DESIGN & FAB. OF EFFECTIVE H₂
PASSAGE AT HEATER HEAD MORE
DIFFICULT
- SEPARATED CYLINDER AND
HX HOUSING CREATE LARGE
BENDING MOMENT ON STRUCTURE
BASE
- ONE-PIECE STRUCTURE CONSISTING
OF 4 CYLINDERS SUBJECTED TO A
GREATER LATERAL THERMAL EXPANSION

- NEED ENHANCED HEAT
TRANSFER
- A GREATER DEVIATION FROM
THE EXISTING ASRE DESIGN

- AXI-SYMMETRIC ANNULAR TYPE HEATER HEAD
ATTRACTIVE FOR CERAMIC ENGINE
- COMBINE RADIATION AND ENHANCE CONVECTION
TO ACHIEVE NEEDED HEAT TRANSFER

FIGURE 3.2 QUALITATIVE ASSESSMENT OF CERAMIC HEATER HEAD CONCEPTS

This preliminary assessment reveals that the preferred CASE design should observe the following general approach:

- Ceramic components should avoid complex contour to avoid potential stress concentration.
- Monolithic heater head concept, if adopted, should consist of four independent domes to reduce stress.
- Joints and seals should be minimized; an annular type regenerator concentric to the cylinder housing is preferred over the can-type regenerator adopted by the ASRE design.

A preliminary effort was carried out to provide guidelines on the preferred operating temperature, heat transfer requirements, and impact on emissions due to a higher temperature operation.

An initial thermal analysis showed that a ceramic Stirling engine could be expected to operate at an engine indicated efficiency of 60% with a hot side temperature of 1000C (1832F), whereas the ASRE engine is anticipated to have an engine indicated efficiency of 53% at a hot side temperature of 800C (1472F) as shown in Figure 3.3.

A preliminary estimate of performance parameters for the Ceramic Stirling Engine relative to the ASRE at maximum efficiency point is given in Table 3.1.

In sizing the heater head area required for heat transfer, preliminary calculations were made to determine the relationship between heat input density (watts/cm^2) and combustion temperature for a given heater head temperature level, Figure 3.4.

Figure 3.5 shows that for an assumed H_2 tube or passage temperature of 1000C (1832F) the selected CASE design condition requires a combustion gas

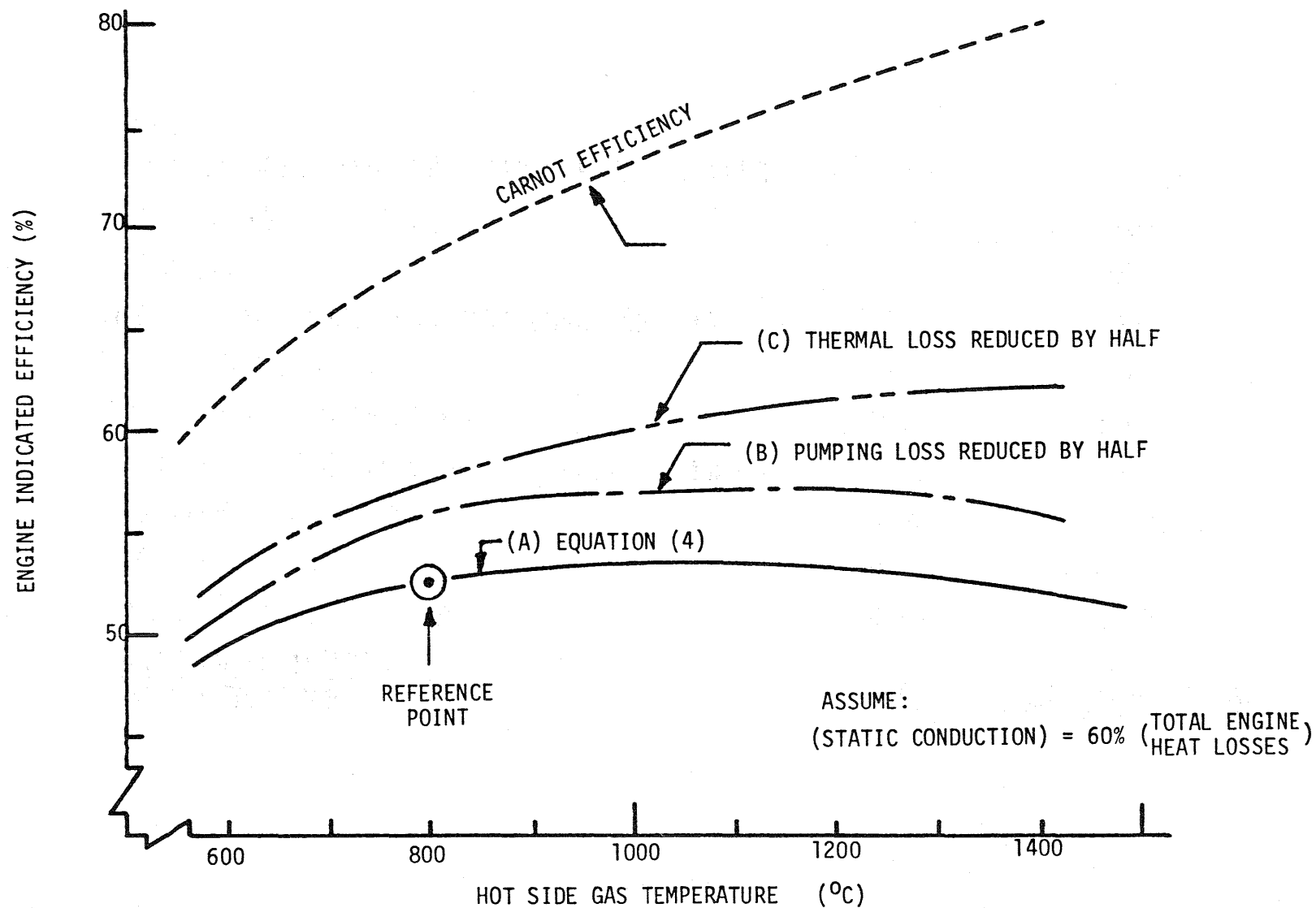


FIGURE 3.3 EFFECT OF HOT SIDE OPERATING TEMPERATURE ON ENGINE INDICATED EFFICIENCY

TABLE 3.1 PRELIMINARY ESTIMATE OF PERFORMANCE OF CERAMIC STIRLING ENGINE RELATIVE TO ASRE
(AT MAXIMUM EFFICIENCY POINT)

ENGINE PERFORMANCE PARAMETERS	ASRE	CASE
		SAME POWER OUTPUT
INDICATED EFFICIENCY	53	60
HEAT INPUT TO ENGINE (KW)	46.9	41.3
FIRING RATE, KW	50.7	44.6
FUEL FLOW RATE, LB/HR	9.35	8.38
TOTAL COMBUSTION AIR FLOW RATE (10% EA) LB/HR	156.53	140.29
AVG. HEATER HEAD TEMP, (°C)	820	1000
AVG. COOLER TEMP, (°C)	60	60
COMB. GAS ΔT REQ'D FOR HEAT TRANSFER (°C)	1305	1283
SPEED (RPM)	1100	SAME
HEAT FLUX DENSITY W/CM ²	~ 50	~ SAME
NUMBER OF HEAT TRANSFER UNITS FOR HEATER HEAD (NTU)	~ 3.25	~ 3.63

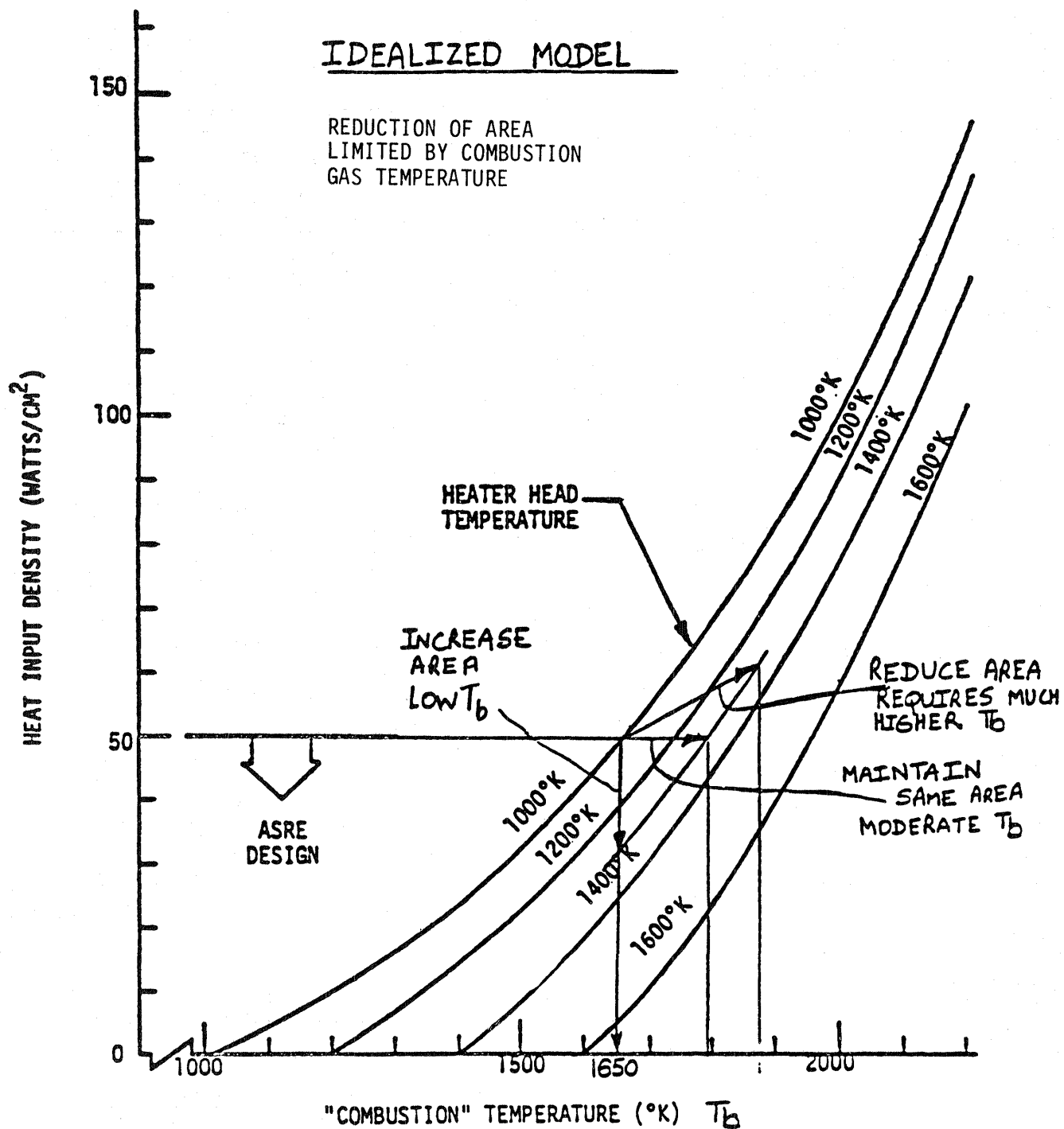
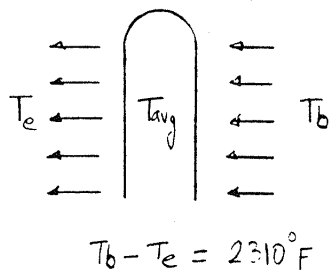


FIGURE 3.4 EFFECT OF EHS WALL AND GAS TEMPERATURE
ON THE HEATER HEAD HEAT INPUT DENSITY



THE REQ'D COMBUSTION GAS TEMP. MAY BE REDUCED BY ENHANCING RADIATIVE HEAT TRANSFER

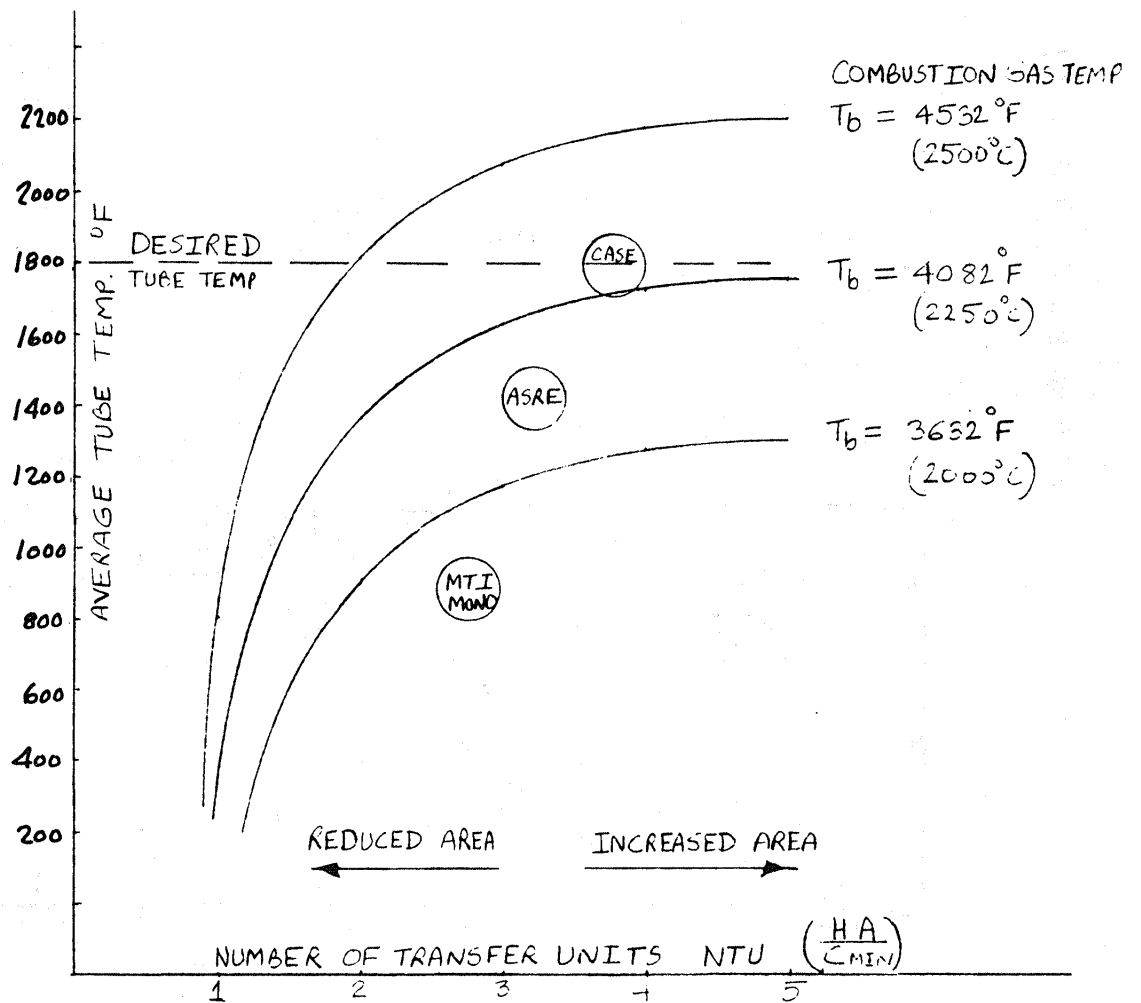


FIGURE 3.5 RELATIONSHIP BETWEEN COMBUSTION GAS TEMPERATURE AND AVERAGE HEATER HEAD TEMPERATURE

temperature of about 2300C (4172F) when the number of heat transfer units

$$NTU = \frac{(HA)}{C_{min}}$$

is about 4,

where H = effective heat transfer coefficient

A = area for heat transfer

C_{min} = specific heat capacity times mass flow rate of combustion gases.

The required combustion gas temperature will be reduced by enhancing radiative heat transfer, i.e., using a radiative panel surrounding the heater head.

A critical part of the design is to maintain NO_x levels at or below EPA requirements while meeting the other engine performance goals. For a 2300C combustion temperature, less than 50% exhaust gas recirculation is required under non-adiabatic conditions. For the same temperature a higher level of recirculation can be achieved under adiabatic conditions. The higher recirculation level may be essential to maintaining NO_x levels. A tradeoff between the percent recirculation, adiabatic vs non-adiabatic condition and the desired flame temperature must be made when establishing the acceptable operating parameters.

3.2 MATERIALS CONSIDERATIONS

3.2.1 INTRODUCTION

The world-wide development of advanced structural ceramics for heat engines has made feasible the consideration of a ceramic Stirling engine. The Automotive Stirling Reference Engine (ASRE) is configured to operate at an H_2 temperature of 820C. The temperature (hence thermal efficiency) limitation is imposed by the properties of available metals of construction.

The structural ceramics which are now available and which are emerging make the successful design and development of a Stirling engine with an H_2 fluid temperature of 1100C (or higher) and pressure of 15MPa (2160 psi) a definite possibility, although many detailed problems will have to be solved to achieve such an ambitious goal.

3.2.2 OPERATING CONDITIONS FOR STRUCTURAL COMPONENTS

Proposed operating conditions for an advanced automotive ceramic engine are listed in Section 2.0. The minimum life of the engine is 4000 hours involving 20,000 cycles of start up and shut down. The peak operating pressure within those components containing the H_2 working fluid is estimated at 15 MPa.

Temperatures of the various components are shown in Table 3.2. The high temperatures and oxidizing environment present a very critical material selection and design problem.

TABLE 3.2 CERAMIC AUTOMOTIVE STIRLING ENGINE
MAJOR CERAMIC COMPONENTS

<u>External Heat System</u>	<u>Material</u>	<u>Operating Temp °F</u>	<u>Key Property</u>
Air Preheater Matrix	Si_3N_4	1500-1800	HIGH THERMAL CONDUCTIVITY
Air Preheater Housing			
Insulation Outer	Alumina-Silicate Fiber	2000	HIGH TEMPERATURE DURABILITY
Insulation Inner	ZrO ₂ Fiber	3000	HIGH TEMPERATURE DURABILITY
Combustor	Si_3N_4 ZrO ₂ Coated	3600-3800	HIGH TEMPERATURE DURABILITY, THERMAL SHOCK CAPABILITY (ZrO ₂ MELTS AT 4800F, Si_3N_4 SUBLIMES AT 3360F, 1 atm)
Ejectors	Si_3N_4	2000	THERMAL SHOCK CAPABILITY
EGR - Valve	Si_3N_4	2000	THERMAL SHOCK CAPABILITY
Fuel Nozzles	SIS 2361 (Water Cool)		
<u>Hot Engine System</u>			
Cylinders & Regenerator Housings	Mullite	1800	LOW THERMAL CONDUCTIVITY, HIGH STRENGTH & FRACTURE TOUGHNESS
Cylinder Head	SiC	1800	HIGH THERMAL CONDUCTIVITY
Heater Tubes	SiC	1800	HIGH THERMAL CONDUCTIVITY
Regenerator Matrix	Alumina-Boro-Silicate Fiber	1800	LOW THERMAL CONDUCTIVITY HIGH SPECIFIC HEAT
Mantel	SiC	2200-2400	HIGH THERMAL CONDUCTIVITY
Displacer	Mullite	1800	LOW THERMAL CONDUCTIVITY
Cylinder Liner	SiC	600	WEAR RESISTANT

Critical considerations are H_2 permeability, strength throughout the operating temperature range (static and long time cyclic, thermal shock), thermal conductivity, and oxidation resistance.

3.2.3 MATERIAL SELECTION

There are generally a number of ceramic materials potentially applicable to each component although some have more development and even commercial experience than others. Engine materials at the highest level of development are:

Sintered α -SiC	}	Hot structural components
Reaction bonded SiC		
Hot pressed Si_3N_4		
Reaction bonded Si_3N_4		
Aluminum silicate	}	Regenerator heat sink
Magnesia alumina silicate (MAS)		

The most applicable materials which have less maturity than those above are:

Sintered Si_3N_4		Hot structural parts
Zirconia-Magnesia-Alumina-Silicate (ZrMAS)	}	Regenerator heat sink
SiC Reticulated Foam		
Zirconia (ZrO_2)	}	Burner wall, air preheater, combustor parts
Zircon ($ZrO_2 \cdot SiO_2$)		
Mullite ($3Al_2O_3 \cdot 2SiO_2$)		

Since the peak temperatures of the engine will occur in the air preheater and burner wall, very refractory, highly oxidation resistant materials will be needed there which can withstand the cyclic thermal stresses.

Table 3.3 lists representative characteristics of advanced ceramic materials

Thermal Conductivity

Among the candidate ceramics the SiC and Si₃N₄ materials have high thermal conductivity (k) while the oxides have low thermal conductivity. Indeed, the sintered α -SiC k is approximately twice that of N155 alloy while that of the Si₃N₄ material is about equal to the metal. Thus, the use of these ceramics will present minimal problems in areas where high thermal conductivity is needed for heat transfer. In addition, the high thermal conductivity coupled with relatively low coefficient of thermal expansion (α) will also be reflected in a lesser susceptibility of the SiC and Si₃N₄ to thermal shock fracture. Various figures of merit have been devised as a measure of resistance to thermal shock fracture which involve strength (σ), modulus of elasticity (E), coefficient of thermal expansion (α), thermal conductivity (k), specific heat (c), and density (ρ). In general, thermal shock damage is minimum with low values of E and α , and high values of σ , k, and c.

H₂ Permeability

In general, ceramics have greater resistance to H₂ permeability than metals. Experience with sintered α -SiC has shown that this material has a low permeability for H₃ (tritium). Figure 3.6 shows diffusion data for various forms of silicon carbide. The diffusion rate is several orders of magnitude less than for metals such as N155. Hence, H₂ permeability is not expected to be a problem with SiC as long as the ceramic components enclosing the H₂ maintain integrity.

TABLE 3.3 TYPICAL PROPERTIES OF STRUCTURAL CERAMICS

(DATA AT ROOM TEMPERATURE UNLESS OTHERWISE NOTED)

Ceramic	Melt (M) or Dissociation (D) Temp °C	Density gm/cm ³	Specific Heat Cal/g °C	Thermal Conductivity Wm ⁻¹ °C ⁻¹	Coefficient of Thermal Expansion 10 ⁻⁶ °C ⁻¹	Modulus of Elasticity GPa	Modulus of Rupture MPa	Fracture Toughness K _{1C} MPa √m
SiC	2700 (D)*	3.1	.24	109 (25C) 71 (300C) 42 (1000C)	4.06 (25-500C) 5.60 (500-1000C)	428	533	2.5-4 (20C) 3-4 (820C)
Si ₃ N ₄	1900 (D)*	2.9	.13	17	3.2 (40-800C)	293	587	4.5-6 (20C) 4.5-6 (820C)
3Al ₂ O ₃ • 2SiO ₂	1830 (M)	3.17	.21 (RT) .26 (500C)	4 (RT) 2.8 (500C)	5.0 (RT-800C)	179	230	2.3 (RT)
Al ₂ O ₃	2045 (M)	3.8	.25	25.5	7.7 (40-800)	390	303	5. (20C) 3.5 (820C)
ZrO ₂	2700 (M)	5.7	.10	2.2 (RT) 2.4 (500C)	8.9 (25-525C) 8.6 (25-925C)	205	600 (RT) 350 (820C)	8-15 (20C) 5 (820C)

* Oxidation limit in air approximately 1600C

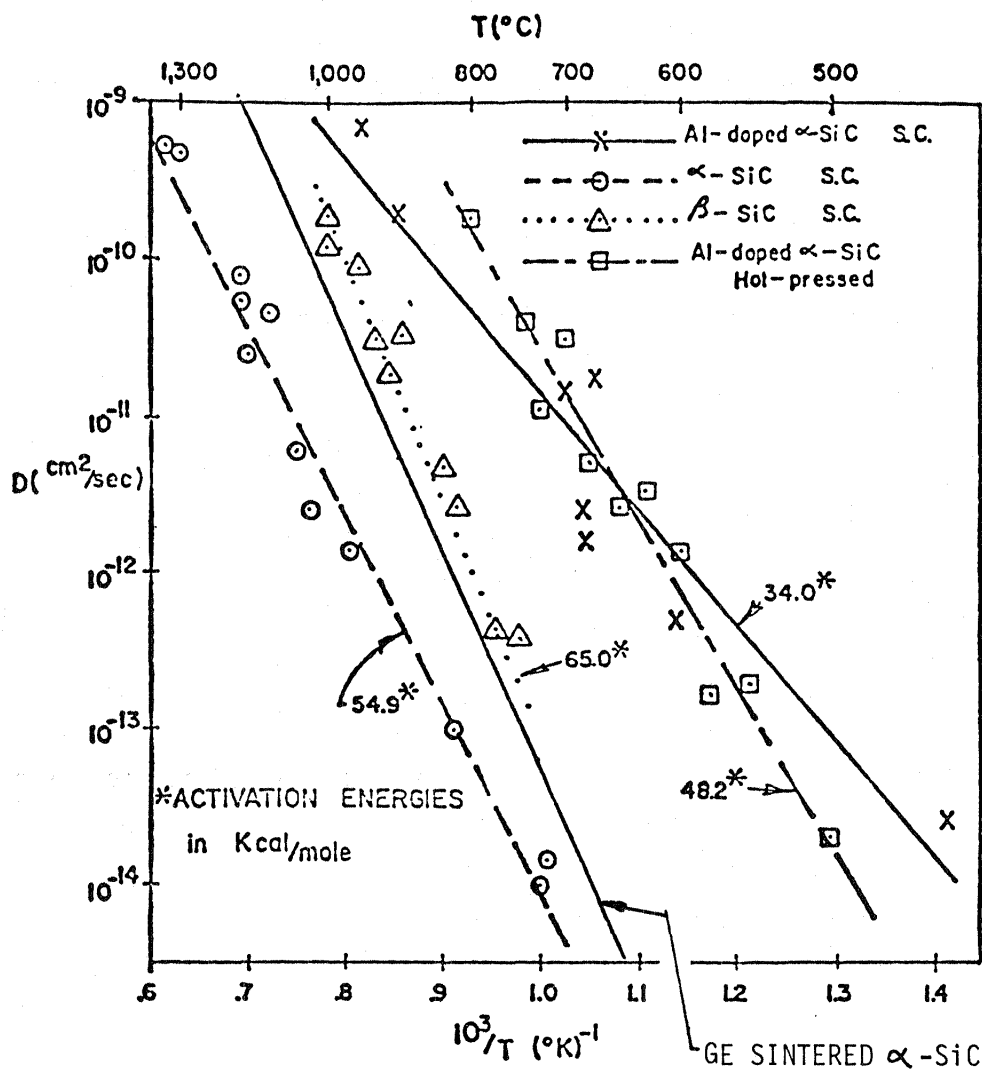


FIGURE 3.6 ARRHENIUS PLOT FOR TRITIUM DIFFUSION IN α AND β -SiC SINGLE CYRSTALS, ALUMINUM DOPED SINGLE CRYSTAL α -SiC AND ALUMINUM DOPED HOT PRESSED α -SiC

Strength

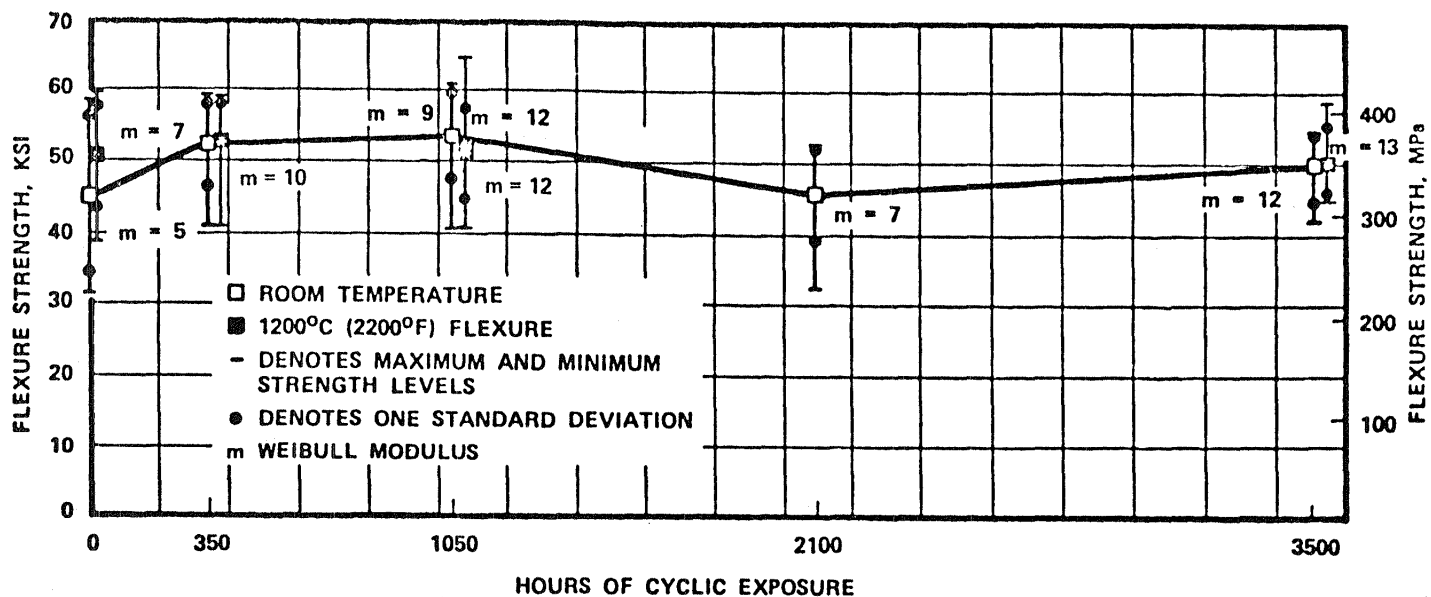
A large data base has been accumulated on strength of the new ceramics as a function of cyclic exposure to stresses and temperatures in heat engines. As an example, excellent data for sintered α -SiC has been accumulated. Materials were exposed to 1200 and 1370C up to 3500 hours in a cyclic test designed to simulate automotive operation. Carborundum Co. sintered α -SiC specimens showed virtually no strength degradation in four point bending after the 3500 hour test. At the 1200C test point, MOR = 350 MPa (Weibull $m = 13$) when tested at both room temperature and 1200C. At the 1370C test point, again there was no loss of room temperature strength after the 3500 hour cyclic test, MOR = 330 MPa (Weibull $m = 13$) but there was a decline in strength when the specimens were tested in four point bending at 1200C, MOR = 230 MPa (Weibull $m = 12$). These data are presented in Figures 3.7 and 3.8.

Oxidation

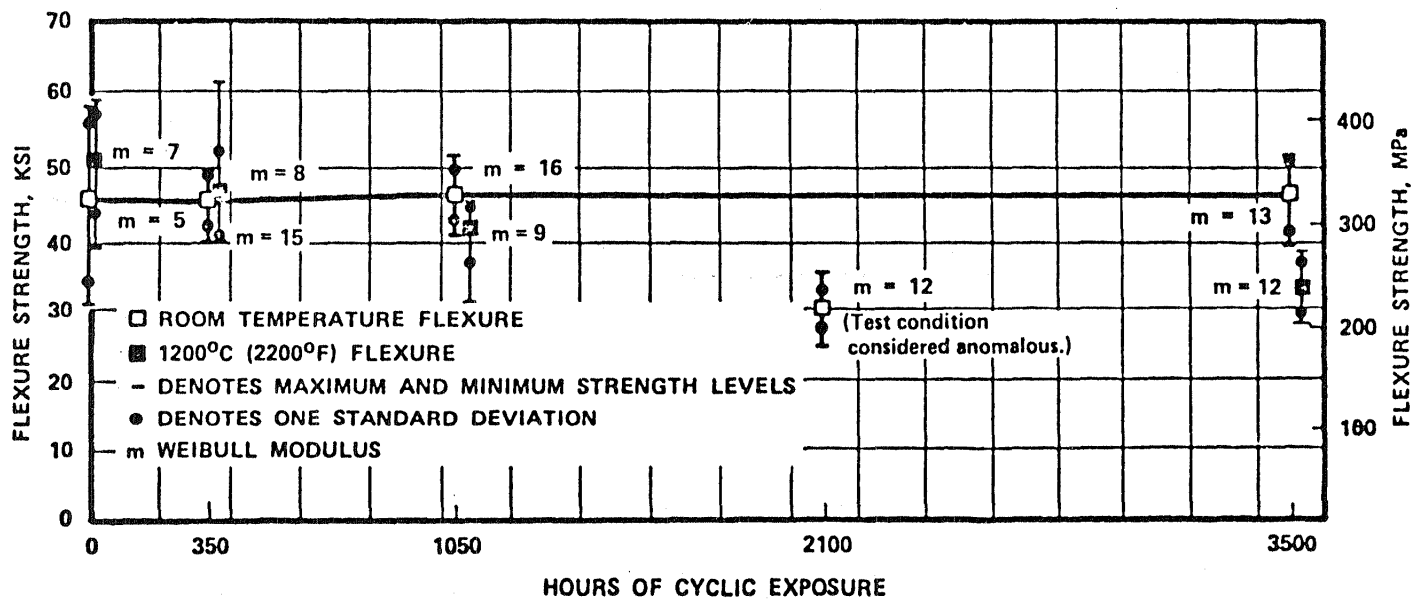
Both SiC and Si₃N₄ are thermodynamically unstable in oxidizing environments, but the rates of oxidation are generally controlled by the mobility of oxygen through the oxide layer. In cases of theoretically dense, chemically pure SiC's and Si₃N₄'s (such as those made by CVD processes) the rates of oxidation are remarkably slow, even at temperatures of 1550 to 1600°C, thus illustrating the excellent potential of pure SiO₂ as a barrier to oxygen diffusion. Spalling, cracking or chemical contamination of the SiO₂ layer will obviously increase the mobility of oxygen through the oxide layer and are therefore undesirable.

Static oxidation tests of sintered α -SiC conducted at General Electric Co. at 1500C for 2000 hours showed little degradation in strength (Fig. 3.9) and weight gain rate of 0.054 mg/cm²/hr^{1/2} thus suggesting a parabolic rate of oxidation. Parabolic kinetics are commonly observed when the rate of oxidation is controlled by the diffusion of oxygen through a coherent, non-spalling oxide layer.

The first few hours of oxidation appear to increase the average strength approximately 10 to 15 percent, possibly through a crack blunting



α-SiC Flexure Strength After Cyclic Exposure to 1200°C (2200°F)



α-SiC Flexure Strength After Cyclic Exposure to 1370°C (2500°F)

FIGURE 3.7 α-SiC FLEXURE STRENGTH AFTER CYCLIC EXPOSURE

3-18

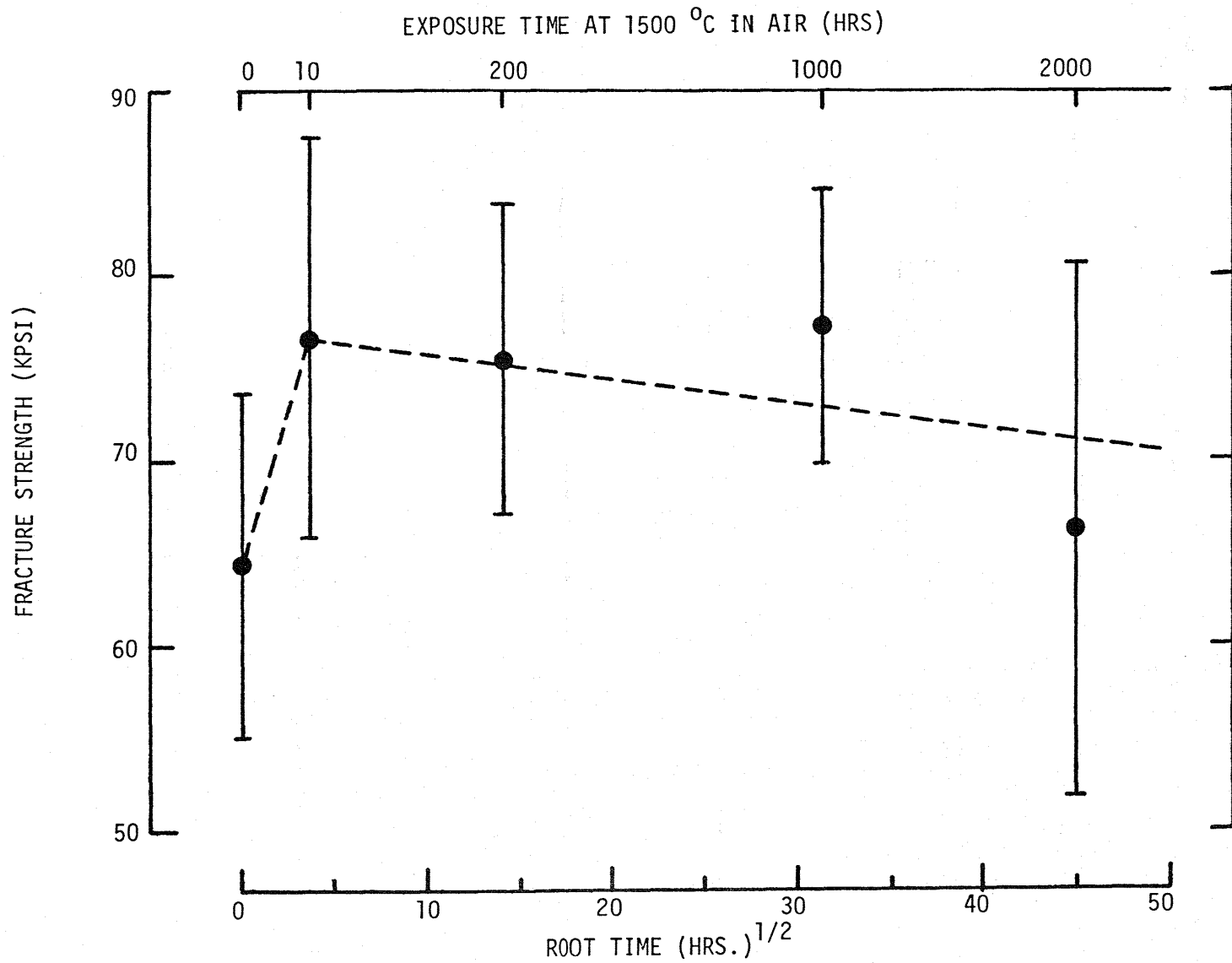


FIGURE 3.8 FRACTURE STRENGTH AS A FUNCTION OF THE SQUARE ROOT OF EXPOSURE TIME AT 1500°C IN AIR

mechanism. An accelerated mode of localized oxidation was found to cause surface pitting and an associated decrease in fracture strength after exposures approaching 2000 hours. Nevertheless, the average strength of specimens tested in bending was no lower after 2000 hours of exposure at 1500°C than the strength of as-machined specimens.

This result suggests that the sintered α -SiC may be suitable for the very high temperature, oxidizing environments found in the air preheater and in the combustor.

Resistance to Chemical Reaction with H₂

Clean, hot hydrogen is a powerful reducing agent and consideration must be given to possible degradation of the ceramic materials in the H₂ atmosphere of the Stirling engine. Evaluations of this potential problem, especially with mullite are being conducted at NASA Lewis Research Center. The temperature at which significant attack might occur and potential H₂ dopants which might mitigate the reducing effects will need to be investigated.

SECTION 4

EXTERNAL HEAT SYSTEM

4.1 PRELIMINARY CONSIDERATIONS

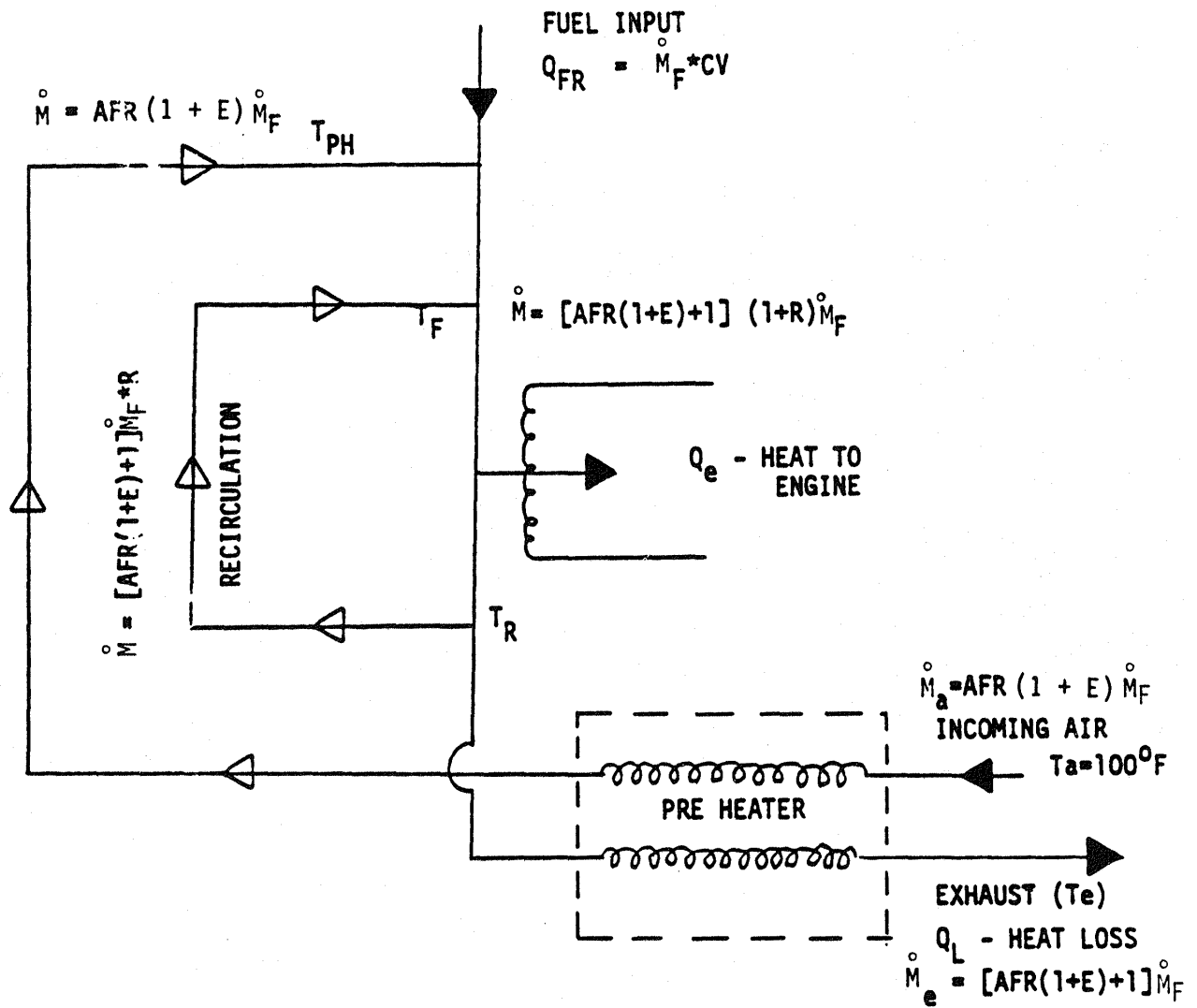
The application of ceramics to the Stirling engine allows consideration of higher operating temperatures.

The ultimate efficiency achievable in a thermodynamic system is the Carnot efficiency governed by hot side and cold side temperature. The cold side temperature is normally limited by the temperature of the available coolant, which in the case of automobile is the radiator coolant. The improvement in hot side temperature on the other hand requires raising the combustion flame temperature. To analyze the effect of higher flame temperature on the overall combustor performance a simple model of the combustor was developed. Although the model was specifically developed for automobile Stirling engine, it is equally useful in analyzing the effect of hot side temperature in any other thermodynamic system with similar combustor configuration.

The results presented here are for a fuel with the calorific value of 18500 BTU/lb requiring an air fuel ratio of 14.31 at stoichiometric conditions. This is typical of most common distillate fuels. Also an excess air level of 10% is utilized. A significant departure from any of these conditions for any other application may require re-evaluation of the optimum point.

4.2 ANALYTICAL REPRESENTATION OF THE EXTERNAL HEAT SYSTEM (EHS)

Figure 4.1 is a schematic depiction of the burner analyzed here. Part of the combustion gases are recirculated within the burner. In principle two types of recirculation can be obtained. One is known as non-adiabatic recirculation wherein the temperature of the recirculation gases may change as they move from their point of origin back upstream. The temperature drop is likely to be more appreciable in external mechanical recirculation system and/or in systems with external heat exchanger. Such a recirculation system is employed in the existing MOD 1 Stirling engine EHS. The second type of recirculation is the adiabatic circulation where the combustion gases are recirculated at the same temperature as they come out of the combustion chamber and without any external heat transfer. In the following analysis of the effect of recirculation on combustion flame temperature an idealized case is considered in which mixing of the gases is considered to be instantaneous, and the flame process is regarded as taking place in a homogeneous reactor flow system in which fully reacted combustion products are recirculated back to the flame front, which is assumed to be at or above ignition temperature. It is to be recognized that under the condition of 100% fuel burnt along the length of the combustion chamber, the flame temperature achieved at all levels of adiabatic recirculation is identical to that achieved at zero level of non-adiabatic recirculation and the results presented here may be interpreted accordingly.



- o COMBUSTION EFFICIENCY = 100%
(CONVERSION OF FUEL TO HEAT)
- o EXTERNAL HEATING SYSTEM EFFICIENCY = $\frac{Q_e}{Q_{FR}} = 1 - \frac{Q_L}{Q_{FR}}$

FIGURE 4.1 A SCHEMATIC REPRESENTATION OF EXTERNAL HEATING SYSTEM

AFR	-	Air fuel ratio
\dot{M}	-	Mass flow rate of fuel and air
\dot{M}_F	-	Mass flow rate of fuel
CV	-	Calorific value of fuel
Q_{FR}	-	Combustor firing rate
Q_e	-	Heat transfer to the engine
E	-	Excess air level
R	-	Recirculation level
T_F	-	Adiabatic flame temperature
T_{PH}	-	Temperature of preheat combustion air
T_R	-	Temperature of recirculated gases
T_e	-	Temperature of exhaust gases
ϵ_{PH}	-	Effectiveness of preheater
ϵ_{HH}	-	Effectiveness of heater head
T_t	-	Heater lead tube temperature
η_c	-	EHS efficiency
C	-	$\dot{M} * C_p$
C_p	-	Specific heat combustion gases

FIGURE 4.1A NOMENCLATURE

In addition to recirculation, a preheater is incorporated into the system. The adiabatic flame temperature is then given by

$$T_F \cdot C_{pT_F} \left\{ AFR (1+E) + 1 \right\} (1+R) = CV + \left\{ AFR (1+E) + 1 \right\} R C_{pT_R} \cdot T_R + AFR (HE) C_{pT_{PH}} \cdot T_{PH} \quad (1)$$

The specific heat of the combustion gases is assumed to be closely related to that of nitrogen and is calculated at the appropriate temperature as per the following equation:

$$C_p = \left\{ 9.47 - \frac{(3.47 \cdot 10^3)}{T} + \frac{(146 \cdot 10^6)}{T^2} \right\} 1/28 \text{ BTU}/16^\circ\text{F} \quad (2)$$

It is noted that because of the temperature dependence of the specific heat an iterative procedure is required. As intuitively expected the flame temperature is independent of firing rate. However, it is dependent on temperature of the recirculated gases and the temperature of the preheated combustion air; which in turn are dependent on the flame temperature. Thus again an iterative procedure is required to obtain a convergent solution.

The temperature of the recirculated gases is calculated from the following relationship:

$$T_R = T_F - Q_e / \left\{ (AFR (1+E) + 1) (1+R) \dot{M}_F \right\} \quad (3)$$

For an assumed effectiveness of the preheater the temperature of the preheated combustion air is calculated from:

$$T_{PH} = \epsilon_{PH} (T_R - 100) + 100 \quad (4)$$

The temperature of the exhaust gases is calculated from:

$$T_e = T_R - \frac{C_{min}}{C_{max}} (T_{PH} - 100) \quad (5)$$

where
$$\frac{C_{min}}{C_{max}} = \frac{AFR (1+E) \times 0.976}{(AFR (1+E) + 1)} \quad (6)$$

The ratio of specific heat of cold and hot fluid is taken as 0.976. It is observed that cold fluid (combustion air) is the fluid with minimum heat capacity.

For the required amount of heat input to the engine the heater head tube temperature which is assumed to be uniform may also be calculated as follows. Since the fluid inside the heater tube remains at almost constant temperature throughout the exchanger, its "specific heat", and thus capacity rate, is by definition equal to infinity and the ratio $C_{min}/C_{max} = 0$. Thus the effectiveness of the heater head heat exchanger is given as

$$\epsilon_{HH} = 1 - e^{-NTU} = \frac{T_F - T_R}{T_F - T_t} \quad (7)$$

Thus for an assumed number of transfer units the temperature of the heater head tubes may be calculated from

$$T_t = T_F - \frac{Q_e}{(R+1)(MC_p)} (1 - \bar{e}^{NTU})^{-1}$$

where \dot{M} is given as

$$\dot{M} = \frac{Q_e}{\eta_c} \frac{\{AFR(1+E)+1\}(1+R)}{CV}$$

It should be noted here that the calculation of the tube temperature is independent of the heat transfer mechanism. The effect of heat transfer mechanism only enters into picture through NTU which is defined as $U_{eff} A/C_{min}$. The EHS efficiency is based on the low heating value of the fuel and is calculated from the exhaust gas temperature. The EHS surface losses, if any, are ignored.

A computer program was developed to obtain the necessary iterative solution. The results of the program were verified by comparison with the published results of the similar kind of burner systems. A listing of the program is given in Appendix I for calculating the adiabatic flame temperature and the combustor performance.

4.3 RESULTS OF THE EHS MODEL

Fig. 4.2 depicts the adiabatic flame temperature as a function of recirculation level for various temperatures of the recirculated gases and the preheated combustion air. The trend shown is that for non-adiabatic or "external" circulation, except that at zero recirculation level the result is identical with adiabatic case. It is observed that as recirculation level is increased, the flame temperature is decreased since the combustion gases at temperature less than the flame temperature are introduced at upstream location. As expected, the flame temperature increases with increase in both the recirculation gas temperature and the preheat air temperature.

In Fig. 4.3 the adiabatic flame temperature is plotted as a function of EHS efficiency for three different values of recirculation levels and preheater effectiveness. It is of interest to note here that the adiabatic flame temperature diminishes as the EHS efficiency is increased. This result is the direct outcome of the fact that for a fixed preheater effectiveness as the exhaust gas temperature diminishes, both the preheat air temperature and the temperature of the recirculated gases is decreased. The temperatures of the recirculation gases and the preheated air are independent of the recirculation level, but increase with preheater effectiveness as seen from Figs. 4.3 and 4.4. It is desirable to maintain the temperature of the recirculated gases which is also the temperature of the gases after they have transferred heat to the heater head, sufficiently high (close to the tube temperature) so that high overall heater head temperature can be maintained.

Fig. 4.5 represents the heater head tube temperature as a function of EHS efficiency. The curves are drawn at a fixed NTU of 4. Thus it gives the maximum achievable tube temperature since any further increase in NTU does not improve the heat transfer effectiveness. An important result is that the tube temperature decreases with increase in EHS efficiency.

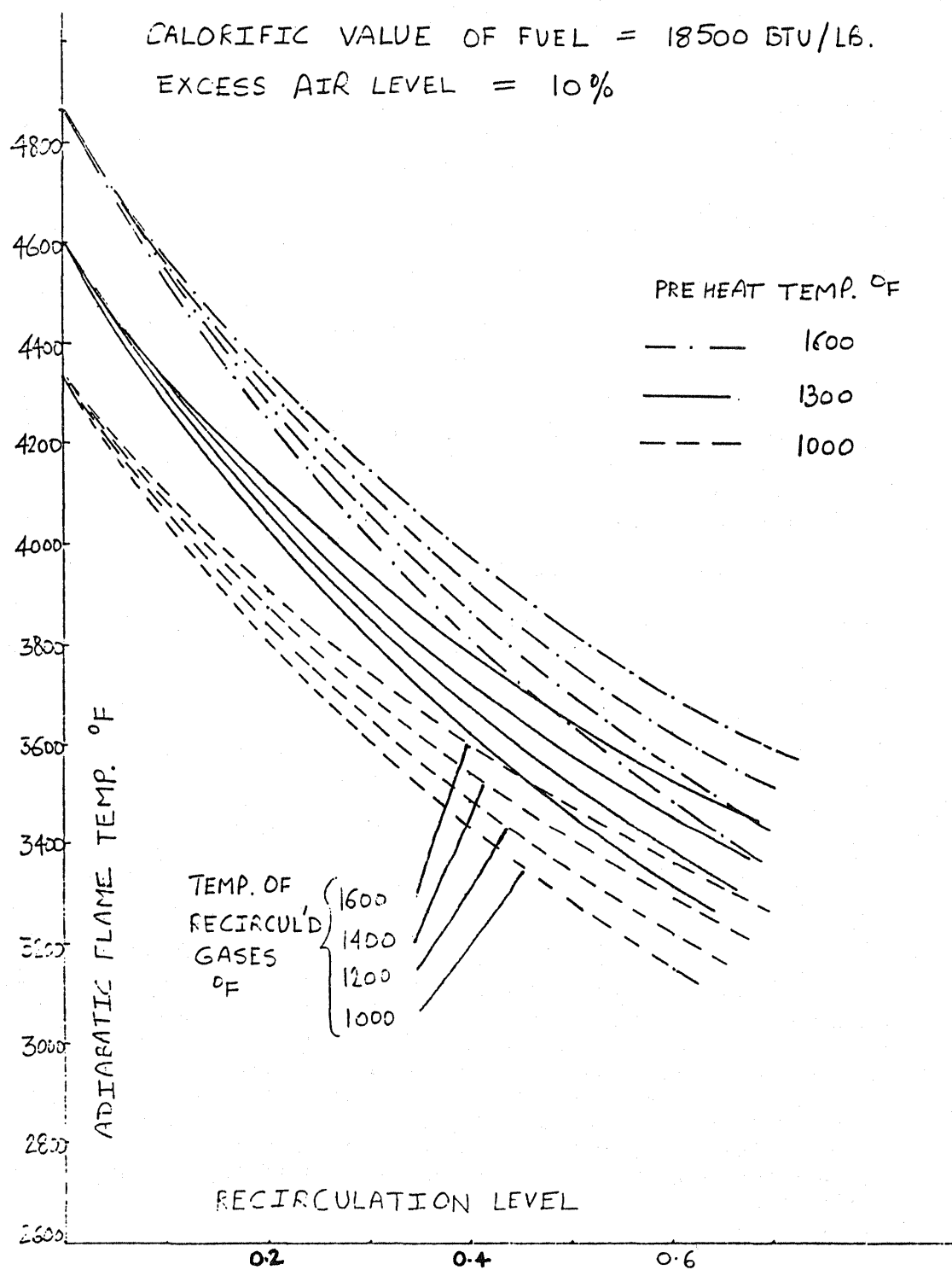


FIGURE 4.2 ADIABATIC FLAME TEMPERATURE CALCULATION

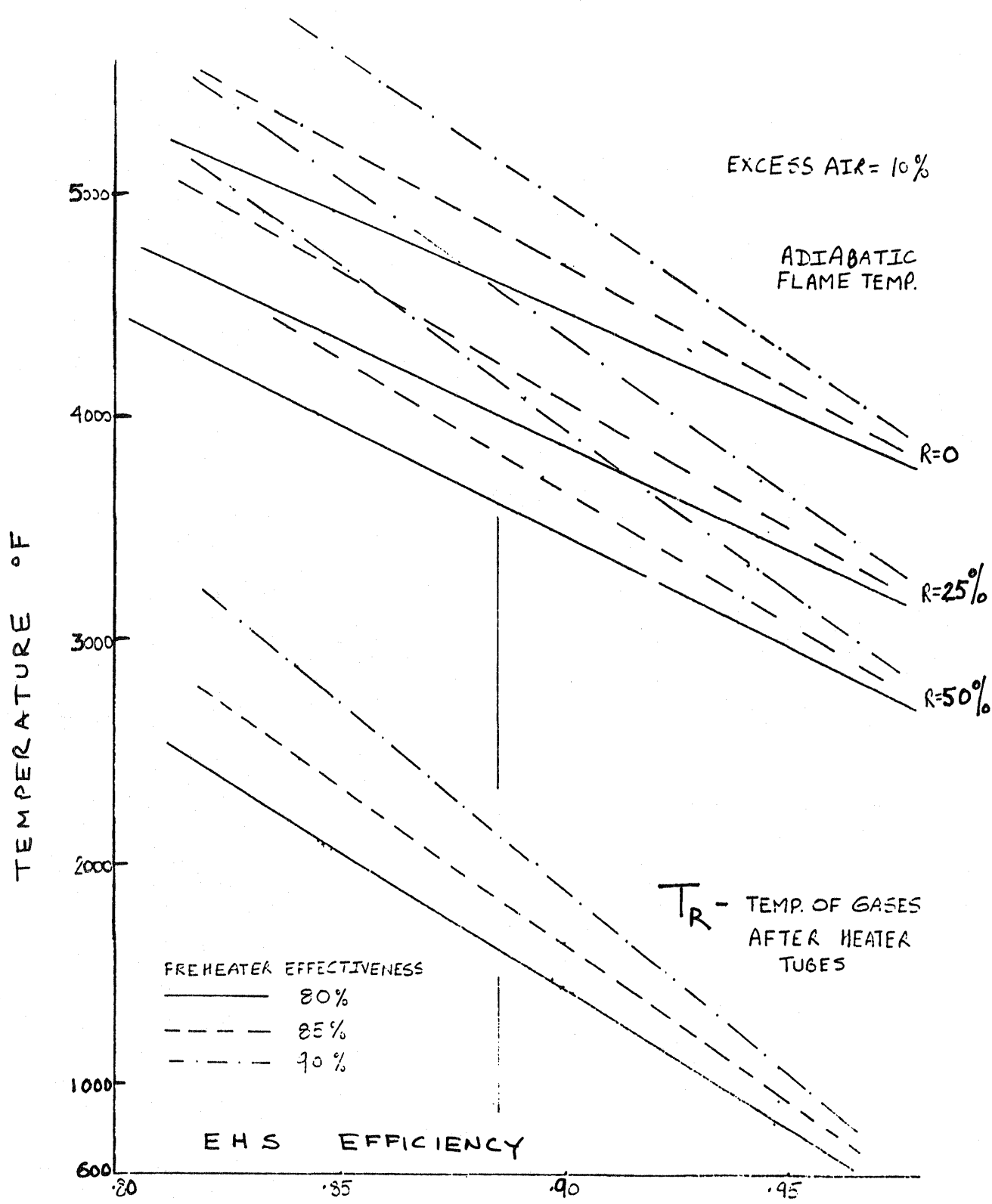


FIGURE 4.3 ADIABATIC FLAME TEMPERATURE AS A FUNCTION OF EHS EFFICIENCY

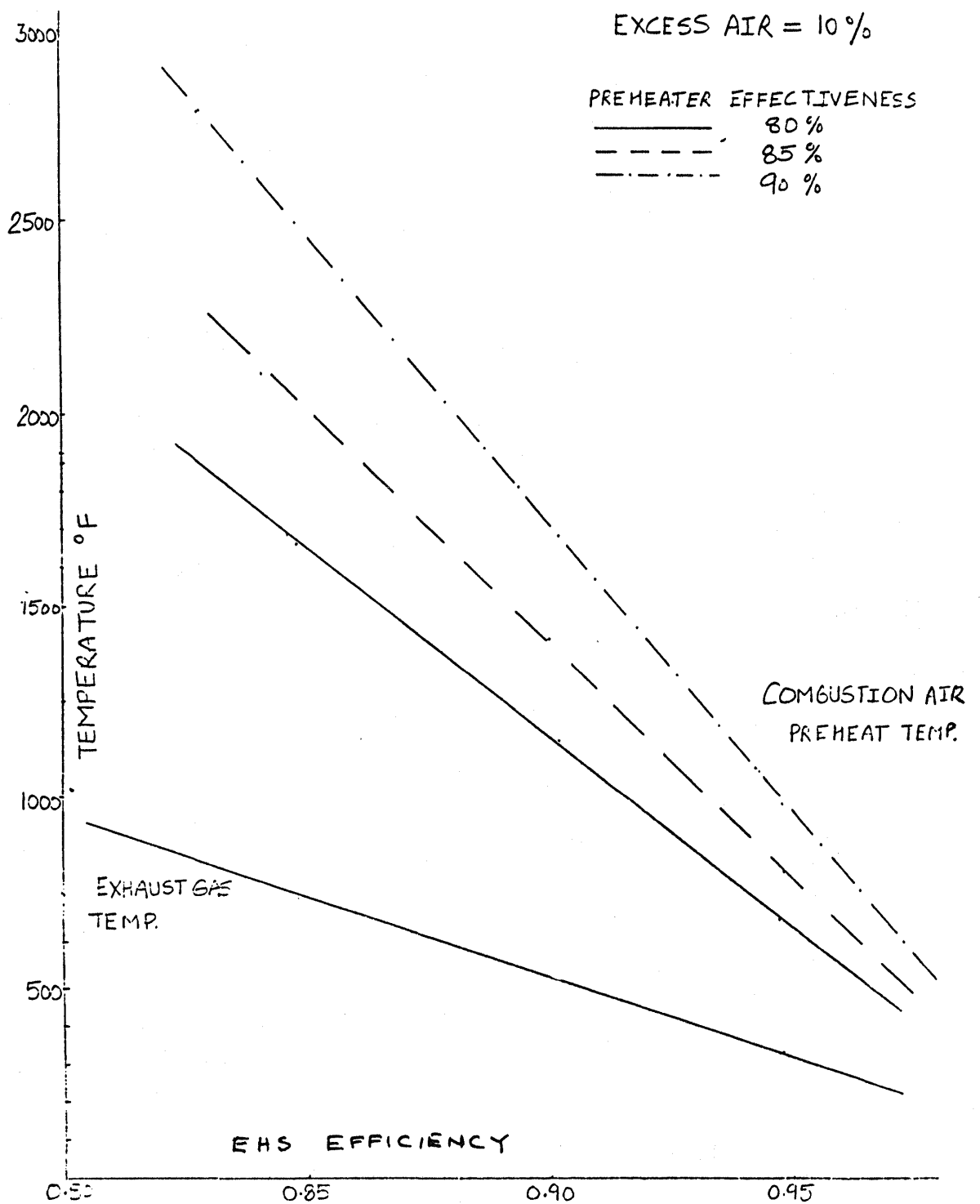


FIGURE 4.4 PREHEAT AND EXHAUST GAS TEMPERATURE AS A FUNCTION OF EHS EFFICIENCY

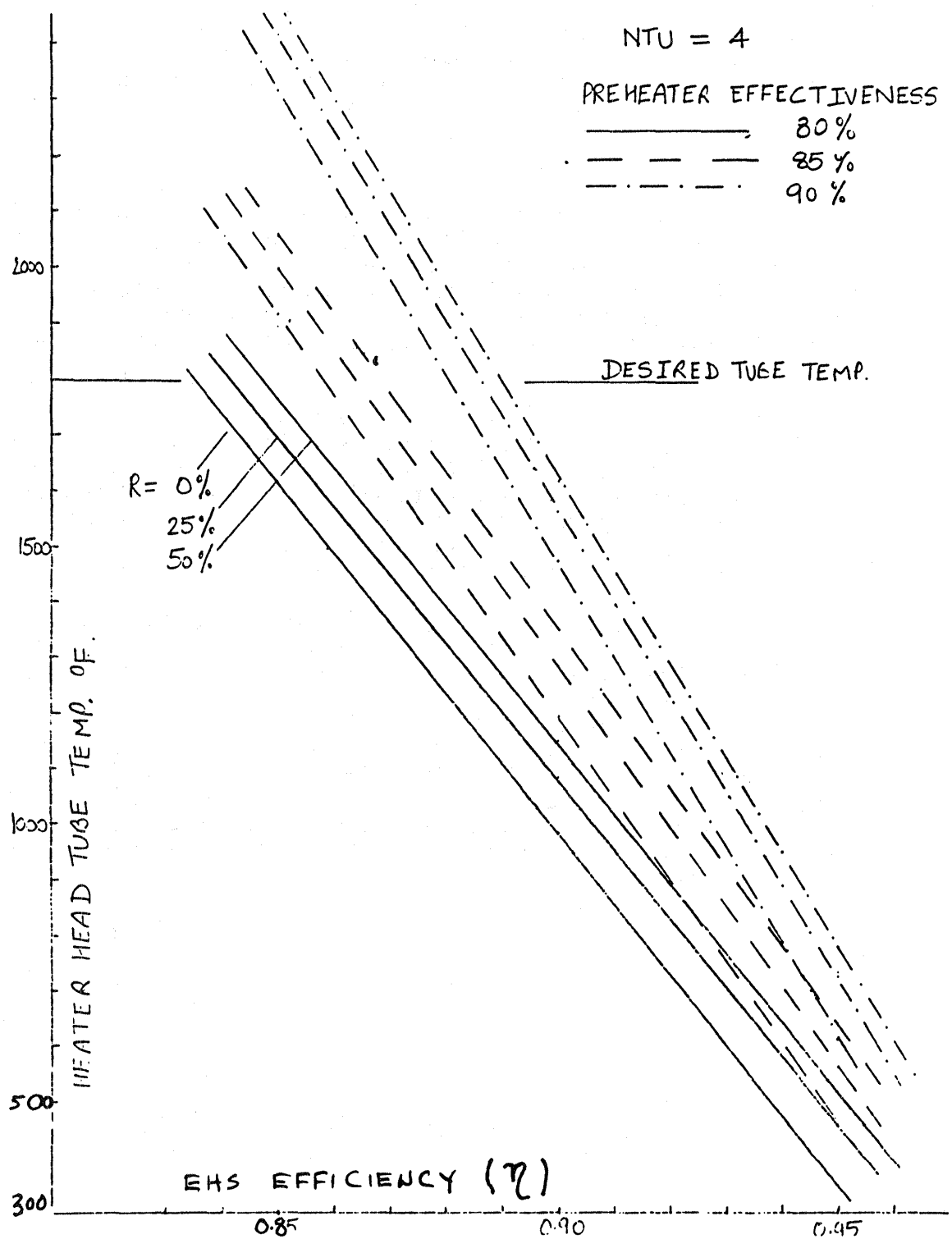


FIGURE 4.5 HEATER HEAD TUBE TEMPERATURE AS A FUNCTION OF EHS η

Thus for a recirculation level of 50% and the preheater effectiveness of 90%, and for the desirable heater head temperature of 1800°F, the maximum achievable EHS efficiency is 89%. Another important result is that the heater head temperature can be raised by increasing the mass flow rate (increased non-adiabatic recirculation), despite the fact that it incurs lower flame temperature.

Thus, one can achieve higher heater head tube temperature, albeit at the expense of reduced EHS efficiency by maintaining the recirculation level and increasing the preheater effectiveness. If further increase in EHS efficiency is required, one can in theory increase the preheater effectiveness even higher. However, after a certain limit the size of the preheater becomes questionable for a given application.

The best design point for CASE thus appears to be at 89% EHS efficiency with 1800°F heater head tube temperature. This point requires 90% preheater effectiveness and 50% recirculation. At this point the adiabatic flame temperature will be 4100°F and preheat temperature of 1875°F. Although higher flame temperature is required for higher heater head tube temperature, it is not as high as that would be required if the recirculation across the heater head tubes were to be decreased.

Fig. 4.6 shows the effect of NTU on the heater head tube temperature for EHS efficiency of 89% and 92%. The typical ASRE design point is at 1400-1500°F tube temperature and about 90.5% EHS efficiency. The NTU for ASRE design lies between 2 and 2.5. In order to raise the heater head tube temperature for CASE design, it thus appears that one need only raise the NTU to between 3 and 3.5. However, a small penalty of about 1-2 points in EHS efficiency will be incurred. The effect of this reduced EHS efficiency with gain in Carnot efficiency in going to higher heater head temperature needs to be evaluated. If EHS efficiency must be maintained at 89% or above then NTU must be raised to about 4.

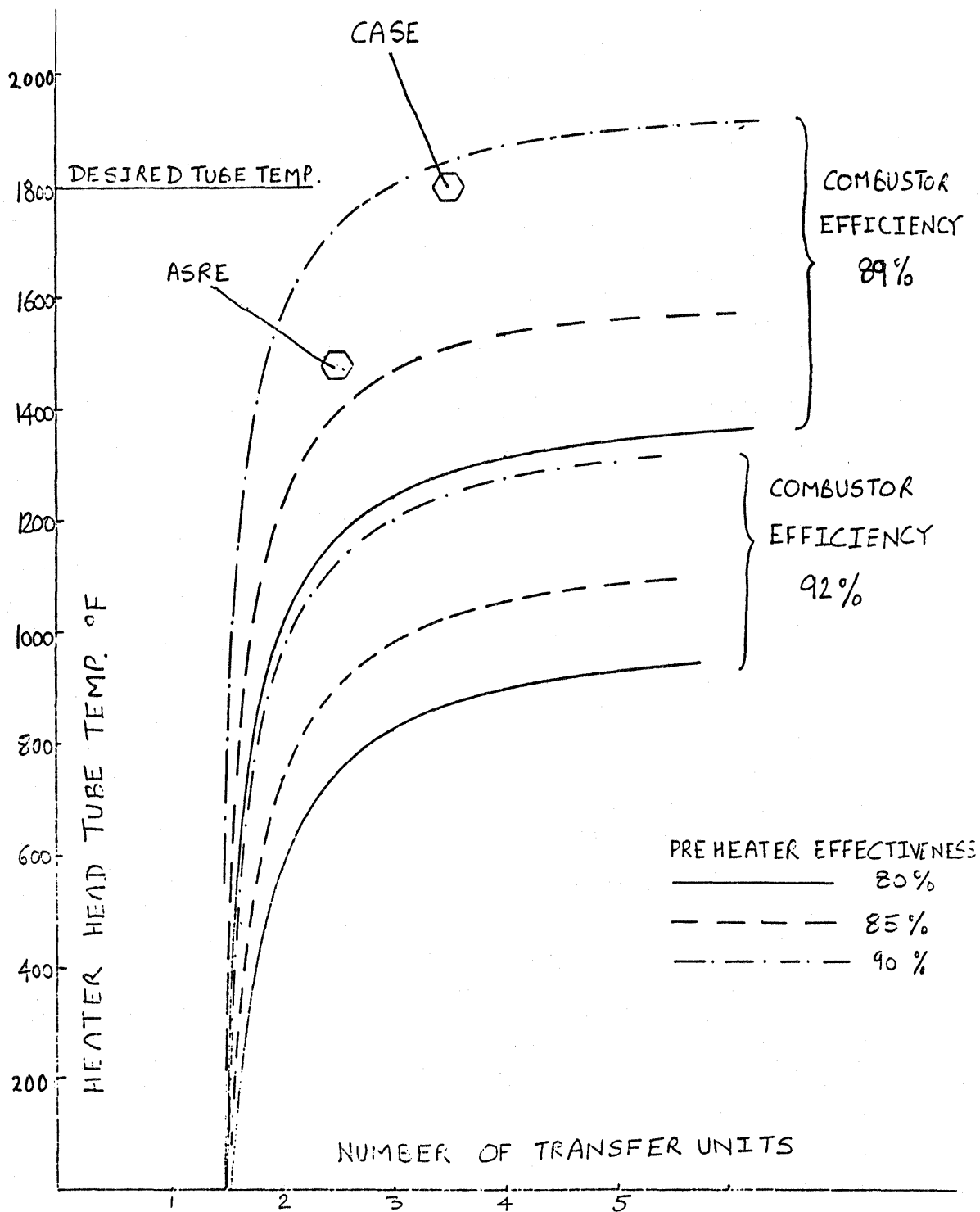


FIGURE 4.6 HEATER HEAD TUBE TEMPERATURE AS A FUNCTION OF NTU

4.4 SUMMARY AND CONCLUSIONS

A computer program was developed to analyze the effect of increased heater head tube temperature on External Heat System (EHS) performance in the case of ceramic Stirling engine. The results, however, are quite general and would apply to any other thermodynamic system where high hot side temperature is essential in maintaining high Carnot efficiency. Flame temperature, recirculation gas temperature, preheat combustion air temperature, exhaust gas temperature heater head tube temperature are obtained as a function of EHS efficiency, preheater efficiency, recirculation level and number of heat transfer units. Some of the more important results and those that are of immediate concern to CASE design are summarized here.

- o The level and type of combustion gas recirculation inside the EHS plays an important role in obtaining high heater head temperature while maintaining the overall effectiveness at a reasonable value.
- o High level of recirculation across the heat exchanger (non-adiabatic recirculation) is essential for maintaining uniformly high heater head tube temperature, even though increased non-adiabatic recirculation implies lower flame temperature.
- o In general, a penalty must be paid in lower EHS efficiency if the heater head tube temperature must be raised without being impractical on heat exchanger design. If it is essential that EHS efficiency must be maintained high one might consider a condensing heat exchanger.

The following comments pertain specifically to CASE design.

- o It appears that in order to raise the heater head tube temperature from 1500°F for ASRE design to 1800°F for CASE design, the EHS efficiency must be reduced by 2 points; from 91% to 89%. The gain in Carnot efficiency due to increased heater head tube temperature must be weighed against reduction in EHS efficiency. If additional engine losses due to increased hot side temperature are incorporated, the gain in overall system efficiency due to high temperature operation may be completely nullified.
- o In order to achieve aforementioned design point the preheater effectiveness must be raised to 90% (compared to ~88% for ASRE) while maintaining the same recirculation level (50%).
- o An outcome of above is that flame temperature in the case of CASE will be higher (4100°F) compared to that for ASRE (3600°F). The required flame temperature would however be much higher if the recirculation level across the heater tubes were to be reduced.

SECTION 5

HOT SIDE

5.1 GENERAL

The engine hot section comprises all ceramic components, except the outer EHS housing and engine retainer rings and bolts. The gas cooler and regenerator are annular in cross-section.

The concept has the following key features:

1. Four separate cylinders having symmetric heater head/regenerator/cooler assembly provide good structural integrity and producibility of the ceramic components and ensure uniform heat distribution.
2. Combination of jet impingement and radiation heat transfer offers high heat flux density at the heater head, thereby allowing the use of a structurally sound ceramic heater at moderate lengths and curvatures.
3. The overall engine envelope remains similar to ASRE.

The basic EHS design concept is similar to the ASRE design but utilizes ceramics. The air-preheater can be constructed with staggered, finned heat exchanger plates which are extruded from Si_3N_4 or SiC material as illustrated in Figure 1.3. As shown in Figure 1.4, the engine cylinder, including the annular regenerator housing, is made of mullite ($3\text{Al}_2\text{O}_3 \cdot 2\text{SiO}_2$) and has internal flow passages in its dome for connection with the external heater tubes. Twenty-four spiral heater tubes evenly surround the engine cylinder at 135° offset and connect the cylinder head and the regenerator housing. A cylindrical bell-shaped mantle covers the engine cylinder pressure vessel including the spiral heater tubes.

The combustion gases, after heating the mantle dome which radiates heat to the cylinder head, are directed to the perforated portion of the mantle and create jet streams impinging against the heater tubes. The perforated mantle transfers heat to the heater tubes by radiation. The combination of radiative and jet impingement convective heat transfer not only results in very effective heat transfer, but also ensures a uniform heater tube temperature distribution. The enhanced heat transfer also allows the use of a shorter heater tube, and thus reduces the engine void volume for greater efficiency.

To reduce the stress level in the ceramic cylinder structure during initial heat up, porous ceramic insulation is placed at the O.D. of the engine cylinder. This insulation reduces the outer surface temperature of the structural ceramic cylinder so that the radial thermal gradient in the ceramic wall is minimized as are the stresses due to such a thermal gradient.

A single EHS unit supplies heat to all four engine cylinders which are symmetrically located around a central point. The heat is transferred to the engine cylinder first at the dome. The hot combustion gases, after transferring some of the heat at the dome, pass through an annular passage surrounding the engine cylinder and transfer the heat, mostly by convection, to a perforated mantle which in turn radiates heat to the engine fin-tube assembly. The combustion gases which may still be sufficiently hot, especially at full load condition, transfer the remaining heat by impinging on the fin-tube assembly. Thus, the heater tubes and the cylinder are maintained at a uniform temperature by properly distributing the heat around the engine cylinder. The advantage of being able to transfer heat at the dome lies in the fact that at maximum load conditions, one need not provide as much heat transfer surface area at the tubes (reduced void volume) and that there is some merit in being able to transfer heat closest to the expansion space. Moreover, during start-up condition, the temperature difference between the tube assembly and the engine cylinder is reduced, thereby relieving the thermal stresses generated at the interconnections.

The CASE heater head heat exchanger consists of a single row of twenty-four closely spaced spiral tubes in a swirling cross flow. The amount of heat that is not transferred by radiation at the dome and at the fin-tube assembly must be transferred by convection at the fin-tube assembly, and this amount of heat determines the heat transfer area required at the tubes.

5.2 THERMAL PERFORMANCE ANALYSIS OF PROPOSED CERAMIC STIRLING ENGINE

5.2.1 INTRODUCTION

In principle, the indicated efficiency of the Stirling engine can be raised by raising the hot side temperature due to increase in carnot efficiency. This rise in indicated efficiency is however limited by the corresponding rise in thermal losses which occur due to greater ΔT between hot and cold side. Ceramic engine offers the possibility of minimizing these thermal losses due to the lower thermal conductivity of ceramics. With improved engine design, especially that of the heater head, one can in addition lower the void volume and the internal gas pumping losses. With this understanding a preliminary estimation of the indicated efficiency that can be achieved in the proposed design ($\sim 60\%$), was made. Based on this estimation the corresponding requirements for the firing rate, air and fuel mass flow rates, etc., were determined for three design points; namely part load condition, maximum efficiency condition and full load condition as shown in Table 5.1. The heater head thermal analysis presented in the next section is based on these estimations.

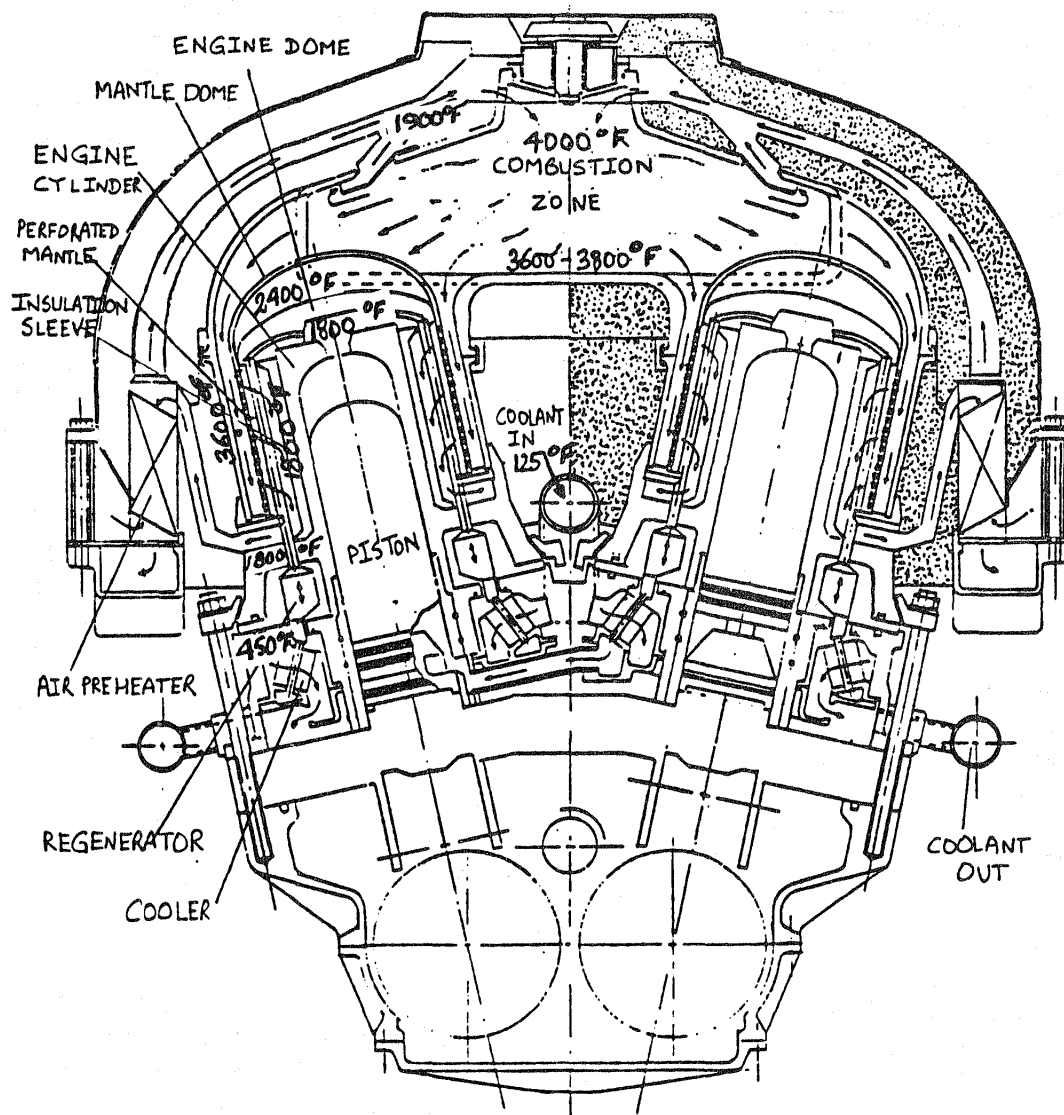
5.2.2 HEATER HEAD THERMAL ANALYSIS

Fig. 5.1 shows the schematic representation of the proposed engine design. A single EHS unit supplies heat to all the four engine cylinders which are symmetrically located around a central point. The adiabatic flame temperature was determined previously (Section 3.1) to be about 4100°F . For the purpose of analysis it is assumed that surface losses from around the EHS are negligible. The heat is transferred to the engine cylinder first at the dome. The hot combustion gases after transferring some of the heat at the dome pass through an annular passage surrounding the engine cylinder and transfer the heat mostly by convection to a perforated mantle which in turn radiates heat to the engine fin-tube assembly. The combustion gases which may still be sufficiently hot, especially at full load condition, transfer the remaining heat by impinging on the fin tube assembly. Thus, the temperature of the heater tubes and the cylinder is maintained at a uniform temperature by properly distributing the heat around the engine cylinder. The exact shape and size of the combustion gas flow passages can be optimized after some experiments to achieve uniform temperature around the mantle cylinder and the dome.

TABLE 5.1 HEATER HEAD THERMAL ANALYSIS

CASE Thermal Design Parameters

	<u>Part Load</u>	<u>Max. Eff.</u>	<u>Full Load</u>
Indicated Power (KW)	7.9	24.8	73.3
Indicated Efficiency (%)	54.7	60.0	52.2
Heat Input to Engine (KBtu/Hr)	49.3	141.0	478.4
Firing Rate (KBtu/Hr) (Combustor Eff. 89%)	55.4	158.5	537.5
Fuel Flow Rate (lb/Hr)	3.0	8.6	29.1
Air Flow Rate (lb/Hr) (with 10% ea)	47.1	134.8	458.1
Available Heat Capacity (Btu/Hr ^{OF})	14.53	41.6	141.3
Average Heater Head Tube Temp. (^{OF})	1800	1800	1800



TEMPERATURE DISTRIBUTION

FIGURE 5.1 CONCEPTUAL DESIGN LAYOUT FOR CERAMIC AUTOMOTIVE STIRLING ENGINE

5.2.3 HEAT TRANSFER AT THE DOME

Most of the heat from the flame zone to the mantle dome is transferred by radiation. The emissivity of the flame for a typical kerosene flame for an equivalent mean beam length is about 0.1 and that of ceramics about 0.9. This heat is subsequently transferred from the mantle dome to the engine cylinder head, again mostly by radiation. The results of the heat balance on the mantle dome are presented in the lower part of Fig. 5.2. It is seen that when the cylinder head temperature is about 1800°F and the flame temperature about 4000°F, the mantle dome temperature will be 2400°F and approximately 14000 BTU/hr will be transferred to each cylinder.

The top portion of the same figure shows the temperature of the combustion gases after it has transferred the aforementioned amount of heat to the dome and as it enters the annular channel. At 50% recirculation level and at maximum efficiency point the temperature of the gases is about 3200°F. On the other hand, at part load condition, all of the heat required by the engine will be transferred at the dome and the temperature of the combustion gases will drop down to the same level as the effective heater head tube temperature, and no further transfer will take place. It should be recognized that in reality the heat transfer process is self regulating. For example, if the heat transfer at the dome is higher than what the engine can absorb (due to low speed and charge pressure at part load condition), the temperature of the heater head will rise - which will reduce the heat transfer to the level that can be absorbed by the engine and since the enthalpy relationship indicates that after the required amount of heat has been transferred, the temperature of the gases do not drop below the tube temperature (1800°F) no reverse heat transfer is likely. The advantage of being able to transfer heat at the dome lies in the fact that at maximum load condition one need not provide as much heat transfer surface area at the tubes (reduced void volume) and that there is some merit in being able to transfer heat closest to the expansion space.

5.2.4 HEAT TRANSFER AT THE HEATER HEAD TUBES

Johnson et.al. [1] have presented the results of jet impingement heat transfer system for GPU-3 Stirling engine. It shows an overall increase of 65-70% in the effective heat transfer coefficient. Combustion gas inside a silicon carbide jet shell is forced through holes in the shell, impinging on the heater tubes. The directed jets break up the boundary layer on the surface of the tubes and thereby improve the heat transfer. Part of the improvement evidently comes from the presence of shell itself which enhances the radiative heat transfer. Since the results are presented only on the overall basis, it is not clear what portion of the total heat transfer is due to radiative effect. In addition, an excess air level of the order of 80% was used; any variation in this level would also affect the relative contribution of radiative and convective heat transfer. Nevertheless, the results seem to agree with the results obtained by separating the effects of radiative and convective heat transfer.

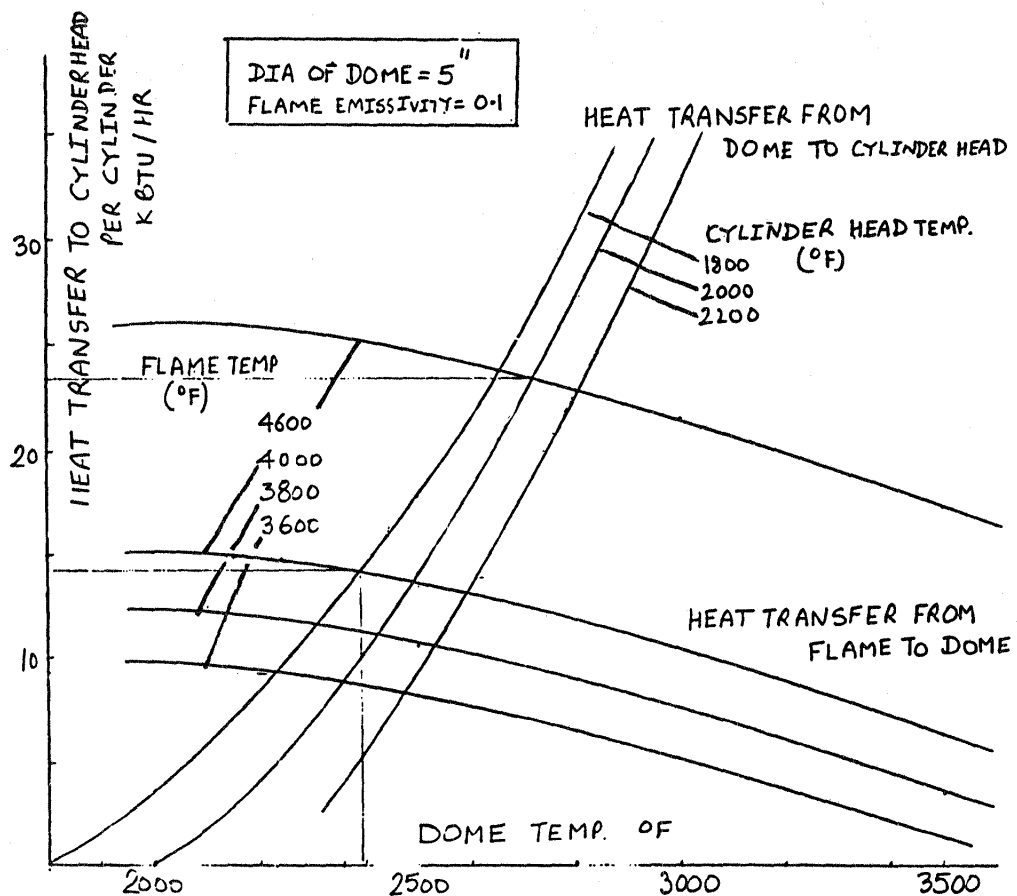
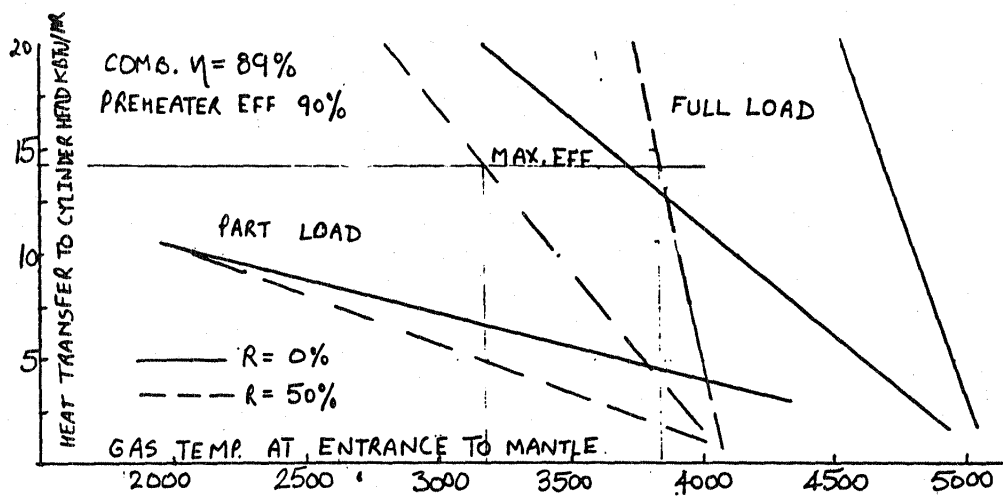


FIGURE 5.2 HEAT BALANCE AT MANTLE DOME

The CASE heater head heat exchanger consists of a single row of twenty-four closely spaced spiral tubes in a swirling cross flow. In general, data is available in the literature for banks of straight tubes containing several rows that are perpendicular to the direction of flow. For single rows of tubes, only a limited amount of data is available. Bankston and Back [2] have correlated the data for a system consisting of a swirl combustor with a cross flow heat exchanger composed of a single row of 48 closely spaced curved tubes used in DSSR engine. The data is correlated in terms of tube diameter and spacing and shows a significantly enhanced heat transfer characteristic for a single row of closely spaced curved tubes in a swirling cross flow of high temperature combustion gases.

The results of aforementioned analyses are utilized for analyzing the proposed design. In the annular part, the combustion gases first transfer heat to the porous mantle which in turn radiates heat to the fin tube assembly. The remaining heat is transferred directly by combustion gases to the fin tube assembly by convection. The heat transfer to the mantle is augmented by the presence of holes. The holes act to create a suction boundary layer. It has been shown by Hartnett and Eckert [3] that depending on the suction parameter the heat transfer to a plate with suction boundary layer can be enhanced several folds over that without suction. Similar results are obtained by Nealy and Reider [4] and Grootenhuys et.al. [5], although the application in these cases was the cooling of the wall. The results indicate availability of flexibility in design approach for the mantle, in order to achieve proper heat transfer and pressure drop characteristics.

The results of the heat balance on the mantle are shown in the lower half of the Figure 5.3 for recirculation level of 50%. For the heater head tube temperature of 1800°F approximately 14000 BTU/hr will be transferred by radiation from the mantle to each cylinder at maximum efficiency condition. The average mantle temperature under this condition will be about 2150°F. This temperature will rise to about 2450°F at maximum load condition and the corresponding heat transfer to each cylinder will be 35000 BTU/hr. The temperature of the gases as they exit from the mantle is given in the top part of the same figure. As can be seen, whereas not much heat is left in the combustion gases at maximum efficiency point, significant amount of heat yet remains to be transferred at maximum load condition.

This remaining amount of heat is transferred by convection to the tubes and determines the amount of area required for the tubes. In Figure 5.4 the available heat transfer coefficient is plotted as a function of Reynolds number. The rise in heat transfer coefficient from maximum efficiency point to maximum load point falls short to cover the additional heat transfer requirement at maximum load condition. And this deficiency is overcome by providing spiral fins on the tubes. Thus, as shown in Figure 5.5, while most of the heat under part load condition will be transferred by radiation at the dome, a large amount of heat must be transferred by convection to tubes at maximum load condition.

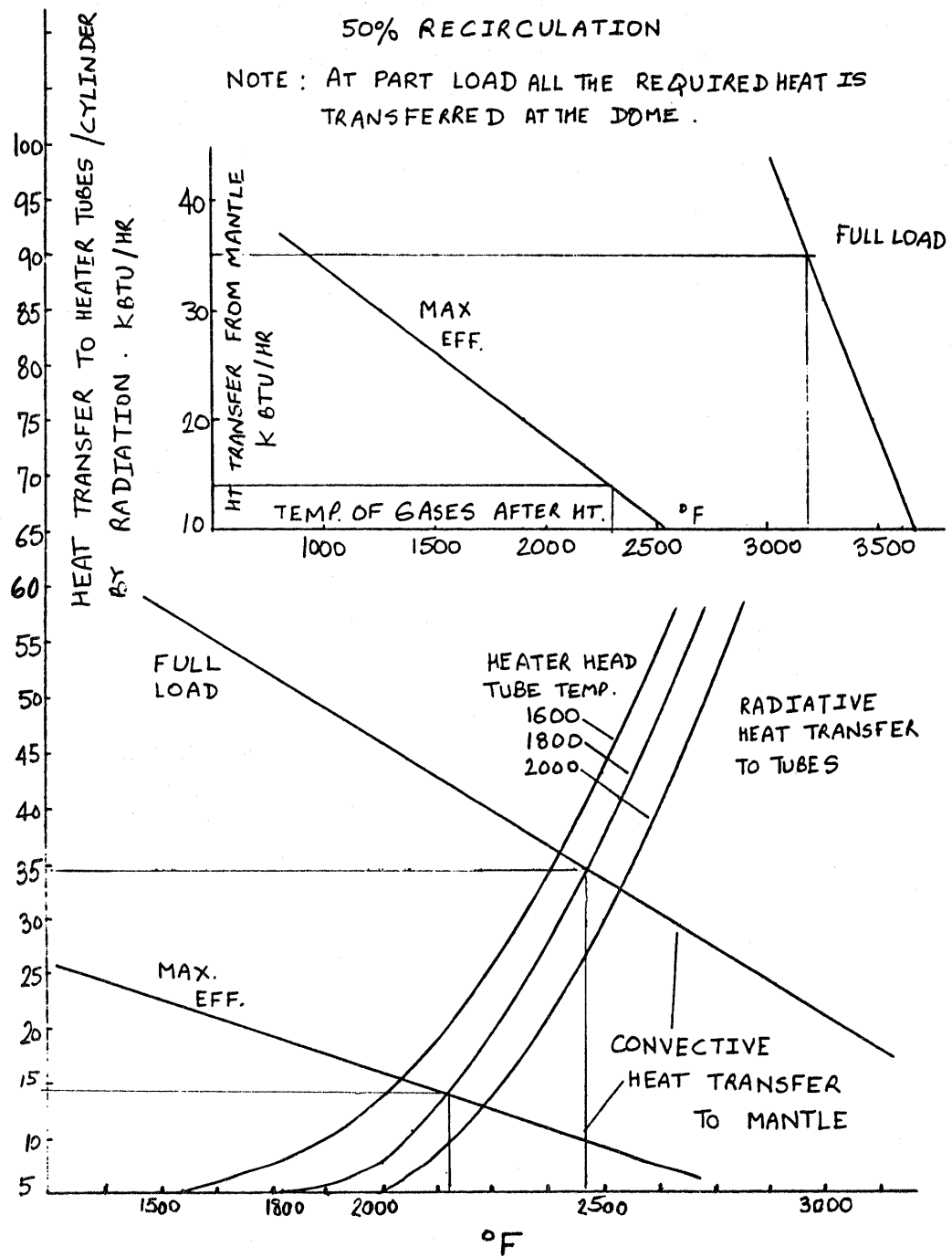


FIGURE 5.3 HEAT BALANCE ON MANTLE

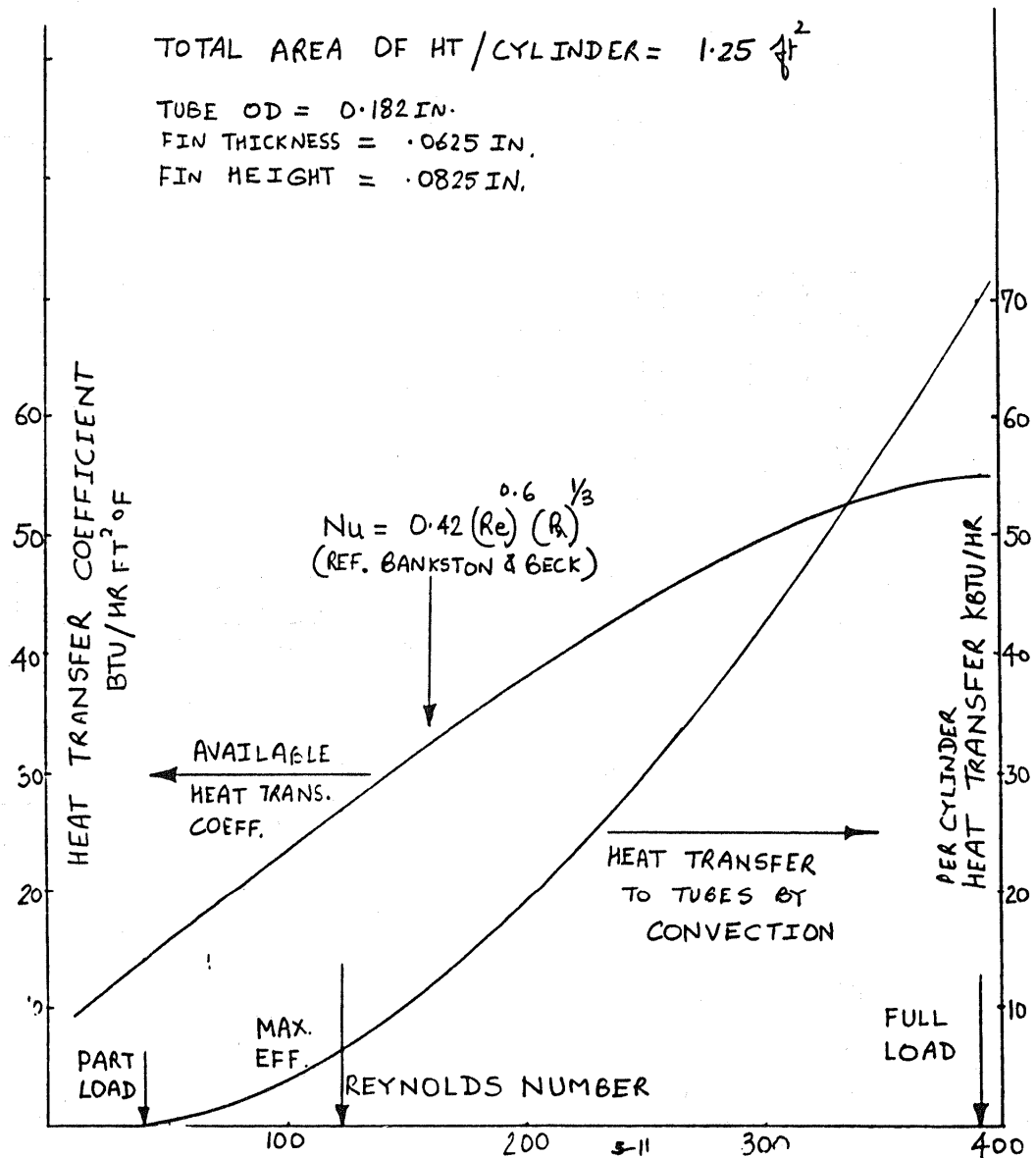


FIGURE 5.4 CONVECTIVE HT TO TUBE BANK AT
AVERAGE HEATER HEAD TEMPERATURE OF 1800°F

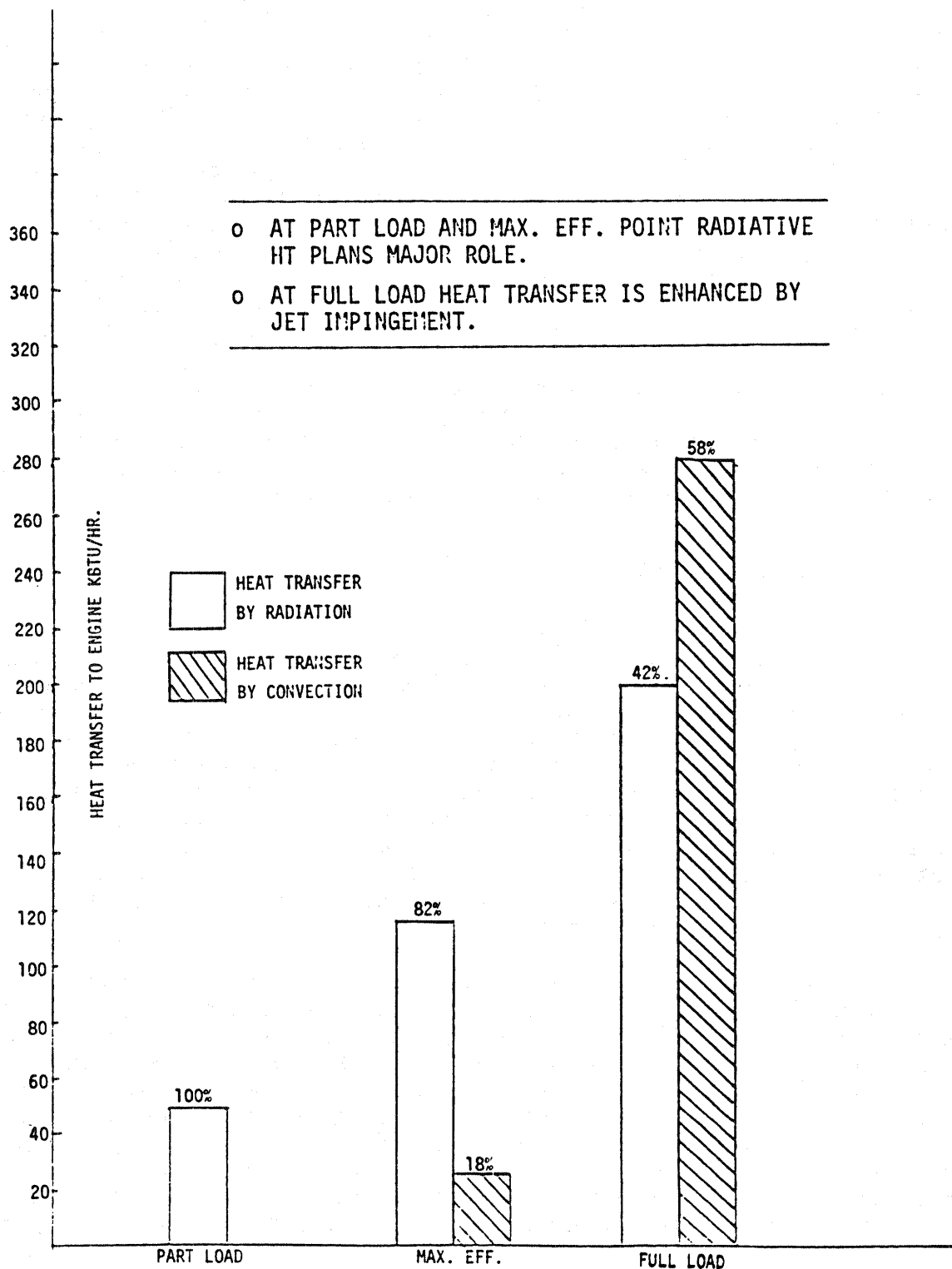


FIGURE 5.5 RADIATIVE VS. CONVECTIVE CONTRIBUTION

5.3 PERFORMANCE ANALYSIS

5.3.1 CASE DESIGN FEATURES AND THERMODYNAMIC ANALYSIS

The CASE design is a double acting Siemens (or Rinia) arrangement. In this arrangement the piston (reciprocating element) in each cylinder serves two functions. It acts as a "displacer" shuttling the working gas (hydrogen) through the regenerator and the associated heat exchangers between the hot expansion space of one cylinder (above the reciprocating element) and the cold compression space (below the reciprocating element) of the adjacent cylinder. It also acts as a power piston, compressing and expanding the working gas in the cylinder and transmitting power to the engine drive shaft. The cylinders in the CASE design are arranged in a vee allowing a favorable cold side connecting duct arrangement. However, the basic arrangement of ASRE design, namely two crank shafts with two pistons coupled to each crankshaft, is maintained. Twin gears are used to couple the crankshaft. This arrangement allows maintenance of overall compactness.

For the engine to operate properly, motion of the pistons must be synchronized. In this arrangement pistons in adjacent cylinders are 90° out of phase. As described in Figure 5.5A in order to obtain positive work output for any one cycle, expansion space volume variation must lead compression space volume variation, thus requiring proper relationship between crankshaft rotation and the relative lead of the power piston.

5.3.2 THERMODYNAMIC ANALYSIS

In order to analyze the performance of the CASE design, an updated version of Martini's second order code [6] was utilized. The second order code consists of relatively simple computational procedures that are particularly useful in optimizing the design of a Stirling engine from inception. This code has been updated to include correction factors for adiabatic effects. The code first computes the basic power output and heat input, which are then modified by the various identifiable energy loss terms. The fluid friction losses and mechanical friction losses are subtracted from the basic power output to obtain net power output. Similarly, reheat loss, shuttle conduction, gas and solid conduction, pumping loss, temperature swing loss, etc. are added to the basic heat input requirements to obtain the net heat input to the engine which includes a credit for frictional heating at the hot end.

In order to gain confidence in the ability of the code to predict the performance of the proposed CASE design, it was first checked out against the known performance of ASRE at four points of maximum load condition, maximum efficiency condition, part load condition and low load condition. The performance of ASRE design at four chosen points is given in Table 5.2. Most of the information required for input to the program was available; where not available, an estimation was made based on published data for similar engines. The list of this input data is given in Table 5.3 and the results of the match are given in Table 4. The results of the comparison between ASRE design and Martini prediction indicates that the predictions are within 5% in all the cases except for very low load condition. Some deviation is to be expected at very low load condition since the results were obtained without changing the input data except the engine charge pressure and speed. The results appear to be in excellent agreement for the Martini code to be able to predict the performance of the proposed design.

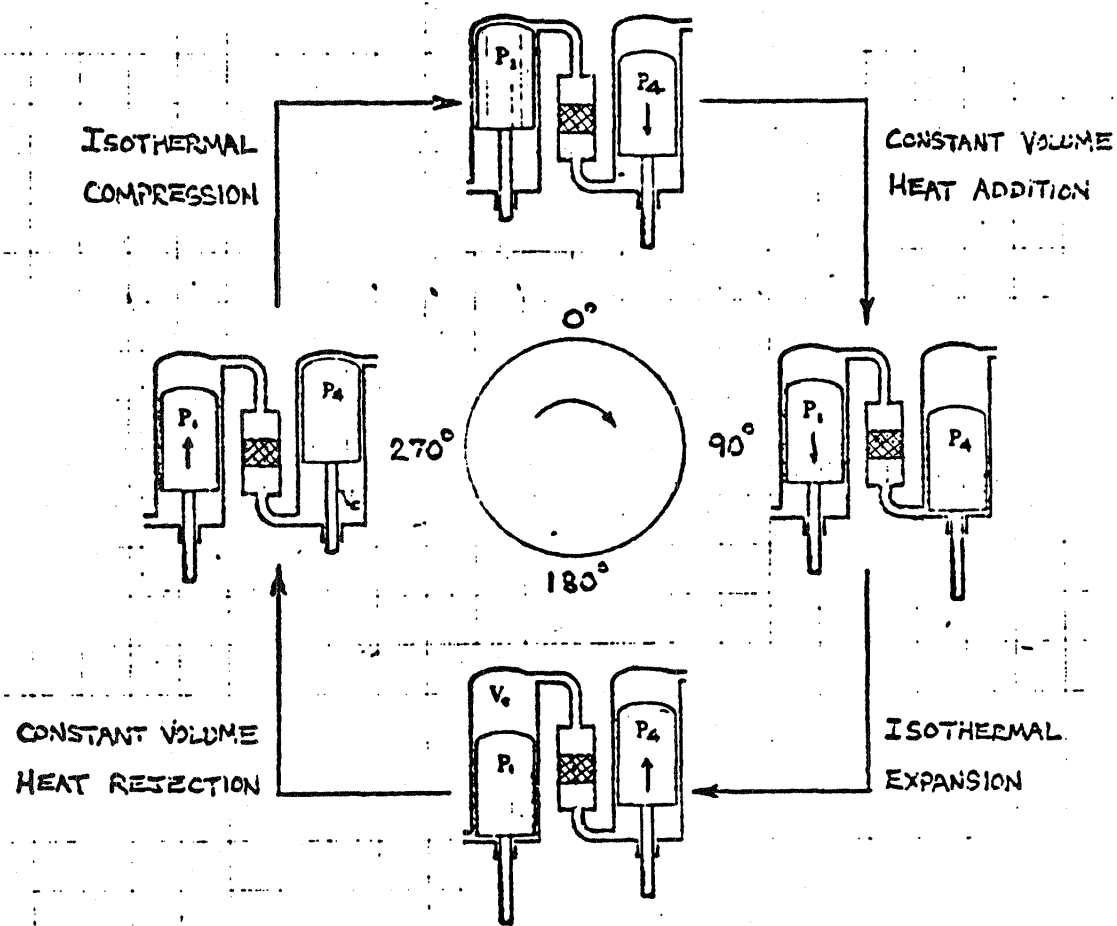


FIGURE 5.5A STIRLING THERMODYNAMIC CYCLE (DOUBLE ACTING PISTON)

TABLE 5.2 HEAT BALANCE IN ASRE

The Heat Flows in Reference Engine

- \dot{Q}_f = Heat from the fuel
- \dot{Q}_{ex} = Heat losses in heat generating system
- \dot{Q}_E = Heat to the heater head
- \dot{Q}_{cb} = Heat losses in cylinders and regenerators
- \dot{Q}_C = Rejected heat in the cycle coolers
- P_i = Indicated power

A = Full load, $p = 15$ MPa, $n = 4000$ rpm

B = Part load, $p = 5$ MPa, $n = 2000$ rpm

C = Maximum efficiency load, $p = 15$ MPa, $n = 1100$ rpm

D = Load low, $p = 5$ MPa, $n = 1000$ rpm

All values in kW

	A	B	C	D
\dot{Q}_f	175.8	32.2	50.7	18.2
\dot{Q}_{ex}	16.0	2.6	3.8	1.8
\dot{Q}_e	159.1	29.6	46.9	16.4
\dot{Q}_{cb}	2.2	2.4	2.3	2.4
\dot{Q}_C	85.8	14.5	22.1	8.4
P_i	73.3	15.0	24.8	7.9

TABLE 5.3 PROGRAM IS082. FOR INPUT TABLE FOR ASRE ENGINE

OPERATING CONDITIONS

NUMBER	SYMBOL	MEANING	VALUE	UNITS
01	SP	ENGINE SPEED		RPM
02	PS	CHARGE PRESSURE		PSIA
03	TMEXP	TEMP. METAL IN EXP. SPACE HEAT EXCHANG		DEG. C
04	TMCMP	TEMP. METAL IN COMP. SPACE HEAT EXCH.		DEG. C
05	OG	OPERATING GAS; 1=H2, 2=HE, 3=AIR		--
06	NDF	CASE NUMBER (ASSIGNED BY USER).		--
07	ZM	BASE CASE ENGINE OPTIONS:		--
		1 - GENERAL MOTORS 4L23		
		2 - GENERAL MOTORS GPU-3		
		3 - UNITED STIRLING P-40		
		4 - STIRLING POWER SYSTEMS V-160		
		5 - MACHINE WITH 12 POINTS OF SPECIFIED VOLUMES		
08		OPEN		
09		OPEN		
10		OPEN		

DIMENSIONS

NUMBER	SYMBOL	MEANING	VALUE	UNITS
***** METAL PROPERTIES ***** (300 SERIES STAINLESS STEEL)				
--	KM	THERM. COND.=EXP(AA+BB*LN(T))		W/CM K
11	AA			-4.565
12	BB			0.4684
13	RHOM	DENSITY		G/CC
14	CPM	HEAT CAPACITY		J/G K
15	--	OPEN		--
***** MECHANICS *****				
16	NCYL	NUMBER OF CYLINDERS PER ENGINE		--
17	JEMO	ENGINE MOTION OPTIONS:		--
		1 - SIEMENS ARRANGEMENT WITH CRANK		
		2 - RHOMBIC DRIVE		
		3 - TWO PISTON SINGLE ACTING (RYDER)		
18	AL	PHASE ANGLE		DEGREES
19	DCEXP	BORE OF EXPANSION CYLINDER		CM
20	DCCMP	BORE OF COMPRESSION CYLINDER		CM
21	STCR	STROKE OF CRANKS (2X CRANK RADIUS)		CM
22	CR	LENGTH OF CONNECTING RODS		CM
23	ECC	ECCENTRICITY IN RHOMBIC DRIVE		CM
24	DD	ROD DIAMETER IN COMPRESSION SPACE		CM
25	ECEXP	EXP. SP. END CLEARANCE		CM
26	ECCMP	COMP. SP. END CLEARANCE		CM
27	ME	MECHANICAL EFFICIENCY		%
28	ADVEXP	ADDITIONAL D. V. IN EXP. SPACE		CM3
29	--	OPEN		--
***** DISPLACER AND CYLINDER WALL CONDUCTION *****				
30	SC	DISPLACER WALL THICKNESS		CM
31	XLB	LENGTH OF DISPLACER OR HOT CAP CAP		CM
32	SE1	CYL. WALL THICKNESS AT EXP. SP. END		CM
33	SE3	CYL. WALL THICKNESS AT COMP. SP. END		CM
34	SE4	CYLINDER WALL THICKNESS AT A MID POINT		CM
35	LB	LENGTH OF TEMP. GRADIENT IN ENGINE CYL.		CM

36	LBM	L. FROM EXP. SP. TO A MID POINT IN T. C.	CM	6.5
37	GAP	GAP BETWEEN DISP. OR HOT CAP AND CYL. W.	CM	0.04
38	NRS	NUMBER OF RAD. SHIELDS IN DISPL OR H.C.	--	1
39	EMIS	EMISSIVITY OF RADIATION SHIELDS	--	0.5
***** HEATER *****				
0	NH	NUMBER OF TUBES PER CYLINDER	--	20
41	LH	MEAN TUBE LENGTH	CM	28
42	LI	HEAT TRANSFER LENGTH	CM	25.2
43	IH	ID OF TUBES	CM	0.3
44	V1	VELOCITY HEADS DUE TO ENTR. EXIT & BENDS	--	1.07
45	ADVH	ADDITIONAL D. V. IN HEATER	CM3	15.0
46	--	OPEN	--	
***** REGENERATOR *****				
47	NR	NUMBER PER ENGINE CYLINDER	--	1
48	LR	LENGTH	CM	5.43
49	DR	DIAMETER OF MATRIX	CM	6.40
50	SR1	WALL THICKNESS AT EXP. SP. END	CM	0.70
51	SR2	WALL THICKNESS AT A MID POINT	CM	0.50
52	LRM	DIST. FROM EXP. SP. END TO THE MID POINT	CM	3.0 **
53	SR3	WALL THICKNESS AT THE COMP. SPACE END	CM	0.3
54	MM	OPTION FOR MATRIX MATERIAL: 1 - MET NET (.05-.20) 2 - STACKED SCREENS	--	1
55	DW	WIRE DIAMETER	CM	.005
56	FF	MATRIX FILLER FACTOR	%	30
57	WSM	MESH OF WIRE SCREEN (BOTH DIRECTIONS)	1/CM	79.0
58	NWML	NUMBER OF WIRE MESH LAYERS	--	550
59	ADVR	ADDITIONAL D. V. IN REGENERATOR	CM3	23
60	--	OPEN	--	
***** COOLER *****				
1	NC	NUMBER OF TUBES PER CYLINDER	--	365
62	LC	MEAN TUBE LENGTH	CM	7.0
63	LD	HEAT TRANSFER LENGTH	CM	5.6
64	IC	ID OF TUBES	CM	0.1
65	V2	VELOCITY HEADS DUE TO ENTR. EXIT & BENDS	--	0.75
66	--	OPEN	--	
***** COLD END CONNECTING DUCTS *****				
67	NE	NUMBER OF DUCTS PER CYLINDER	--	1
68	LE	MEAN DUCT LENGTH	CM	0 ***
69	ID	ID OF DUCT	CM	0 ***
70	V3	VELOCITY HEADS DUE TO ENTR. EXIT & BENDS	--	1.12
71	ADVCE	ADDITIONAL DEAD VOLUME IN COLD END	CM3	35.0
72	--	OPEN	--	
***** MISCELLANEOUS *****				
73	RCMCN	RADIAL CLEARANCE OF POWER PISTON SEAL	MICRONS	2.5 *
74	XSLAN	LENGTH OF POWER PISTON SEAL	CM	0.5 *
75	--	OPEN	--	

*

* ASSUMED SAME AS GPU3

** ESTIMATED

*** THESE ARE USED ONLY IN CALCULATING THE VOID VOLUME
WHICH IS GIVEN AS LUMP SUM

TABLE 5.4 MARTINI CODE VALIDATION

	<u>MAX. EFFICIENCY</u>			<u>MAX. LOAD</u>			<u>PART LOAD</u>			<u>LOW LOAD</u>		
ENG. SPEED (RPM)	1100			4000			2000			1000		
CHARGE PRESS (MPa)	15			15			5			5		
5-17 HOT SIDE TEMP (°C)	820			820			820			820		
COLD SIDE TEMP (°C)	50			50			50			50		
PERFORMANCE	ASRE	MART	△	ASRE	MART	△	ASRE	MART	△	ASRE	MART	△
INDICATED POWER (KW)	24.8	25.7	+3.6%	73.3	75.5	-3.0%	15.0	14.9	- .7%	7.9	7.3	-7.6%
INDICATED EFFICIENCY	52.9	52.36	-1.0%	46.0	45.93	- .2%	50.7	49.51	-2.3%	48.2	45.13	-6.4%
HEAT INPUT TO ENGINE (KW)	46.9	49.1	+4.7%	159.1	164.3	3.3%	29.6	30.2	2.0%	16.4	16.2	-1.2%

5.3.3 CASE DESIGN OPTIMIZATION

After making some minor changes in the Martini code to account for different materials and configuration, it was utilized to optimize the engine design. The data input for the CASE design are given in Table 5.5. The most significant design change was that of heater head and the engine cylinder. The engine cylinder being made of mullite does not conduct as much heat to the cold side as the metal cylinder does, even though it has greater wall thickness. For similar reasons heat conduction loss along the piston wall is also reduced.

The heater head consists of 24 spiral tubes arranged circumferentially around the engine cylinder. Each tube has an ID of 0.118 in. and OD of 0.182 in. The length of each tube is about 8 in. Near the hot side of the engine cylinder the tubes are attached to a manifold which is attached to the engine cylinder dome. Since the heat is also being transferred at the dome the effective length for heat transfer is greater than 8 in. Because of lack of sharp bends in the tubes they are likely to reduce the internal pressure loss and because of spiral configuration add to the internal heat transfer coefficient. Because of the particular design of external heat transfer system, the entire tube section is maintained at uniform temperature and has the isothermalization effect on the expansion process. Since the tubes are proposed to be made of silicon carbide, no significant temperature drop across the tube is expected. The drop however may be significant at full load condition and must be accounted for in predicting the performance at this condition.

An annular regenerator is utilized and is made of mullite, which again decreases the conduction losses. The annular construction reduces the wall thickness requirements from pressure stress consideration. The matrix inside the regenerator is proposed to be Nextel 312*, which in terms of their metal oxides are (by weight) 62% aluminum oxide (Al_2O_3), 14% boron oxide (B_2O_3) and 24% silicon dioxide (SiO_2). According to the manufacturer, it retains its strength and flexibility at continuous temperature of up to 2200°F. The lower density of ceramic fibers is almost completely compensated by higher specific heat relative to metals. An advantage of these fibers is that they can be made in diameter as small as .00044 in. However, the smallest diameter selected is determined by the strength and thermal shock considerations. It is claimed by the manufacturer to have withstood rapid quenching from 2000°F to freezing temperature. An added advantage is that the thermal losses within the matrix are reduced because of lower thermal conductivity of ceramic matrix compared to metal matrix.

In the proposed design the ceramic - metal interface occurs at the cold end of the regenerator. The cooler is envisioned to be of all metal construction and of basically identical design as ASRE, except that it will also be annular in construction. Thus the basic design parameters of the cooler from ASRE design are retained. The void volume in the connecting duct is somewhat increased to account for the fact that the connection between adjacent cylinders occurs on the cold side.

* Registered Trade Mark, 3M Company
St. Paul, MN 55144

TABLE 5.5 PROGRAM ISO82. FOR INPUT TABLE FOR CASE ENGINE

OPERATING CONDITIONS

NUMBER	SYMBOL	MEANING	VALUE	UNITS
01	SP	ENGINE SPEED	RPM	1100
02	PS	CHARGE PRESSURE	PSIA	2176
03	TMEXP	TEMP. METAL IN EXP. SPACE HEAT EXCHANG	DEG. C	982
04	TMCMP	TEMP. METAL IN COMP. SPACE HEAT EXCH.	DEG. C	50
05	OG	OPERATING GAS, 1=H2, 2=HE, 3=AIR	--	1
06	NDF	CASE NUMBER (ASSIGNED BY USER)	--	2
07	ZM	BASE CASE ENGINE OPTIONS: 1 - GENERAL MOTORS 4L23 2 - GENERAL MOTORS GPU-3 3 - UNITED STIRLING P-40 CASES 4 - STIRLING POWER SYSTEMS V-160 5 - MACHINE WITH 12 POINTS OF SPECIFIED VOLUMES	--	3
08		OPEN		
09		OPEN		
10		OPEN		

DIMENSIONS

NUMBER	SYMBOL	MEANING	VALUE	UNITS
***** METAL PROPERTIES ***** (MULLITE)				
--	KM	THERM. COND.=EXP(AA+BB*LN(T))	W/CM K	
11	AA			-3.69
12	BB			0
13	RHOM	DENSITY	G/CC	3.17
14	CPM	HEAT CAPACITY	J/G K	1.09
15	--	OPEN	--	
***** MECHANICS *****				
16	NCYL	NUMBER OF CYLINDERS PER ENGINE	--	4
17	JEMO	ENGINE MOTION OPTIONS: 1 - SIEMENS ARRANGEMENT WITH CRANK 2 - RHOMBIC DRIVE 3 - TWO PISTON SINGLE ACTING (RYDER)	--	1
18	AL	PHASE ANGLE	DEGREES	90.0
19	DCEXP	BORE OF EXPANSION CYLINDER	CM	6.0
20	DCCMP	BORE OF COMPRESSION CYLINDER	CM	6.0
21	STCR	STROKE OF CRANKS (2X CRANK RADIUS)	CM	3.4
22	CR	LENGTH OF CONNECTING RODS	CM	9.5
23	ECC	ECCENTRICITY IN RHOMBIC DRIVE	CM	
24	DD	ROD DIAMETER IN COMPRESSION SPACE	CM	1.26
25	ECEXP	EXP. SP. END CLEARANCE	CM	0.099
26	ECCMP	COMP. SP END CLEARANCE	CM	0.094
27	ME	MECHANICAL EFFICIENCY	%	91.1
28	ADVEXP	ADDITIONAL D. V. IN EXP. SPACE	CM3	3.6
29	--	OPEN	--	
***** DISPLACER AND CYLINDER WALL CONDUCTION *****				
30	SC	DISPLACER WALL THICKNESS	CM	0.23
31	XLB	LENGTH OF DISPLACER OR HOT CAP GAP	CM	14.50
32	SE1	CYL. WALL THICKNESS AT EXP. SP. END	CM	1.04
33	SE3	CYL. WALL THICKNESS AT COMP. SP. END	CM	1.04
34	SE2	CYLINDER WALL THICKNESS AT A MID POINT	CM	1.04

35	LB	LENGTH OF TEMP. GRADIENT IN ENGINE CYL.	CM	14.38
36	LBM	L. FROM EXP. SP. TO A MID POINT IN T. G.	CM	7.19
37	GAP	GAP BETWEEN DISP. OR HOT CAP AND CYL. W.	CM	.04
38	NRS	NUMBER OF RAD. SHIELDS IN DISPL OR H.C.	--	3
39	EMIS	EMISSIVITY OF RADIATION SHIELDS	--	0.8
***** HEATER *****				
0	NH	NUMBER OF TUBES PER CYLINDER	--	24
41	LH	MEAN TUBE LENGTH	CM	20.32
42	LI	HEAT TRANSFER LENGTH	CM	22.85
43	IH	ID OF TUBES	CM	0.300
44	V1	VELOCITY HEADS DUE TO ENTR. EXIT & BENDS	--	1.07
45	ADVH	ADDITIONAL D. V. IN HEATER	CM3	10.74
46	--	OPEN	--	
***** REGENERATOR *****				
47	NR	NUMBER PER ENGINE CYLINDER	--	1
48	LR	LENGTH	CM	5.43
49	DR	DIAMETER OF MATRIX	CM	6.40
50	SR1	WALL THICKNESS AT EXP. SP. END	CM	0.635
51	SR2	WALL THICKNESS AT A MID POINT	CM	0.635
52	LRM	DIST. FROM EXP. SP. END TO THE MID POINT	CM	1.5
53	SR3	WALL THICKNESS AT THE COMP. SPACE END	CM	0.635
54	MM	OPTION FOR MATRIX MATERIAL:	--	1
		1 - MET NET (.05-.20)		
		2 - STACKED SCREENS		
55	DW	WIRE DIAMETER	CM	0.005
56	FF	MATRIX FILLER FACTOR	%	28.0
57	WSM	MESH OF WIRE SCREEN (BOTH DIRECTIONS)	1/CM	74.0
58	NWML	NUMBER OF WIRE MESH LAYERS	--	550
59	ADV R	ADDITIONAL D. V. IN REGENERATOR	CM3	23
60	--	OPEN	--	
***** COOLER *****				
1	NC	NUMBER OF TUBES PER CYLINDER	--	365
62	LC	MEAN TUBE LENGTH	CM	7.0
63	LD	HEAT TRANSFER LENGTH	CM	5.6
64	IC	ID OF TUBES	CM	0.1
65	V2	VELOCITY HEADS DUE TO ENTR. EXIT & BENDS	--	0.75
66	--	OPEN	--	
***** COLD END CONNECTING DUCTS *****				
67	NE	NUMBER OF DUCTS PER CYLINDER	--	1
68	LE	MEAN DUCT LENGTH	CM	0
69	ID	ID OF DUCT	CM	0
70	V3	VELOCITY HEADS DUE TO ENTR. EXIT & BENDS	--	1.12
71	ADVCE	ADDITIONAL DEAD VOLUME IN COLD END	CM3	40.0
72	--	OPEN	--	
***** MISCELLANEOUS *****				
73	RCMCN	RADIAL CLEARANCE OF POWER PISTON SEAL	MICRONS	2.5
74	XSLAN	LENGTH OF POWER PISTON SEAL	CM	0.5
75	--	OPEN	--	

*

After incorporating the aforementioned design considerations in the Martini code it was used to predict the performance of the proposed engine. Figures 5.6 to 5.9 show the effect of varying some of the more critical parameters about the selected design point.

Fig. 5.6 shows the effect of changing the bore size on the indicated efficiency and indicated power. By reducing the bore size one can improve the indicated efficiency, albeit at the expense of power. The result almost directly emanates from reduced swept volume and reduced working gas flow in the engine which result in reduced power output and reduced pumping and thermal losses respectively. In order to minimize the effect on the drive system design and maintain overall engine envelope, the piston stroke was fixed at the same value as ASRE design.

Varying the equivalent regenerator diameter to length ratio had a very pronounced effect on the indicated efficiency as shown in Figure 5.7. The overall volume of the regenerator is maintained to be same as ASRE design. The trend for best efficiency is towards lengthening the regenerator compared to its diameter which has the added benefit of reducing the pressure stresses on the regenerator housing. The maximum length is however restricted from overall engine envelope constraints and the minimum diameter is restricted by the fact that a certain diameter is required to provide room for heater tube attachment. Since the same volume of regenerator was maintained, no loss in regenerative capacity occurs, and hence no effect on power output is indicated. Thus, for CASE design the equivalent D/L ratio is same as the ASRE design.

The effect of regenerator filling factor on indicated efficiency over the range depicted in Figure 5.8 is relatively small. It however noticeably decreases if the filling factor is increased above 40% since pressure losses become high. Whereas with increasing filling factor one observes some gain in power due to increased capacity of the regenerator, one begins to see less than desired power output at less than 28% filling factor.

The regenerator matrix fiber diameter is also one of the critical parameters in determining the regenerator effectiveness, and hence overall engine indicated efficiency. As seen from Figure 5.9 it is advantageous to go lower on fiber diameter which apparently provides more surface area for heat transfer per unit volume. However, the minimum diameter selected is limited by the producibility of the fibers and their capability to go through thermal cycling without breaking apart.

Based on this optimization process the performance of the CASE design at four points was compared with that of the ASRE design. This comparison is shown in Table 5.6. The average improvement in indicated efficiency over the entire range of load conditions is about 15% over ASRE design. The effect of average heater head temperature on indicated efficiency is compared in Fig. 5.10 for CASE and ASRE design. Although it is superficial to raise the hot side temperature of the ASRE design beyond its present limit, it nevertheless gives an idea as to what portion of the overall effect is due to Carnot effect. It appears almost half of the overall improvement is due to Carnot effect and the other half due to design improvement.

Fig. 5.11 shows the typical speed and power curves as a function of heater head temperature. At a constant speed as the heater head temperature is raised the indicated power also increases. In order to obtain the same power at the design point as ASRE engine the bore size of the engine was reduced. It is also to be noted that one can achieve the same mean pressure during the working cycle when operating at a higher temperature with lower working gas inventory. The effect of

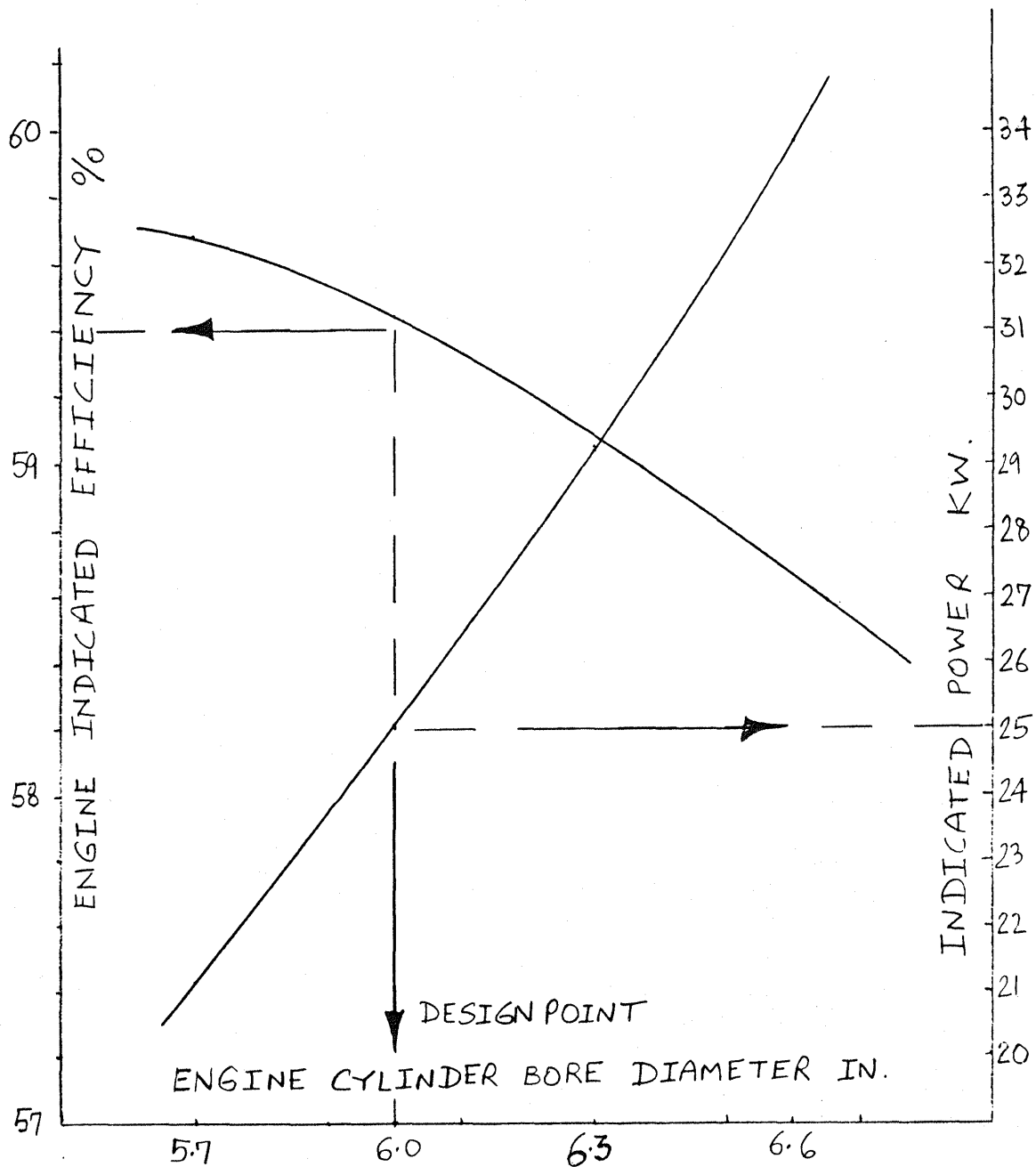


FIGURE 5.6 EFFECT OF ENGINE BORE SIZE VARIATION AROUND OPTIMUM DESIGN POINT AT MAXIMUM EFFICIENCY

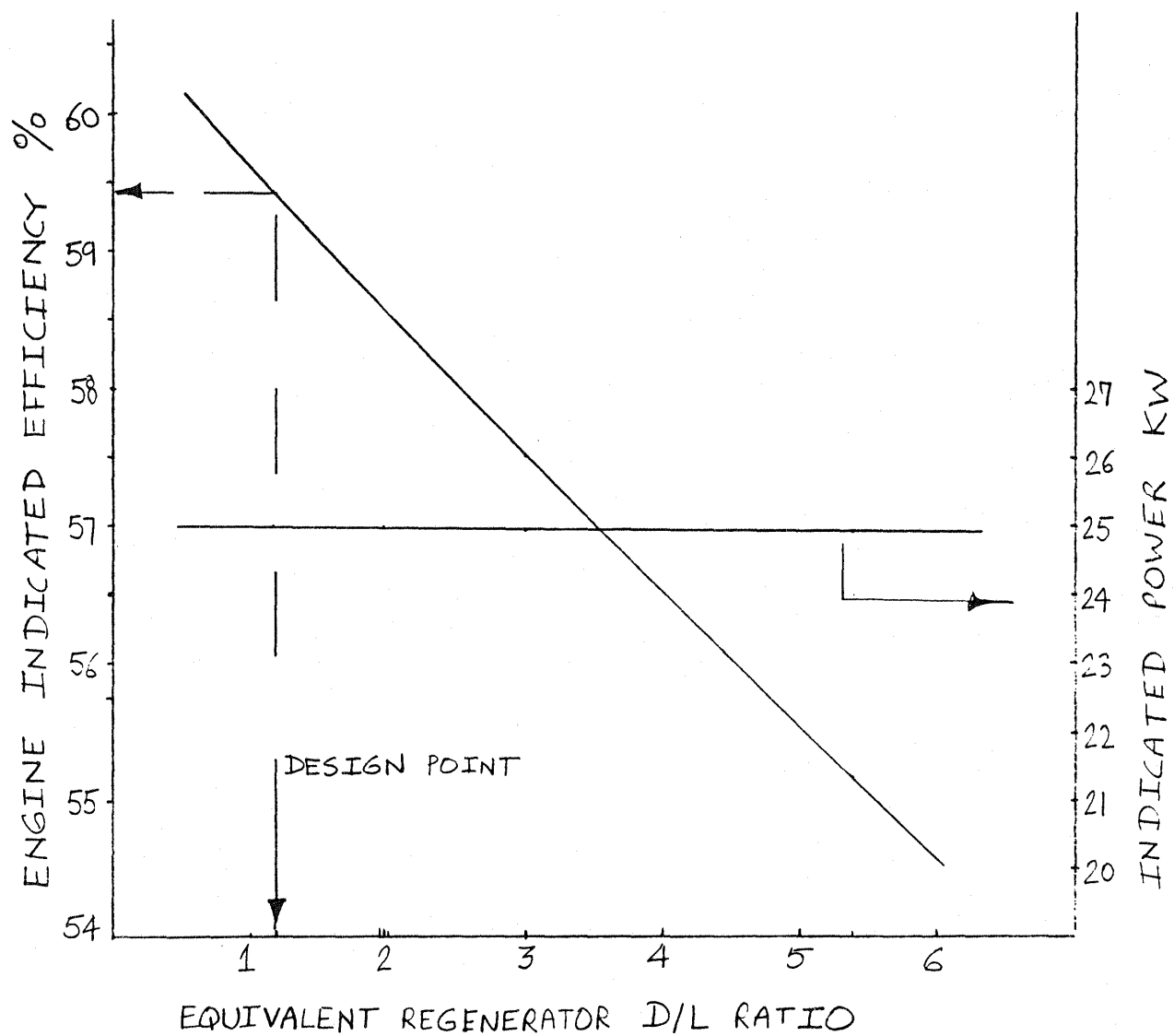


FIGURE 5.7 EFFECT OF REGENERATOR D/L RATIO VARIATION AROUND OPTIMUM DESIGN POINT AT MAXIMUM EFFICIENCY

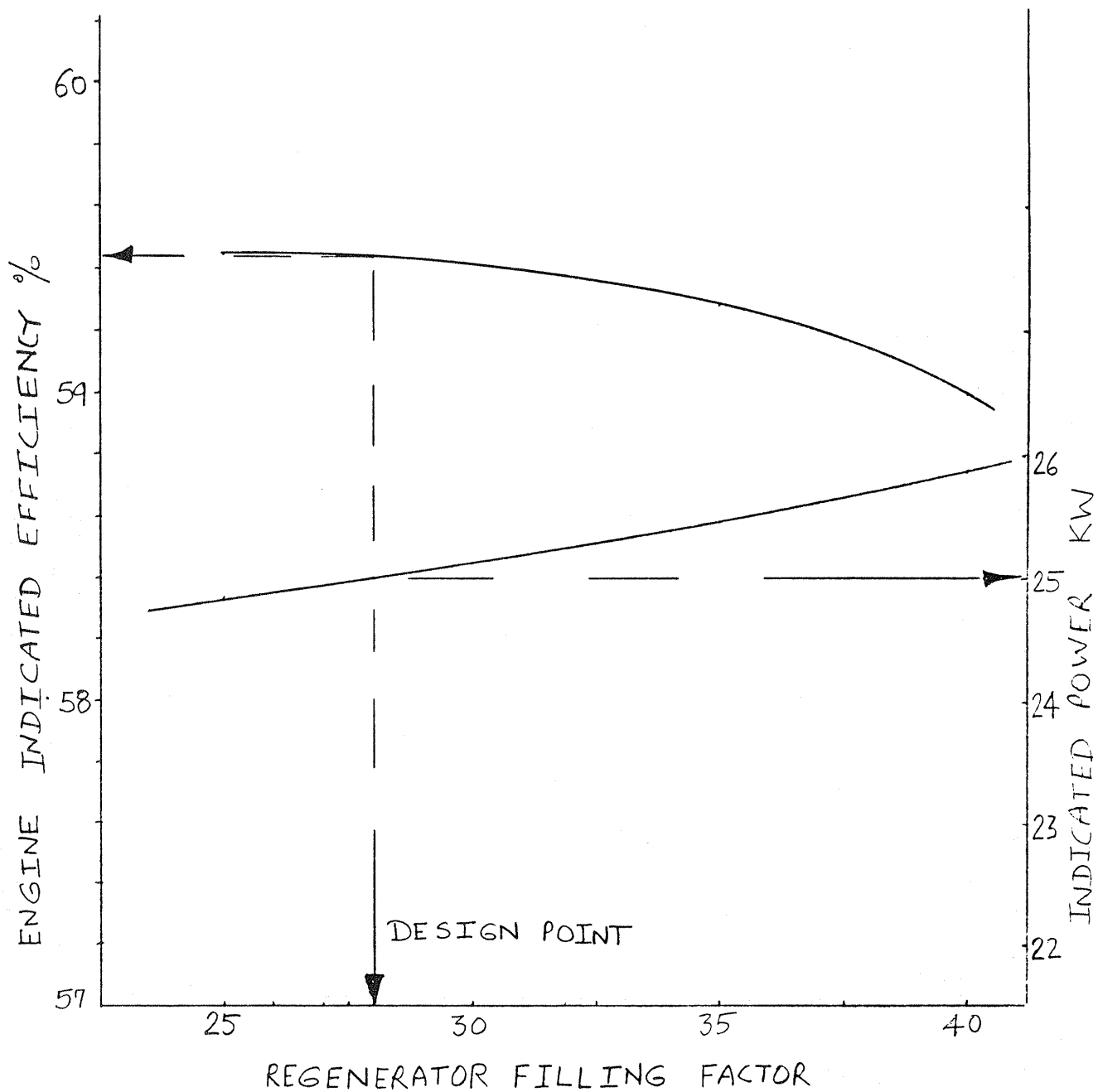


FIGURE 5.8 EFFECT OF REGENERATOR FILLING FACTOR AROUND OPTIMUM DESIGN POINT AT MAXIMUM EFFICIENCY

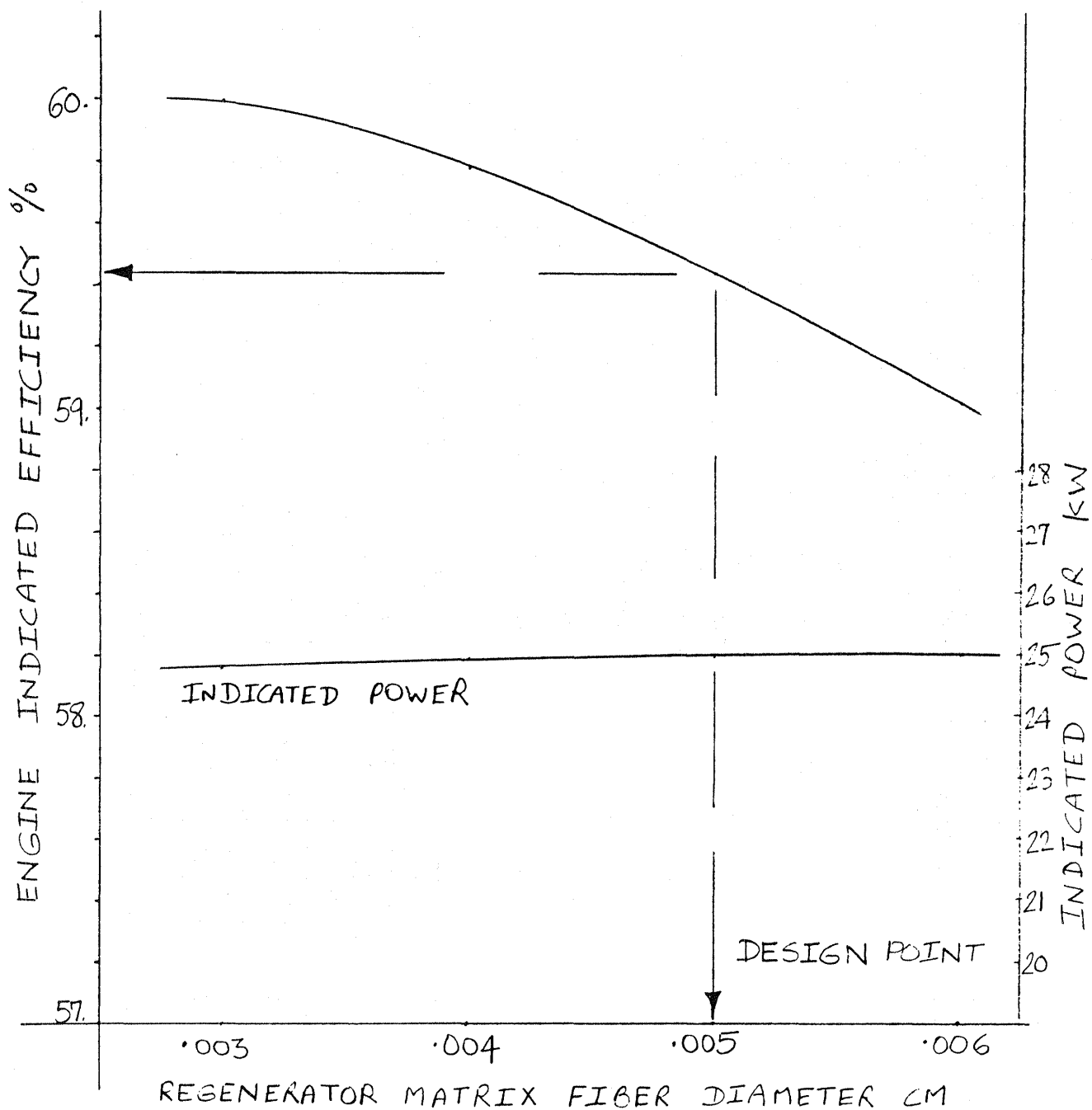


FIGURE 5.9 EFFECT OF REGENERATOR MATRIX FIBER DIAMETER AROUND OPTIMUM DESIGN POINT AT MAXIMUM EFFICIENCY

TABLE 5.6 RELATIVE PERFORMANCE OF ASRE AND CASE DESIGN

	<u>MAX. EFFICIENCY</u>	<u>MAX. LOAD</u>	<u>PART LOAD</u>	<u>LOW LOAD</u>
ENG. SPEED (RPM)	1100	4000	2000	1000
CHARGE PRESS (MPa)	15	15	5	5
HOTSIDE TEMP (°C)	982	982	982	982
COLD SIDE TEMP (°C)	50	50	50	50

PERFORMANCE	ASRE	CASE	Δ	ASRE	CASE	Δ	ASRE	CASE	Δ	ASRE	CASE	Δ
INDICATED POWER (KW)	24.8	25.0	+0.8%	73.3	80.7	+10.1%	15.0	14.8	-1.3%	7.9	7.15	-9.5
INDICATED EFFICIENCY	52.9	59.44	+12.4%	46.0	53.89	+17.2%	50.7	58.17	+14.7%	48.2	55.3	+14.7%
HEAT INPUT TO ENGINE (KW)	46.9	42.0	-10.4%	159.1	149.8	-5.8%	29.6	25.4	-14.2%	16.4	12.93	-21.2%

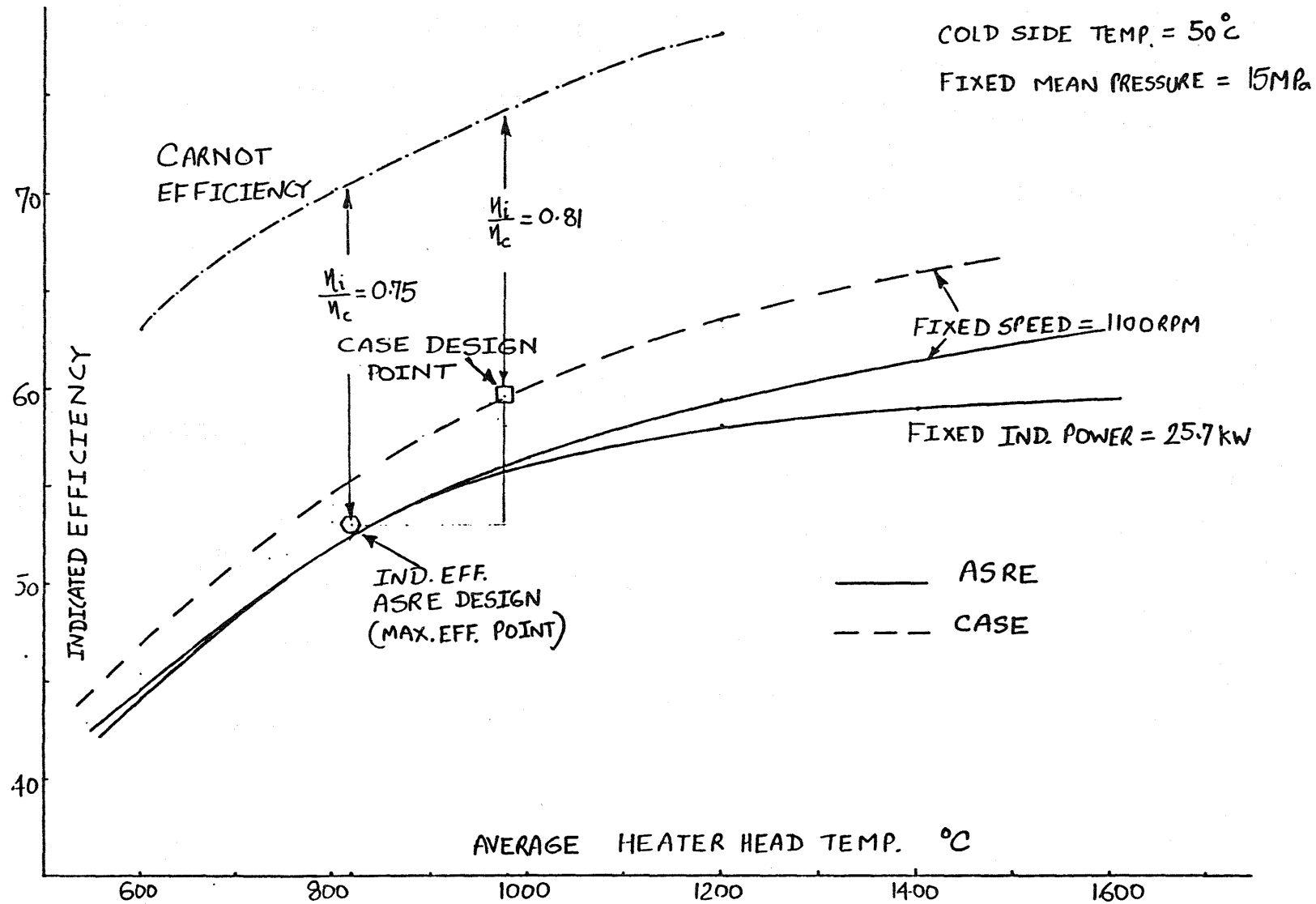


FIGURE 5.10 INDICATED EFFICIENCY VS. HEATER HEAD TEMPERATURE

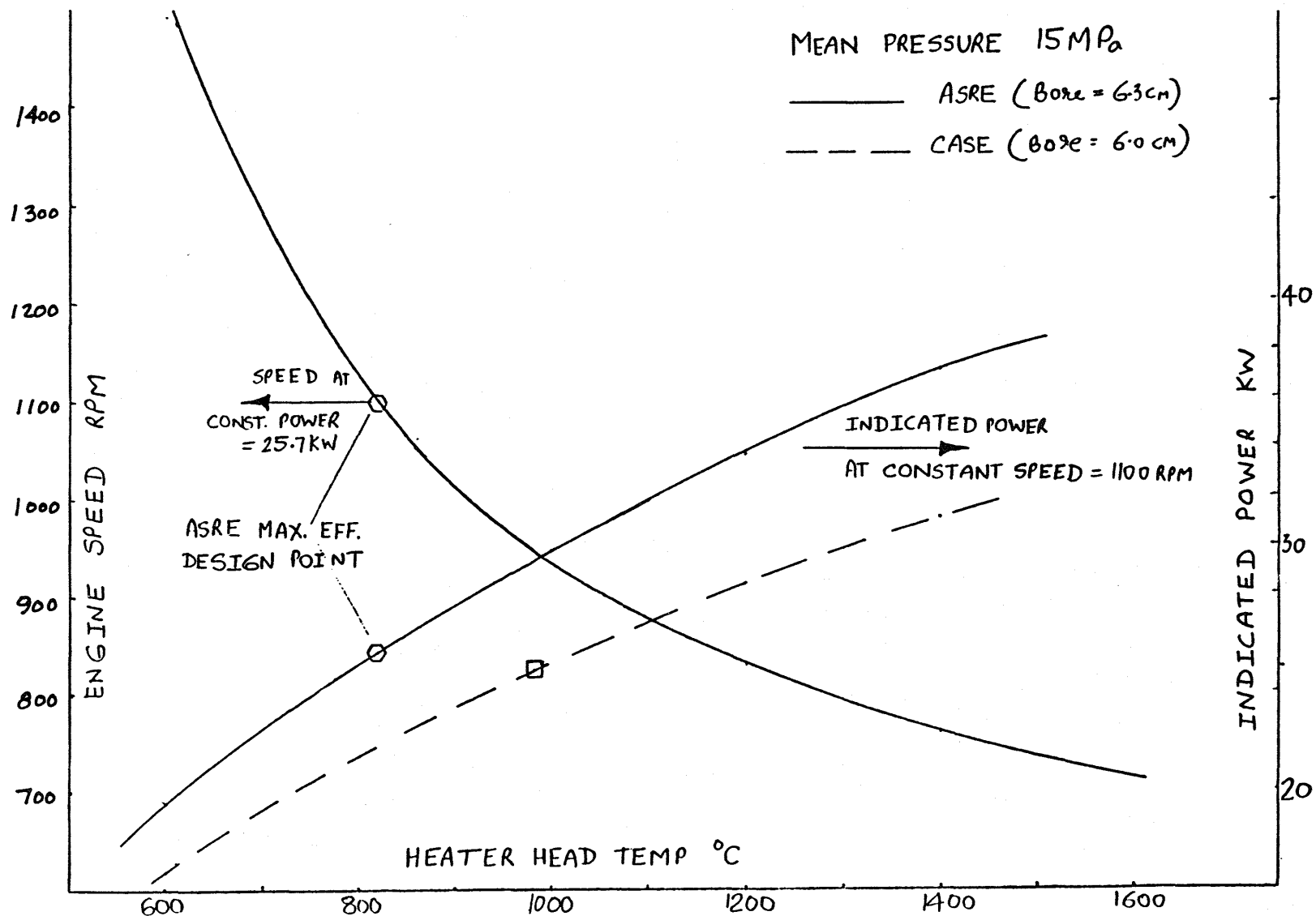


FIGURE 5.11 ENGINE SPEED AT CONSTANT POWER AND ENGINE POWER AT CONSTANT POWER

this reduced gas inventory does not appear to be significant in reducing the internal engine losses and the major gain in indicated efficiency is still limited by the thermal losses due to higher temperature operation.

The thermal and dynamic losses occurring in two designs, ASRE and CASE, are compared in Table 5.7. Major reduction in thermal losses are due to the use of ceramic walls which cuts down on conduction losses. The shuttling losses are reduced mainly because D/L ratio of displacer is reduced. The heater flow losses are reduced because of smaller heater head tube length and increased number of tubes.

5.4 SUMMARY AND CONCLUSIONS

It was shown in an earlier analysis (Section 4.3) that in order to raise the temperature of the heater head tubes, it is necessary to raise the number of available heat transfer units (NTU) from ~ 2.5 for ASRE design to about 3.3 to 3.5 for the proposed CASE design. This was accomplished by utilizing the radiative and convective heat transfer (augmented by impingement) mechanisms in the proposed design. The analysis presented here shows that aforementioned NTU is achievable in the proposed design.

In order to check the performance of the proposed design Martini Code was utilized (made available through courtesy ORNL). The code was validated by matching the predictions of the code with four ASRE performance points, and was utilized to optimize the engine performance. Based on these predictions it is found that the indicated efficiency of the engine of the proposed design at maximum efficiency point will be around 60%.

TABLE 5.7 RELATIVE LOSSES IN ASRE AND CASE DESIGN (MAXIMUM EFFICIENCY POINT)

<u>THERMAL LOSSES (W)</u>	<u>ASRE</u>	<u>CASE</u>
CORR. FOR ADIABATIC HX.	2791.55	2477.15
REHEAT LOSS	1262.19	1236.46
SHUTTLE LOSS	763.64	554.08
PUMPING LOSS	1032.44	1105.63
TEMP. SWING	57.9	52.56
CYL. WALL COND.	523.84	116.4
DISP. WALL COND.	315.97	25.74
REG. WALL COND.	1071.11	200.76
CYL. GAS COND.	27.58	19.42
REG. MTX. COND.	94.24	105.58
RADIATION IN DISP.	35.47	52.84
<u>DYNAMIC LOSSES (W)</u>		
ADIABATIC CORR.	1303.26	533.52
HEATER FLOW LOSS	239.76	99.26
REGENERATOR FLOW LOSS	198.88	129.61
COOLER FLOW LOSS	16.01	10.01

REFERENCES

1. Johnson, D.C., Congdon, C.W., Begg, L.L., Britt, E.J., and Thieme, L.G. "Jet Impingement Heat Transfer Enhancement for the GPU-3 Stirling Engine" DOE/NASA 151040-33. October 1981.
2. Bankston, C.P., Back, L.H., "Heat Transfer from Combustion Gases to a Single Row of Closely Spaced Tubes in a Swirl Crossflow Stirling Engine Heater." J. Heat Transfer, Feb. 1982, vol. 104, p. 55.
3. Hartnett, J.P., Eckart, E.R.G., "Mass-Transfer Cooling in a Laminar Boundary Layer with Constant Fluid Properties." Trans. ASME, Jan. 1957, p. 247.
4. Nealy, D.A., and Reider, S.B., "Evaluation of Laminated Porous Wall Materials for Combustor Liner Cooling." Trans. ASME, April 1980, p. 268.
5. Grootenhuis, P., Mackworth, R.C.A. and Saunders, O.A., "Heat Transfer to Air Passing Through Heated Porous Metals," Proc. Inst. of Mech. Engineers, Sept. 1951, p. 25.
6. W. R. Martini, "Stirling Engine Design Manual" Second Edition, DOE/NASA/ 3194-1, NASA CR-68088, January 1983.

SECTION 6

COLD SIDE

6.1 CONFIGURATION

The cold side of the engine below the engine cylinders is similar to the ASRE with the major exception that a V configuration has been employed. The cold section below the engine cylinder and the drive system are all metal parts just as in the ASRE design.

The cylinder is attached to the engine mounting block using a circular retaining ring which is bolted to the colder metal plate. The design of the retaining ring and its ceramic interface represents one of the critical design areas for the ceramic engine since maximum stress of the ceramic vessel occurs at this interface.

Since the cooler and regenerator assembly are of annular type, a V-type cylinder configuration was selected to maintain the overall dimensions close to ASRE design. The V-configuration also reduces the length of interconnect passage of working gas between cylinders.

During the course of this study in connection with the long range ceramic Stirling engine (CASE II), the possibility of the application of a hot piston ring was assessed. In addition the problems associated with the piston rod seal were considered. Possible use of a pressurized crank case to minimize the demands on the piston rod seal and the incorporation of dry/self lubricated bearings to eliminate the need for an oil pump and oil distribution system have been considered.

A calculation of the friction power loss associated with the two ring design indicated 0.4 to 0.6 KW power consumption per cylinder.

The development of an effective Pumping Lennigrader (PL) seal was identified as a critical problem unless a pressurized crank case is introduced. A pressurized crank case may be feasible based on emerging high strength graphite fiber reinforced composites.

A detailed discussion of the above mentioned problems is included in the following sections.

6.2 ADVANCED CONCEPTS FOR SEALS AND BEARINGS FOR CERAMIC AUTOMOTIVE STIRLING ENGINE

6.2.1 SHUTTLE/PUMPING LOSSES

A preliminary evaluation was completed regarding the use of piston ring seals on the displacer to reduce or eliminate the shuttle/pumping loss due to the existence of the clearance volume between the displacer wall and the cylinder liner. The implementation of this concept would require two piston ring seals, one on the displacer hot side and one on the cold side. Several major technical challenges are immediately evident regarding the incorporation of these seals, including the following:

- (a) The high hot side temperature of 1100 C for the CASE II design imposes a very stringent operating environment upon the piston ring seals.
- (b) The hot dry hydrogen operating fluid dictates the need for the seals to operate for a relatively long life with dry film lubrication.
- (c) The use of two piston ring seals as proposed, in conjunction with a charge pressure of 15 MPa (2176 PSIA) and an operating pressure ratio of 1.57, results in a relatively high seal face pressure/frictional loading.

The following discussion addresses these items simultaneously, since they are all interacting.

Operating temperatures in the range of 1000°C to 1100°C quickly lead to the consideration of ceramics for the seal material. A preliminary review of the current ceramics friction and wear technology, however, indicates that an "off-the-shelf" material is not available for this application. As expected, additional development is required. Furthermore, while not a complete survey of recent testing, the above noted technical survey indicated that current testing/studies are directed toward single direction wear characteristics. No oscillating wear tests were noted. It is believed that oscillating wear results could vary considerably from single direction wear, and for the piston ring seal application discussed herein, oscillating wear is a requirement.

Frictional properties presented in the test results surveyed showed friction coefficients ranging from 0.1 to greater than 1.0. It was further noted that the friction coefficients varied as a function of applied load, ambient/operating temperature, sliding velocity, and surface films/coatings, as well as for different materials and their crystal orientation. It is apparent that additional material development is required for this application of piston ring seals.

The results to date indicate, however, that a reasonable coefficient of friction goal for a high temperature ceramic seal on the displacer hot end would be approximately 0.2. Similarly, a reasonable coefficient of friction goal for a seal on the displacer low temperature end (350°F) would be approximately 0.1. This is based upon the friction properties of today's dry film lubricating materials including filled polyimide and PTFE (polytetrafluorethylene).

As shown in Appendix II, this would result in an estimated friction power loss of from 0.37 to 0.56 KW for a displacer having two piston ring seals, one each on the hot and cold ends.

6.2.2 PISTON ROD SEAL

One potential design modification noted for the long range Ceramic Automotive Stirling Engine is the elimination of the piston rod oil seal to reduce motoring friction, using a dry/self-lubricating seal in place of the oil lubricated design. The proposed concept would have an added advantage of eliminating the present problem of oil migrating past the seal and into the hot engine working space. To assess this proposed modification, it is considered necessary that the function of the piston rod seal be reviewed.

The piston rod seal in the Automotive Stirling Engine (ASE), seals the clearance around the piston rod where it penetrates the engine pressure vessel. The pressure differential across the seal is dependent upon the engine charge pressure, which can be as high as 15 MPa (2176 PSI). The piston rod oscillates (approximately sinusoidally) with a peak-to-peak stroke of 3.4 cm at frequencies up to 4000 cycles per minute. An ideal seal, therefore, permits the rod oscillation with no working fluid (hydrogen) leakage from the pressure vessel.

Hydrogen is a very difficult gas to seal, and even the extremely small leak paths (capillaries and pores) permit leakage. Although some leakage is tolerated, considerable effort is made to keep it at a relatively low level (equal to or less than 1 cc/min). The current piston rod seal design used in the ASE is known as a Pumping Leningrader (PL) seal. This seal is a stuffingbox type/oil scraper/cartridge-like seal assembly, incorporating a filled PTFE (or equivalent) sliding seal squeezed around the piston rod mechanically to control the hydrogen leakage, and oil scrapers to prevent the rod-cooling crankcase oil from migrating into the hot engine working space.

The PL seal provides for an active pumping of the oil back down the shaft due to elasto-hydrodynamic effects resulting from the seal configuration and the reciprocating motion of the rod.

The current performance of this seal design is apparently marginal, and it is still under development for both life and leakage improvement. The use of oil with this design serves several functions. It provides a thin lubricating film for the sliding seal members, helps to seal the very small leak paths, and is applied at a flow rate of sufficient magnitude to keep the seal to rod friction from overheating the piston rod and seal assembly. It is, of course, detrimental if the oil migrates into the engine working space.

Eliminating the use of oil at the piston rod seal would eliminate both the oil migration problem and the oil pump parasitic power requirement. New problems would be incurred, however, including a probable higher leak rate through the capillary and pore size leak paths (due to the loss of the oil sealing effects), and a much higher seal assembly operating temperature (due to the loss of the oil cooling flow). While no attempt was made to estimate a seal operating temperature if dependent upon radiation and/or convection cooling, the friction power loss of a PL-type seal is significant and the operating temperature would certainly be elevated substantially, resulting in the requirement of a new seal material and/or design. This would appear to be a very challenging/high risk approach.

An alternate concept for reducing motoring friction would be the use of a pressurized crankcase. With this concept, the piston rod PL-seals would be replaced with more "conventional" dry film lubricated rod seals on each piston rod, plus a single rotary seal where the drive shaft penetrates the crankcase/pressure vessel. Each piston rod seal pressure differential would be reduced from as high as 15 MPa (2176 PSI), engine charge pressure minus ambient pressure, to less than 3.4 MPa (500 PSI), established by the engine operating pressure ratio. The pressure vessel dynamic seal leakage paths would be reduced from four PL-seals on the piston rods to a single rotary seal on the drive shaft. Motoring friction should be reduced proportionally. While seal development would be required, the technical problems would appear to be much less demanding and solvable within the designated long-range time frame for this application.

A new technical problem is introduced by the incorporation of a pressurized crankcase. However, assuming the availability of new materials through technology developments (such as graphite fiber reinforced metals and polymers), and through innovative design, a crankcase pressure vessel design appears to be an attractive and reasonable alternative. Minimum weight, volume, and cost would be of primary concern in this design.

6.2.3 CRANK SHAFT BEARINGS

Dry/self-lubricating bearings, including crank, main, and wrist-pin bearings, offer the advantage of eliminating the need for an oil pump and the related oil distribution system, while also offering the potential for reduced motoring friction. A review of today's dry bearing technology, however, indicates that additional development is necessary to meet the requirements of these bearings. Dry bearing improvements required include higher operating temperatures and longer wear life, while having a low coefficient of friction and relatively high load carrying capability.

One promising concept in the development of dry bearings is the use of ceramics. The rapid advancement in ceramics technology in recent years, including dry ceramics bearing studies, indicates that ceramic bearings are a prime candidate in the development of dry-self/lubricated bearings. Dry/long-life bearings, however, remain a very challenging technology development.

SECTION 7

STRUCTURAL ANALYSIS

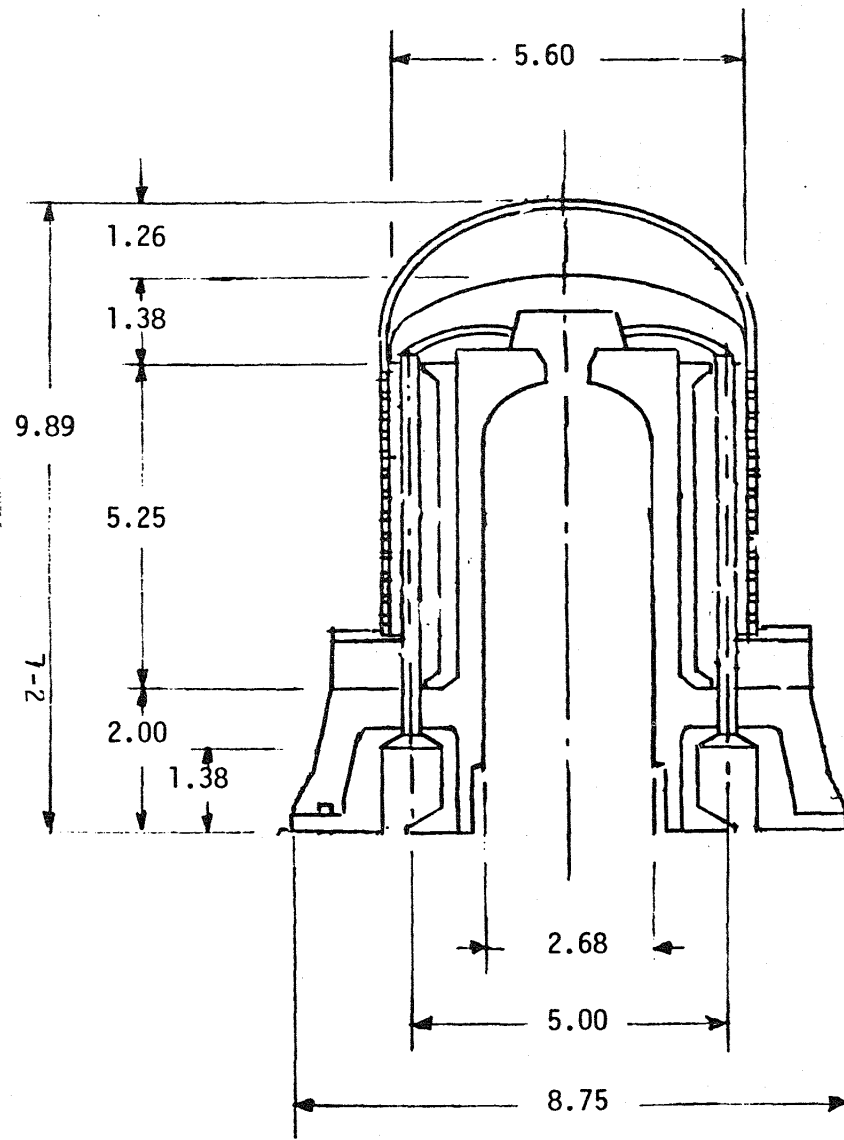
7.1 GENERAL

Thermal heat transfer needs require that the pressure vessel head be made from the high thermal conductivity SiC, while the body of the pressure vessel is fabricated from low conductivity mullite. The reliable joining of these two materials will be a critical process development task which will have to be addressed during further development of the Ceramic Automotive Stirling Engine.

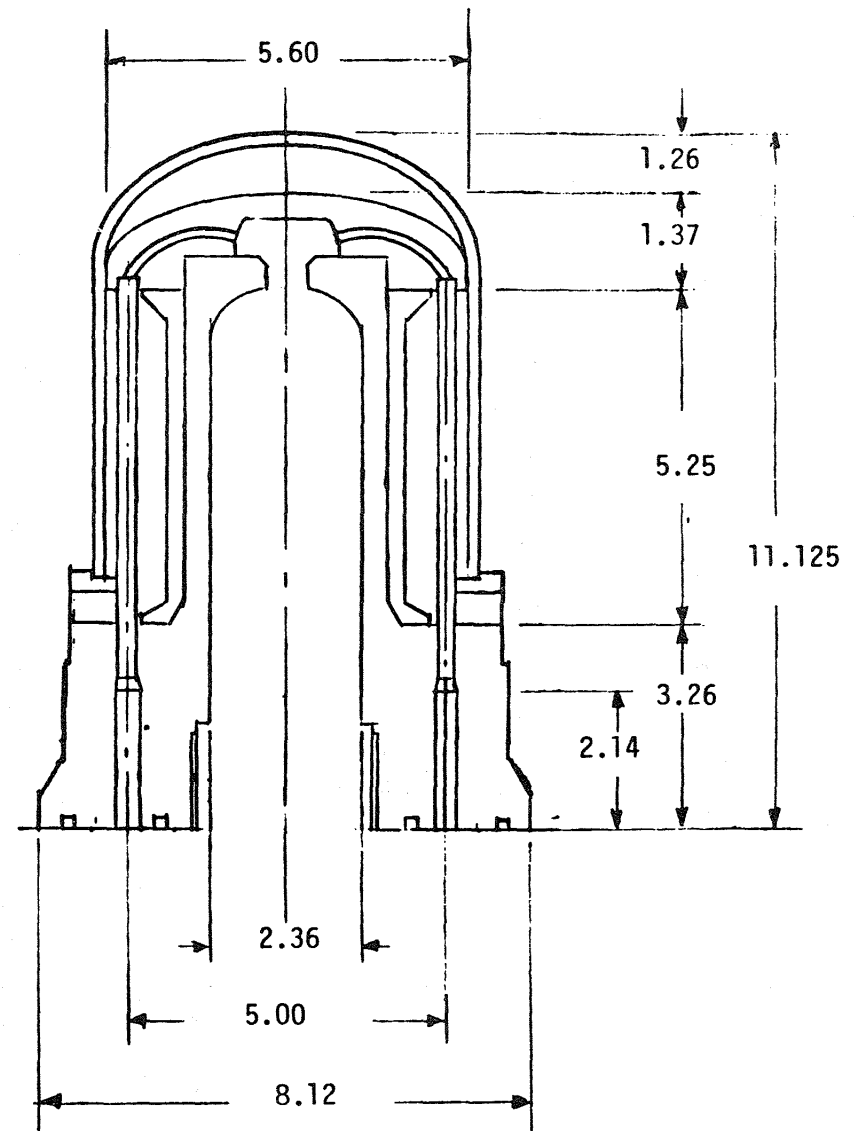
The critical stress problem has been found to be due to the thermal gradient in the pressure vessel in the vicinity of the regenerator. The maximum stress is very sensitive to this gradient. Although we believe that mullite with tensile strength on the order of 100 Ksi (700 MPa) is achievable, we want to keep the peak design stresses down in the 20 to 30 Ksi range to leave room for statistical variations in the properties of the ceramic bodies.

Several iterations of design were required to reduce the predicted stresses to the range desired. The main approach was to change the properties of the regenerator cavity to employ a longer but smaller cross-section concentric regenerator thereby reducing the thermal gradient from top to bottom of the regenerator cavity.

Figure 7.1A shows the cylinder configuration initially adopted while Figure 7.1B illustrates the elongated design required to reduce the axial thermal gradient and thereby the stresses.



A. EARLY VERSION



B. FINAL VERSION

FIGURE 7.1 ALTERNATE CERAMIC CYLINDER DESIGNS

Finite element analysis showed that maximum stresses in the pressure vessel in the range of 23 Ksi are feasible for the selected design temperatures and pressures using mullite.

Stresses in the heater tubes were computed and were found to be in the range of 20 Ksi using SiC. The tubes are 0.243 in. OD (6.17 mm) and 0.118 in. ID (3.0 mm).

7.2 STRESS LEVELS IN CERAMIC HEATER HEAD PRESSURE VESSEL

7.2.1 INTRODUCTION

Finite Element Method models of the Ceramic Heater Head and steel retaining ring were used to determine stresses and begin study of design approaches to cause lower stresses. The NASTRAN (NASA STRuctural ANalysis) code was used to evaluate stresses from internal pressure and equilibrium (operating) thermal gradients using isoparametric axisymmetric elements. The NASTRAN code used in Version 62A as maintained by the MacNeal-Schwendler Corporation and installed on GE's IBM 3033 at the Valley Forge Computer Center. These efforts have led to preliminary definition of low cycle fatigue (start-stop), high cycle fatigue, and maximum stresses.

7.2.2 SUMMARY OF RESULTS

The several models analyzed are shown in Table 7.1 and 7.2. Model "CERAM.11" is the baseline. Stresses due to internal pressure and due to thermal equilibrium temperature distribution were estimated separately and in combination.

Stresses resulting from the thermal gradient were dominant. They are sensitive to geometry and will influence the number of start/stop cycles the head can withstand. The maximum tensile stress predicted was 23,049 psi near the retaining ring in the best model. Differential expansion of the steel retaining ring and ceramic causes some of the stress level predicted. the thermal distribution applied developed less radial growth in the steel ring which was cooler on the average than the ceramic.

High cycle fatigue stress levels due to the internal pressure of 2000 ± 1000 psi are predicted to be about one third of the thermal gradient stresses. Locations of maximum stress from internal pressure do not coincide with locations of maximum thermal stresses. Maximum stress from the internal

TABLE 7.1 MODELS AND MAXIMUM (TENSILE) PRINCIPLE STRESSES IN THE CERAMIC

									NUMBER OF ELEMENTS
52	52	82	82	112	86	142	142	142	
6976	4660	7106	5203	NA	4215	2600 6996.	4300 6989.	4734 PSI	1000 PSI INTERNAL PRESSURE
58405	23771	49223.	46559	MAY RADIAL 14639 HOOP 55272 AXIAL 23728 SHEAR 13926 PRINC. 55272	26224	31831.	31799.	38198.	THERMAL EQUILIBRIUM
NA	26037	52394	47002	NA	27271.	3770 34398.	8241 34358.	39200.	1000 PSI + THERMAL EQUIL
NA	30567	58764	47887	NA	29369.	8778 39538.	16551 39487.	41246.	3000 PSI + THERMAL EQUIL.
.1	.5	.6	.7	.8	.9	.10	.11	.12	TO POINT

BASELINE

TABLE 7.2 EFFECT OF CHAMFER AND LOCAL SMALL TEMPERATURE CHANGES ON MAXIMUM PRINCIPLE TENSILE STRESS IN THE CERAMIC

LOCATION	TEMPERATURE	
(A)	1369 °F	1369
(B)	1319	1000
(C)	450	450
(D)	450	400
NECK	400	300
FLANGE	400	200
	.13	.14

MODEL ID #

LINEAR GRADIENT TO 450°F

CERAM. 14 CERAMIC HEATER HEAD PRESSURE VESSEL
REV C GEOMETRY, THIN WALL, 0.01 INCH, CHAMFERED UNDEFORMED SHAPE

450°F

(C)

(D)

450°F

(A)

(B)

NECK

FLANGE

GAP AT CHAMFER

LOCATION OF MAX STRESS IN THE CERAMIC

1800°F

Z

CHAMFER, 450° @ Z=0; 400°F RING	300°F RETAINING RING CHAMFER; 450°F TO 400°F @ Z=0	COMMENT
6300 PSI	6300 PSI (TOP OF RING)	1000 PSI INTERNAL PRESSURE
30182 PSI	18258 PSI	THERMAL EQUILIBRIUM
31744 PSI	(AT LOCATION SHOWN) 19855 PSI ABOVE	1000 PSI + THERMAL EQUIL
34500 PSI	23049 PSI	3000 PSI + THERMAL EQUIL
CERAM. 13	CERAM. 14	MODEL ID

pressure alone is about 8600 psi \pm 4300 psi in hoop tension on the inner wall. It is sensitive to wall thickness. Increasing the wall thickness from 0.41 inch to 0.75 inch lowers the pressure induced stress to 5000 \pm 2500 psi. However, the combined principle stress is predicted to be 10179 \pm 5090 psi at the regenerator cavity inlet.

When stresses from internal pressure fluctuations are combined with stresses from thermal distortions the principle stress in operation is predicted to range from -3273 psi to +10551 psi at the regenerator cavity inlet due to mostly compressive thermal gradient stresses. At the location of maximum principle tension stress in the ceramic, combined operating stress varies from 34358 psi to 38538 psi at the element centroid, for a low cycle range of 36988 psi and a high cycle stress range of 5180 psi.

However, when the outer edge is chamfered and the retainer is kept cooler (300F) (model CERAM.14) the maximum stress ranges from 19885 to 23049 psi. It is evident that the sensitivities are such that maximum stresses in the pressure vessel can be kept below 30000 psi with judicious design. This occurs near the steel retainer.

The maximum range of high cycle fatigue principle stress at the wall I.D. is 8241 to 16551 psi in the baseline. With the thicker wall, the range predicted is 3770 to 8778 psi.

These high tensile stresses occur in relatively local areas. If the quality of the ceramic body can be controlled to minimize flaws in these regions, then a durable design can be achieved. Also, stresses have been found to respond favorably to geometry changes, leading to some of the recommendations for further analysis to be coordinated with tests.

7.2.3 RECOMMENDATIONS FOR FUTURE WORK

- . Increase the cylinder wall thickness as much as possible without constricting the flow around the heater tubes
- . Increase the base diameter while holding the seal diameter to a minimum, and holding location of the regenerator cavity

- . Evaluate detailed changes to the interface of the retainer with temperature and choice of ceramic.
- . Refine the model accuracy by using more elements after the most promising design features have been analytically selected
- . Use a Three Dimensional Cyclic Symmetry model including the heater tubes and holes for final analysis
- . Determine the natural frequency of the tubes and their dynamic response
- . Integrate the stress distribution over the volume considering the flaw probability to estimate strength (fracture statistics)
- . Test variations of the best analytic design to verify the theoretical fatigue and strength predictions.

7.2.4 DISCUSSION OF ANALYSIS OF CYLINDER STRESSES AND CHOICE OF CERAMICS

Figure 7.1 shows the basic model and loading with boundary conditions. We assumed long bolts would bend at low stress levels to permit radial growth of about 0.01 inch while holding the ring against axial motion from internal pressure induced forces.

The model used six-noded isoparametric axisymmetric elements. Their formulation allows linear variation in strain across the size of the element. This economical method did not allow representation of the heater tubes. Later modeling will include the tubes. Current estimates of the thermal distribution suggest that only the tube inlets should develop significant stresses since they interrupt (as holes) the continuity of the heater head. Since the tubes are at the same temperature as the cylinder for the operating average value, stresses assuming end constraint are conservative but appropriate to make preliminary estimates of transient and cyclic thermal gradients in these low mass tubes.

1
5/8/83
ALL ELEMENTS

7-9

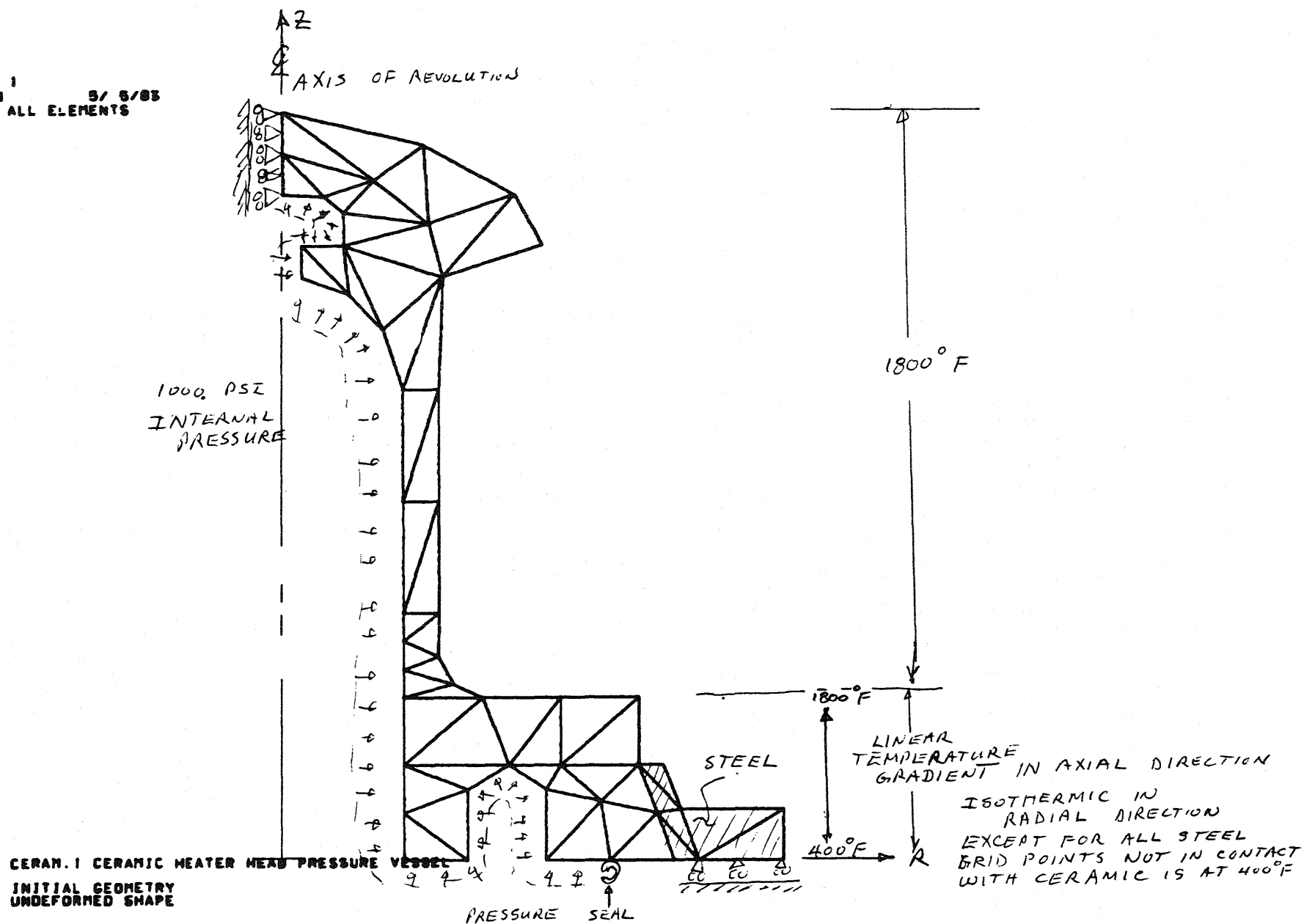


FIGURE 7.1A BASIC BOUNDARY CONDITIONS AND LOADS

The restraint forces at the boundary conditions were checked to partly assess model accuracy. The seal in the baseline model is at a radius of 3.0175 inches. An internal pressure of 1000 psi should develop a restraint force of 28605.162 pounds. A restraint force of 28605.366 pounds was predicted. The thermal distortions should cause no restraint forces since the steel ring was part of the model, and axial thermal growth was unrestrained by the location of the boundary conditions. Restraint forces of zero were predicted for the thermal distortion case.

Fig. 7.2 shows some stresses through the cylinder wall due to 1000 psi internal pressure. Considering the proximity of the base, these values are in good agreement with predictions for thick-walled tubes which are for constant wall thickness far from boundary conditions.

Fig. 7.3 shows deflections from 1000 psi internal pressure. This load case represents the alternating pressure value. Note that the maximum deflection is 0.000673 inch.

Fig. 7.4 shows deflections representing the range of normal operation. At 0.046865 to 0.48211 inch they differ by the amount expected for the 2000 psi pressure range and are several times larger than the deflections from internal pressure alone. Also, the axial growth is consistent with expectations from the hand calculation on the figure.

Table 7.1 shows the evolution of the analysis. The initial model, CERAM.1, had only 52 elements and predicted large thermal stresses as noted in the Table. Increasing the cylinder wall in CERAM.5 made large improvements. By increasing the number of elements, we confirmed in CERAM.6 that high stresses can occur, but still more elements would be needed to improve the prediction. Then, in CERAM.7 we disconnected the steel ring and added axial restraint to the ceramic. This showed that a significant fraction (15%) of the stress levels are due to interaction with the ring.

Continuing in Table 7.1 we ran model CERAM.8 as a test of the severity of the stresses induced by the linear temperature gradient of 1800°F to 400°F in only 2 inches of height. A nine inch high cylinder of 4 inch I.D. and 8 inch O.D. with a regular mesh confirmed that the previous models predictions

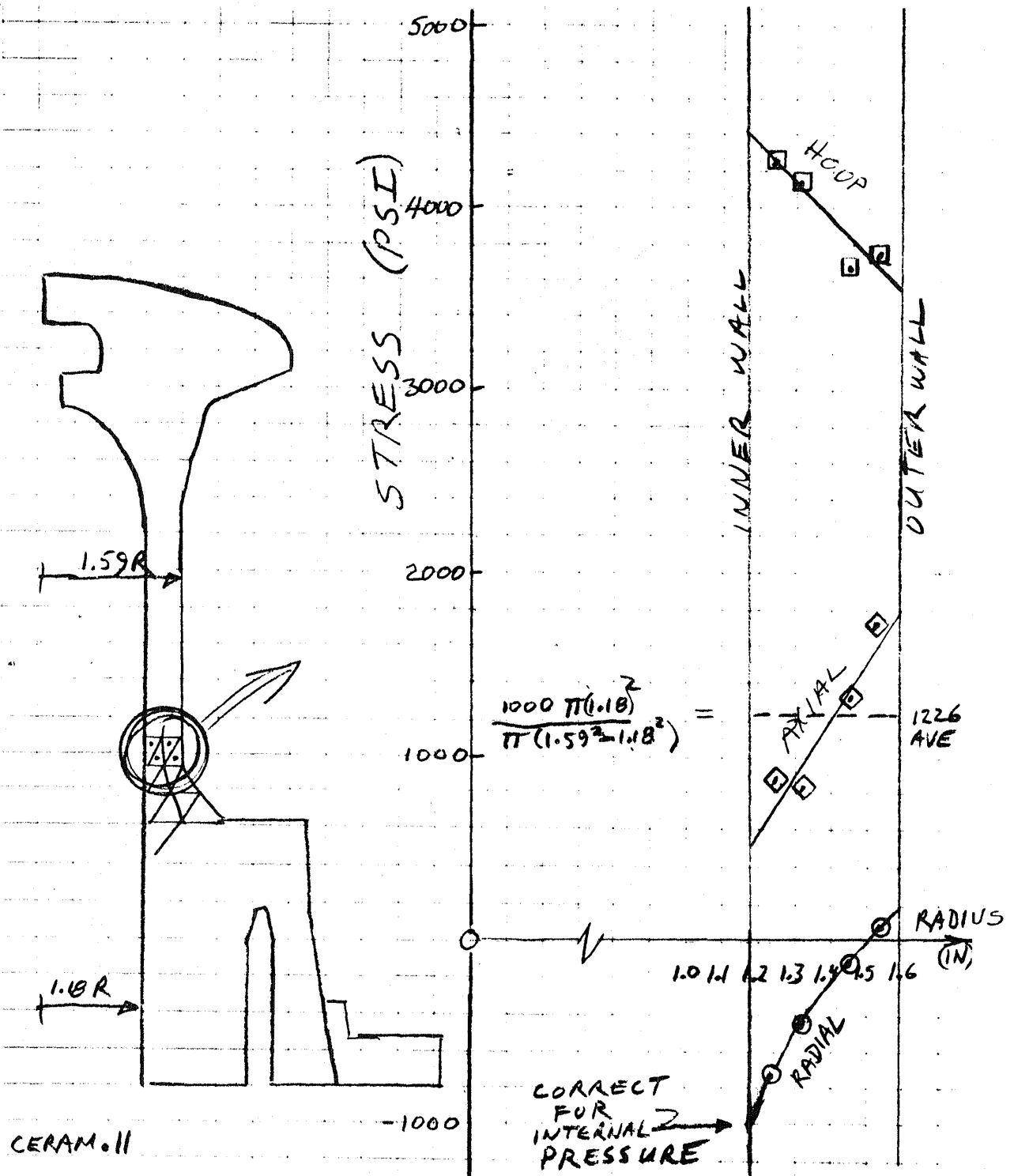
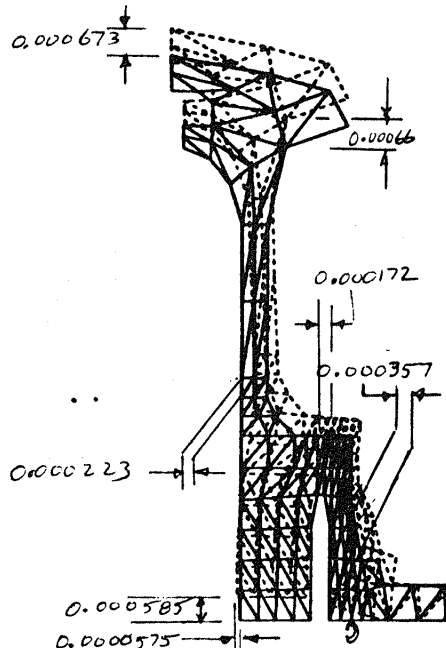


FIGURE 7.2 STRESS ACROSS WALL THICKNESS DUE TO 1000 PSI INTERNAL PRESSURE

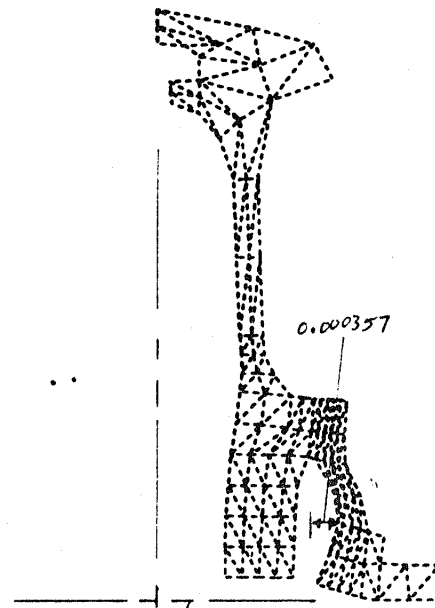
2
2 8/8/83 MAX-DEF. = 0.0000514
ALL ELEMENTS



CERAM. II CERAMIC HEATER HEAD PRESSURE VESSEL
1000 PSI INTERNAL PRESSURE
REV A GEOMETRY, THIN WALL, 0.41 INCH
STATIC DEFOR. SUBCASE 1 LOAD 201

a) UNDEFORMED + DEFORMED MESH

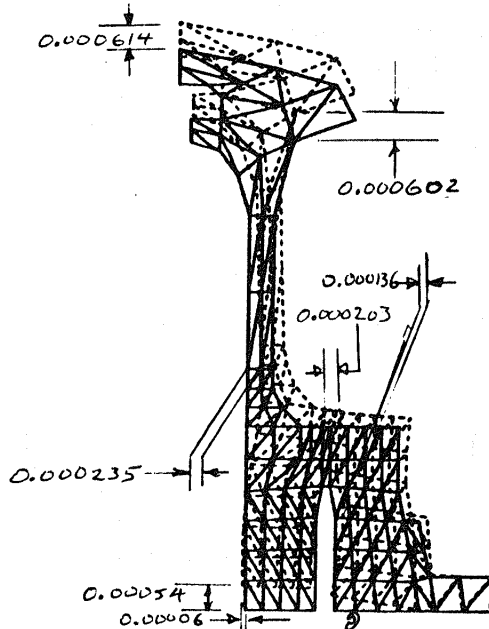
2
2 8/8/83 MAX-DEF. = 0.0000514
ALL ELEMENTS



CERAM. II CERAMIC HEATER HEAD PRESSURE VESSEL
1000 PSI INTERNAL PRESSURE
REV A GEOMETRY, THIN WALL, 0.41 INCH
STATIC DEFOR. SUBCASE 1 LOAD 201

b) AS (a) BUT ONLY DEFORMED MESH

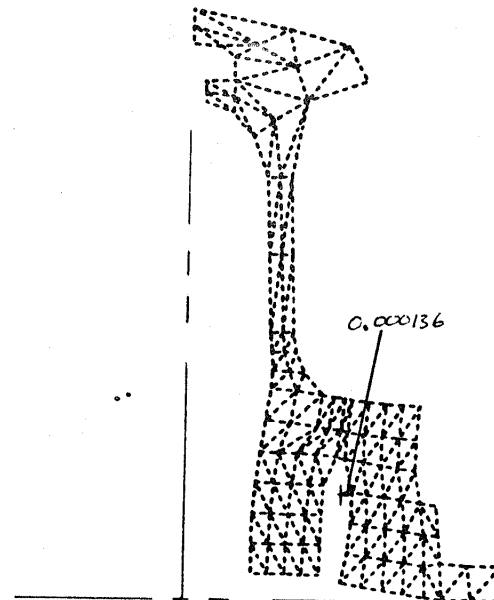
2
2 8/10/83 MAX-DEF. = 0.00002457
ALL ELEMENTS



CERAM. II CERAMIC HEATER HEAD PRESSURE VESSEL
1000 PSI INTERNAL PRESSURE
REV B GEOMETRY, THIN WALL, 0.41 INCH
STATIC DEFOR. SUBCASE 1 LOAD 201

c) AS (a) BUT GREATER O.D.

2
2 8/10/83 MAX-DEF. = 0.00002457
ALL ELEMENTS



CERAM. II CERAMIC HEATER HEAD PRESSURE VESSEL
1000 PSI INTERNAL PRESSURE
REV B GEOMETRY, THIN WALL, 0.41 INCH
STATIC DEFOR. SUBCASE 1 LOAD 201

d) DEFORMED SHAPE

FIGURE 7.3 RESPONSE OF TWO GEOMETRIES TO 1000 PSI

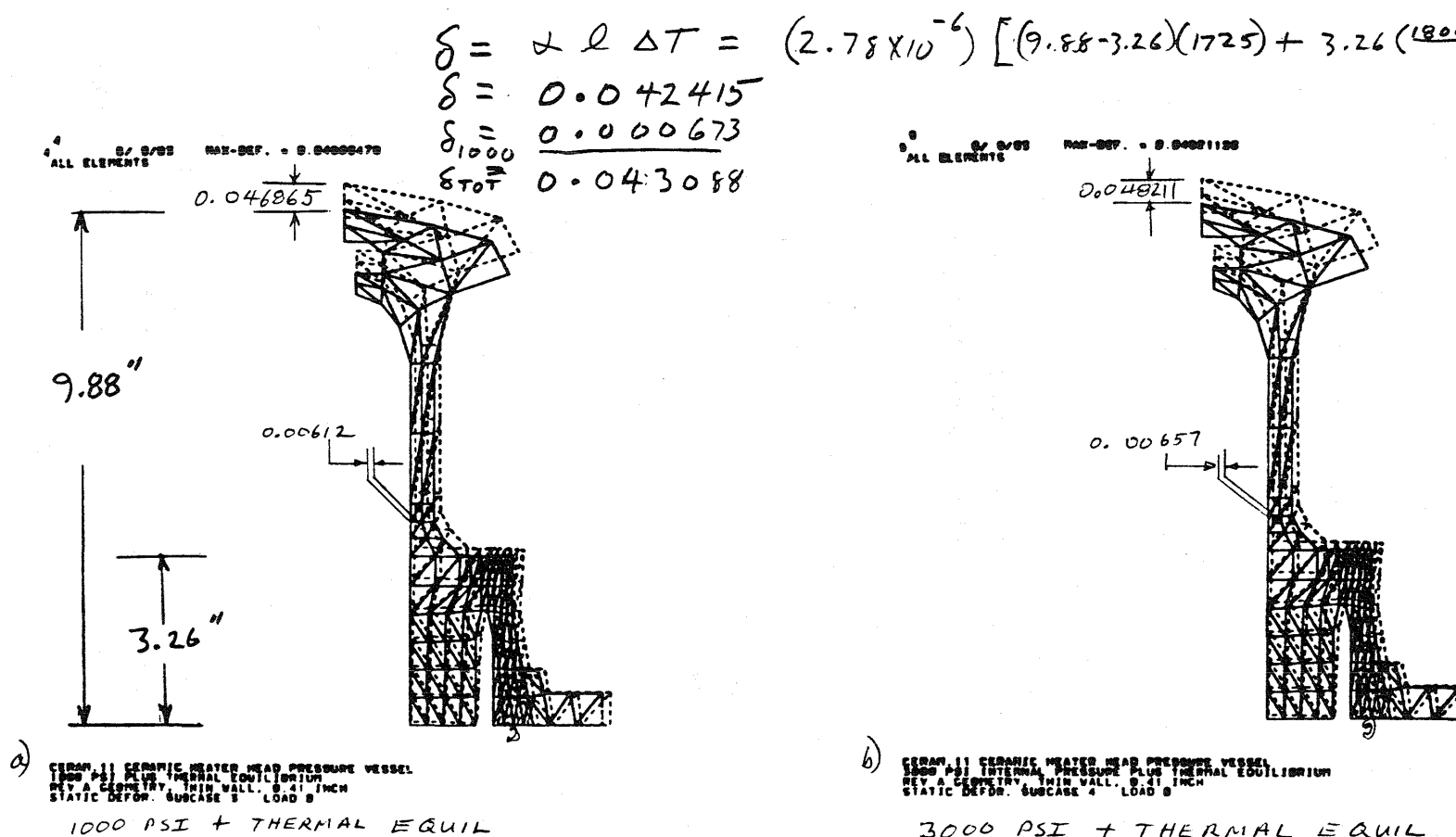


FIGURE 7.4 DOMINANT OPERATING DEFORMATION IS THERMAL

were sensible. The heater head geometry was changed to allow the temperature gradient to run over a 3.26 inch base disc thickness rather than 2.0 inch. Also, the piston diameter and seal diameter were reduced.

Model CERAM.9 of this baseline head was similar in complexity to prior models. This similarity lent credence to the accuracy of comparing stresses to prior models. As shown in Table 7.1 lower stresses were achieved. However, the maximum stresses occurred in a coarse region of the model. More runs were made to numerically test design sensitivity to geometry changes, all with the same element count, or mesh refinement. These geometry variations should have little or no effect on the key functional parts being the bore and stroke and the regenerator geometry.

Fig. 7.5 shows key stresses in the baseline (CERAM.11) with two variations. CERAM.10 has the thick wall, which benefits cylinder wall stresses. CERAM.12 has a greater outer diameter with the same seal location, benefiting the high cycle maximum tensile stress range in the most highly stressed region of the head. CERAM.12 changes also slightly benefit the cylinder wall.

High cycle fatigue stress level is obtained by subtracting the minimum stress from the maximum stress in Figure 7.5. The sensitivity to mean stress and defect size should influence high cycle fatigue life. A defect of sufficient size in either the cylinder wall or near the retaining ring could cause failure by immediate fracture or growth to a critical size. The probability distribution of defect sizes plus a distribution of defect location should be used in conjunction with the stress distribution to estimate risk of failure. These distributions for the flaw size and location must vary with the manufacturing and material processes. If we integrate over the volume of the head, considering the state of stress and the probability of flaw size at each volume element, we should be able to bound the risk of high-cycle fatigue failure since the Weibull model relating strength and volume appears applicable.

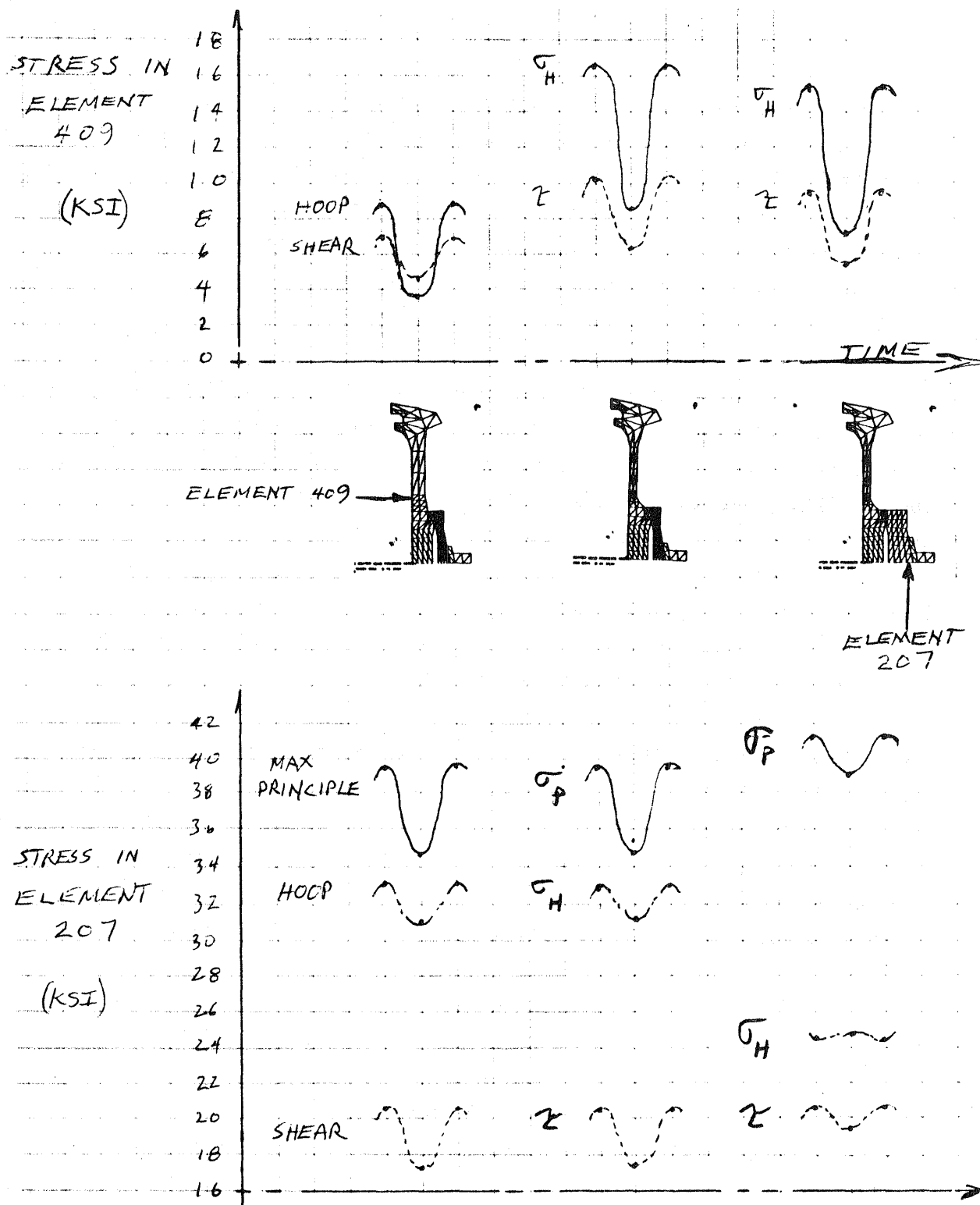


FIGURE 7.5 LOW AND HIGH CYCLE FATIGUE FOR THREE DESIGNS, ALL WITH SAME BORE, STROKE, AND LOADS

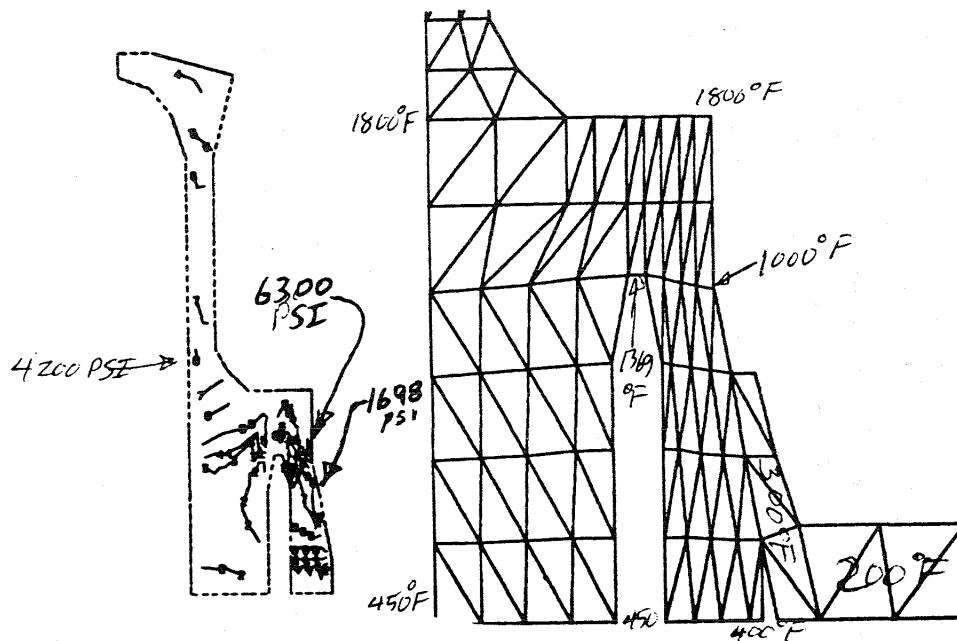
Low cycle fatigue stress range can also be seen in Figure 7.5. The average of the maximum and minimum stress would be this stress range if we assume that the head is stress free at 75°F and with no pressure differential. Every time the head is brought from rest to operation and back to rest, it will have to endure these stress ranges. If we start and stop the engine four times a day, then we have 14600 cycles from zero to 39500 psi to zero in ten years.

The maximum stress of 39500 psi in the baseline model is rather localized. The maximum stress is just 25000 psi only 1/10 inch away. It is also responsive to changes in the interface with the retaining ring, recalling model CERAM.7, Table 7.1, versus CERAM.6. We expect that further work on the local geometry should further reduce stresses.

Future design variations should increase the cylinder wall (CERAM.10 versus CERAM.11), increase the outer diameter, and contour the ring interface, and ensure a relatively cool retaining ring.

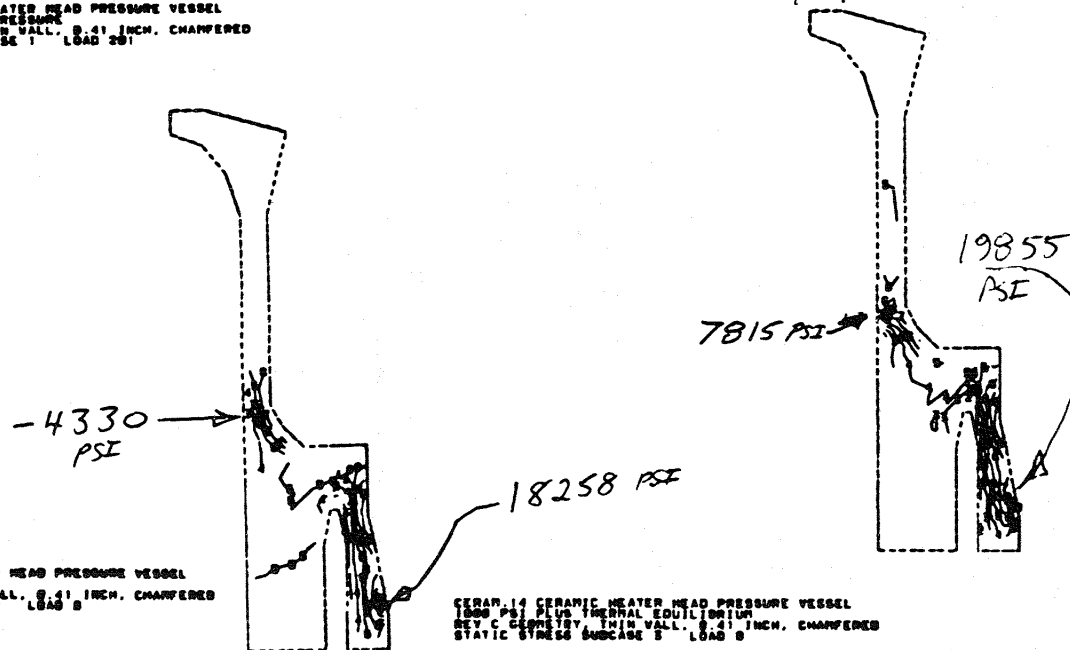
As a check on this hypothesis, two more models were run with the results shown in Table 7.2 and Fig. 7.6 for the best case. First, in model CERAM.13, a chamfer was placed at the outer diameter of the base to relieve interacting with the retainer. Also, the thermal gradient was modestly changed by letting the base lower surface be 450°F rather than 400°F. The maximum stress dropped from 39500 psi (CERAM.11) to 34000 psi.

In model CERAM.14, we lowered the retaining ring temperature from 400°F to 300°F because of its proximity to the engine water jacket. The temperature gradient in the ceramic was also adjusted to represent a radial gradient rather than only an axial gradient as noted in Table 7.2. The maximum principle stress range is from 19855 to 23049 psi, still at the interface with the retainer.



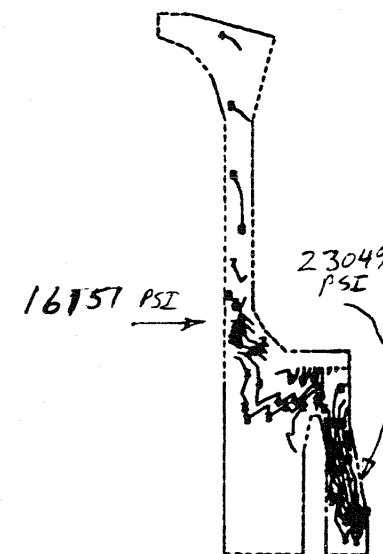
CERAM.14 CERAMIC HEATER HEAD PRESSURE VESSEL
1000 PSI INTERNAL PRESSURE
REV C GEOMETRY, THIN WALL, 0.41 INCH, CHAMFERED
STATIC STRESS SUBCASE 1, LOAD 201

7-17



CERAM.14 CERAMIC HEATER HEAD PRESSURE VESSEL
1000 PSI INTERNAL PRESSURE
REV C GEOMETRY, THIN WALL, 0.41 INCH, CHAMFERED
STATIC STRESS SUBCASE 2, LOAD 0

CERAM.14 CERAMIC HEATER HEAD PRESSURE VESSEL
1000 PSI PLUS THERMAL EQUILIBRIUM
REV C GEOMETRY, THIN WALL, 0.41 INCH, CHAMFERED
STATIC STRESS SUBCASE 3, LOAD 0



CERAM.14 CERAMIC HEATER HEAD PRESSURE VESSEL
1000 PSI PLUS THERMAL EQUILIBRIUM
REV C GEOMETRY, THIN WALL, 0.41 INCH, CHAMFERED
STATIC STRESS SUBCASE 4, LOAD 0

FIGURE 7.6 MAXIMUM PRINCIPLE STRESSES IN MODEL CERAM.14

7.3 STRESS ANALYSIS FOR HEATER HEAD TUBES

7.3.1 SUMMARY AND CONCLUSIONS

The identification of a ceramic nested tubular heater head configuration for potential use in a Stirling engine application has led to the need for completing a structural analysis of the ceramic heater head tube included in this design. Thermal analyses of this concept indicates that acceptable heat transfer will be provided through the tubes if 24 tubes are evenly spaced around the cylinder head/pressure vessel, each tube having the following geometry:

- . exposed length = 8.1 in. (205.7 mm)
- . outside dia. = 0.243 in. (6.17 mm)
- . inside dia. = 0.118 in. (3.0 mm)

The thermal analysis also determined that the maximum tube to pressure vessel temperature difference would be 500°F (260°C), and the maximum internal pressure would be 3000 psi (21 MPa).

A finite element structural analysis was completed to determine the maximum stress levels to be experienced in the proposed heater head tube. Two materials were evaluated, Silicon Carbide and Silicon Mullite. The analyses showed that the maximum tensile and shear stress levels are within the realm of acceptable working stresses for both materials. The calculated values are:

Silicon Carbide

- . Maximum tensile stress = 19,740 psi (136 MPa)
- . Maximum shear stress = 11,130 (77 MPa)

Silicon Mullite

- . Maximum tensile stress = 9,840 psi (68 MPa)
- . Maximum shear stress = 5,660 psi (39 MPa)

It is recommended that a fracture statistics risk analysis be completed to determine the mean fracture strength of the tube, thereby gaining further insight into the acceptability of the tubes/materials for this application.

7.3.2 INTRODUCTION

Conceptual design studies of a Stirling engine with ceramic components have identified a ceramic nested tubular heater head configuration as a potential candidate for this application. Figure 7.7 shows a conceptual design layout incorporating ceramic nested tube heater heads, one heater head per cylinder. Simply described, the heater head assembly consists of a pressure vessel in conjunction with heater tubes nested around the unit. The pressure vessel is cylindrical, having a modified hemispherical "free" end, and a flanged end for attaching the assembly to the engine cylinder block. The heater head tubes, 24 evenly spaced around the periphery of the pressure vessel, are modified helixes with their ends bent to run parallel to the heater head axis at their point of attachment to the pressure vessel. Each tube is slightly less than one-half of one coil.

Pressure and thermally induced stresses are of concern with this design configuration, both in the heater head tubes and in the pressure vessel. The following discussion pertains to the heater head tubular stresses, with the pressure vessel stress evaluation being presented in a separate discussion.

The tubular structural analysis was completed by use of the SAPV.2 Program, "A Structural Analysis Program for Static and Dynamic responses of Linear Systems", developed at the University of Southern California.

7.3.3 STRUCTURAL ANALYSIS PROGRAM

The SAPV.2 Structural Analysis Program is a general purpose program utilizing finite element methods. The program has a family of elements to choose from, including three dimensional straight or curved pipe elements, as required for the evaluation of the subject ceramic heater head tube. The elements are of the more recent iso-parametric formulation approach, and are capable of representing piping with internal pressure, thermal gradients, externally applied forces, and enforced displacements. Static and dynamic solutions are possible. The evaluation reported herein was limited to a static solution with both pressure and thermal gradient considerations.

7.3.4 HEATER HEAD TUBE CONFIGURATION

The heater head tube evaluated is a modified helix as depicted in Figures 7.8 through 7.11. Tube dimensions are:

- . Outside dia. = 0.243 in. (6.17 mm)
- . Inside dia. = 0.118 in. (3.0 mm)
- . Total exposed length = 8.1 in. (205.7 mm)

Tube materials/properties evaluated are:

Silicon Carbide

- . Modulus of elasticity = 54×10^6 psi (3.72×10^5 MPa)
- . Coef. of thermal expansion = 2.67×10^{-6} ($4.8 \times 10^{-6}/^\circ\text{C}$)

Si Mullite

- . Modulus of elasticity = 26×10^6 (1.79×10^5 MPa)
- . Coef. of thermal expansion = $2.78 \times 10^{-6}/^\circ\text{F}$ ($5 \times 10^{-6}/^\circ\text{C}$)

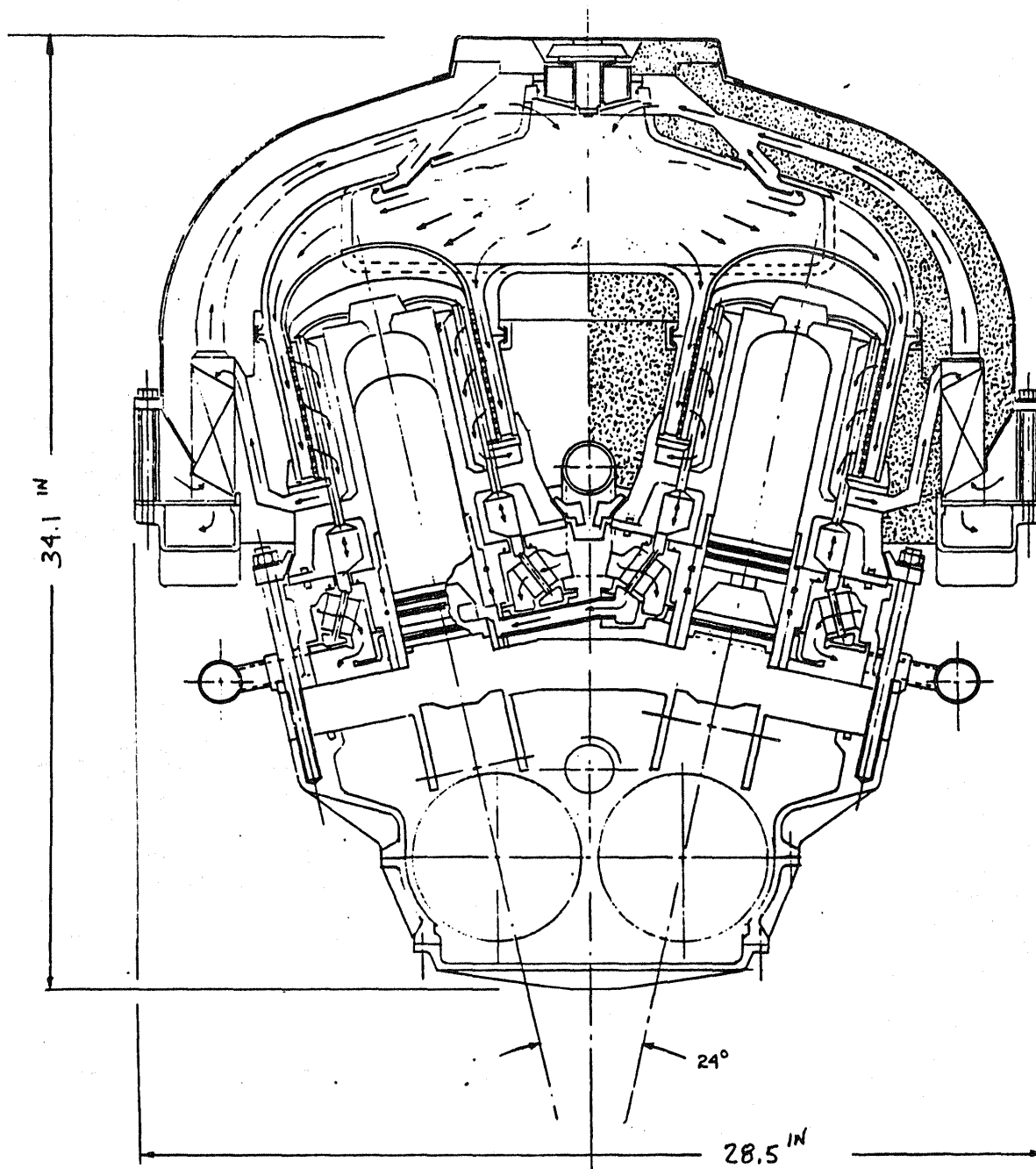


FIGURE 7.7 CONCEPTUAL DESIGN LAYOUT FOR CERAMIC
AUTOMATIC STIRLING ENGINE.

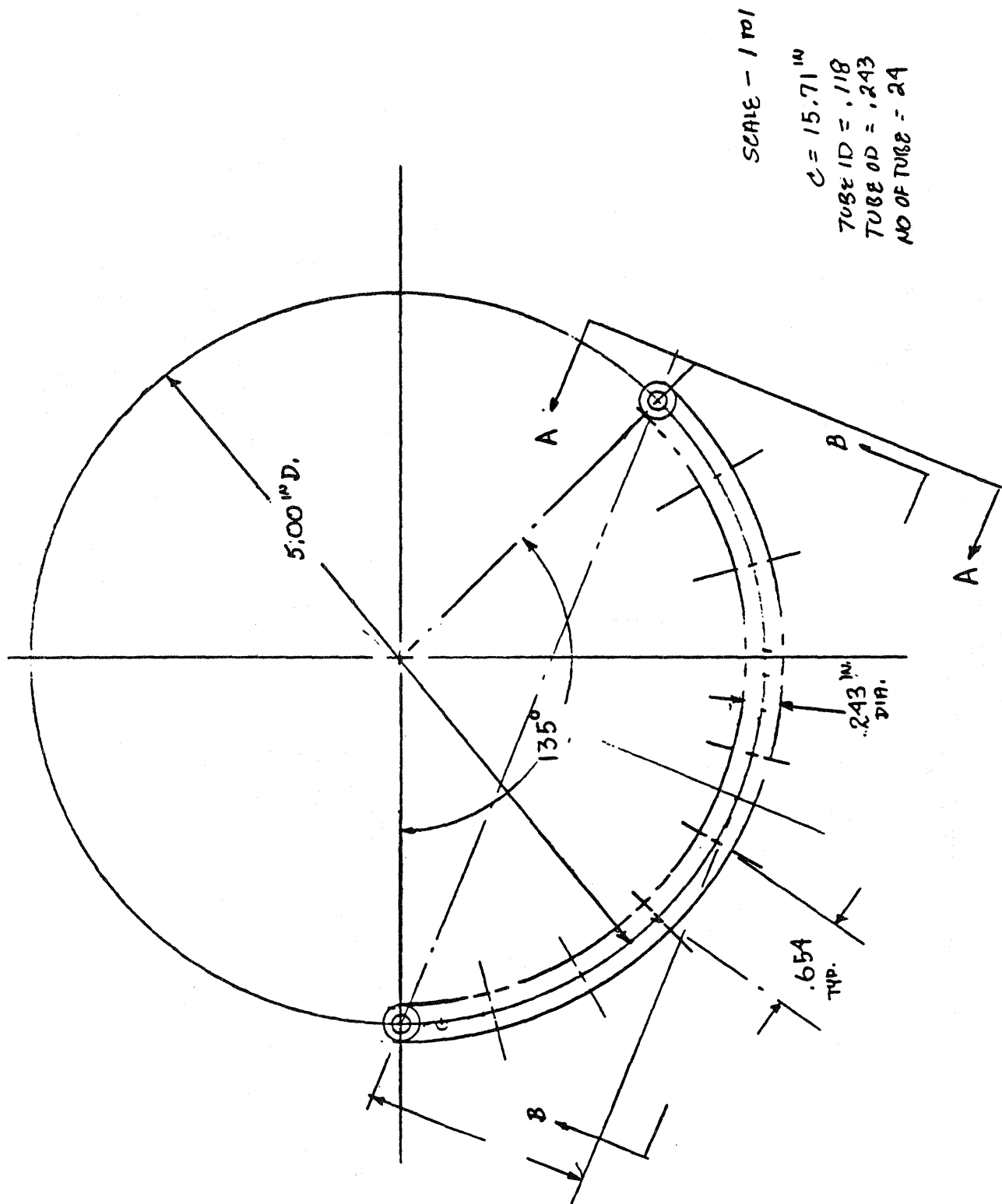


FIGURE 7.8 HEATER HEAD TUBE
END VIEW

(REFERENCE FIGURE 7.8)

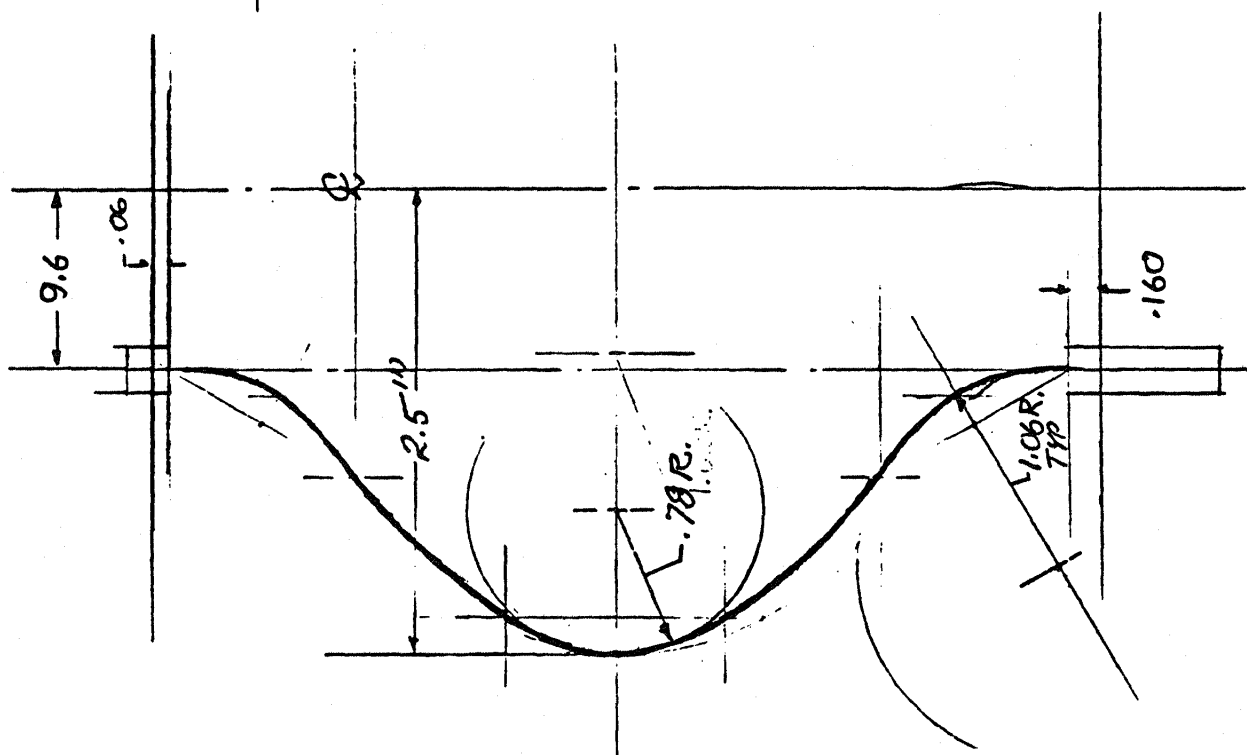


FIGURE 7.9 HEATER HEAD TUBE
TRUE VIEW PROJECTION
VIEW AA

(REFERENCE FIGURE 7.8)

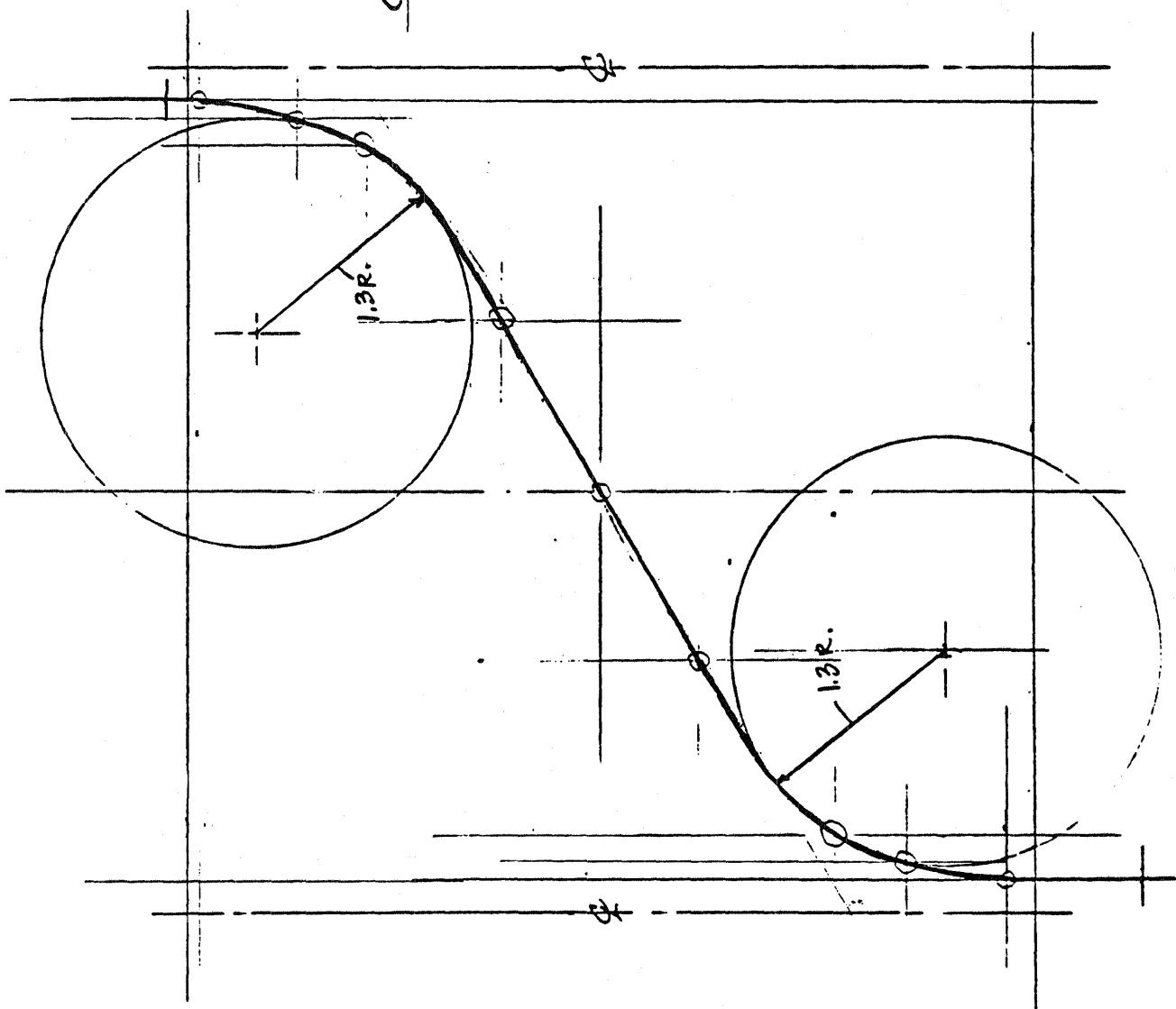


FIGURE 7.10 HEATER HEAD TUBE
TRUE VIEW PROJECTION
VIEW BB

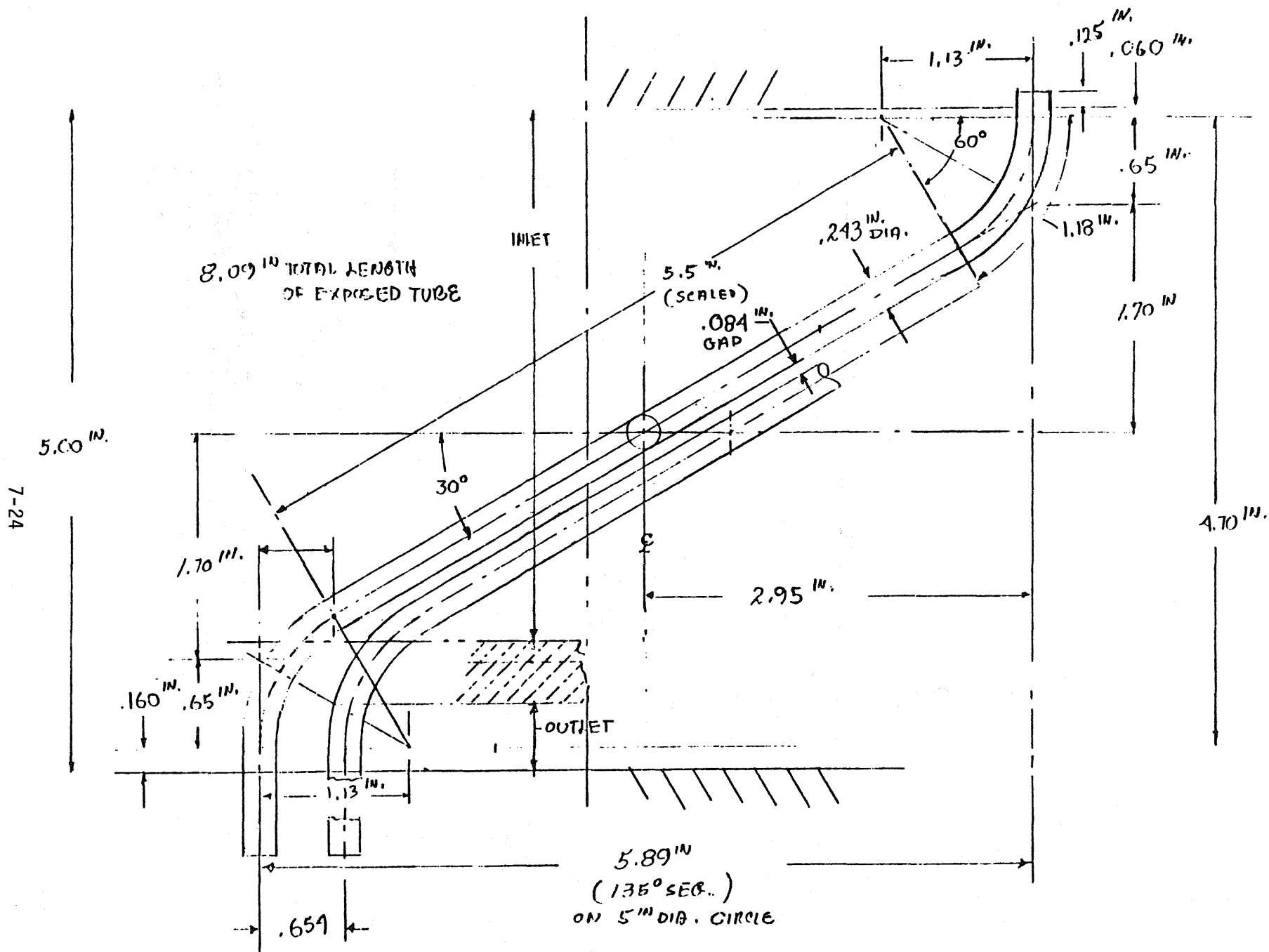


FIGURE 7.11 HEATER HEAD TUBE
PROJECTED FLAT PATTERN VIEW

7.3.5 LOAD CONDITIONS ANALYZED

The following load conditions were analyzed for both tube materials:

- Temperature difference acting on element = 500°F (260°C)
- Tube internal pressure = 3000 psi (21 MPa)
- Static solution

7.3.6 STRESS ANALYSIS RESULTS

The SAPV.2 program output has been included as Appendix III of this report. This output includes tables providing displacements, forces, and moments at the pre-assigned nodal points, plus top and side view plots of the undeformed and load deformed tubular shapes. Maximum stress levels at the various nodal points are obtained by combining the outputted forces and moments by use of Mohr's circle relationships. The maximum tensile and shear stress levels for the tubes were determined to be as follows:

Silicon Carbide Tube

- Maximum tensile stress = 19,740 psi (136 MPa)
at element no. 31, j-end.
- Maximum shear stress = 11,130 psi (77 MPa)
at element no. 32, j-end.

Silicon Mullite Tube

- Maximum tensile stress = 9,840 psi (68 MPa)
at element no. 31, j-end.
- Maximum shear stress = 5,660 psi (39 MPa)
at element no. 1, i-end.

The Silicon Mullite stresses are lower than the silicon Carbide stresses by a factor of approximately 2 to 1 since its modules of elasticity is lower by the same ratio, while its coefficient of thermal expansion is approximately the same.

The above noted maximum stress levels are considered to be within the realm of acceptable working stresses for the proposed ceramic heater head tubulars. Further insight into the acceptability of these materials for this application can be gained by completing a risk analysis via fracture statistics, to determine the mean fracture strength. It is recommended that this analysis be completed.

SECTION 8

PERFORMANCE MAPPING OF THE PROPOSED

CERAMIC AUTOMOTIVE STIRLING ENGINE DESIGN

8.1 INTRODUCTION

The performance map of the CASE design covers the entire range of acceptable speed and mean pressure conditions. The maximum and minimum mean pressure levels of the engine are 15 MPa and 3 MPa respectively. The minimum and maximum limits on the operating speed for ASRE are 500 and 4500 rpm respectively. The engine performance curves (indicated power vs. speed) are presented in Fig. 8.1 with constant indicated efficiency and constant mean pressure level lines. In order to obtain net power and net efficiency for the CASE system, one must subtract the auxiliary power consumption and the losses associated with friction and seals. The overall system efficiency must also include the efficiency of the external heating system. An extra power demand of 0.3 Kw at 4000 rpm and higher was also assumed for the V-belts.

8.2 PARASITIC POWER REQUIREMENTS

The parasitic power is required for the following items.

- EHS blower
- Water pump
- Alternator
- Lubricating oil pump
- Hydrogen gas compressor

Excluded from the auxiliary power demand for ASRE are the air conditioning compressor, power steering pump and the air atomizer compressor.

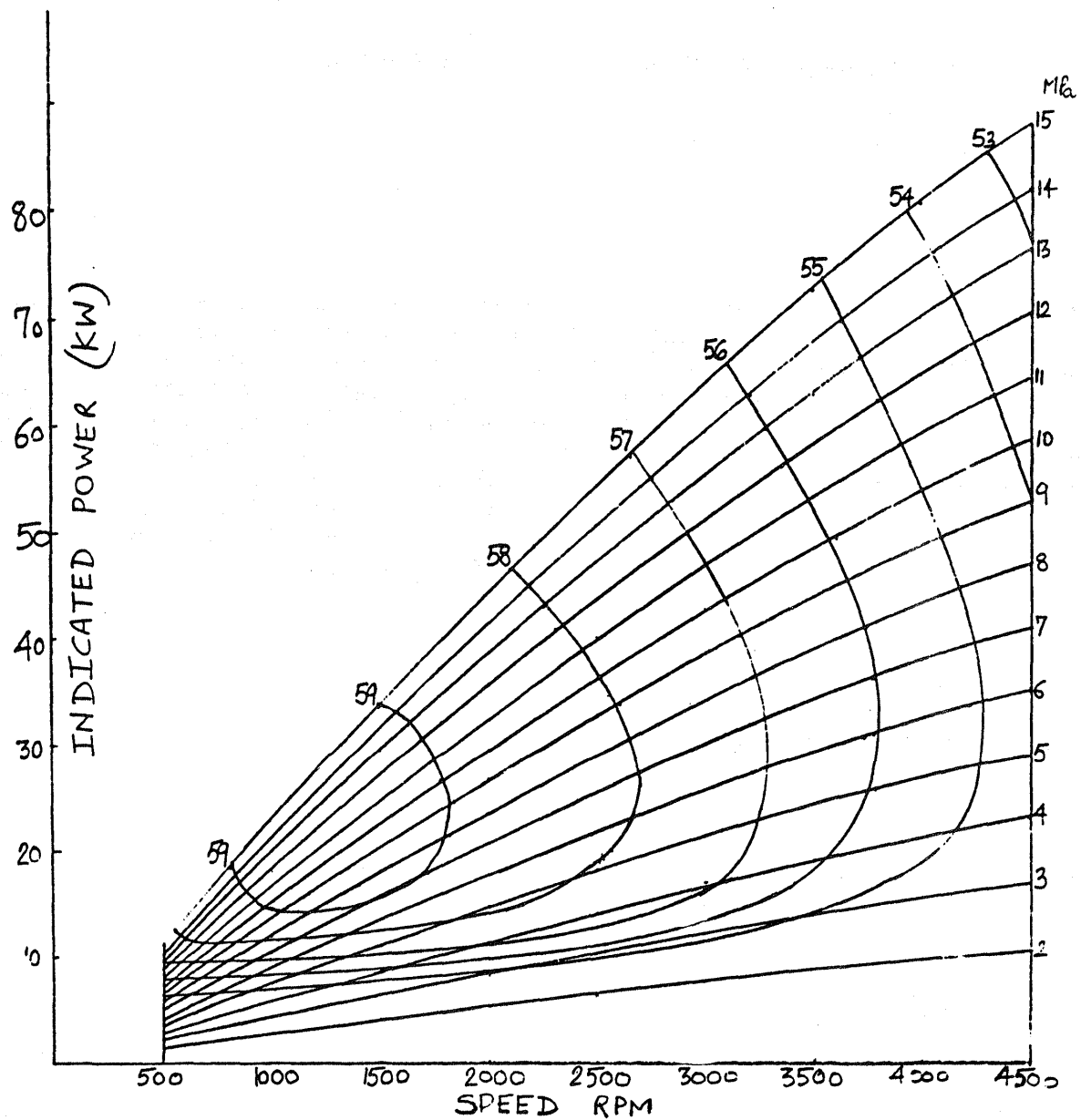


FIGURE 8.1 PERFORMANCE MAP OF CASE CURVES OF CONSTANT INDICATED EFFICIENCY (%) AND CONSTANT MEAN PRESSURE (MPa)

8.2.1 EHS BLOWER

The power required for the EHS air blower is calculated from:

$$P_b = \left(\frac{\Delta P}{\rho_a} \dot{m}_a \right) \left(\frac{1}{\eta_B \eta_v} \right)$$

where,

ΔP = Total air pressure drop (Pa)

\dot{m}_a = Air mass flow (kg/sec)

ρ_a = Air density 1.19 kg/m³

η_B = Blower efficiency

η_v = Variable ratio belt drive efficiency

The blower power as a function of air mass flow rate is presented in Figure 8.2 for ASRE design. For the calculation of blower power for CASE, same relationship is used assuming that the overall pressure drop in the external heating system is identical to ASRE design. The air flow required is calculated from the relation

$$\dot{m}_a = 4.11 * 10^{-7} \frac{P_i}{\eta_i} \text{ kg/sec}$$

to account for the reduced air flow requirement at higher indicated efficiency.

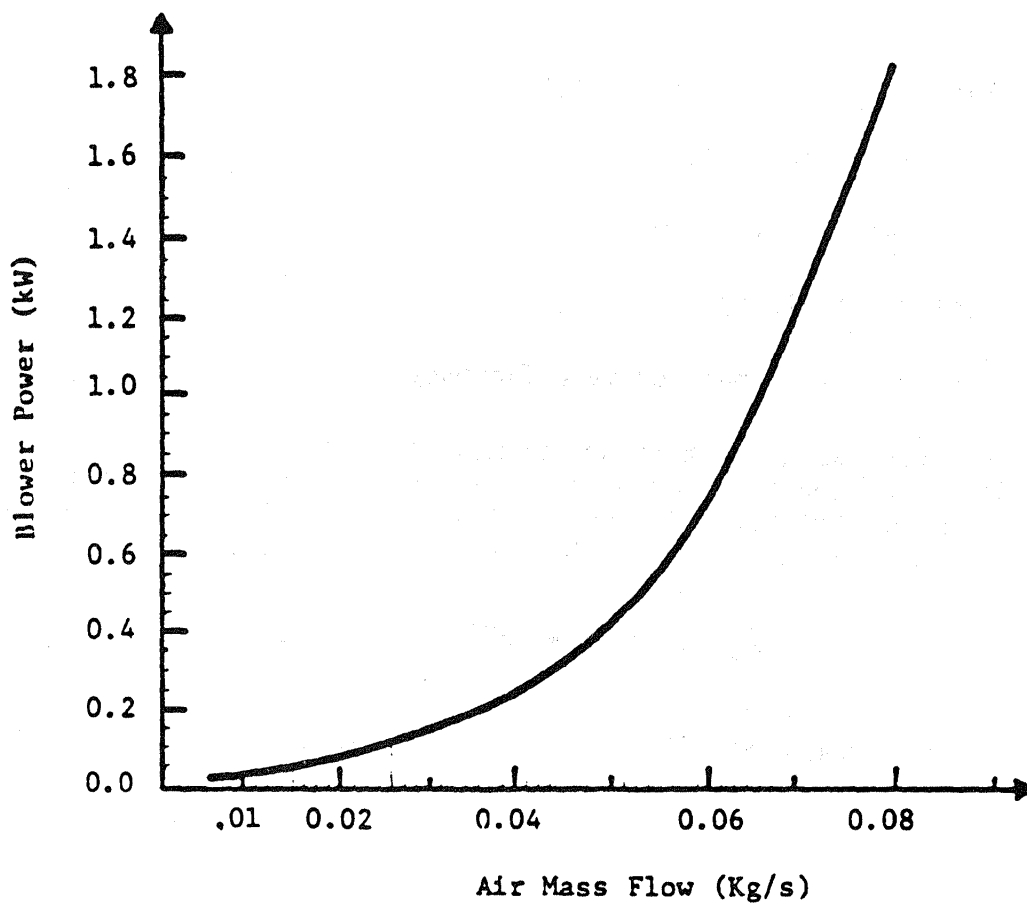


FIGURE 8.2 BLOWER POWER DEMAND

8.2.2 WATER PUMP

The power demand for the water pump is shown in Fig. 8.3 for the ASRE design as a function of engine speed. This power demand is based on the water flow requirement of 4.23 kg/s at full engine speed and load, and it must be proportionately adjusted to account for reduced heat rejection requirements for a more efficient engine. This is accomplished using the following relationship.

$$\frac{\text{Power 2}}{\text{Power 1}} = \left\{ \frac{\eta_{i1} (1 - \eta_{i2})}{\eta_{i2} (1 - \eta_{i1})} \right\}^2$$

8.2.3 ALTERNATOR

The alternator power demand is based on the following electric devices:

- Electronics
- Ignition
- Fuel pump
- Solenoid valves
- Fuel valve
- Air throttle

In addition to the above continuous power demand, there are intermittent power demands from the electric blower motor, starting motor, lights and radio, etc. This, however, does not affect the mileage calculations if a fully charged battery is assumed. Also, except for the fuel pump power requirement which is efficiency dependent, the power requirement for all the rest of the items is speed dependent. The power requirement of the fuel pump is relatively small; hence, its efficiency dependence is ignored. Thus, the overall alternator power demand is based on the curve in Fig. 8.4. It is, however, noted that the assumed power demand of the alternator for the ASRE design is much less than that given in this figure. Accordingly, the calculated power requirement for the alternator for CASE design is adjusted.

8.2.4 LUBRICATING OIL PUMP

The pump is used for pressurizing the lubrication oil for the main shaft and crank shaft bearings. This oil is also used to get rid of the generated heat from the seals. The power consumption curve for the oil pump is shown in Fig. 8.5.

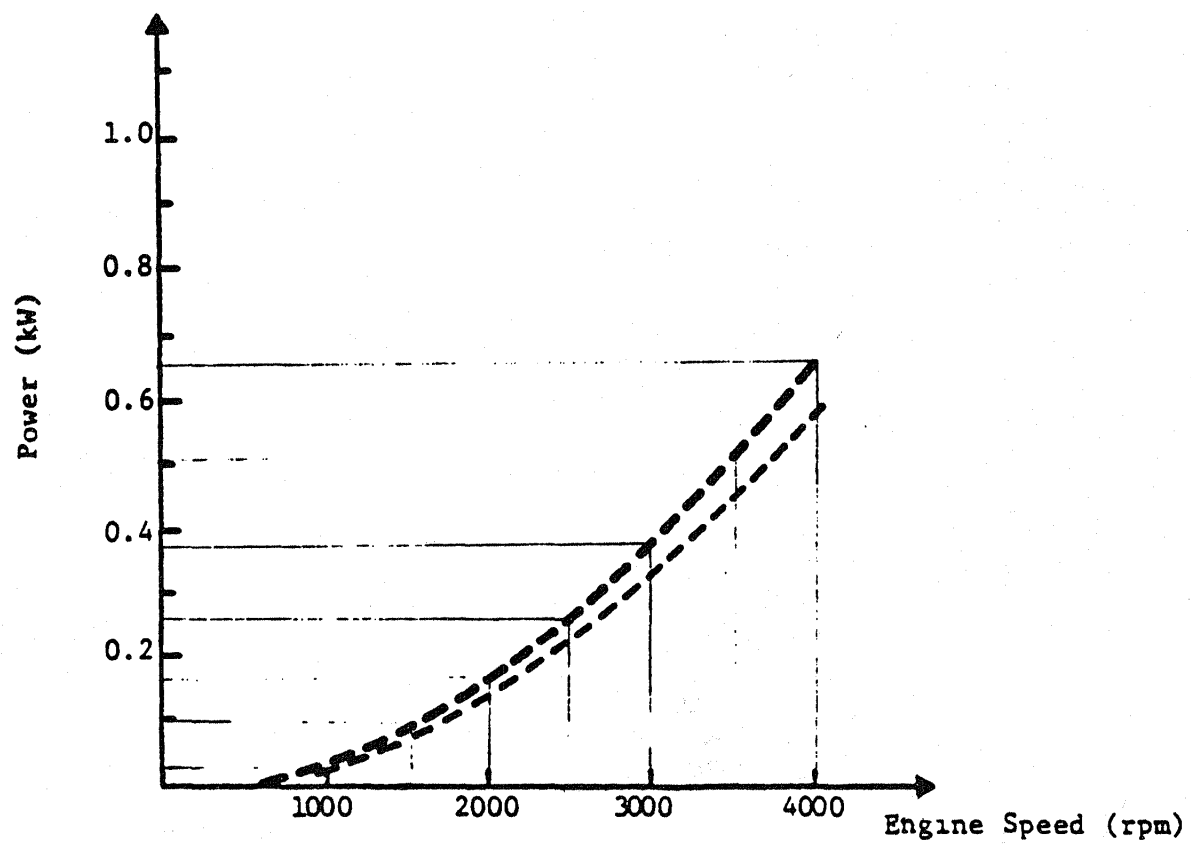


FIGURE 8.3 WATER PUMP POWER DEMAND

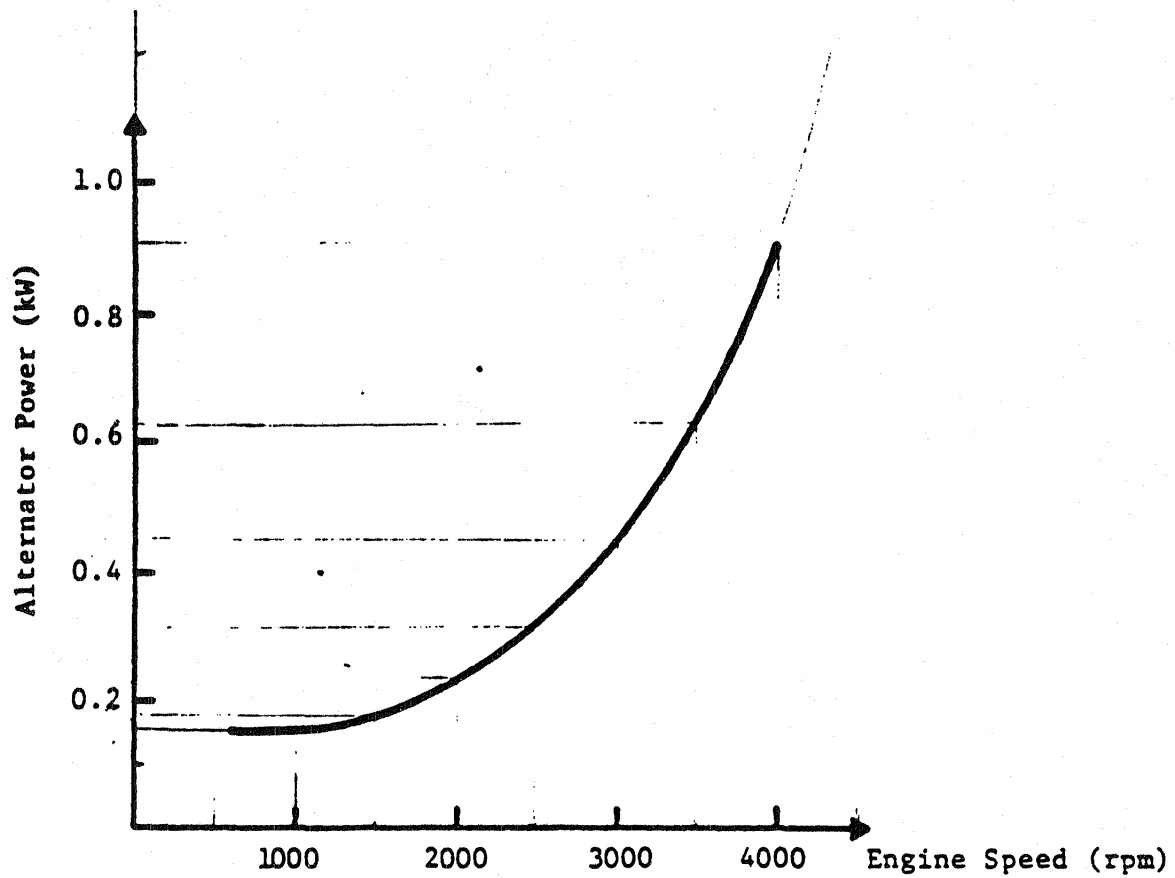


FIGURE 8.4 ALTERNATOR POWER DEMAND

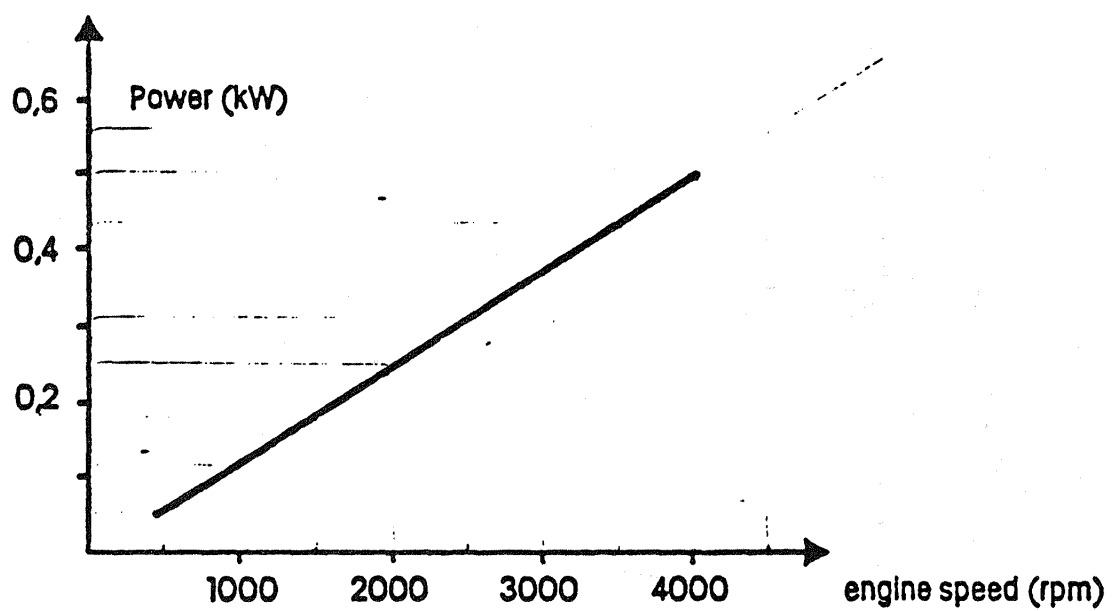


FIGURE 8.5 POWER CONSUMPTION - OIL PUMP

8.2.5 HYDROGEN GAS COMPRESSOR

The power consumption for the hydrogen gas compressor is shown in Figure 8.6.

8.3 FRICTION POWER

The mechanical friction losses for the MOD 1 engine are estimated based on experimental tests on P40 and P75 engines. This is a function of both the speed and the pressure level as shown in Figure 8.7. The friction power used for the performance calculation of the ASRE is less than shown in the above figure. The exact value depends on load condition and varies from 68% at full load condition to 52% at low load condition. An average of 60% of the value calculated from Figure 8.7 is assumed for friction losses for CASE design.

8.4 EXTERNAL HEATING SYSTEM EFFICIENCY

The efficiency of the external heating system assumed for ASRE design is shown in Figure 8.8. It is dependent on the heat input requirements of the engine. At a very low heat input rate, the efficiency drops because sufficient recirculation level cannot be maintained across the heater head. On the other hand, at high heat input rate, the efficiency drops due to limitations of the heater head design. It is one of the basic deficiencies of the ASRE design in that it relies almost entirely on convective heat transfer and hence on the available total mass flow rate. In the proposed CASE design, since most of the heat, especially at low load conditions is transferred by radiation, it is a function of temperature and not mass flow rate. Thus, the efficiency of the external heating system in the CASE design is expected to remain fairly uniform over the entire load conditions. It was shown earlier (Section 4.3) that because of higher temperature operation of the CASE, a penalty must be taken in the external heating system efficiency. Accordingly, a constant external heating system efficiency of 89% is assumed for the CASE design.

8.5 PERFORMANCE MAP FOR CASE

Figure 8.9 shows the performance of CASE as a function of speed. It is noted from the figure that whereas the load requirements under maximum efficiency and part load conditions can be met at speeds the same as ASRE design, at full load condition, the load requirement can be met at much reduced speed of 3300 rpm compared to ASRE design. This has the added benefit of reduced wear and longer life, and it may require rematching of the torque converter and overall optimization reference with federal driving cycle.

The performance of the CASE at four load points is compared with ASRE design in Table 8.1. It is seen that most significant gain occurs at full load condition for reasons cited before. A moderate gain of 10 to 15% is expected near the low load condition. It was projected earlier that additional gains in net efficiency can be achieved by going to higher heater head temperature. The loss in external heating system efficiency is more than compensated by gain in engine efficiency as shown in Table 8.2.

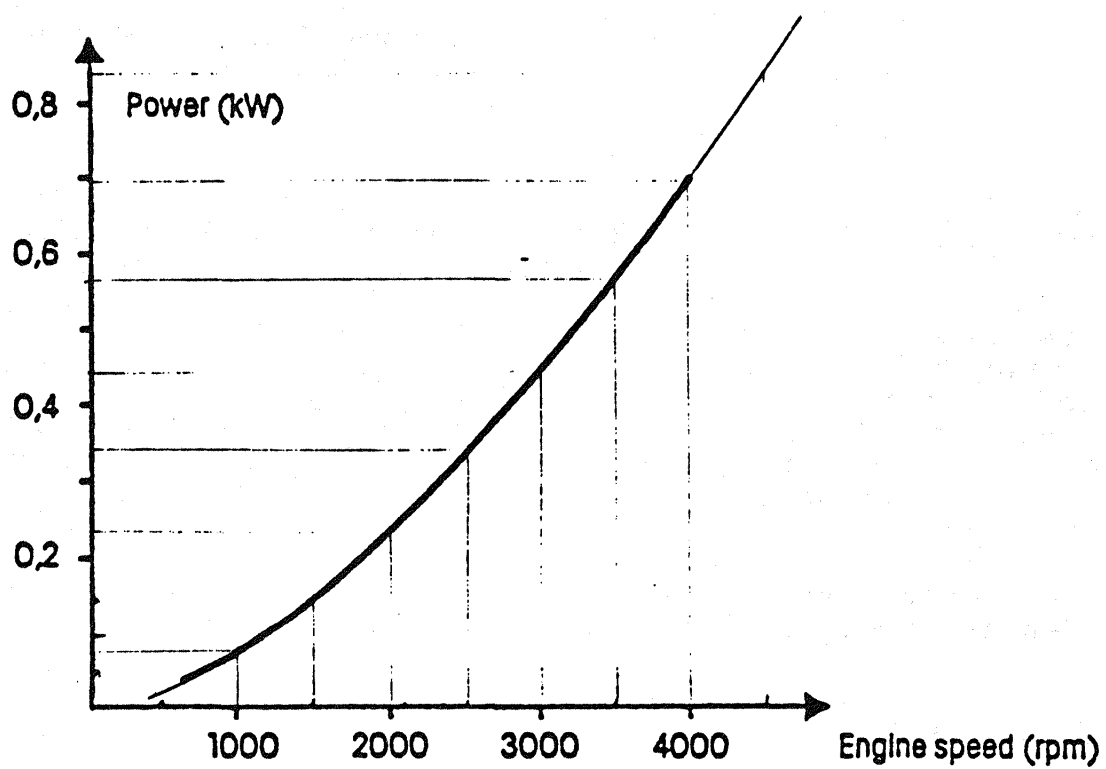


FIGURE 8.6 HYDROGEN GAS COMPRESSOR POWER CONSUMPTION

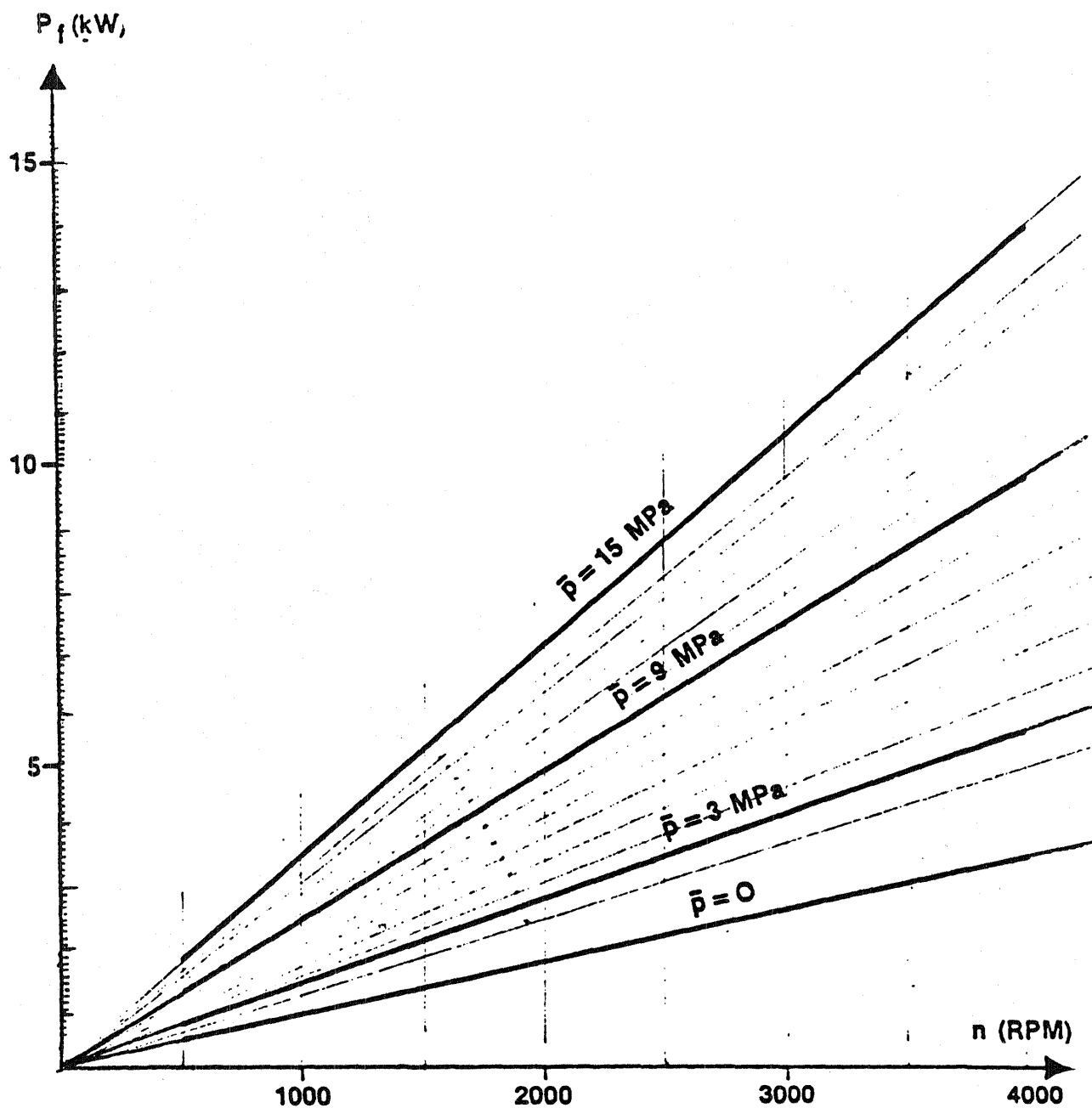


FIGURE 8.7 MECHANICAL FRICTION VERSUS ROTATIONAL SPEED, MEAN PRESSURE AS PARAMETER (H_2 WORKING GAS)

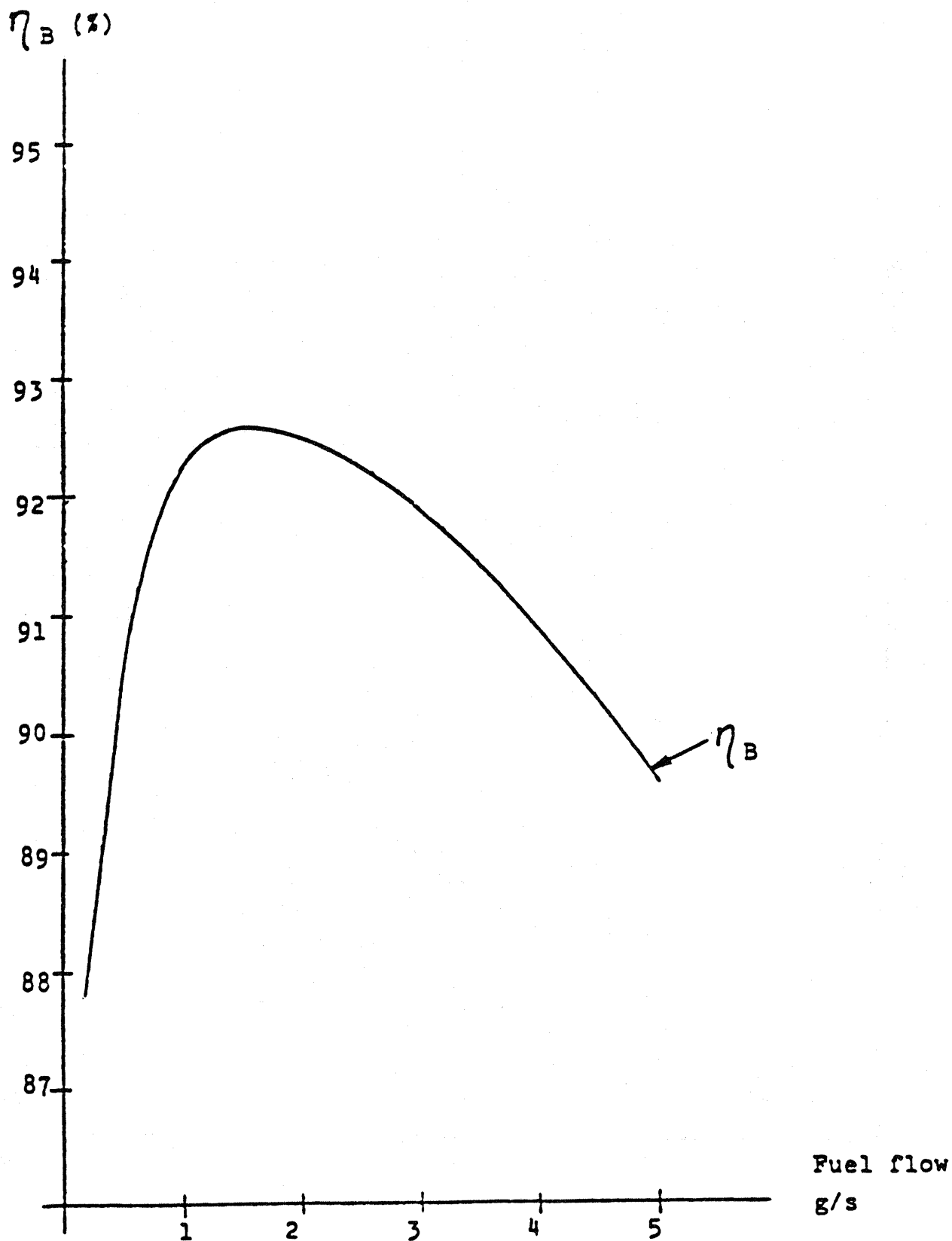


FIGURE 8.8 η_B VERSUS FUEL FLOW FOR ASRE

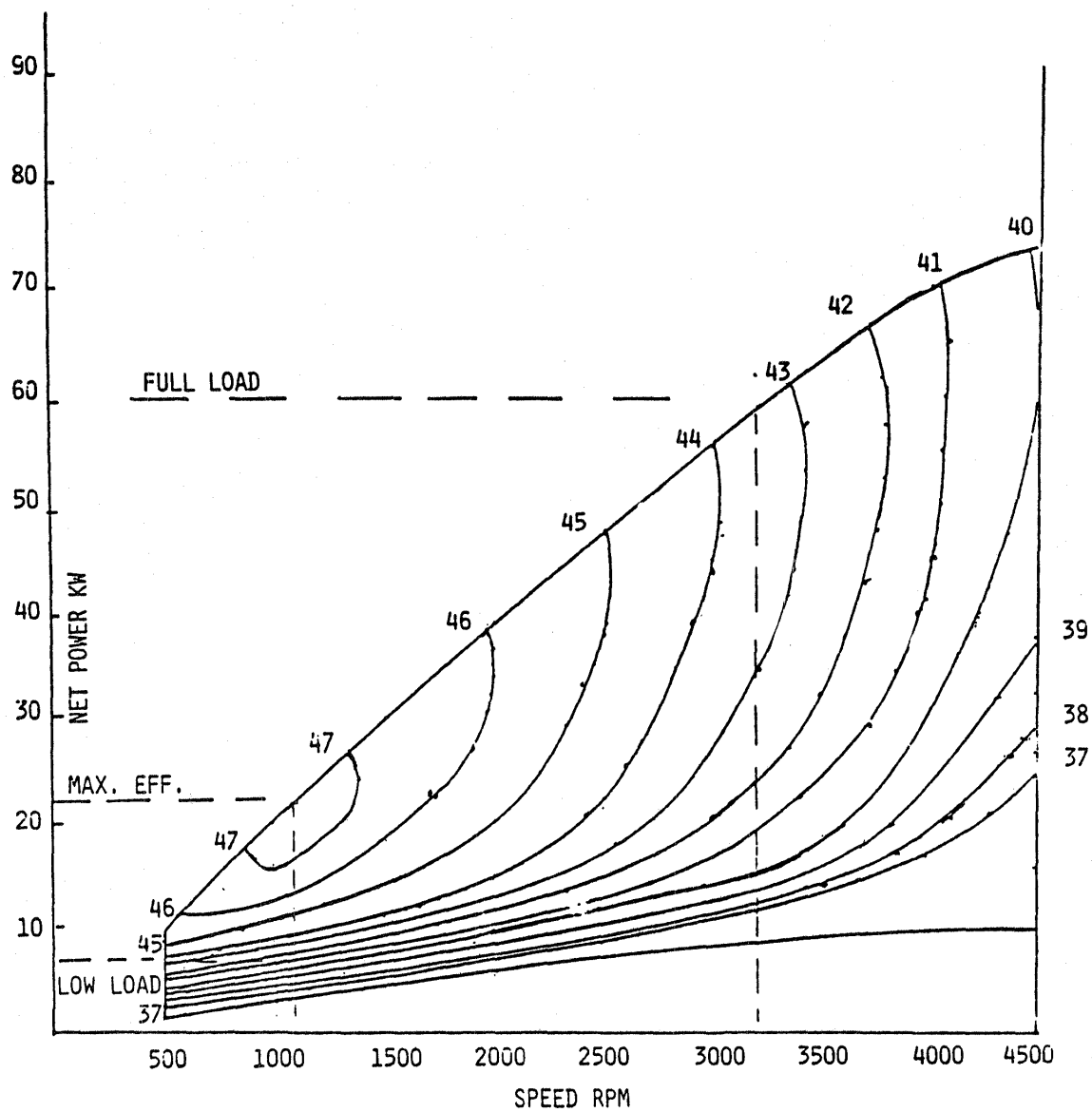


FIGURE 8.9 PERFORMANCE MAP OF CASE: CURVES OF CONSTANT NET EFFICIENCY (%)

TABLE 8.1 PERFORMANCE COMPARISON OF CASE AND ASRE DESIGN

		FULL LOAD		MAX. EFFICIENCY		PART LOAD		LOW LOAD	
		CASE	ASRE	CASE	ASRE	CASE	ASRE	CASE	ASRE
ENGINE SPEED	(RPM)	3300	4000	1100	1100	2000	2000	1000	1000
CHARGE PRESSURE	(MPa)	15	15	15	15	5	5	5	5
INDICATED POWER	(KW)	69.2	73.3	25.0	24.8	14.8	15.0	7.2	7.9
8-14 FRICTION	(KW)	6.9	9.6	2.2	2.2	2.0	2.0	0.9	0.9
AUXILIARIES	(KW)	1.8	3.6	0.3	0.5	0.7	0.8	0.3	0.4
NET POWER	(KW)	60.5	60.1	22.5	22.1	12.1	12.2	6.0	6.6
EXTERNAL HEATING SYSTEM EFFICIENCY	(%)	89	90.5	89	92.4	89	91.7	89	89.8
INDICATED EFF.	(%)	55.57	46.1	60.0	52.8	58.17	50.9	55.3	48.5
NET EFFICIENCY	(%)	43.2	34.2	48.1	43.5	42.4	37.7	41.0	36.4
PERCENTAGE GAIN OVER ASRE		26.3%		10.6%		12.5%		12.6%	

TABLE 8.2 CASES DESIGN POINTS AT MAXIMUM EFFICIENCY OPERATING CONDITIONS

NTU	TUBE °F	TEMP °C	PREHEATER EFFECT.	COMB EFF.	FLAME TEMP °F	EXH' ST TEMP °F	ENG. IND. EFF. %	$\frac{N_e}{N_C}$	PARASITIC PWR WRT ASRE		$N_{co}^* N_e$	% GAIN OVER ASRE	COMMENTS
									BLOWER	COOLER			
-	1500	820	0.87	0.91	3600	450-500	52.9	.75	1	.1	.48		ASRE DESIGN
3.3	1800	982	0.90	0.89	4100	563	60.0	.81	0.83	0.59	0.53	10.4	PRESENT DESIGN
4.0	1800	982	0.90	0.89	4100	563	61.8	.83	0.83	0.59	0.55	14.6	PRESENT DESIGN WITH ADD'L IMPROVEMENTS
4.0	1550	840	0.90	0.91	3800	488	57.2	.81	0.91	0.81	.52	8.3	EFFECT OF RAISING PREHEATER EFFECTIVENESS
4.0	1900	1038	0.95	0.91	4180	488	62.4	.83	0.76	0.53	.57	18.8	
4.0	2223	1217	0.98	0.91	4500	488	64.9	.83	0.71	0.66	.59	22.9	
4.0	1873	1023	0.90	0.89	4100	563	62.2	.83	0.80	0.55	.55	14.6	EFFECT OF RAISING COMBUSTOR EFFICIENCY
4.0	1698	926	0.90	0.90	3950	525	59.8	.82	0.85	0.66	.54	12.5	
4.0	1550	840	0.90	0.91	3800	488	57.2	.81	0.91	0.81	.52	8.3	
4.0	2000	1093	0.95	0.905	4260	513	63.6	.83	0.74	0.49	.60	25.	
4.0	2518	1381	0.95	0.88	4720	610	67.6	.84	0.70	0.35	.64	33.	

8.6 SUMMARY AND CONCLUSIONS

The performance mapping of the proposed CASE design was completed. The results are based on the auxiliary power losses and friction losses identical to those assumed for ASRE performance mapping. Credit is taken for savings in blower and coolant pump power losses because of improved overall efficiency level which results in reduced air flow and heat rejection requirements.

The results indicate that a net gain of 10 to 26% over ASRE design can be expected depending on the load condition. Most significant gain occurs at full load condition. It is noticed that because of overall improved performance, the maximum rated power of the engine (60 Kw) can be obtained at a lower speed of 3300 rpm compared to 4000 rpm for ASRE design. This has the added benefit of reduced wear and longer life, especially of the piston rings and seals. Further gain in net efficiency can be obtained if the heater head temperature can be further raised with the advancement in materials technology.

SECTION 9

CERAMIC PROCESSES

9.1 MATERIALS SELECTIONS

Materials selections for the key elements of the Ceramic Automotive Stirling Engine are summarized in Table 9.1. Heat transfer considerations led to the choice of mullite for the cylinder and regenerator housing and the displacer where, in addition to structural strength, low thermal conductivity is needed to minimize heat losses. The cylinder head, the heater tubes, and the mantle require high thermal conductivity as well as structural strength and, therefore, SiC was chosen for those components. In addition, a low thermal conductivity ceramic fiber core for the regenerator will reduce thermal losses. A commercially available alumino-borosilicate fibrous material was chosen for this element.

From the point of view of material integrity at high temperatures, the most critical component is the combustion housing where temperatures up to 3800°F (2093°C) must be sustained. A ZrO₂ coated Si₃N₄ is proposed for this element. In an oxidizing environment ZrO₂ is chemically stable up to 4800°F. A thin coating on the order of 20-30 mils is anticipated to reduce the temperature at the Si₃N₄/ZrO₂ interface to approximately 2500°F (1371°C), which the Si₃N₄ can tolerate. Due to a large difference in the expansion coefficients, a gradient bond will be required.

The air preheater choice was Si₃N₄ although SiC would also serve. Manufacturing problems and manufacturing costs will ultimately be decisive in this choice. The high thermal conductivities of the materials are needed for an efficient air preheater heat exchanger design.

<u>COMPONENT</u>	<u>MATERIAL</u>	<u>OPERATING TEMP °F</u>	<u>CRITICAL SELECTION CRITERIA</u>
<u>External Heat System</u>			
Air Preheater Matrix	Si_3N_4	1500-1800	HIGH THERMAL CONDUCTIVITY & THERMAL SHOCK RESISTANCE
Air Preheater Housing			
Insulation	Alumina-Silicate Fiber	2500-2800	HIGH TEMPERATURE DURABILITY
Combustor	Si_3N_4	2500-2800	THERMAL SHOCK CAPABILITY
Ejectors	Si_3N_4		
CGR - Valve	Si_3N_4		
Fuel Nozzles	SIS 2361 (Water Cool)		
Flame Shield	ZrO ₂ Coated Mullite	3200-3500	HIGHEST TEMPERATURE AREA, REQUIRES DEVELOPMENT OF COATINGS (ZrO ₂ MELTS AT 4800F) (MULLITE MELTS AT 3500F)
<u>Hot Engine System</u>			
Cylinders & Regenerator Housings	Mullite	1800-2000	LOW THERMAL CONDUCTIVITY, HIGH STRENGTH & FRACTURE TOUGHNESS
Heater Tubes	SiC } integral		
Tube Fins		1800-2000	HIGH THERMAL CONDUCTIVITY
Regenerator Matrix	Alumina-Boro-Silicate Fiber	1800-2000	LOW THERMAL CONDUCTIVITY (NEXTEL), HIGH SPECIFIC HEAT
Coolers	Aluminum		
Mantel	SiC	2200-2400	HIGH THERMAL CONDUCTIVITY
Displacer	Mullite	1800-2000	LOW THERMAL CONDUCTIVITY

FIGURE 9.1 CERAMIC AUTOMOTIVE STIRLING ENGINE MATERIALS

From the point of view of mechanical strength, the high temperature developmental structural ceramics are already approaching the 700 MPa modulus of rupture strength level. Advances in fracture toughness by composite technology and transformation toughening, as well as improvements in Weibull modulus, are anticipated in the 1990 technology base. In this conceptual design, stress levels below 25 kpsi (172 MPa) have been maintained. Not every component has been analyzed; hence, much design effort remains to be performed if the ceramic Stirling concept is pursued further.

The relatively low stress level allowed in this design may be too modest as the ceramic fabrication technology advances and performance of the structural ceramics becomes less susceptible to statistical variations.

9.2 PRODUCTION AND PROCESS EVALUATION (CASE)

The methods and equipment to produce the CASE in a quantity of 300,000 per year are estimated as we conceive them to be in the 1990's decade. Much of this equipment is not yet in existence, but based on present knowledge, we know that it is feasible to build when the demand arises for a large-scale ceramics processing industry.

9.3 GLOSSARY OF TERMS

Slip Casting - The process consists of suspending finely powdered raw material in a liquid (called a "slip") and pouring this controlled mixture into a porous mold (such as plaster of paris). The porosity of the mold permits absorption of the liquid in the slip, leaving a layer of solid material at the mold surface. The wall thickness of the part is allowed to build up on the inside wall of the mold and the excess "slip" is poured out. The thickness of each part is time/temperature dependent and the number of mold re-uses (limited to about 100 times) will change these parameters somewhat, so precise control of part wall thickness is difficult. This method does permit forming odd hollow shapes not achievable by other means.

Uniaxial Pressing - The process begins with the insertion into a mold of prepared dry powder, applying pressure to both or either end until the part is dense enough to be sintered. The process has a short cycle time and will permit accuracy within 1 to 2% of finished size. It is limited to short parts with a low length/dia. ratio. This is because uneven densification occurs due to mold wall friction if the mold becomes long in relation to cross section. Fairly close shape profiles can be faithfully reproduced.

Isostatic Pressing - This method allows the application of equal pressure in all directions to densify the powder. The piece is pressed in an elastic mold, sometimes over a metal mandrel if the part is hollow and cylindrical. The mold is immersed in a fluid which is hydrostatically compressed. The cycle time is longer than that for the uniaxial process. Relatively close tolerances can be held on the surfaces conforming to the inner mandrel, with only rough-shape profiles being held on the outer surfaces formed by the elastic mold.

Injection Molding - Is similar to the common practice of injection molding plastics, except harder, more wear-resistant dies must be employed. The ceramic powder is mixed with a plastic as a binder in twin-screw extrusion equipment, which can be set up to feed directly into injection molding machines or may be extruded into a rod, cooled, and pelletized for later reheating and processing.

In some cases a fugitive inner core may be needed to form complex shapes. This part can be made of thermoplastic and inserted in the mold prior to injection molding the ceramic mixture. After molding the part is now fairly dense, and may be handled and machined to gain closer tolerances or un-molded features.

After the injection molding is removed from the press, it requires oven drying at about 600°C to remove the plastic binders (and the fugitive core, if used). The part is now in a relatively fragile condition and is ready to be sintered at high temperatures to final size and density.

Electrophoresis Deposition - This process may be compared to a plating operation in which the electrolyte solution contains charged ceramic particles. The mold core on which the deposition takes place is a low-cost plastic injection molded part, made electrically conductive by carbon-coating or other means.

The core is immersed in a solution of charged ceramic particles which are deposited on the core surface until sufficient wall thickness is built up. The coated core is removed from the bath, dried, and oven baked to melt out the core, leaving a green ceramic part, which is ready for final sintering.

The process has the advantage of allowing unusual part geometry without the difficulty of outer mold release and removal.

Tape-forming-doctor blade - A thick slurry of ceramic powder mixed with thermoplastic materials in a twin screw extruder is deposited on a moving belt or carrier substrate such as cellulose acetate. The slurry is spread behind a knife edge which can be notched or shaped to produce a ribbon of controlled cross section on the carrier. The part can be cut off to predetermined lengths by a flying shear. Portions of the cross section can be altered on localized areas of the part by automated machinery before the tape-form is completely dried.

The piece is carefully dried as the belt progresses and is subsequently placed on conveyORIZED handling equipment to carry it through the sintering furnace. The cellulose carrier belt is vaporized in the final operation.

Plasma Spray Coating - In this process a flow of inert gas such as argon is directed through a nozzle, which contains high voltage electrodes. Most of the gas flows through the arc and is heated to very high temperatures (15,000°C) and accelerated to supersonic speed. A part of the gas is used as a cooling layer next to the nozzle wall. Powdered zirconia introduced into the arc is melted and accelerated in the supersonic gas plasma. When the melted particles strike the ware, they impact and cool into a high purity coating. The spray is usually a spot about 1.0 to 1.5 inches diameter at a working distance of 3 inches. Consequently, a moving head or moving workpiece is needed to traverse all areas to be coated.

9.4 MANUFACTURING PROCESS AND COST ANALYSIS

An approach for the manufacture of ceramic Stirling engines in quantities of 300,000 units per year as well as an estimate of unit costs are presented in Sections 10 and 11.

SECTION 10

MANUFACTURING PROCESSES

10.1 INTRODUCTION

This section describes the processes which are envisioned for the manufacture of the CASE I ceramic Stirling engine.

Initially, based on the primary design (Figure 10.1) a parts list was completed, along with an assembly tree. Each part was rough-sketches and scaled dimensions applied.

In addition, three assembly flow-charts were made which show the assembly sequence of the top end of the engine. These are diagrammatic layouts of an assembly line showing the order of parts build-up as the engine progresses to final form. Figure 10.2 illustrates the main assembly, while figures 10.3 and 10.4 show major subassemblies, cylinder heater head, and cold-side components respectively.

Figure 10.5 shows the cylinder heater head assembly for which the assembly procedure is depicted in Figure 10.3. Similarly, 10.6 shows the cold side components assembly for which the assembly procedure is represented in Figure 10.4.

The manufacturing process was defined for each part, giving consideration to its shape, quantity required, and material from which it is made. At the same time, the capital equipment required, and an estimate of capacity,

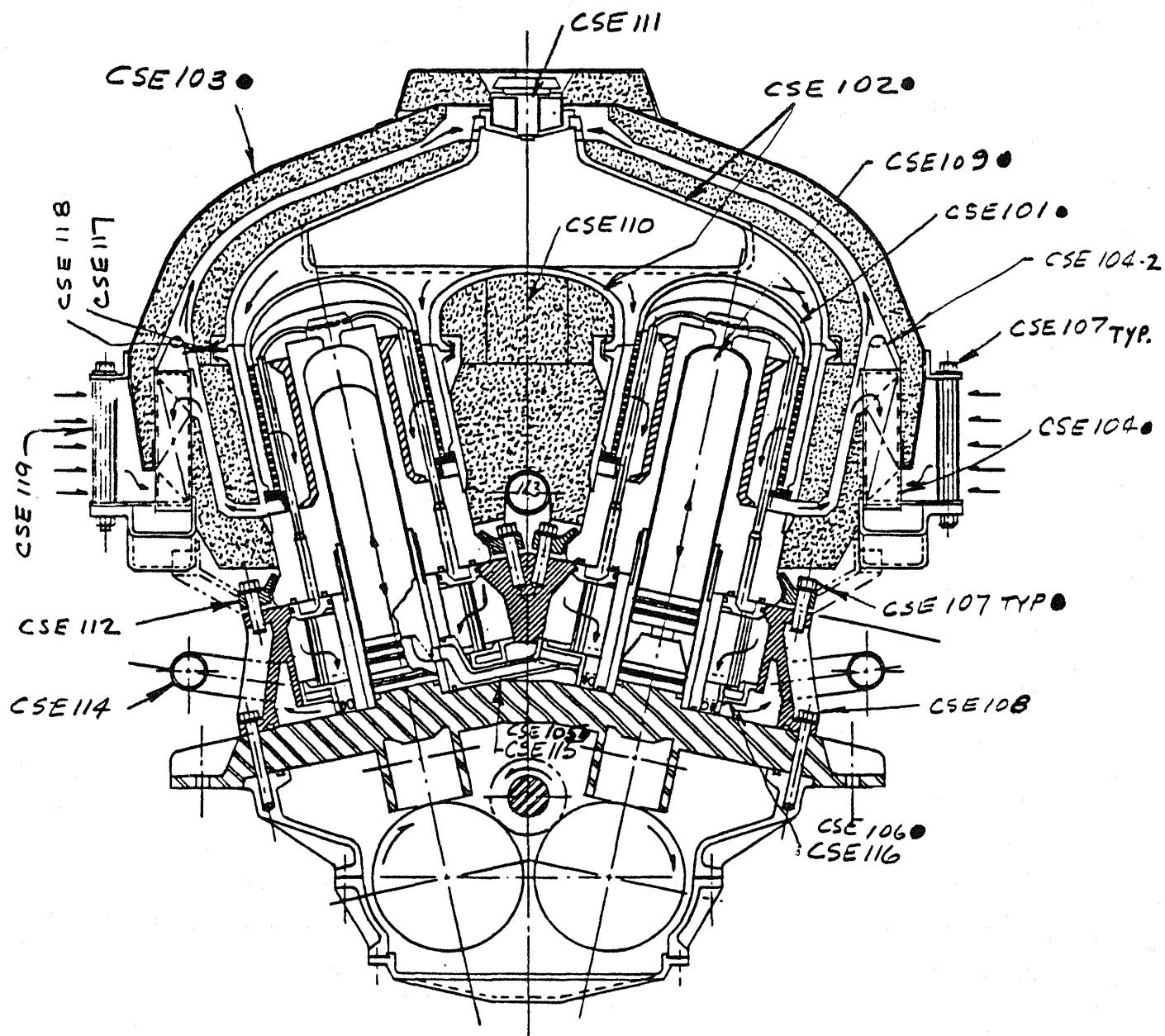


FIGURE 10.1 CERAMIC AUTOMOTIVE STIRLING ENGINE
10-2

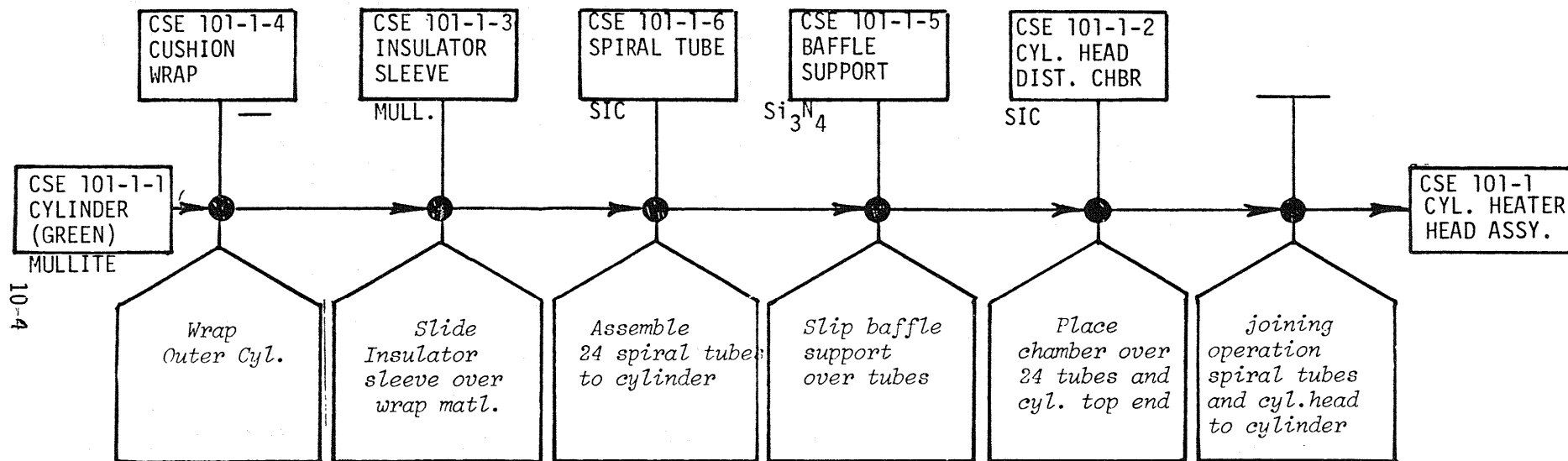
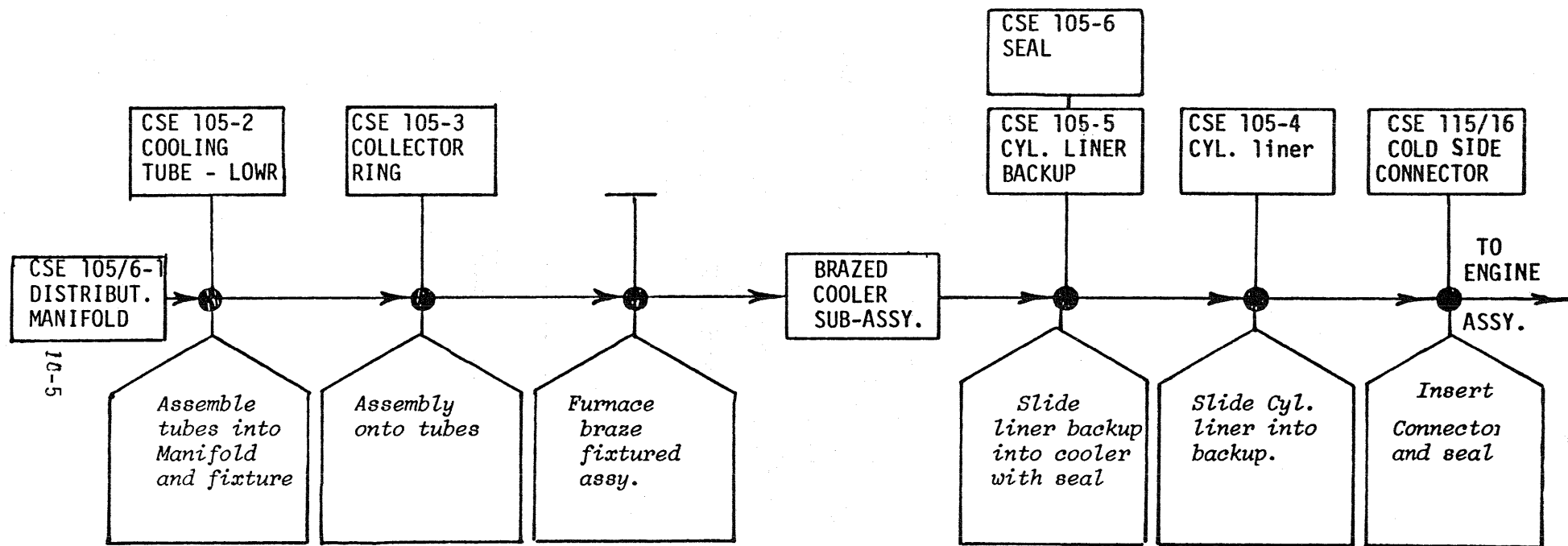


FIGURE 10.3 CSE 101-1 ASSEMBLY



MANUFACTURING FLOW CHART

FIGURE 10.4 CSE 105/6 - COLD SIDE COMPONENTS AND CYLINDER LINER

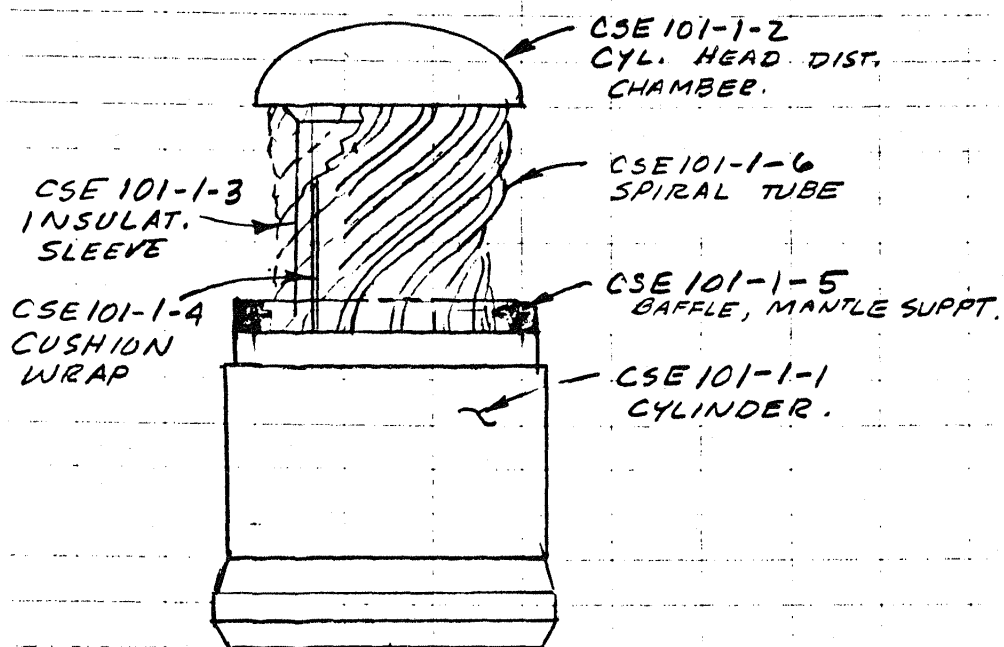


FIGURE 10.5 CSE 101-1 CYLINDER HEATER HEAD ASSEMBLY

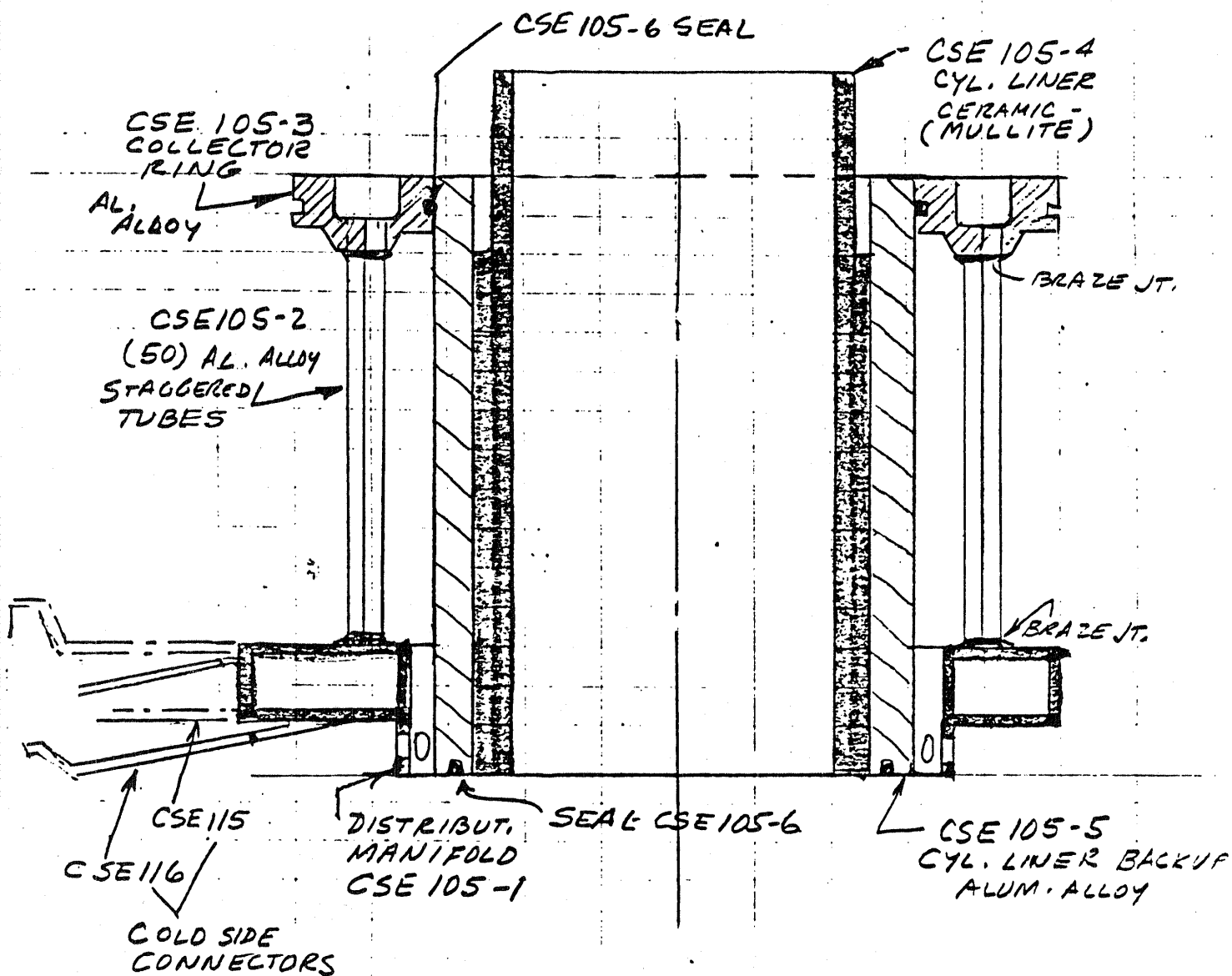


FIGURE 10.6 COLD SIDE COMPONENTS ASSEMBLY

physical size, and cost was made. In general, because of the production volume levels needed, most of this equipment will be dedicated. That is, only one part will be produced on that facility.

As a general case, the nature of these processes will require around the clock operation, with some portion of that time allocated to maintenance of the facilities.

For ceramic parts then, roughly the following baseline figures were used:

- 300,000 Engines/Year
- 300 Production Days/Year
- 20 Hours/Production Day
- 6,000 Production Hours/Year
- 1,000 Engines/Day
- 50 Engines/Hour

For the cost analysis (Section 11), labor costs were estimated in hours per unit or per 100 units, and hourly costs applied in 1984 dollars, at industry rate. Capital Equipment Investment and tooling expenditures were also estimated in 1984 dollars, material costs were estimated at volume rates, and appropriate scrap rates applied where the process requires reasonable losses to various causes.

10.2 DETAILED PARTS ANALYSIS

Detailed sketches of the major ceramic components are shown in Appendix IV. Included on each drawing are the selected material, piece part volume, and piece part weight. For each part, a process was then defined upon which the piece part cost was estimated. Table 10.1 lists the individual parts, quantity per engine, material selection, volume and weight of each.

10.2.1 MANUFACTURING PROCEDURES FOR PIECE PARTS

The following is a brief discussion of the manufacturing procedures applied to each ceramic part. The considerations of size, production rates, and some space requirements for processing are given that determined our final estimates for costing each piece found on the Manufacturing Summary Sheets.

CSE 102 - COMBUSTION CHAMBER - (SiC - 1 per engine)

General - This is by far the largest and one of the most difficult parts to handle, due to its unusual shape. It is this size/shape which has led to the choice of slip casting as the primary fabrication method. The inner surfaces of the part are subjected to 3,600°C temperatures in service, necessitating a coating of zirconia by plasma spray methods, utilizing revolving heads that extend through the five openings.

Slip casting requires the use of plaster of paris molds which have a life expectancy of 100 castings each. A recycling and renewal system for the molds is necessary to maintain continuous production.

Process Details

1. Mixing - Two mixers having a capacity of 700 lb/hr. each and occupying 200 sq. ft. of floor space are required to prepare the slip material for pouring into molds.
2. Pouring - With the given rate of 50 parts/hr, about 25 molds will be active at any given time, given the following pour-process times:
 - a. Pour mix in plaster mold - 5 min.
 - b. Wait for absorption of liquid into mold walls - 5 min.
 - c. Pour excess slip out of mold - 5 min.
 - d. Await solidification of residual slip - 10 min.
 - e. Remove mold from part - 5 min.

TABLE 10.1 CASE 1 MATERIAL WEIGHTS HEATER SYSTEM

PT. NO.	NAME	WT. (EA.)	QTY/ENG.	WT. /ENG		MATERIALS
				LB.		
CSE 102	COMB. CHAMBER	29.05	1	29.10		Si ₃ N ₄
CSE 101-2	CYL. OUTER SLEEVE	6.18	4	24.72		Si ₃ N ₄
CSE 101-1-1	CYL. HEATER HD.	14.50	4	58.00		MULLITE
CSE 101-1-2	HTR. HD. DIST. CH.	2.53	4	10.12		SiC
CSE 101-1-6	HEATER HEAT TUBE	.15	96	14.10		SiC
CSE 109	DISPLACER	.77	4	3.08		MULLITE
CSE 109A	RADIATION SHIELD	.04	12	.48		MULLITE
CSE 101-3	INSULTAING SLEEVE	1.50	4	6.00		MULLITE
CSE 101-3	RAD. MANTLE DOME	2.15	4	8.60		SiC
CSE 101-5	MANTLE-BAFFLE	.13	4	.52		Si ₃ N ₄
CSE 105-4	CYL. LINER	1.66	4	6.64		MULLITE
CSE 104-1	PRE HEATER PLATES	.035	800	<u>28.00</u>		SiC
TOTAL				<u>189.66</u>		

WEIGHT BREAKDOWN BY MATERIAL (LB)	Si ₃ N ₄	MULLITE	SiC
	54.34	74.2	61.12
SPECIFIC HEAT BTU/16°F	0.17	0.275	.186

TIME CONSTANT $\tau = \frac{\rho_c V}{h A}$ FOR MULLITE PARTS SIGNIFICANTLY LONGER THAN OTHERS.

3. Drying - A controlled-humidity dry cycle for 24 hours will require storage space for 1,000 parts. These will be stacked 5 high by 2 wide on rollaround carts. The humidity controlled room must hold 100 carts occupying 32 sq. ft. each. The total space needed will be 9,600 sq. ft., including handling areas and aisles.
4. Mold Handling, Drying Ovens - The molds will be split in two; occupying about 32 sq. ft. each.
 - a. Two re-drying ovens at 150°C having a 2 hour cycle that can process 50 molds per hour are needed.
 - b. The oven size will be 32 ft² by 50 molds = 1,600 ft² each and should be 8 ft wide x 200 ft long for optimum continuous use.
 - c. Additional loading/handling space of 1,600 ft² will be required.
 - d. New molds will be required after 100 cycles.
5. Sintering Operation - The furnace will require approximately a 4-hour cycle (a 2-hour rise from ambient to 1,900°C, dwell 1/2 hour, cool to 1,200°C 1/2 hour). This furnace will be continuously fired, having a nitrogen (Inert-gas) atmosphere evacuated to 100 microns. Such a furnace, complete with conveyors, parts setters and auxiliary equipment will cost 3 million dollars and will occupy 4,480 sq. ft. of space. (Similar furnaces will be used for other SiC and Si₃N₄ parts.)
6. Grinding - The part is designed so that five surfaces must be held within close relationship to each other. The four cylinder sealing areas, and the fuel-injector surface. These will be ground simultaneously on automatically controlled Blanchard type grinding equipment that can take plunge-cuts along the frontal planes of the engine, thus assuring the angularity of the cylinder sealing surfaces and spacing to the injector location. Two machines running 25 parts per hour each (or two minutes/part) are needed.
7. Plasma Spray Coating - The surface volume of CSE-102 is 940 in² at .03 in. thick, or 28 in³. Weight of zirconia to be applied per part: 28 in³ x .21 lb/in³ = 6.1 LB. Number of nozzles required:

6.1 LB/Min x 60 Min/Hr, using a 10 LB/HR nozzle = 37 nozzles

Therefore, from the above calculation, we will require eight five-nozzle stations to produce 1 part per minute. Each of these is estimated to cost about 1 million dollars complete with programmed robotic controls, and all peripheral handling equipment. Approximate floor space for such equipment is 2,048 ft² and with adequate service and loading facilities, will need 6,100 ft² of plant area.

CSE 101-2 OUTER SLEEVE - (Sic 4 PER ENGINE)

General - The geometry of this part will be nicely suited to the isostatic pressing process and will permit the forming of two pieces at a time, top-to-top. After pressing, and while in the unfired condition, the pieces are gang-cut apart, accurately determining the "green" length. Outside details of this part are not critical, and the inside is formed against a steel mandrel. Final grinding in the dense form may be needed to assure a close fit of the internal step area. Because of service temperatures, the part is plasma-coated with zirconia on inside surfaces.

Process Details

1. Powder preparation - Ball mill to specification.
2. Isostatic pressing - Each press will have a cycle process time of about 1 minute. Therefore, we will require two presses, producing two parts per cycle to achieve the required rate of 4 parts/minute.
3. Green Cutoff/Grind - Two grinding machines, with a cycle time of 30 sec. are needed to separate the pressed parts and trim the inside step of each end.
4. Sintering Furnace - A similar furnace to that used for the CSE 102 Combustion Chamber will be required. The operating temperature cycle will be different because a 3 hour bake period at 600°C will precede the 1900°C sintering process. Total time cycle will be about 5 hours.
5. Dense Grinding - The part must be final-trimmed to length so that all four sleeves mate with CSE-102 Combustion Chamber. The step area inside has to be located precisely with respect to the sealing surfaces at the other end of the part, and must seat closely on CSE-101-1-1 cylinder heater head.
6. Zirconia Plasma Spray - Equipment somewhat like that used to plasma spray the CSE-102 Combustion Chamber will be used for this operation. The fixturing set up for the nozzles may be simpler because the parts are right circular cylinders.

Each sleeve has an inside area of 60 in.² and will be coated .03 in. thick, for a zirconia volume of 1.8 cu. in., which weighs .4 lb. At a nozzle rate of 10 lb./hr., it will take 2.4 minutes to coat each sleeve. Since we need four parts per minute, ten spray heads will be used. These will be program controlled rotating heads spiralling up and down through the center of the cylinders, or stationary heads, with the sleeve parts being rotated.

CSE 101-1-1 CYLINDER HEATER HEAD (Mullite - 4 PER ENGINE)

General - The shape of this part lends itself well to the isostatic pressing process. There are many details on this piece that must be controlled to close tolerances, requiring attention to the grinding/machining processes that follow initial forming. Being made of mullite, a different type of furnace will be needed, using air atmosphere (instead of the nitrogen used on the SiC and Si₃N₄ parts.) Such a furnace will cost more because the heating element must be protected from consumption in the presence of the oxygen, which is necessary to sinter the mullite.

Process Details

1. Powder Processing - Ball milled material to specification.
2. Isostatic Pressing - The size and shape of this piece will dictate the use of 1 part per press cycle of 1 minute each. Therefore, four presses are needed to maintain the desired rate. The inner shape will be fairly well defined because of the steel tool mandrel, but the outer surfaces will be approximate.
3. Green-State Machining - The part may be handled and machined readily in the unfired condition with single-point tools. The outer contour may be trimmed to shape, as required. The regenerative matrix cavity will be turned at this time.

A drilling operation to produce 12 holes, then index will be needed to yield the 24-hole receptacles for spiral tube assembly.

4. Bake Out/Sintering - A continuous processing air-atmosphere oven/furnace will bake out binders and dry the green part at 500°C for 2 hours. The temperature will then rise to 1750°C for a 2 hour sintering cycle. Total cycle time will be 5 hours, including heating and cool down periods at the beginning and end of the process.

The size of this processing system will be about the same as the nitrogen atmosphere furnaces previously discussed.

5. Dense Grinding - The details defined in the green state will be reduced after firing, but may not all be within required tolerances for this part:
 - a. Machine grinding will be required to finish the inside shape and stepped areas - 4 machines having a cycle time of 1 minute each part.
 - b. Machine grind the area that fits the CSE 101-1-2 heater head cap, and the outside shoulder that mates with the sleeve CSE 101-2, 4 machines required.
 - c. The 24 holes will be gang-drilled (12 per pass) to final diameter for the tube-end sockets.

CSE 101-1-2 CYLINDER HEAD DISTRIBUTION CHAMBER (Silicon Carbide - 4 PER ENGINE)

General - The intricate (for ceramics) shape of this piece with its 24 curved passages will require the use of a fugitive (lost wax) core. To minimize the amount of dense-grind machining that might otherwise need to be done, injection molding is the choice for fabrication.

Process Details

1. Mixing - The dry silicon carbide powder is intimately mixed with a heated thermoplastic vehicle using a twin screw extrusion machine of the type often used in the reinforced thermoplastics industry. The capacity required will be 2.5 lb/part times 4 or 10 lbs. per engine. At 50 engines per hour we will need a capacity of 500 lb/hr. The factory arrangement will be for two machines to feed the injection mold machines directly with hot mixed material.
2. Injection Molding
 - a. Fugitive Core Molding - This part will be small, molded of polyethelene, and will resemble a "spider", having 24 legs that define the internal features. The cycle time for this part will be short (about 30 sec.) and a 4 cavity die can be used so that only one machine will be needed to make 200 pieces per hour.
 - b. Part Molding - The core "spider" pieces will be hand-placed in a four-cavity die. The injection molding machine will be fed with material directly from the extruder-mixer. Cycle time for this part, and with the ceramic material is longer than for normal thermoplastics, about 4 minutes each. Four machines are required to meet the rate of 200 parts/hr.

3. Oven Dry and Core Removal - A seven-day (168 hour) bakeout cycle at 600°C in evacuated ovens is done to remove the thermoplastic vehicle and the spider core material from the as-molded part. Approximately 28,000 pieces will be in-process at any given time.

Such ovens will accommodate about 1400 parts (1 shift output) at a time, each oven being about 8 ft. in diameter and 10 ft. long. Twenty ovens will be needed to accommodate all parts in process. The parts being loaded will be reasonably strong, but after bakeout, they will be fragile and require careful handling. These parts are still green, not yet having been sintered.

4. Sintering - A continuous, inert nitrogen atmosphere 2100°C furnace similar to that used for CSE-102 combustion chamber et al will be used for sintering these SiC pieces. A short, 2 hour cycle may be used, 5 loads per day of 800 parts each will yield the necessary 4000 pieces per day.
5. Final Dense Machining - Tolerances to within 1/2% will be realized on the injection molded piece, which will be satisfactory over most of the part, with the exception of the inside diameter to fit CSE 101-1-1 Cylinder Heater Head. A dense-grind operation to true-up this area and to ream the 24 hole tube sockets will require two grinders to finish the part.

CSE 101-1-6 SPIRAL TUBES

General - The configuration of these parts is such that the usual process methods are not practical. A degree of accuracy must be attained in respect to locating the end points of these tubes, as well as keeping a reasonably uniform spiral shape so there is no difficulty in assembly or final positioning. Since 24 of these are used per cylinder (96 per engine) the process must yield nearly 20,000 parts per day (500 per hour, 100 per minute). The manufacturing following process described is untried but feasible, as the elements in this technique are all used in other industries.

Process Details

1. Injection Mold a spiral core "cage" from polyethelene. The spiral tube inside diameter and the shape of the 24 tubes will be defined by this cage. The spirals are connected at top and bottom by circular rings which may be split to permit easy release of this part from the die. After mold release these are rejoined by ultrasonic welding or other means. Two injection-molding machines using two-cavity dies will produce cores at a 15 sec. cycle rate.

2. Carbon Coating - The cores must be made electrically conductive. The simplest way may be to load (mix) the core material with enough carbon to accomplish this, but there are portions of the core that we do not wish to be conductive. Therefore, we have chosen to dip-coat the cores in a carbon solution, which may conveniently be done on a conveyor-rack system, and then selectively remove the carbon from unwanted areas.
3. Localized Carbon Removal - The coating must be removed at the top and bottom surfaces of the core rings so that ceramic material is selectively not plated out on these areas in the subsequent operation. This will leave the tubes open and a place for the melted core to run out when it is removed later.

The carbon-cleaning is done automatically on the conveyor by passing the core cage through rotating abrasive surfaces spaced a precise distance apart.

4. Electrophoresis Process - This equipment will consist of a vat containing a conductive slurry of silicon carbide. Controls must be applied to the bath to assure continuous quality of the slurry (i.e., - conductivity, acidity percent solids). A recirculation-makeup system will be required to sample and maintain the properties in the vat solution. The same conveyor used through carbon coating processing will be continued in the Electrophoresis deposition bath.
5. Drying - Melt Out Cycle - Humidity-controlled environmental conditions are to be provided while the green ceramic-coated core-cage dries out for one hour. This process is continued on the same conveyor line that transported the parts through carbon coating, selective removal, and Electrophoresis coating. The conveyor system is designed to carry 4 core-cages abreast each of which may be spaced one foot apart. Thus, a line rate of one foot per minute will yield the required production rate, and a drying tunnel 60 feet long will be sufficient (or shorter, if the line is looped within a wider oven).

Toward the end of the drying cycle, the temperature is raised to 150°C to melt out the thermoplastic core, and the green ceramic cage is carefully removed from the conveyor and placed in setters for the sintering furnace.

6. Sintering - A furnace similar to those described for the other silicon carbide parts will be used to sinter the spiral cages.

7. Cut Off and End Machining - A very close fit is required for the ends of the spiral tubes into the mating sockets that have been machined into the heater head and distribution chamber. Care must be exercised in machining the tube ends so that no stresses are imposed due to misalignment of the end points.

The tubes are first separated from the end rings of the core cage by precisely spaced cut-off grinding wheels. Two grinders, having a 30 second cut off cycle will meet production needs. Once the correct length is determined, the outside diameter of the ends that are inserted into the sockets are machined in precision-fixtured grinders that remove material simultaneously from both ends in pencil-sharpener fashion. A total of sixteen grinding machines, each having a ten second cycle will produce the required number of 96 tubes per minute.

CSE-109 - DISPLACER (MULLITE - 4 PER ENGINE)

General - The manufacturing processes and equipment to produce this part are very similar to others already discussed. The sintering furnace required will be shared with other parts to follow, which can be placed on the setters to save space or, when possible will be sent through with like parts, together with some allowances for the inevitable losses. Design detail of this part is not complete in that methods to fasten it to the piston are not resolved. However, we assume a small change in configuration will not significantly change the cost. Possibly, three internal ridges on the I.D. of the displacer would be machined to retain the spring-loaded radiation domes.

Process Details

1. Powder Preparation - Dry powder is Ball Milled to specification before use.

2. Isostatic Pressing - One part per press cycle (1 minute each) requires an investment of four presses to maintain production rate.
3. Cut Off/Trim - The end of the piece will be gauged from the dome end and cut to length. A second operation to machine-fit the piston end internal diameter and to trim the outside diameter to within .002 is then performed. Two machines, with a 30 sec./part cycle will be used to green-machine the parts.
4. Sintering Furnace - This facility will be similar to that used for CSE101-1-1 cylinder heater head. This furnace is an air atmosphere unit operating at a maximum of 1750°C, after a pre-bake cycle of 500°C for 3 hours.
5. Final Dense Grinding - Both outside diameter and the inside of the displacer must be closely maintained to match mating surfaces or to keep clearances to cylinder walls. Four machines with cycle times of one minute per part are needed to meet rates.

CSE 109A RADIATION SHIELD (MULLITE - 12 PER ENGINE)

General - There are three of these parts applied to each displacer. This is an application of a ceramic "spring" where the lobed skirt of the domed parts has a slightly larger free diameter than the inside of the displacer. The displacer may (or may not) have three locating ridges inside to help space and retain these pieces which are tensioned as they are pushed up inside the displacer.

Process Details

1. Powder Preparation - The dry powder is ball-milled to specifications of fineness and purity before use.
2. Premixing - The powder is thoroughly mixed with thermoplastic in a twin-screw extruder in a machine comparable to those used for the cylinder distribution head, CSE 101-1-2. The heated, molten output from this machine is run directly into the injection molding machine. One 100 lb/hr. machine will handle this job.
3. Injection Molding - The part being molded is lightweight (.04 lb.) and, therefore, a shorter molding cycle of 15 sec. each may be used. If we use a three-cavity mold, one press will be adequate for the twelve parts per minute rate (600 per hour, 12,000 per day).

4. Oven Dry - The parts must be dried out and the plastic melted out of the ceramic powder binder, leaving the "beanie" shaped radiation shield. The oven will be at 600°C for 20 hours to accomplish this task. Capacity for a 20-hour output, or 12,000 parts, will be needed per batch-load. Only one oven of the size used for CSE-101-1-2 will be needed.
5. Sintering - These parts may be sintered by placing them over specially formed setters so that as shrinkage takes place in the oven, the part conforms to the exact shape and finished size desired. The spring leaves of the part will emerge from the sintering oven with the oversize outside diameter desired, enabling a spring fit into the CSE 109 displacer. The small size of the part enables us to share furnace space with the displacer.

CSE 101-1-3 CYLINDER INSULATION SLEEVE (MULLITE - 4 PER ENGINE)

General - This part is purposely not densified as much as other mullite pieces because of its application to help retain heat within the cylinder walls surrounding the displacer. The piece is not a precise part and will not require any machining other than cutting-off operations.

Process Details

1. Powder Preparation - Ball mill to specifications. The powder will be coarser than normal to produce a 70% of normal-density piece.
2. Isostatic Pressing - Two parts may be pressed at one time over a common mondrel. The normal rate of one cycle a minute can be met with two presses.
3. Cut-off/Trim - The pair of parts formed in the Isopress can be trimmed to length in a gang-saw grinder, with a 30 sec. cycle time. Two such grinders are needed to meet production rate.
4. Sintering - The same furnace as used for Displacer parts CSE 109, 109A can be used. If necessary, these sleeves may be placed over the outside of the displacer to save space when sintering. Special setter fixtures may be needed to space intermixed pieces to assure even heating and shrinkage.

CSE 101-3 RADIATION MANTLE-DOME (SiC - 4 PER ENGINE)

General - The mantle will require more machining than most parts due to the requirement for a staggered hole pattern. The process to produce is similar to a number of other pieces discussed.

Process Details

1. Powder Preparation - Ball-Milled powder to specification will be used.
2. Isostatic Pressing - The part will be pressed to shape over a steel mandrel, defining internal features closely, and the external shape in a general fashion. Four presses at one-minute cycles will produce the four pieces per minute rate.
3. Green Machining - The part must fit the CSE 101-1-2 cylinder head dist. chamber on the inside, and at the foot, mate with the inside step of the outer sleeve, CSE 101-2. Both of these areas are machined in one operation, which also will size the part length. A second indexing/drill operation will produce the six 25 hole rows in this part. Four machines having a one min./cycle rate, and using specialized controls will produce these parts.
4. Sintering - The machined green part will be sintered in an evacuated nitrogen atmosphere furnace like those used with other Silicon-Carbide pieces.
5. Final Grinding - Grinding in the dense state after sintering will be necessary to produce parts that fit at the foot and inside step area. Four grinding machines each for the two areas will be used for this setup, each having a one-minute grinding time per operation.

CSE 101-1-5 MANTLE BAFFLE (SILICON NITRIDE - 4 PER ENGINE)

General - This part is short, with a relatively large diameter. Therefore, it is well-suited to uniaxial pressing. The piece is critical in length, and must fit beneath the foot of the CSE101-3 mantle.

Process Details

1. Powder Preparation - Dry ball-milling of the powder to specification.
2. Uniaxial Pressing - Cycle time is short, needing only 15 seconds per part. One press will meet production needs. A press die will cost about \$50,000. No green machining will be needed.
3. Sintering - The part will share the furnace used for CSE 101-2, outer sleeve. This part will nest inside the larger one on a special spacing setter.

4. Dense Grinding - The length of the part will be ground to final height on two grinders having a 30 second cycle time each.

CSE 105-4 CYLINDER LINER (MULLITE - 4 PER ENGINE)

General - The general form and size of this part are not unlike other parts already planned and discussed. Sintering furnace facilities may be shared with other pieces. Both I.D. and O.D. of this part must be held to close tolerances.

Process Details

1. Powder Processing - Dry mullite powder is ball milled to specification.
2. Isostatic Pressing - Two parts will be made head-to-head as in similar pieces before. Two presses at 1 minute per cycle will meet production needs. The inside, being formed over a steel mandrel will be closely sized.
3. Green Machining - The outside diameter and the stepped area are turned to bring the part within close unsintered dimensions at this time. Two grinding machines, with a 30 second cycle time will first machine the outside features, then part the liners, with a trim to length cut at the same time.
4. Sintering - This part will share the same furnace used for the displacer and insulating sleeve. Separate setters probably would be best to position the parts, rather than nest them within unlike pieces, because of the closeness of sizes.
5. Dense Machining - After sintering the parts should be within 1/2% of final size. However, this liner must be held to closer tolerances to mate with the reciprocating piston assembly on the inside, and to fit within the metal cold-side components. Four grinders are planned for the operations, having 30 sec. cycle times for each.

CSE 104-1 PREHEATER PLATE - (SiC - 800 PER ENGINE)

General - Excepting for the interrupted ribs, the preheater plates can easily be made by conventional tape - casting procedures. The rib voids, however, will be removed by a process similar to carving or slicing with a razor-sharp knife, that will drop in position and swiveled as the tape proceeds along a conveyor, then lifted at the proper time. The volume required (800/min.) will dictate multiple process setups.

Process Details

1. Dry Powder Preparation - Ball mill powder to specifications.
2. Mix Slurry - The dry powder will be mixed in twin screw extruders to produce a heavy mixture for the doctor blade machines. At 800 pieces per engine weighing .036 lbs. each, about 1,800 lb/hr of mix must be prepared.
3. Doctor Blade Machines - Since each part is roughly 1/2 feet long, we will need $800 \times .5 = 400$ ft./min. of tape. A reasonable belt speed will be 5 ft/min. With a part width of 1.50 in., a manageable size machine could extrude 8 strips at once. Therefore, we will use 10 machines operating in tandem to make the parts. Each machine, with vent hoods, heat lamps and robotic razor scoring trim arms will cost \$250,000.
4. Drying and Sintering - As the parts are doctor-bladed and scored on the cellulose carrier tape, they are dried under a heat-lamp section before being automatically feed onto setters for sintering. The parts may be stacked 5 high and fed into an evacuated nitrogen furnace similar to that used for other silicon-carbide pieces. The part will emerge ready to use with no further machining needed.

SECTION 11

COST ANALYSIS

11.1 INTRODUCTION TO COST ANALYSIS

The cost analysis of the ceramic components is based on the manufacturing processes described in the previous Section 10. All money values are given in 1984 dollars.

A summary of the manufacturing data for the ceramic parts is provided in Appendix I of this section.

A sizeable portion of the cost in producing the component parts lies in the raw material powder cost. The engine cost analysis was conducted at three levels, I, II and III, for various assumed raw material costs. Currently, high quality powders required for high performance ceramic parts are expensive: For example, SiC or Si₃N₄ powder of high quality costs in the neighborhood of \$80./lb., mullite is \$30./lb. while zirconia is approximately \$10./lb. Since we are contemplating 1990's production, we arbitrarily set the three levels at considerably reduced levels anticipating a significant "learning curve" cost reduction for powder as follows:

	Powder Cost \$/Lb.		
	Level I	Level II	Level III
Si ₃ N ₄	5	10	20
SiC	5	10	20
Mullite	1	3	5
Zirconia	2	5	10

The metal component costs were assumed to be the same as those projected for the Mod 1 engine by Mechanical Technology, Inc. (MTI) as reported in "Manufacturing Cost Analysis" - Report Dec. 9, 1981 under contract DEN-3-32.

The summary of the CASES cost analysis is provided in Table 11.1. The MTI Mod 1 estimated cost is \$1498 compared to the CASES estimates of \$1942, \$2634, and \$4017 at the three levels.

The complete analysis is given in Appendix IV of this section.

TABLE 11.1 CASES ENGINE COST (1984) EXTRAPOLATED FROM MOD-1 ENGINE COST DATA

	(1)	(2)	(3)	(4)			(5)		
	Est. Basic Engine Cost <u>(Mod 1 Design)</u>	Est. Cost ¹ Equivalent Top Side <u>Components</u>	Est. Cost ¹ Lower Engine Block <u>Components</u>	Cost Equivalent ² Ceramic Engine <u>Top Side Components</u>			CASES Est. Basic Cost <u>(Col 3 + Col 4)</u>		
				⁴ <u>Level I</u>	<u>Level II</u>	<u>Level III</u>	<u>Level I</u>	<u>Level II</u>	<u>Level III</u>
Matl.	887.91			629.54	1,339.78	2,609.20			
Labor	155.50			114.87	114.87	114.87			
Burden	445.34			328.98	328.98	328.98			
Scrap ³	8.98			36.05	66.99	130.46			
	<u>1,497.73</u>	<u>664.82</u>	<u>832.91</u>	<u>1,109.44</u>	<u>1,850.62</u>	<u>3,183.51</u>	<u>1,942.35</u>	<u>2,683.53</u>	<u>4,016.92</u>

NOTES:

1. From Report dated 12/9/81, by Mechanical Technology, Inc. Under Contract DEN3-32
2. Equivalent parts exchange where clear identification is possible.
3. For ceramic parts, 5 percent of material is considered normal loss factor.
4. Level refers to material cost projections, see Section 11.1 of this report.
5. Burden is 28% of labor.

SECTION 12

LONG RANGE CERAMIC STANDARD ENGINE (CASE II)

12.1 INTRODUCTION

At the conclusion of the effort on the "primary design", CASE I, an additional investigation was carried out to assess the potential for a ceramic automotive Stirling engine based on the year 2000 ceramic technology and somewhat more radical departures from conventional design approaches.

Based on the evaluation of various candidate component concepts, a reference design for the Long Range Ceramic Standard engine concept was developed and is illustrated in Figure 12.1.

12.2 DESCRIPTION OF CONCEPT FOR CASE II

A pulse combustor which enhances heat transfer is located at the top center of the engine. Another advantage of the pulse combustor is its compactness, higher efficiency of burning and lower CO and NO_x in the exhaust products. There is a noise penalty which will need to be treated with muffling devices.

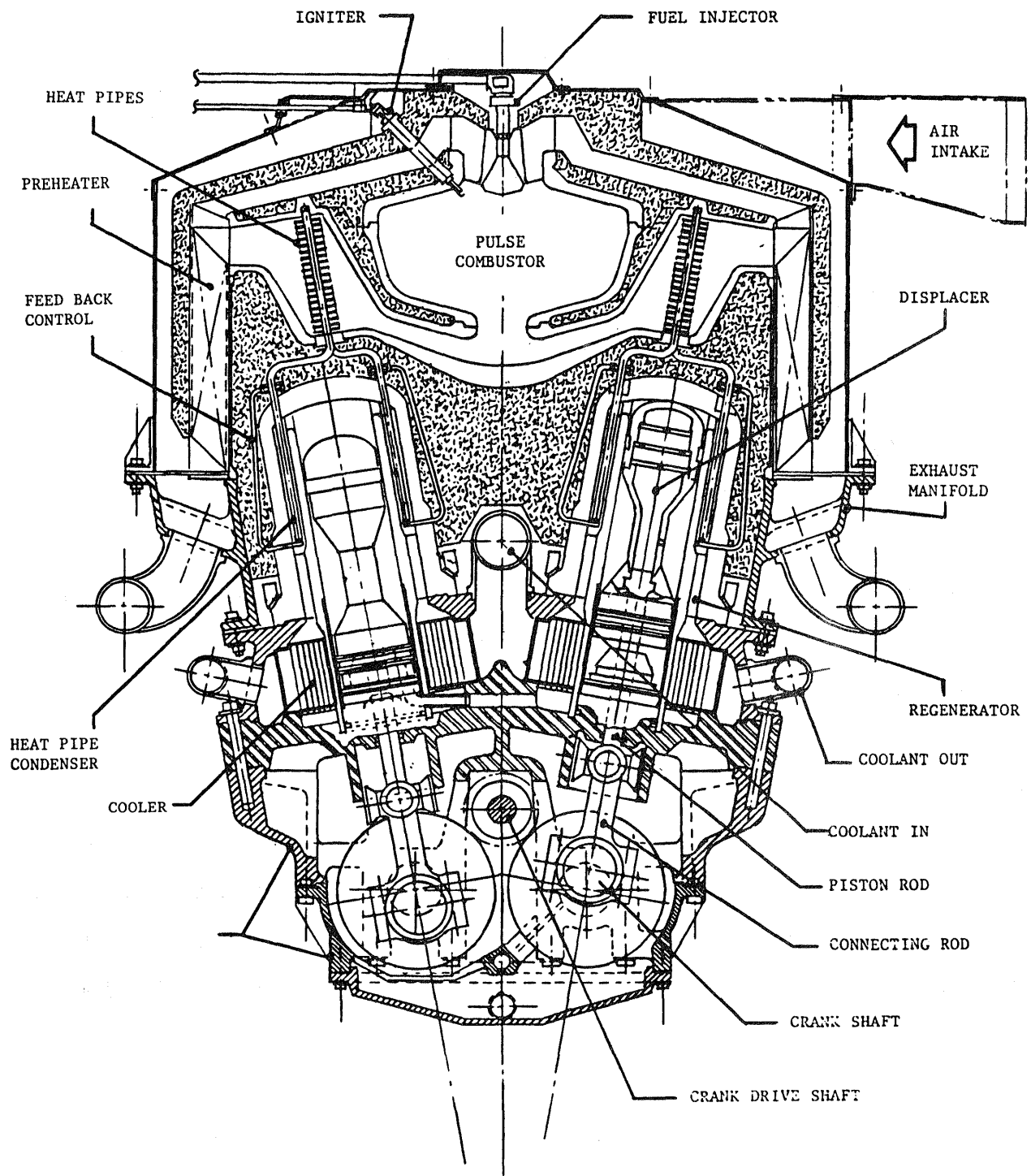


FIGURE 12.1 LONG RANGE AUTOMOTIVE STIRLING ENGINE CONCEPT
UTILIZING HEAT PIPES AND PULSE COMBUSTION

The engine consists of four double acting cylinder/displacer assemblies. Heat pipes with lithium as the transfer medium carry energy from the pulse combustor to the cylinder wall and hence to the working fluid. One of the most important characteristics of the heat pipe is its capability of nearly isothermal operation thus effecting an efficient thermodynamic cycle for the engine. The hot side temperature for this design was raised to 1100°C (improved to 980°C for the primary design CASE I over 800°C for the ASRE). The high temperature imposes a need for ceramic heat pipes in the CASE II design.

At the maximum efficiency point the net efficiency gain is 25% on the ASRE design (54.2% vs 43.5%). Although the concept was aimed to automobile application, these design concepts can be applied, as well, to other future Stirling engine applications. The performance comparison of the CASE I, CASE II, and the ASRE designs is provided in Table 12.1 .

Another feature of this design is a seal ring on the hot side of the displacer as well as a ring on the cold side to minimize gas shuttling losses.

By raising the hot side temperature to 1100°C (2012°F), the flame temperature increases over the earlier designs to 4300°F (2371°C) thus improving a severe condition for the wall of combustion chamber. In fact, the combustion chamber design in both CASE I and CASE II will be a critical issue.

Other novel features of the CASE II design concept include pressurized crankcase to minimize problems associated with the piston rod seals and a dry lubrication system which will involve ceramic bearings.

TABLE 12.1 PERFORMANCE COMPARISON OF CASE AND ASRE DESIGN

		FULL LOAD			MAX EFFICIENCY			PART LOAD			LOW LOAD		
		CASE 2	CASE 1	ASRE	CASE 2	CASE 1	ASRE	CASE 2	CASE 1	ASRE	CASE 2	CASE 1	ASRE
ENGINE SPEED	(RPM)	3400	3300	4000	1100	1100	1100	2000	2000	2000	1000	1000	1000
CHARGE PRESSURE	(MPa)	15	15	15	15	15	15	6	5	5	6	5	5
INDICATED POWER	(KW)	68.5	69.2	73.3	24.6	25.0	24.8	16.2	14.8	15.0	8.5	7.2	7.9
FRICTION	(KW)	7.2	6.9	9.6	2.2	2.2	2.2	2.1	2.0	2.0	1.0	0.9	0.9
12-4 AUXILIARIES	(KW)	1.3	1.8	3.6	0.3	0.3	0.5	0.6	0.7	0.8	0.3	0.3	0.4
NET POWER	(KW)	60.0	60.5	60.1	22.1	22.5	22.1	13.5	12.1	12.2	7.2	6.0	6.6
EXTERNAL HEATING SYSTEM EFFICIENCY	(%)	90	89	90.5	90	89	92.4	90	89	91.7	90	89	89.8
INDICATED EFF.	(%)	63.38	55.57	46.1	67.1	60.0	52.8	62.48	58.17	50.9	63.8	55.3	48.5
NET EFFICIENCY	(%)	50.0	43.2	34.2	54.2	48.1	43.5	47.1	42.4	37.7	48.6	41.0	36.4
PERCENTAGE GAIN OVER ASRE		46.2	26.3		24.6	10.6		24.9	12.5		33.5	12.6	

12.3 DESIGN OF CASE II

Candidate concepts incorporating long range technologies (year 2000) have been evaluated in order to explore the performance potential of a Long Range Ceramic Standard design for a Ceramic Automotive Stirling Engine (CASE). This activity has led to the development of a reference design based on which performance potential and the future technology needs will be identified. The following subjects are covered in this section:

- 12.3.1 Review of CASE I Design
- 12.3.2 Potential Design Improvement
- 12.3.3 Candidate Long-Range Ceramic Standard Design Concepts
- 12.3.4 Reference Conceptual Design for the Long Range Ceramic Standard

12.3.1 REVIEW OF CASE I DESIGN

One of the key constraints in the initial phase of the conceptual study of a Ceramic Automotive Stirling Engine (CASE) was that the design be based on projected 1990 technology. The conceptual design developed in the initial study (CASE I) is shown in Fig. 12.2. It consists of four separate cylinders each having a symmetric heater head/regeneration/cooler assembly to provide good structural integrity to ensure uniform heat distribution and for producibility of the ceramic components. The design incorporates a unique combination of jet impingement and radiation heat transfer, and offers high heat flux density at the heater head. The operating temperature is limited, however, to 1800F at the heater tube since the peak temperature at the hottest location of the combustor wall approaches 3800F which is pushing the projected 1990 state-of-the-art temperature limitation of known ceramic materials. In addition, the heat transfer components and engine designs for CASE I follow closely with the state-of-the-art Stirling engine practice based on technology readiness of 1990. Thus far, the results of the CASE I design study are quite favorable for the feasibility of a Ceramic Automotive Stirling engine with a modest (10 to 15%) improvement in the engine efficiency over the metallic reference engine (ASRE).

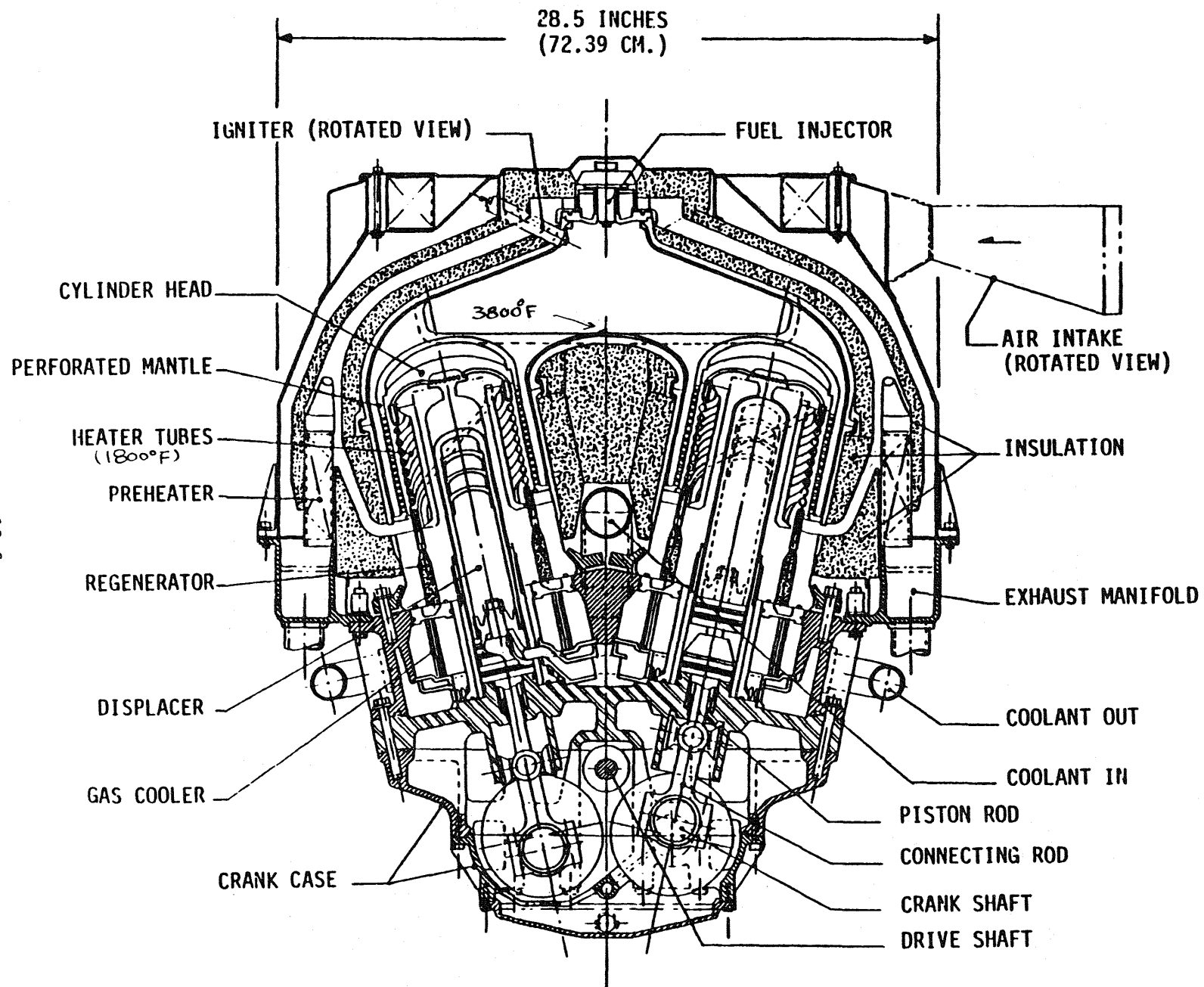


FIGURE 12.2 CERAMIC AUTOMOTIVE STIRLING ENGINE

The performance of a CASE can be further improved by assuming the availability of additional technology developments in engine components and materials through the year 2000. In order to identify the key areas for potential engine components and material improvement, it is beneficial to re-examine where the major heat and power losses are in the CASE I design. Table 12.2 itemizes these losses for the ASRE and CASE I designs at the maximum efficiency operating point (1100 rpm, 15 Mpa charge pressure).

As indicated in Table 12.2 the major losses in the CASE engine design are due to:

- o Adiabatic compression and expansion processes in the engine working spaces
- o Regenerator ineffectiveness
- o Shuttling and pumping losses at the displacer clearance volume
- o Conduction losses along the walls.

In addition, exhaust heat dissipated from the external heating system, parasitic power requirement and motoring friction contribute to lowering the engine net efficiency. More importantly, the basic heat dissipation to the engine cooler can be further reduced by increasing the Carnot efficiency. Potential means to improve these design deficiencies are discussed in the following sections.

12.3.2 POTENTIAL DESIGN IMPROVEMENT

The general approaches to the design improvements for those areas identified in the last section are also summarized in Table 12.2. These design modifications are discussed below.

12.3.2.1 Carnot Efficiency

As discussed in the previous section, the engine heater tube temperature for CASE I was limited to 1800F due to the requirement that no part of the combustor wall exceed 3800F. Thus, the Carnot efficiency for CASE I is only 74%. The oxidation limit for SiC is approximately 2900F (1600C). Therefore, it is reasonable to assume that the engine hot side temperature can be operated at 2550F (1400C) and yield a higher Carnot efficiency of 80%.

This higher heater head temperature can be accomplished in practice only if the combustor wall temperature is not significantly higher than that of the heater tubes. One potential means to limit the combustor wall temperature is to effectively cool the wall either by the preheated air or by incorporating an integrated combustor wall/engine heater head. More discussion on such a concept is presented in Section 4.0 Reference Design.

TABLE 12.2 RELATIVE LOSSES IN ASRE AND CASE DESIGN AND POTENTIAL IMPROVEMENT
(MAXIMUM EFFICIENCY POINT)

	ASRE	CASE I	POTENTIAL MODIFICATION
Carnot Eff.	70%	74%	o Increase T_H to 1400°C
External Heat System Eff.	91%	89%	o Improve E_{PH} from 90% to 95%, pulsed combustion
<u>THERMAL LOSSES (W)</u>			
Corr. for Adiabatic	2791.55	2477.15	o Isothermalization o Heat-Pipe Heater Head
Reheat Loss	1262.19	1236.46	o Improve regenerator effectiveness
Shuttle Loss	763.64	554.08	o Hot side ceramic piston ring
Pumping Loss	1032.44	1105.63	o Displacer re-configuration
Temp. Swing	57.9	52.56	
Cyl. Wall Cond.	523.84	116.4	
Disp. Wall Cond.	315.97	25.74	o Improve material strength to allow use of thinner walls
Reg. Wall Cond.	1071.11	200.76	o Reduce thermal conductivity of material.
Cyl. Gas Cond.	27.58	19.42	
Reg. Mtx. Cond.	94.24	105.58	
Radiation in Disp.	35.47	52.84	
<u>DYNAMIC LOSSES (W)</u>			
Adiabatic Corr.	1303.26	533.52	o Isothermalization
Heater Flow Loss	239.76	99.26	o Reduce or eliminate heater tube
Regenerator Flow Loss	198.88	129.61	o Internal regenerator
Cooler Flow Loss	16.01	10.01	o Reflex boiler
Parasitic Power	0.5 KW	0.3 KW	o Lower blower power, pulsed combustion o No or smaller cooling pump o No oil pump
Motoring Friction	2.2 KW	2.2 KW	o Dry bearing and gas bearings o Reduce speed

12.3.2.2 External Heating System Efficiency

As the heater head temperature is increased, the temperature of the exhaust gases emitted to the atmosphere is increased for an identical preheater design. This results in a lower external heating system (EHS) efficiency. In order to maintain a high EHS efficiency, the air preheater effectiveness must be improved, from 90% to the 95% range. This can be accomplished by using thinner wall, narrower flow paths, a larger overall size of the preheater, or other enhancement in the heat transfer.

A pulse combustion system appears to be an excellent candidate for this application. It offers several advantages over the conventional system as summarized in Table 12.3. Having a pulsating flow along the heat transfer path will allow a substantial improvement in the preheater effectiveness and thus a higher EHS efficiency.

12.3.2.3 Engine Internal Losses

Corrections for Adiabatic Processes

The compression and expansion processes for an ideal Stirling cycle are isothermal. However, the variable volume spaces in a conventional Stirling engine are usually of such size and shape that their compression and expansion are essentially adiabatic since little heat can be transferred to the walls. Adiabatic processes are less efficient and allow more heat to be dissipated to the engine cooler. As indicated in Table 12.2 the losses due to

TABLE 12.3 ADVANTAGES OF A PULSE COMBUSTION SYSTEM

- o Heat transfer rate 3 to 5 times more than conventional system
- o Self powered - Reduce blower power
- o Excess air requirements are reduced
- o Capability of operating in condensing mode
- o For a given firing rate, heat exchanger area is reduced
- o Self cleaning
- o Pollution free exhaust

the adiabatic processes for CASE I design are by far the greatest among all other internal engine losses.

A potential approach to ensure isothermal processes is to incorporate an effective heat transfer device in the engine expansion and compression spaces. One of the most effective means to transfer heat in this application is the employment of heat pipes. The heat pipes offer the following advantages.

- o extremely high heat flux density
- o near isothermal heat exchange
- o compact
- o flexibility in configuration

The extremely high heat flux density of an alkali metal heat pipe allows the compact design of a Stirling engine heater head, thus reducing the void volume and improving the engine power density and efficiency.

Reheat Loss

The reheat loss also contributes a significant penalty to the engine efficiency. The loss will increase further as the temperature gradient between the hot and cold ends of the regenerator ($T_H - T_C$) increases. An improvement in the regenerator effectiveness will reduce the reheat loss. However, the regenerator effectiveness for CASE-I design already exceeds 99%. A substantial increase in the regenerator size and a reduction in regenerator matrix filament size will be required to improve the effectiveness. However, the penalty in additional flow friction across the regenerator needs to be taken into account.

Shuttle/Pumping Losses

These losses are associated with the existence of the clearance volume between the displacer wall and the cylinder liner. The shuttle loss is due

to the heat conduction loss between the displacer wall and the cylinder wall via a narrow gap (typically 0.01") containing hydrogen. To reduce this heat loss, the clearance space between the two walls should be increased.

An increase in the clearance space, however, will increase the pumping loss which is due to the thermal loss generated by pumping the hydrogen in and out of the clearance space. To reduce or eliminate the pumping loss, the clearance space and the engine expansion volume should be sealed off by, for instance, a piston ring seal capable of maintaining the operating temperature at the engine hot side. A dry lubricant or a gas bearing can be considered as a potential candidate for prolonging seal life. The hot seal problem was discussed in Section 6.

Conduction Losses

Heat conduction losses across the cylinder wall, displacer wall, and regenerator housing and matrix can be reduced by:

- o using thinner walls
- o reducing thermal conductivity of material

Additional improvement in ceramic material strength and Weibull modulus will allow the design of thinner walls for various engine components. It is believed that, by the year 2000, the allowable design strength can be developed to a level approaching 50 K psi range, about twice as high as that anticipated for 1990. The possibility of reducing the thermal conductivity of the structural ceramic materials may be achievable by use of additives, porosity or other novel approaches. Trade-off of decreased thermal conductivity versus the potential reduction in the material strength will have to be considered.

Other Losses

The other losses, including the flow friction losses across the heater, regenerator and cooler, appear to be insignificant. No particular efforts will be devoted to reduce these losses in this effort.

12.3.2.4 Parasitic Power

Use of a pulse combustion system will allow a significant reduction in the blower power requirement. The blower is needed for the start-up. After the combustion is stabilized, the pulsation of the combustion gas provides significant driving force to move the air and combustion gas.

A more efficient engine with improved cold side heat transfer will allow the use of a smaller water pump. Dry bearings in the crank-shaft, if developed successfully, will completely eliminate the need for an oil pump.

12.3.2.5 Motoring Friction

The development of dry bearings has been continuing for years. Dry bearings not only eliminate the need for oil lubrication, but also have the potential of reducing the motoring friction. This is particularly significant for a kinematic Stirling engine. The conventional Stirling engine requires a sophisticated seal design at the piston rods to prevent oil from migrating to the hot working space. This not only presents a very challenging technology development for a long life and reliable seal, but also adds a significant increment to the motoring friction. Elimination of the oil seal will reduce the motoring friction.

12.3.2.6 Vehicle System Improvement

Even though vehicle improvement, other than the engine itself, is beyond the scope of this study, it is worth noting that the improvement in the vehicle fuel efficiency (in terms of MPG) is also greatly influenced by the improvements of other vehicle subsystems and components. Some of the more noticeable examples are the uses of a CVT (Continuously Variable Transmission) and electronic control.

12.3.3 CANDIDATE LONG-RANGE CERAMIC STANDARD DESIGN CONCEPTS

Several design concepts have been considered to implement the potential design improvements discussed in Section 12.3.2. Two classes of concepts appear to be attractive from performance, structural integrity and producibility considerations. Both concepts have the following common features:

- o Monolithic heater head with annular heater head, regenerator and cooler assembly to ensure maximum structural integrity and compactness.
- o Displacers having both hot and cold side seal rings and enlarged displacer wall to cylinder wall clearance space to reduce/eliminate shuttle and pumping losses.

The first concept, as shown in Fig. 12.3 utilizes the cylinder wall as the "heat pipe" condenser section and the combustor wall as the "heat pipe" evaporator. It is a relatively simple construction. However, it appears to be a longer and larger design than an alternate approach (discussed below) due to the required surface area for adequate heat transfer to the monolithic heater head. It also requires larger ceramic components (heat pipe evaporator) needed to be in single-piece construction.

A second concept utilizes a bundle of tubular heat pipes as illustrated in Fig. 12.4. Heat pipes penetrate the cylinder head into both the heater head tubes and the expansion space. Since a sufficient number of

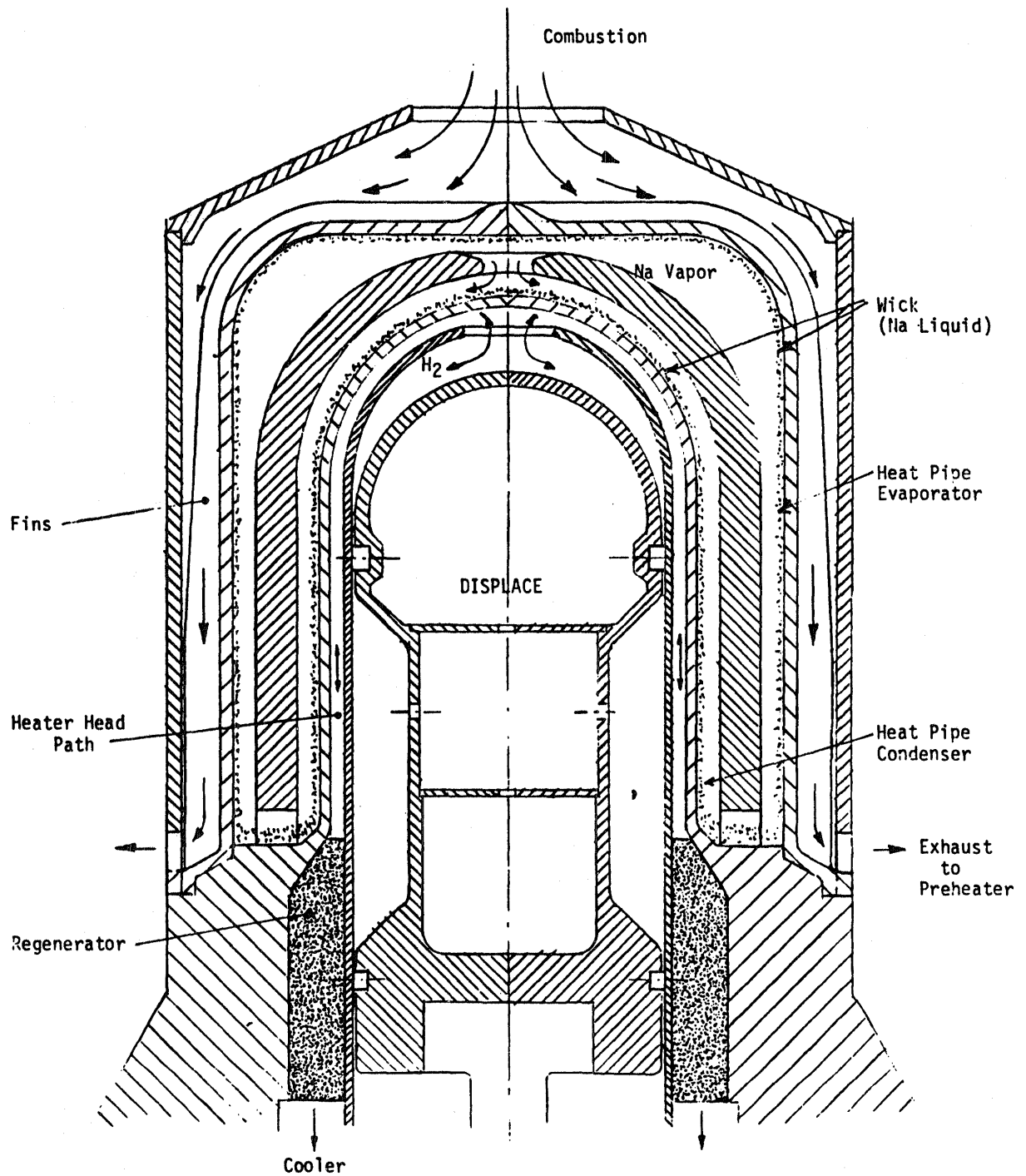


FIGURE 12.3 MONOLITHIC HEAD HEAT PIPE CONCEPT

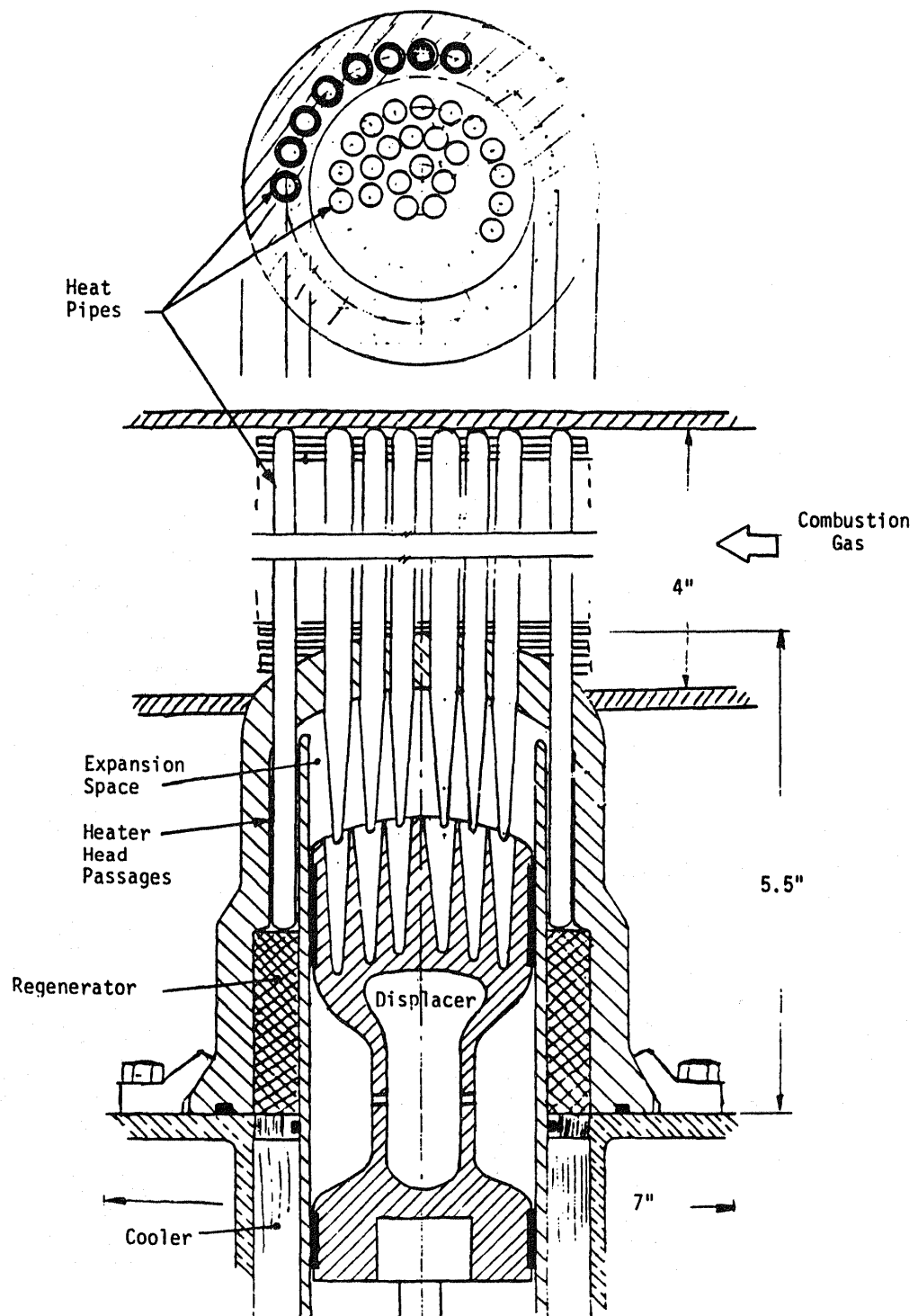


FIGURE 12.4 TUBULAR HEAT-PIPE HEATER HEAD CONCEPT

tubes can be incorporated into each cylinder, the hot section of the engine can be designed with a relatively short length, thus further reducing the void volume. The heat pipes in the expansion space will ensure isothermal compression and expansion. This tubular heat pipe approach forms the basis for a Long Range Ceramic Standard reference conceptual engine design.

12.3.4 LONG RANGE CERAMIC STANDARD REFERENCE CONCEPTUAL DESIGN

Based on the evaluation of various candidate component concepts, a reference design for the Long Range Ceramic Standard engine concept was developed and is illustrated in Figure 12.1.

A pulse combustor is located at the top center of the engine which consists of four double acting cylinder/displacer assemblies. It is noted that most of the combustor wall is embedded with heat pipes, thus being maintained at a relatively low temperature acceptable to the ceramic material. Additional evaporator sections of the heat pipes are located downstream of the combustor prior to the preheater.

It is apparent that the detailed design and development of the heat pipe for this application represents a great challenge in the future. Nevertheless, this concept is attractive in providing high temperature operation. The heater head temperature can potentially be operated at 1400C (2550F), with the combustor wall temperature being limited to 1600C (2900F) range which is the oxidation limit for Si C material. The combination of a pulse combustor and heat pipe also offers a compact design. The initial layout of this concept indicates that the overall envelop of the engine has the potential of being equal to or less than that of the ASRE design.

Preliminary estimate of the heat pipe sizing has been carried out during the process of generating this reference design. Utilizing lithium heat pipes having .25" O.D. and 2" penetration into the engine working space, approximately 50 heat pipes/cylinder are required to provide adequate heat input at the full load, assuming the same engine efficiency as the CASE I design. The requirement on the heat pipe will be less stringent as the engine efficiency for this advanced design is improved.

12.4 APPLICATION OF HEAT PIPES TO CERAMIC AUTOMOTIVE STIRLING ENGINE

12.4.1 INTRODUCTION

The use of heat pipes in Stirling engines has been envisioned to offer the following advantages [1]:

- o Freedom to design the expansion space heat exchanger to satisfy the heat transfer and fluid dynamic requirements in an optimal fashion.
- o Ability to use a remote heat source.
- o Ability to maintain a more uniform temperature at the heater head.

These advantages, however, must be carefully weighed against the requirements of the Ceramic Automotive Stirling engine application. The requirements for CASE I design are indicated in Table 12.4. It is seen that almost 10:1 turndown ratio is required from full load to low load condition necessitating a self-regulating mechanism for heat pipes to maintain a constant hot side temperature. Also, the temperature levels and the heat input density limit the selection of size, shape, and working fluid for the heat pipe.

12.4.2 SOME BASIC DESIGN CONSIDERATIONS

A typical heat pipe consists of an evaporator section where the heat is supplied from an external source to the working fluid in the heat pipe; an

TABLE 12.4 CASE THERMAL DESIGN PARAMETERS

	<u>Part Load</u>	<u>Max. Eff.</u>	<u>Full Load</u>
Indicated Power (KW)	7.9	24.8	73.3
Indicated Efficiency (%)	54.7	60.0	52.2
Heat Input to Engine (KBtu/Hr)	49.3	141.0	478.4
Firing Rate (KBtu/Hr) (Combustor Eff. 89%)	55.4	158.5	537.5
Fuel Flow Rate (lb/Hr)	3.0	8.6	29.1
Air Flow Rate (lb/Hr) (with 10% ea)	47.1	134.8	458.1
Available Heat Capacity (Btu/Hr ^o F)	14.53	41.6	141.3
Average Heater Head Tube Temp. (^o F)	1800	1800	1800

adiabatic section, and a condensing section where the heat is rejected to the environment. The condensate is "pumped" through the wick to the evaporator by capillary action. If the heat pipe is operated in a gravitational field, the pumping power of the wick must overcome the viscous losses and the gravitational field as well.

The heat transfer from the source to the sink is effected mainly by six simultaneous and independent processes: (1) heat transfer from the source through the container wall and wick-liquid matrix to the liquid-vapor interface; (2) evaporation of the liquid at the liquid-vapor interface in the evaporator; (3) transport of the vapor in the core from the evaporator to the condenser; (4) condensation of the vapor on the liquid-vapor interface in the condenser; (5) heat transfer from the liquid-vapor interface through the wick-liquid matrix and container wall of the sink; and (6) return flow of the condensate from the condenser to the evaporator caused by capillary action in the wick. Each one of these processes offers thermal and flow resistance and limits the selection and application of heat pipes to a practical system.

One of the most important characteristics of a heat pipe is its capability of nearly isothermal operation. Within the working limits of a pipe, an increase in heat input will be followed by an increase in working fluid evaporation rate, a transfer of the heat down the pipe, and subsequent increased condensation. For a given heat input, the pipe establishes an associated isothermal operating temperature. Its operating temperature must vary with heat input; however, since its heat rejection area is fixed. This condition is not desirable for Stirling engine application where a fixed hotside temperature should be maintained under varying load conditions (10:1 in the case of the automotive Stirling engine).

The temperature at the outside wall of the heat pipe may be either "fixed" or "floating" depending on the type of constraints imposed by source or sink. At the evaporator, a "floating" temperature is usually the result of forcing some sort of heat flux boundary condition upon the heat source. Such is the case in automotive Stirling engine application, where the source temperature may change with heat flux related to load condition. At the condenser, a "floating" temperature is commonly effected by radiative cooling. However, in the Stirling engine, the temperature of the heater head must be kept constant under all load conditions for maximum efficiency. Thus, Fig.12.5 illustrates the temperature profile which results if the sink temperature is fixed and the source temperature is allowed to float. As shown by profiles a and b, the source temperature and the vapor temperature increase with increasing heat flux and there is corresponding increase in the temperature gradient at the evaporator and condenser. Where large turndown ratio is required, this increase in temperature may be substantial.

In order to limit the temperature variation, a control system can be devised based on the fact that any inert (non-condensable) gas present in the heat pipe quickly gathers at the far end of the condenser section and tends to limit the available condensing area. An inert gas reservoir can be added as

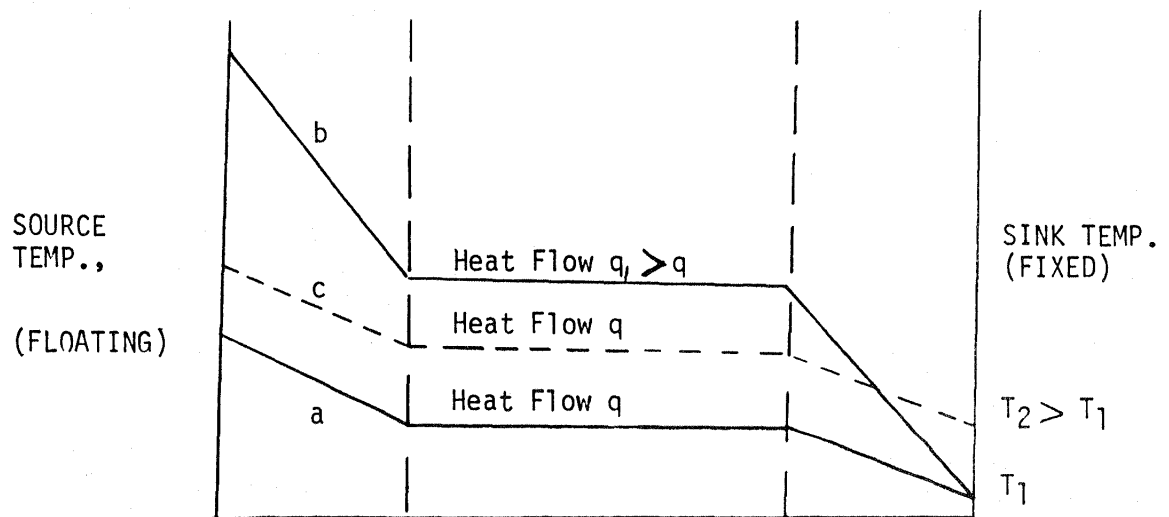


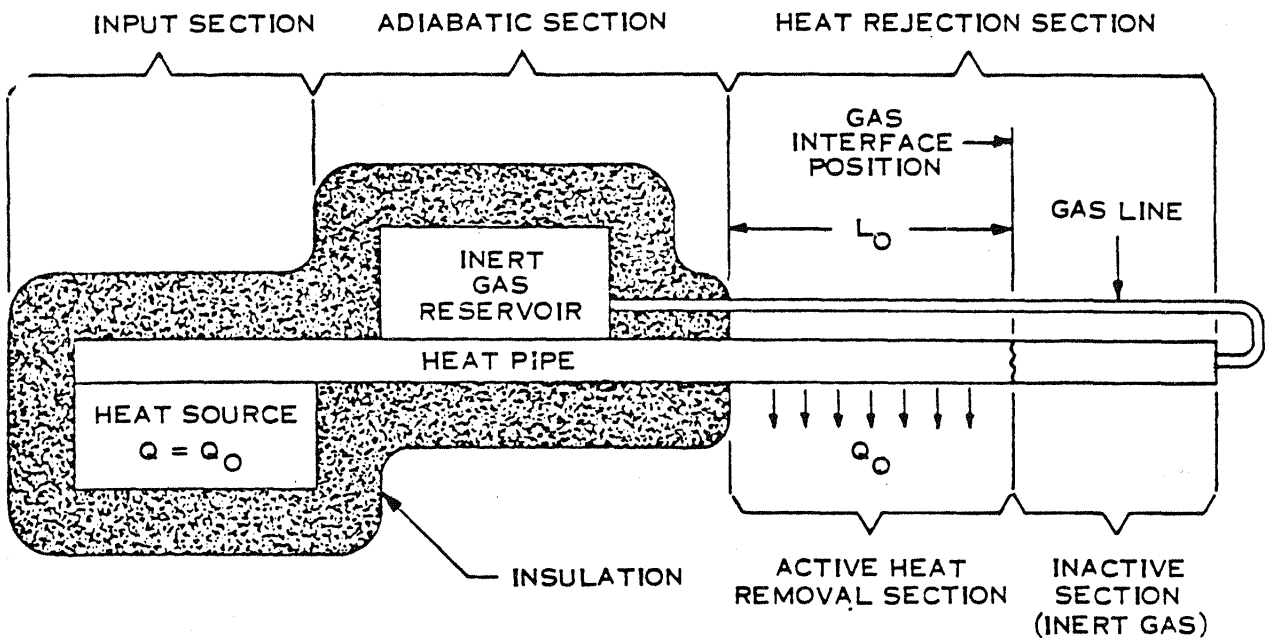
FIGURE 12.5 QUALITATIVE TEMPERATURE PROFILES ALONG HEAT FLOW PATH

shown in Fig. 12.6 and the heat pipe working fluid vapor pressure, and hence, the pipe operating temperature could then be controlled by sensing either the pipe temperature or the reservoir pressure, and controlling the reservoir pressure accordingly. By placing the gas reservoir in contact with the active portion of the heat pipe, a self-controlling mechanism can be devised. The specific design characteristics selected serve to fix the operating temperature of the pipe regardless of its surroundings, provided only that some heat is being added and the vapor/gas interface is somewhere in the heat rejection portion of the pipe. This mechanism employs the following physical relationships:

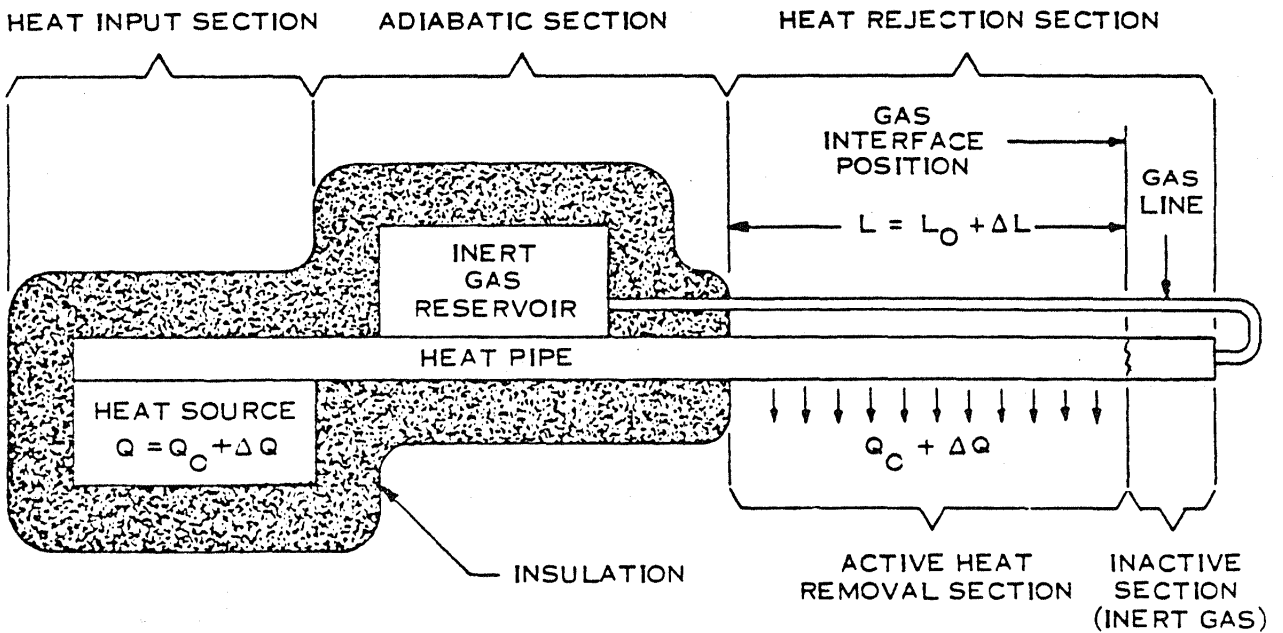
- a. The pressure of the working fluid vapor is dependent only on the temperature of the liquid phase of the working fluid.
- b. The pressure of the working fluid vapor increases exponentially with temperature.
- c. The pressure of the control gas is dependent mainly on the available volume for the gas (in the present instance the bulk of the control gas is in thermal contact with the heat pipe - its temperature is nearly constant over most of its volume).
- d. During steady state operation, the pressure of the control gas is uniform and equal to the working fluid vapor pressure at the vapor/gas interface.

The interaction of the above factors results in a sensitive thermal control device as explained in Fig. 12.7. During steady state operation, the control gas volume is fixed at V_0 . Assuming a constant environment, an increase in the heat load will result in an increase in the temperature of the evaporator. Due to the sensitivity of the equilibrium vapor pressure with temperature, a slight increase in the evaporator liquid temperature increases the equilibrium vapor pressure and pushes the vapor/gas interface back, thus providing more heat rejection area. The increase in heat rejection area limits the temperature rise to a nominal amount for large changes in heat input. The motion of the interface also results in an increase in the control gas pressure towards point 1 since its available volume has been decreased.

Conversely, a decrease in heat input will lower the evaporator temperature. This causes a decrease in the equilibrium vapor pressure, and the inert gas pressure pushes the vapor/gas interface towards the evaporator and point 2 in the figure. By choosing the proper relative values of heat pipe volume and inert gas reservoir volume, and by choosing the proper pressure drop characteristics for the pipe connecting the gas reservoir to the heat pipe, a stable system can be achieved in which the transition to a new equilibrium condition occurs quickly and repetitively.



(A) CONTROLLED HEAT PIPE OPERATION AT $Q = Q_0$



(B) CONTROLLED HEAT PIPE OPERATING AT $Q = Q_0 + \Delta Q$

FIGURE 12.6 SELF-CONTROLLED HEAT PIPE

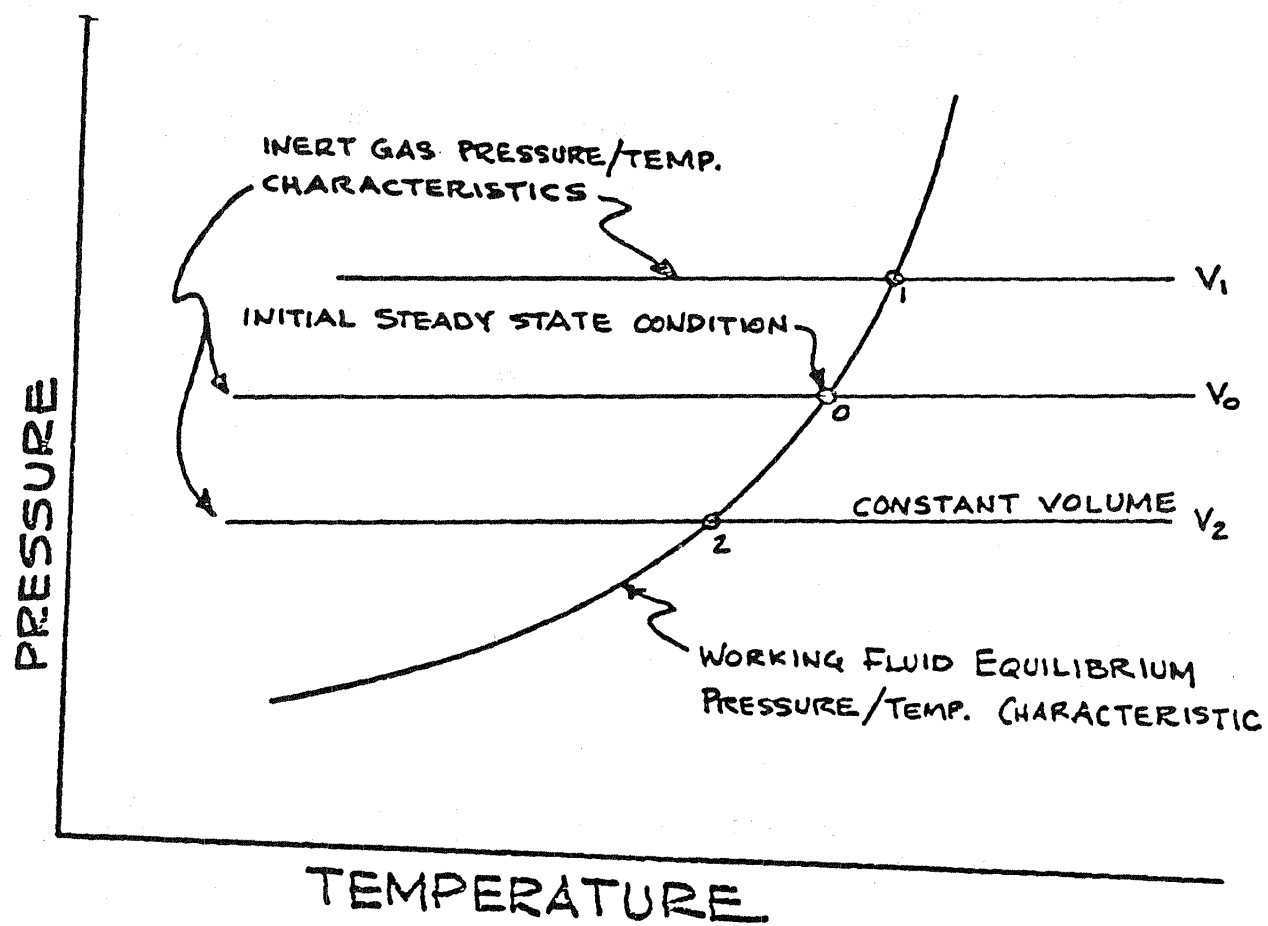


FIGURE 12.7 PRESSURE-TEMPERATURE RELATIONSHIPS

12.4.3 SELECTION OF HEAT PIPE WORKING FLUID

The high operating temperature of a ceramic Stirling engine ($> 1000^{\circ}\text{C}$) requires that the heat pipe be constructed of ceramic also. In addition, to transfer heat at this temperature level, an alkali metal is required as the working fluid. Thus, a corrosion-resistant vacuum-tight enclosure, compatible with the alkali metal is required. The alkali metal working fluids which are appropriate to the operating temperature range of the ceramic heat pipes are not generally compatible with ceramic materials. The ceramic material must be protected from contact with the working fluid. This can be accomplished by using chemical vapor deposition (CVD) to line the interior of the ceramic tube with a layer of refractory metal such as tungsten, molybdenum and niobium. As for the ceramic itself, silicon carbide is considered to be the primary candidate due to its excellent thermal shock resistance, good thermal conductivity, and resistance to both oxidizing and reducing atmospheres. In addition, silicon carbide has an extremely low hydrogen permeability. Predictions based on the measurements give the tungsten-silicon carbide heat pipe a life of more than 20 years at an operating temperature of 1300°C with a tungsten layer thickness of 0.25 mm. [2]

The selective properties of the two most likely working fluids for the heat pipe are shown in Table 12.5. The maximum use temperature for sodium is restricted to about 900°C , beyond which its vapor pressure rises substantially. On the other hand, lithium has a working range of up to 1400°C . Also, lithium has a better surface tension and latent heat of vaporization. One of the drawbacks of using liquid metal heat pipes in this application is the high melting temperature of liquid metals (357°C for lithium). Thus, during startup, the temperature must be raised to this temperature before the heat pipe becomes operational. Provisions may have to be made to prevent the formation of hot spots during startup when full blast of the hot combustion gases impinge on the heat pipes.

12.4.4 SIZING OF HEAT PIPES

For the purpose of preliminary estimation of heat pipe size required for CASE II, the same basic heat input requirements were assumed as for CASE design as shown in Table 12.4. The heat pipes are sized for full load requirements. At other load conditions, appropriate control system as mentioned before can be utilized to maintain the same hot side temperature. The maximum heat input per engine cylinder is about 120K Btu/Hr. Assuming 16 heat pipes per cylinder, the heat carrying capacity required per pipe is about 2200W.

The constraint imposed on the radial heat flux is based on the heat flux map prepared based on a large number of empirical data as shown in Fig. 12.8 to relate heat pipe diameter and heat flux density. The maximum evaporative and condensing heat flux lies in the range of 1×10^5 to 2×10^5 Btu/Hr ft^2 [3]. This range is selected after contrasting the phenomena that occur in heat pipes at the liquid-vapor interface with boiling and condensing alkali

TABLE 12.5 SELECTIVE PROPERTIES OF CANDIDATE LIQUID METALS

	<u>Sodium</u>	<u>Lithium</u>
Normal Boiling Point °F	1621 (883°C)	2400 (1316°C)
Liquid Density lbm/ft ³	46.1	28.83
Liquid Surface Tension lbf/ft	7.9×10^{-3}	25.8×10^{-3}
Liquid Viscosity lbm/ft hr	0.42	1.1
Liquid Thermal Conductivity Btu/ft hr °F	31.8	28
Latent Heat of Vaporization Btu/lbm	1700	8422
Vapor Viscosity lbm/ft hr	0.056	
Vapor Density lbm/ft ³	0.017	
Heat Capacity Btu/lb °F		1.0
Normal Melting Point °F	208 (98°C)	357°F (181°C)
Vapor Pressure PSI at 1800-2000°F	90.0	2.0

metals. In heat pipes, it is recommended that the vaporization of the working fluid should be confined to surface evaporation below the nucleate boiling region so that formation of hot spots in the wick can be avoided.

The design of heat pipe to meet the requirements of this application can be initially scoped by stating the pressure drop criterion:

$$\text{Available Capillary Pressure} \geq \text{Viscous Drop in Liquid} + \text{Viscous and Inertial Drop in Vapor} + \text{Gravitational Drop}$$

The pressure head developed in the wick as a function of hydraulic pore radius is given in Fig. 12.10. A reasonable hydraulic pore radius to expect with ceramic heat pipes is about 0.005 to 0.01 in. and for lithium as the working fluid, it will develop a capillary head of about 0.5 psi. Based on the capillary pore radius of 0.005 in., the wick pressure drop from Fig. 12.8 is about 0.2 psi. For small pore radii, the liquid pressure drop dominates compared to the vapor pressure drop which is expected to be about 0.1 psi. The gravitational pressure drop for a vertical heat pipe is about 0.2 psi. Thus, in summary, the capillary head developed balances the overall pressure drop expected in the heat pipe.

Assuming 4 in. length of the evaporator and condenser section, the radial heat input density required is 6.6 kw/ft. From Fig. 12.8 A the inner radius of the heat pipe for this input density is about 0.1 in., and the OD of the heat pipe is 0.27 in. Table 12.6 gives the preliminary design parameters for the heat pipes for automotive Stirling engine CASE II design.

12.4.5 BASELINE CONCEPTUAL DESIGN

Based on the design considerations presented here, a conceptual design for the advanced automobile Stirling engine was generated as shown in Fig. 12.9. As shown, the heat pipes are arranged circumferentially inside the engine cylinder head. A monolithic heater head is utilized to simplify the construction of ceramic parts. The heat pipes are straight-through type which are bent to bring them out on a single diameter around the combustion chamber as shown in Fig. 12.10. This has the advantage of keeping the temperature fairly uniform on the front and back side of the heat pipes and eliminates the significant amount of temperature gradient observed when two or more rows of heater head tubes are used. An inert gas reservoir is provided in contact with the operating length of heat pipe to provide self-regulation of temperature of the heat pipe with varying load. With this concept, the void volume can be closely controlled and minimized; limited only by the permissible pressure drop of the working fluid inside the engine. It is noted that the placement of heat pipes directly inside the expansion space from top restrict the available length of the condenser section to the stroke of the piston. The stroke of the piston for CASE is 1.34 in. For the same heat input density, it means about four times as many heat pipes; which not only make it difficult to incorporate a control system, but also create difficulty in arranging them so that minimum temperature gradient is created between the rows of heat pipes.

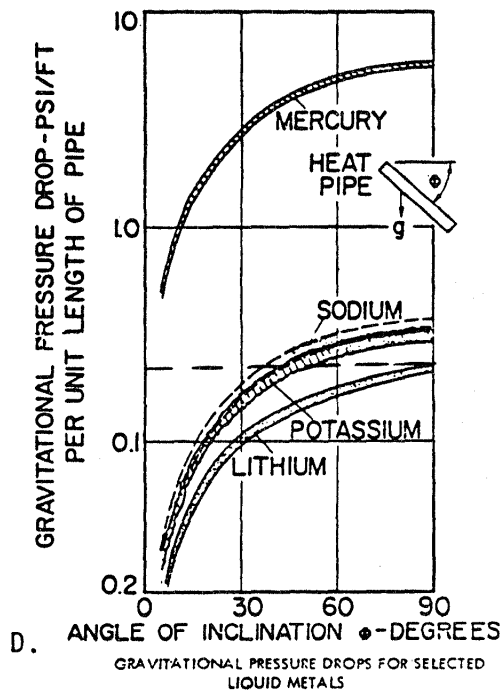
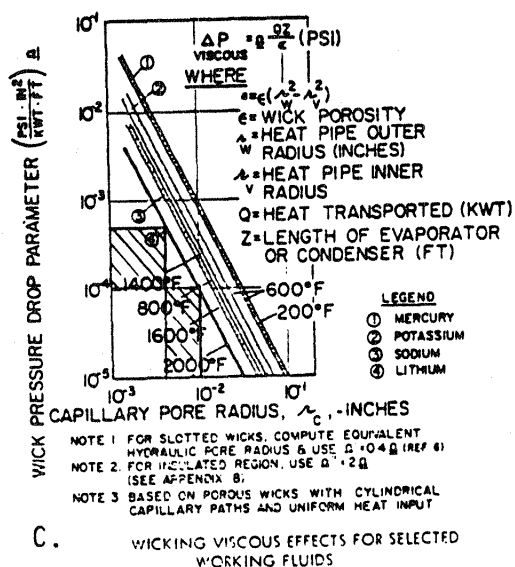
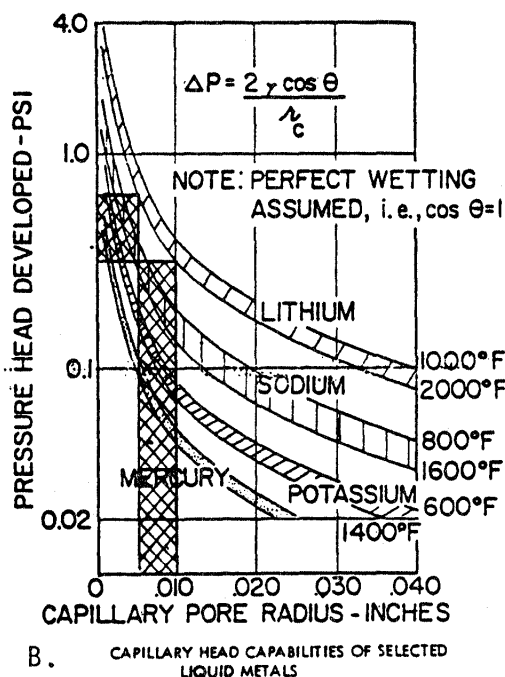
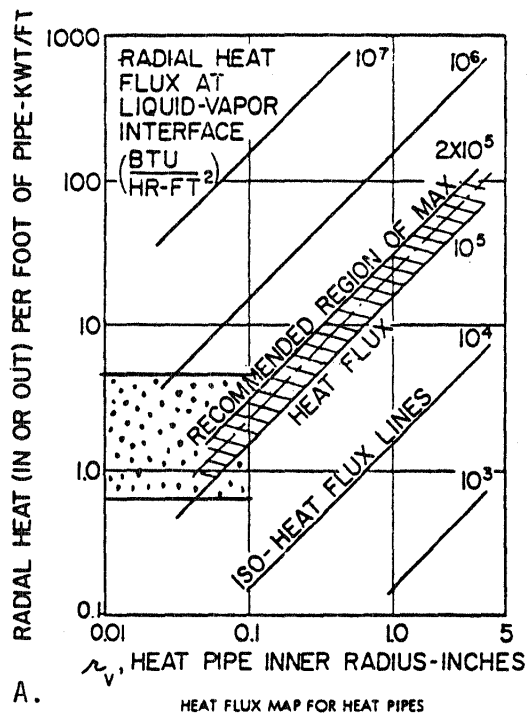
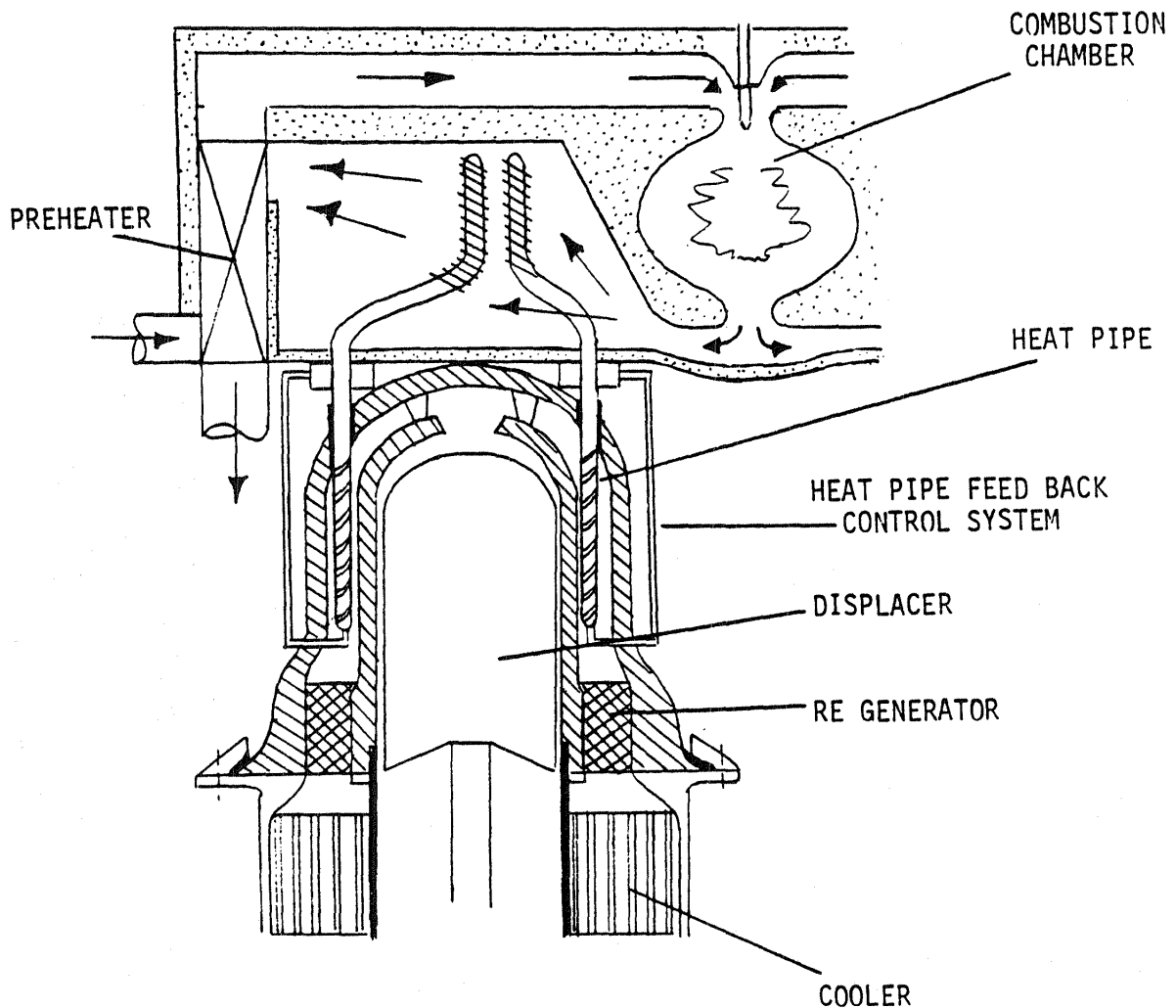


FIGURE 12.8 SELECTION AND SIZING OF HEAT PIPES

TABLE 12.6 HEAT PIPE DESIGN PARAMETERS

Number of heat pipes/cylinder		16
Length of condenser and evaporator section	in.	4
Heat pipe inner diameter	in.	0.2
Heat pipe wick pore diameter	in.	0.01
Wall thickness	in.	0.03
Heat pipe OD	in.	0.28
Ratio of fin area to base area at evaporator		5:1
Maximum heat input/engine cylinder	Kw	35
Heat carrying capacity/pipe	W	2200
Radial heat input density	Kw/Ft	6.6



KEY FEATURES

- 0 A SINGLE ROW ARRANGEMENT OF HEAT PIPES IS PREFERRED IN THE COMBUSTION CHAMBER TO REDUCE ΔT ACROSS THEM.
- 0 10:1 HEAT INPUT RATIO FROM FULL LOAD TO NO LOAD IS ACHIEVED BY UTILIZING A FEEDBACK CONTROL SYSTEM.
- 0 USE OF HEAT PIPES REDUCED THE VOID VOLUME AND ACHIEVES ISOTHERMALIZATION IN THE EXPANSION SPACE.
- 0 RAPID RESPONSE.

FIGURE 12.9 BASELINE DESIGN FOR HEAT PIPE APPLICATION TO AUTOMOTIVE STIRLING ENGINE

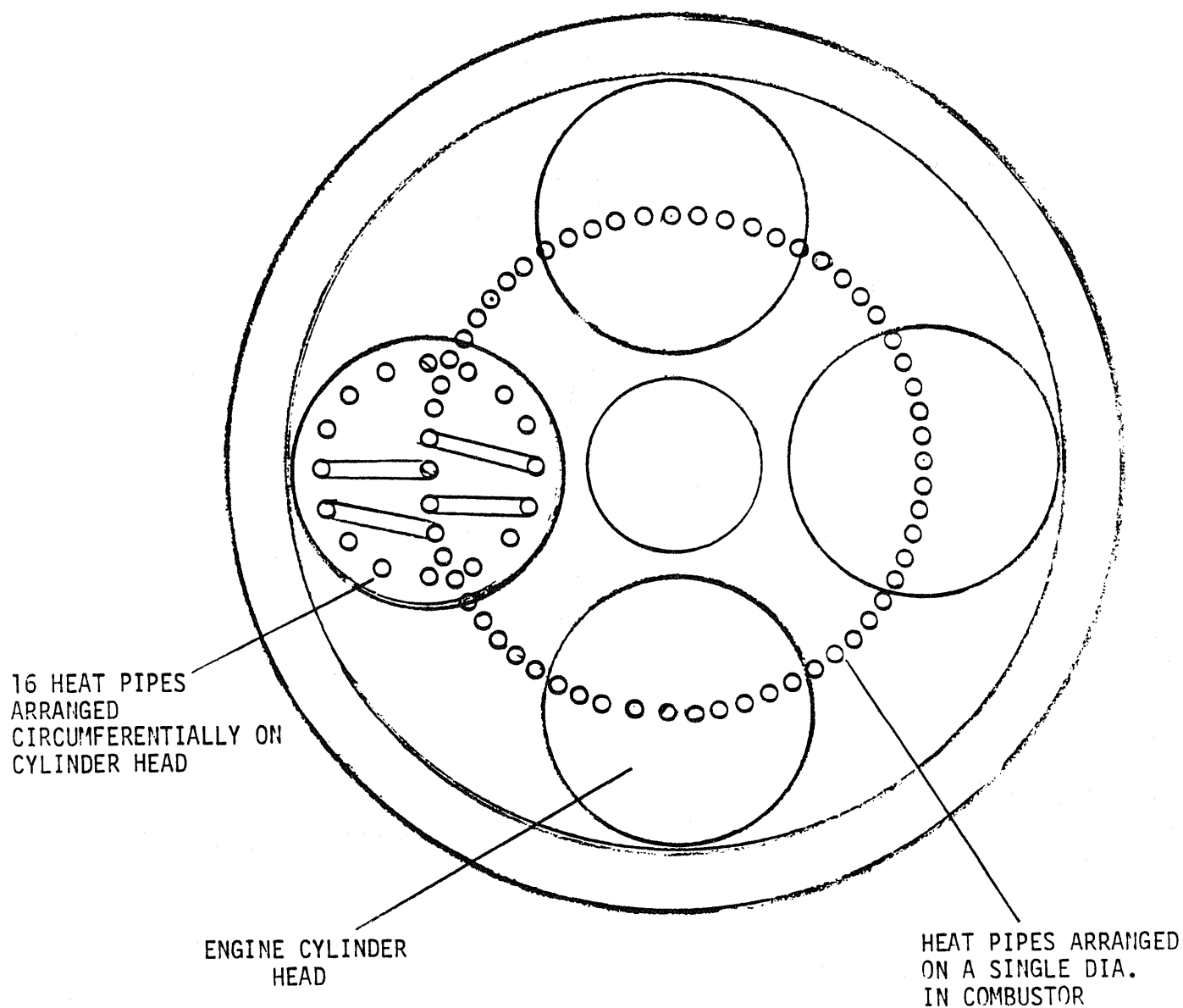


FIGURE 12.10 CROSS-SECTIONAL VIEW OF HEAT PIPE ARRANGEMENT

A pulse combustion system provides the necessary high heat flux density at the evaporator end of heat pipes. Also convection and radiation are prominent modes of heat transfer to the working fluid inside the engine. The heat pipes radiate to the surrounding walls of the engine which in turn transfer heat by convection to hydrogen. If necessary, the external surface of the heat pipe condenser section can be ribbed to further enhance the heat transfer.

12.5 APPROACH FOR REDUCTION IN VARIOUS LOSSES

Several areas of thermal and power losses in the Stirling engine were identified during CASE 1 study. These are given in Table 12.7. In conventional Stirling engines the hot side working space and the cold side working space are separated by a long cylinder. The cylinder is made long enough so that the heat transferred along the temperature gradient is relatively small. Also, normally the seal is located on the cold side of the cylinder which permits the use of conventional sealing materials. The movement of the piston inside the cylinder results in two major sources of losses. One known as the pumping loss is due to the flow of gas in and out of the clearance gap, when the engine is subjected to cyclic pressure variation. Since the gas does not necessarily leave the clearance volume at the same temperature at which it entered, there is a net energy transport from the hot side to the cold side.

From Martini's code it is deduced that in order to reduce the pumping loss, the following actions can be taken:

- o Reduce the cylinder diameter - affects power output
- o Reduce ($P_{\max} - P_{\min}$) - affects size, increases reheat loss
- o Reduce speed - affects power output, increases reheat loss
- o Reduce ($T_H - T_C$) - affects Carnot efficiency

- o Reduce clearance - further reduction not practical, increases displacer losses
- o Reduce length of hot gap - requires seal on the hot side

The Martini code nomenclature is given in Table 12.15.

TABLE 12.7 VARIOUS THERMAL AND POWER LOSS MECHANISMS IN STIRLING ENGINES

THERMAL LOSSES (W)

CORR. FOR ADIABATIC HX.

REHEAT LOSS

SHUTTLE LOSS

PUMPING LOSS

TEMP SWING

CYL. WALL COND.

DISP. WALL COND.

REG. WALL COND.

CYL. GAS COND.

REG. MTX. COND.

RADIATION IN DISP.

DYNAMIC LOSSES (W)

ADIABATIC CORR.

HEATER FLOW LOSS

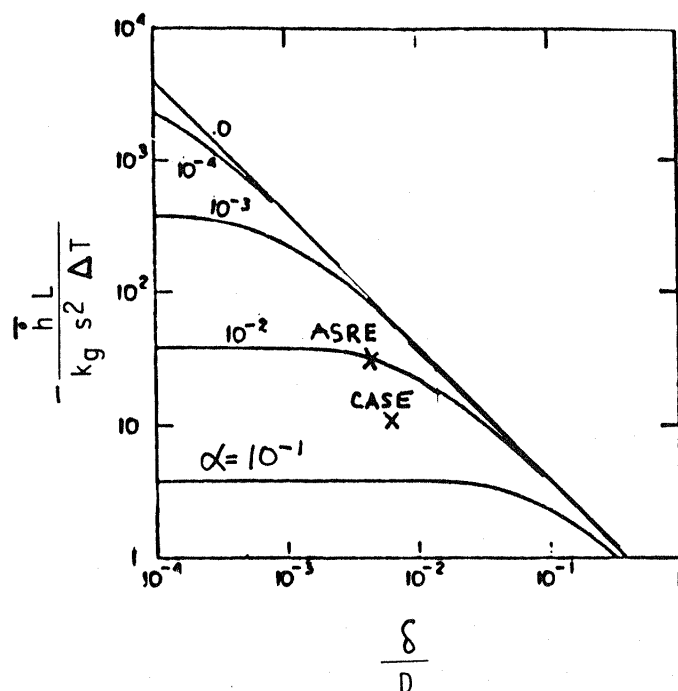
REGENERATOR FLOW LOSS

COOLER FLOW LOSS

Of all these possibilities only the last one appears to be most effective. It is seen that by placing the seal near the hot side, the flow of gas in and out of the clearance space can be almost completely avoided. The use of another seal at the cold end keeps the gas enclosed and prevents the energy exchange on the cold end side also. In the absence of flow, the gas contained inside the clearance space will quickly come to an equilibrium average temperature. Thus, the major heat loss will now be due to conduction and convection through the gas.

The second major loss is heat transfer due to motion of the displacer and the heat capacity of the walls. This is referred to as shuttle conduction and occurs any time the displacer oscillates between a temperature difference. The displacer absorbs heat during the hot end of its stroke and gives off heat during the cold end of its stroke. Shuttle conduction in the Martini's code is calculated according to the theory postulated by Rios [4]. It is based on the assumption that as the displacer moves toward the high temperature end of the cylinder, the temperature of a point on the displacer surface will be generally lower than the temperature of the adjacent point on the cylinder wall surface. Therefore, during this part of the cycle, heat will be transferred radially inward from the cylinder wall to the displacer. Similarly, when the displacer is moving towards the low temperature end of the cylinder, the heat transfer will be radially outward. In the conventional design of Stirling engines, since the heat transfer takes place across a gap which is filled with the working gas, the temperature difference between the displacer and the cylinder is finite, and the radial heat transfer takes place irreversibly. On the average, the temperature of the displacer surface is colder when it is moving toward the warm end than when it is moving in the opposite direction, so that a net axial heat transfer results from the radial heat transfer.

In the proposed concept, it is seen that since the seals are placed at both ends, the gas is entrapped in the clearance space and it moves back and forth with the displacer. Because of rapid mixing of the gas in this space, it will be maintained at an equilibrium temperature. Also, in the proposed design, since the heat pipes are arranged around the periphery of the inner cylinder over much of the length of the displacer, the entire length of the cylinder wall up to the regenerator is likely to be at a uniform temperature. And in the absence of any manifested temperature gradient, the shuttle conduction losses will be negligible. It is also to be noted that since the radial clearance between the displacer and the cylinder is increased, the heat transfer loss will decrease because the larger gap acts as an insulator and as per the theory, the radial conduction predominates over the axial conduction in the conventional designs. Figure 12.11 shows the effect of changing the radial clearance, which is equivalent to moving along a curve and the effect of varying the material properties, which is equivalent to going from one curve to the other vertically. It is seen that the choice of materials at very high speeds is not critical, since the curves fall very close together. However, in the range of speed for the ASRE design, going from metal to ceramics has considerably reduced the shuttle heat transfer. It can be seen that further improvement in the CASE 2 design would come by increasing the radial clearance and also at the same time, reducing the temperature difference along the displacer.



τ = average rate of axial enthalpy flow

L = displacer length

K_g = thermal conductivity of gas

s = stroke

D = displacer diameter

δ = radial clearance

ΔT = difference between temperature at the boundary with the working space and temperature at the seal.

l_{T1} = wall thickness at T_1 (temperature of displacer)

l_{T2} = wall thickness at T_2 (temperature of cylinder wall)

k_1 = thermal conductivity of displacer surface

k_2 = thermal conductivity of cylinder surface.

$$\alpha = \frac{1}{2\pi} \frac{k_g}{\delta} \left(\frac{l_{T1}}{k_1} + \frac{l_{T2}}{k_2} \right)$$

CHOICE OF MATERIALS AT VERY HIGH SPEED NOT CRITICAL

IN THE ASRE RANGE OF SPEED GOING FROM METAL TO CERAMICS
REDUCED THE SHUTTLE HEAT TRANSFER.

FURTHER REDUCTION FROM INCREASED RADIAL CLEARANCE.

FIGURE 12.11 EFFECT OF RADIAL CLEARANCE AND MATERIAL PROPERTIES ON SHUTTLE CONDUCTION LOSS

Another major source of loss in the Stirling engine is the reheat loss due to inefficiency of the regenerator. The inefficiency of the regenerators mostly arises due to the temperature difference that must exist between the gas and the matrix so that the entire thermal load may be transferred to and from the gas during each cycle. When the gas leaves the cold heat exchanger and is heated in the regenerator, the gas temperature must be slightly lower than the matrix temperature in order to cause finite heat transfer rate. When the flow is reversed, the opposite is true. The net effect, therefore, is that there is a net enthalpy flux through the regenerator. This enthalpy flux is a measure of regenerator ineffectiveness. Under steady state cycle operation, the regenerator enthalpy flux is the same at all points within the regenerator, provided the regenerator is well insulated and the axial conduction is negligible. This enthalpy flux also manifests itself as the heating and cooling load required to maintain steady state conditions. Since a significant phase shift between the mass flow and pressure variations occur in the Stirling engine, the heater and cooler load are also influenced by the work of compression and expansion. The regenerator effectiveness is defined as the ratio of the amount of heat absorbed in the regenerator to the total amount passing through it and is given as:

$$E = \frac{FR \dot{M} C_p (T_H - T_C) - \text{Reheat Loss}}{FR \dot{M} C_p (T_H - T_C)}$$

The effectiveness of the regenerator is also defined in terms of the dimensionless parameter $\Lambda = hAL/VC_p$ and is given as:

$$E = \frac{\Lambda}{2 + \Lambda}$$

Therefore, the reheat loss in the regenerator becomes equal to:

$$RH = FR \dot{M} C_p (T_H - T_C) \frac{2}{\Lambda + 2}$$

Here FR is the fraction of time that the gases are flowing through the regenerator in one direction.

Thus, in order to reduce the reheat loss, the most direct way is to further improve the regenerator effectiveness. This can be done by increasing the dimensionless parameter Λ . This in turn implies that the heat transfer be increased. Both of these can be accomplished by going to finer fiber diameter of the matrix. Thus, in the proposed advanced concept a fiber diameter of 0.001 cm is utilized.

Because of the practical difficulties in supplying heat during the expansion process and due to finite times required for compression and expansion, the majority of practical Stirling cycle machines have in-line arrangement of cooler, regenerator and heater and do not approximate the ideal Stirling cycle. These machines have been characterized as operating on pseudo Stirling cycle. There are two basic implications of this type of engine design. One is that the working gas is cooled in the cooler after it has been heated during the compression process and similarly it is heated in the heater after it has been cooled during the expansion process. The second implication is that since no heat transfer surfaces are in the hot and cold spaces, except for the point in the cylinder when the clearance space essentially disappears, very little heat transfer is possible between the bulk of the gas in that space and the walls. Since little heat can be transferred during the compression and expansion processes ($\Delta Q = 0$), these processes are essentially adiabatic. In real Stirling machines, a large portion of the gas is in the dead volume which is compressed nearly isothermally, so the loss of work per cycle is not as great. It was shown by Martini [5] that there is not much difference between the specific heat input for an isothermalized and a non isothermalized machine. The basic advantage of isothermalizing the expansion and compression space emanates from the fact that it cuts down the dead volume.

In the case of Martini's analysis, a series of calculations have been made to compare a cycle analysis assuming that the expansion space and compression space behave adiabatically. It is determined that for practical engine designs, the relationship between the power output assuming adiabatic spaces and power output assuming isothermal spaces, depends only upon the ratio between the heat input temperature and the heat output temperature and also upon the fraction of dead volume in the machine.

Also, the heat requirement for the adiabatic case is related to the heat requirements for the isothermal case by the same two ratios of temperature and dead volume. The temperature corrected volume ratio in the Martini's code is defined as:

$$S = \frac{T_C}{V_L} \left(\frac{H_D}{T_H} + \frac{R_D}{T_R} + \frac{C_D}{T_C} \right)$$

NOMENCLATURE

C_D - Cold space dead volume

T_H - Effective hot space temperature

H_D - Hot space dead volume

T_R - Regenerator temperature

R_D - Regenerator dead volume

V_L - Swept volume

T_C - Effective cold space temperature

The larger S is, the less dramatic the effect of adiabatic spaces. It is seen from Fig. 12.12 that both adiabatic power correction and adiabatic heat input correction diminishes with the volume ratio. The effect on the indicated power and the indicated efficiency is shown in Fig. 12.13. With increasing volume ratio, the power drops and the efficiency levels off. Thus, for the required power output of about 25 kW at the maximum efficiency point the efficiency is 67%. The most dramatic effect is observed to be that of the cold side dead volume. With the increase in cold dead volume, although the power output decreases, the efficiency increases and the optimum volume ratio is about 1.85.

Based on the aforementioned design analysis a comparison of the relative losses in ASRE and CASE design at maximum efficiency point are shown in Table 12.8. It is seen that the maximum improvement occurs in the areas identified earlier. The indicated efficiency as a percentage of Carnot efficiency has been raised to 88 percent compared to 75 percent for ASRE design as shown in Figure 12.14. A significant portion of this improvement is due to advancement of the design itself.

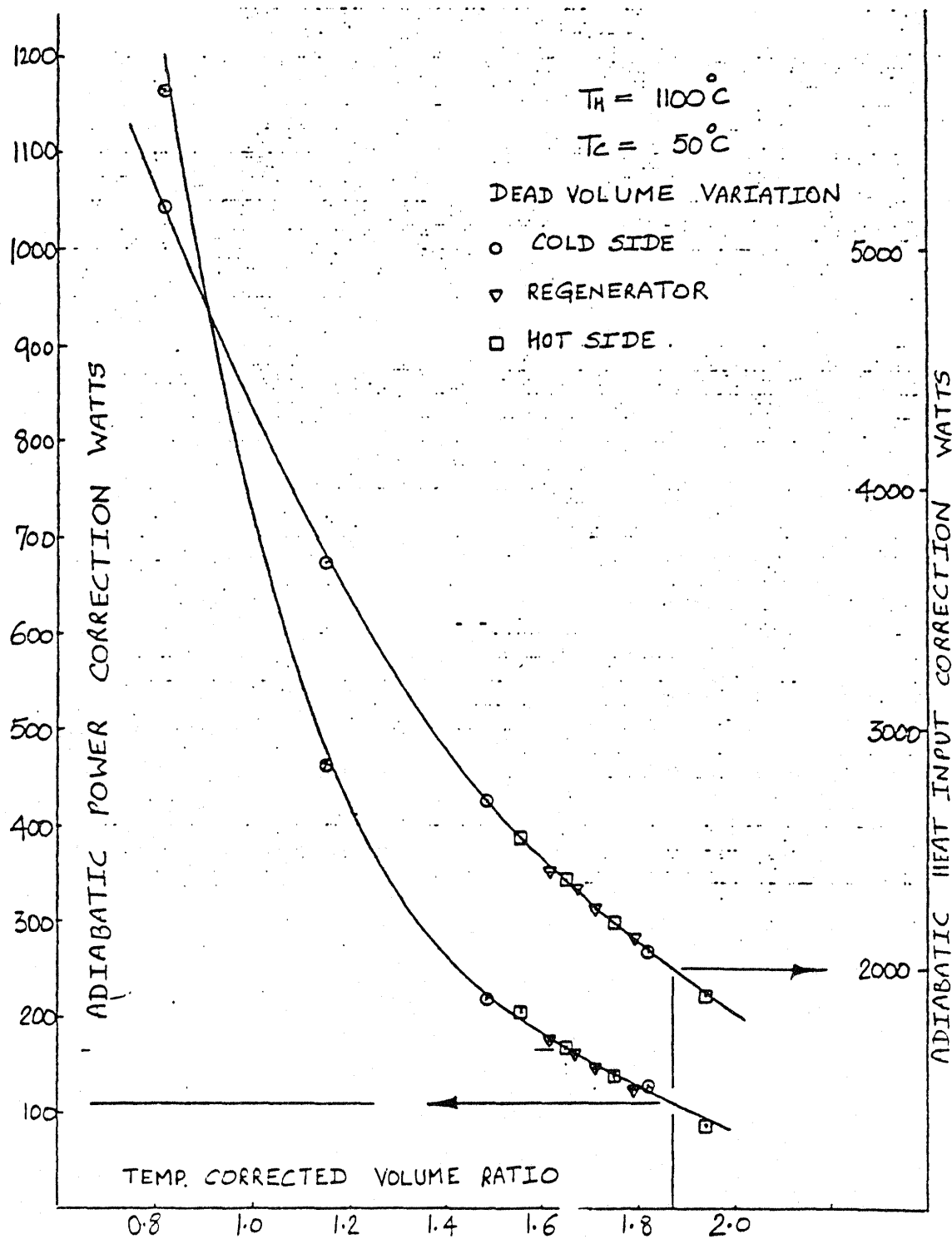


FIGURE 12.12 EFFECT OF VOLUME RATIO ON CORRECTION FACTORS

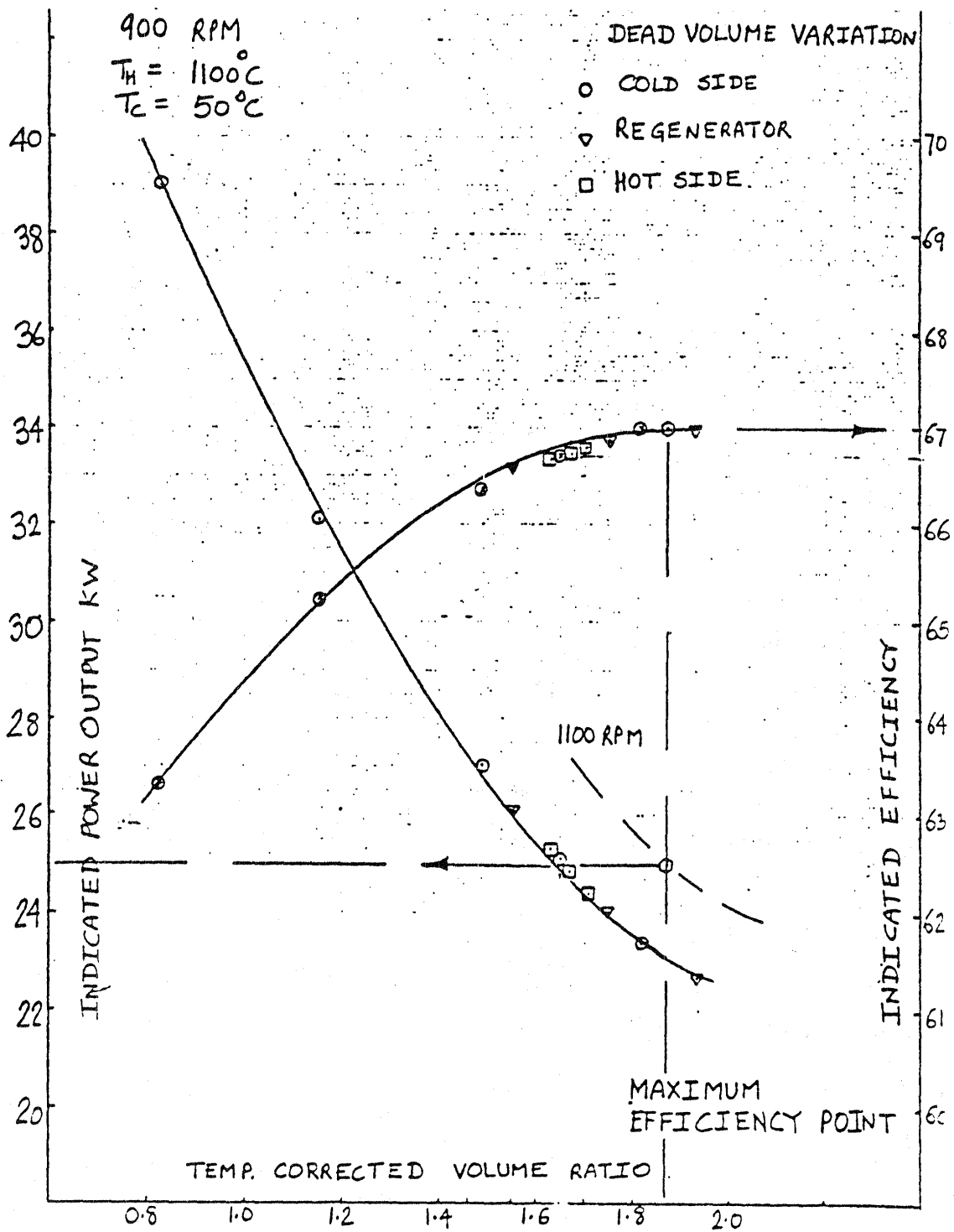


FIGURE 12.13 EFFECT OF VOLUME RATIO ON INDICATED EFFICIENCY AND POWER

TABLE 12.8 RELATIVE LOSSES IN ASRE AND CASE DESIGN
(MAXIMUM EFFICIENCY POINT)

<u>THERMAL LOSSES (W)</u>	<u>ASRE</u>	<u>CASE 1</u>	<u>CASE 2</u>	<u>KEY ATTRIBUTE</u>
CORR. FOR ADIABATIC HX.	2791.55	2477.15	2146.42	REDUCED VOID VOLUME
REHEAT LOSS	1262.19	1236.46	425.97	IMPROVED REGENERATOR
SHUTTLE LOSS	763.64	554.08	29.41	RECONFIGURED DISPLACER
PUMPING LOSS	1032.44	1105.63	90.050	HOT DISP. RING
TEMP SWING	57.9	52.56	38.35	
CYL. WALL COND.	523.84	116.4	21.16	REDUCED WALL THICKNESS
DISP. WALL COND.	315.97	25.74	6.78	
REG. WALL COND.	1071.11	200.76	151.33	
CYL. GAS COND.	27.58	19.42	15.69	
REG. MTX. COND.	94.24	105.58	127.3	
RADIATION IN DISP.	35.47	52.84	55.63	
<u>DYNAMIC LOSSES (W)</u>				
ADIABATIC CORR.	1303.26	533.52	121.33	REDUCED VOID VOLUME
HEATER FLOW LOSS	239.76	99.26	106.26	
REGENERATOR FLOW LOSS	198.88	129.61	658.46	SMALLER REG. FILAMENT SIZE
COOLER FLOW LOSS	16.01	10.01	5.46	

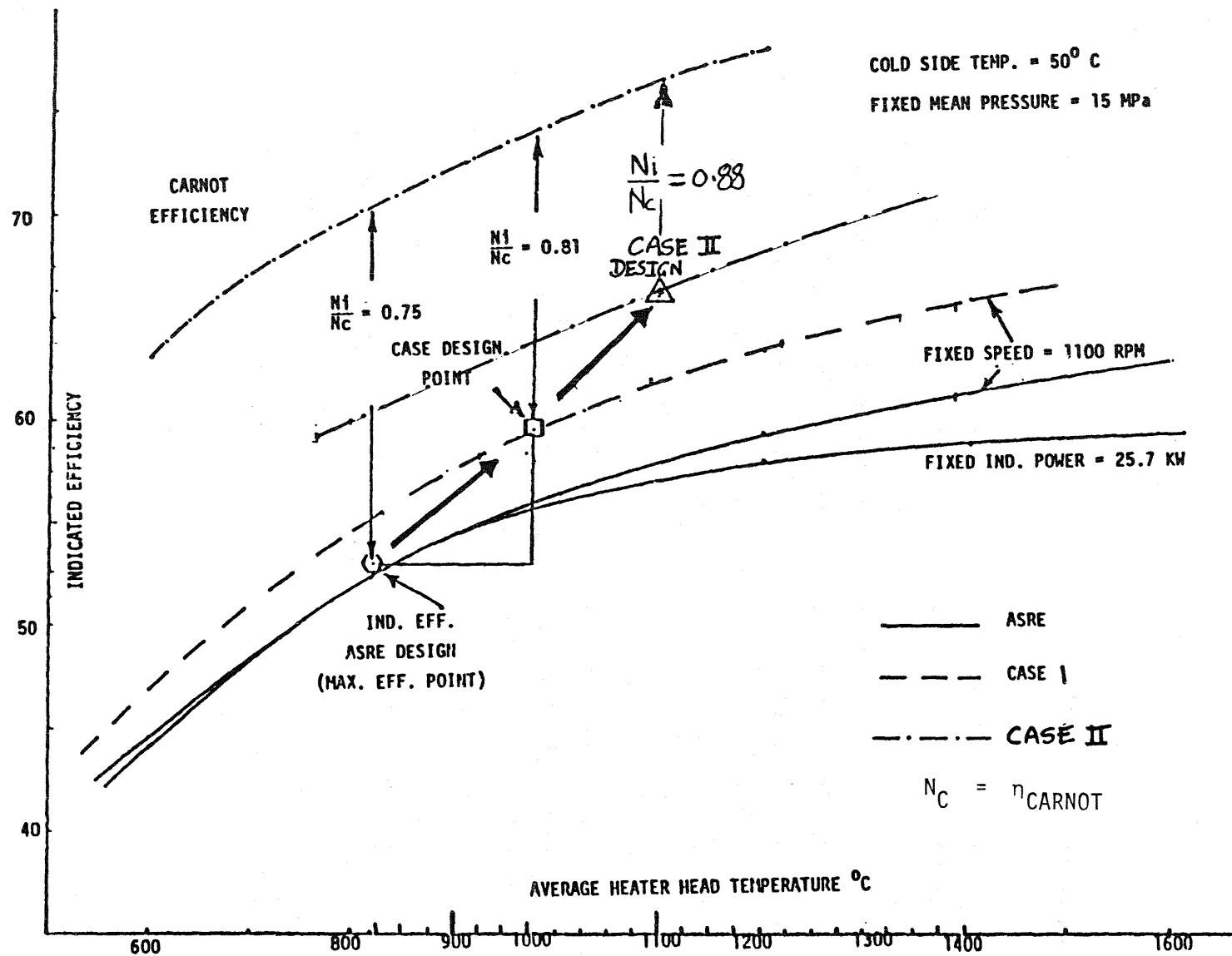


FIGURE 12.14 INDICATED EFFICIENCY VS. HEATER HEAD TEMPERATURE

12.6 EXTERNAL HEATING SYSTEM

One of the implications of raising the hot side temperature of the Stirling engine is the corresponding increase in the flame temperature and decrease in the external heating system efficiency. In order to maintain the reasonable level of external heating system efficiency, the preheater effectiveness is assumed to be 95%. Also, it was decided that the heating system should not operate in the condensing mode. Thus, from Fig.12.15 for about 2000°F hot side temperature and the 95% preheater effectiveness the efficiency of the external heating system will be 90%. At this EHS efficiency, from Figure 12.16 the exhaust gas temperature and preheat temperature are 500°F and 2100°F respectively. From Fig.12.17 the adiabatic flame temperature is 4300°F. It is seen that increase in the heater head temperature to 2200°F would lower the EHS efficiency to 89% and raise the flame temperature to 4450°F. Since the analysis is made for heat exchanger NTU of 4, any further improvement in the heat transfer coefficient would bring in diminishing returns except making the heat exchanger smaller. Further, reduction in the heat exchanger size would require increase in heat pipe heat carrying capacity. The acceptable level of flame temperature would also limit the highest temperature of the heater head in view of NO_x formation. However, it has been suggested that the possibility of NO_x formation is reduced in the case of pulse combustion since it requires very little or no excess air.

A typical comparison of steady state burning and pulsating burning is given in Table 12.9

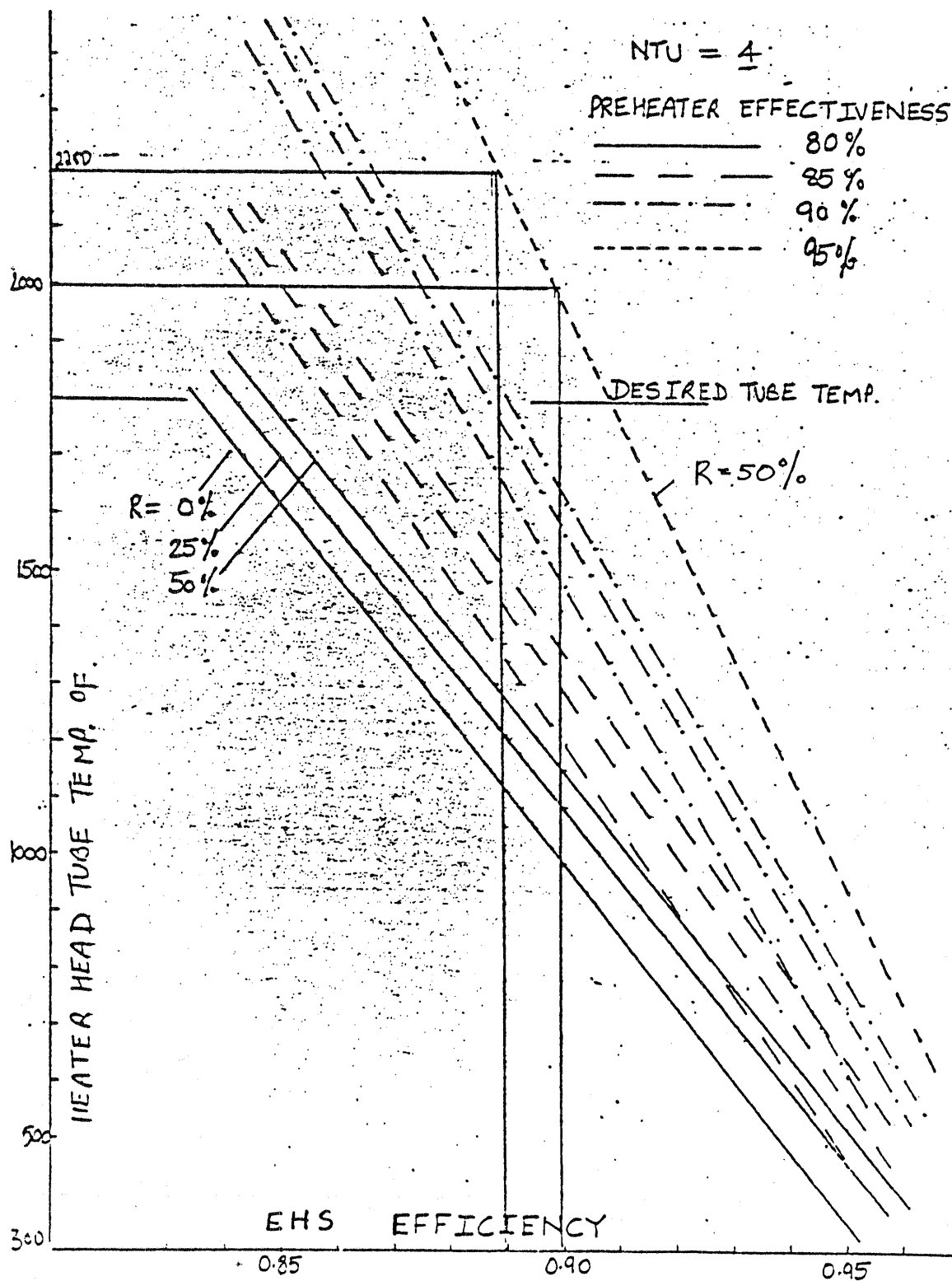


FIGURE 12.15 EHS EFFICIENCY AS A FUNCTION OF HOT SIDE TEMPERATURE

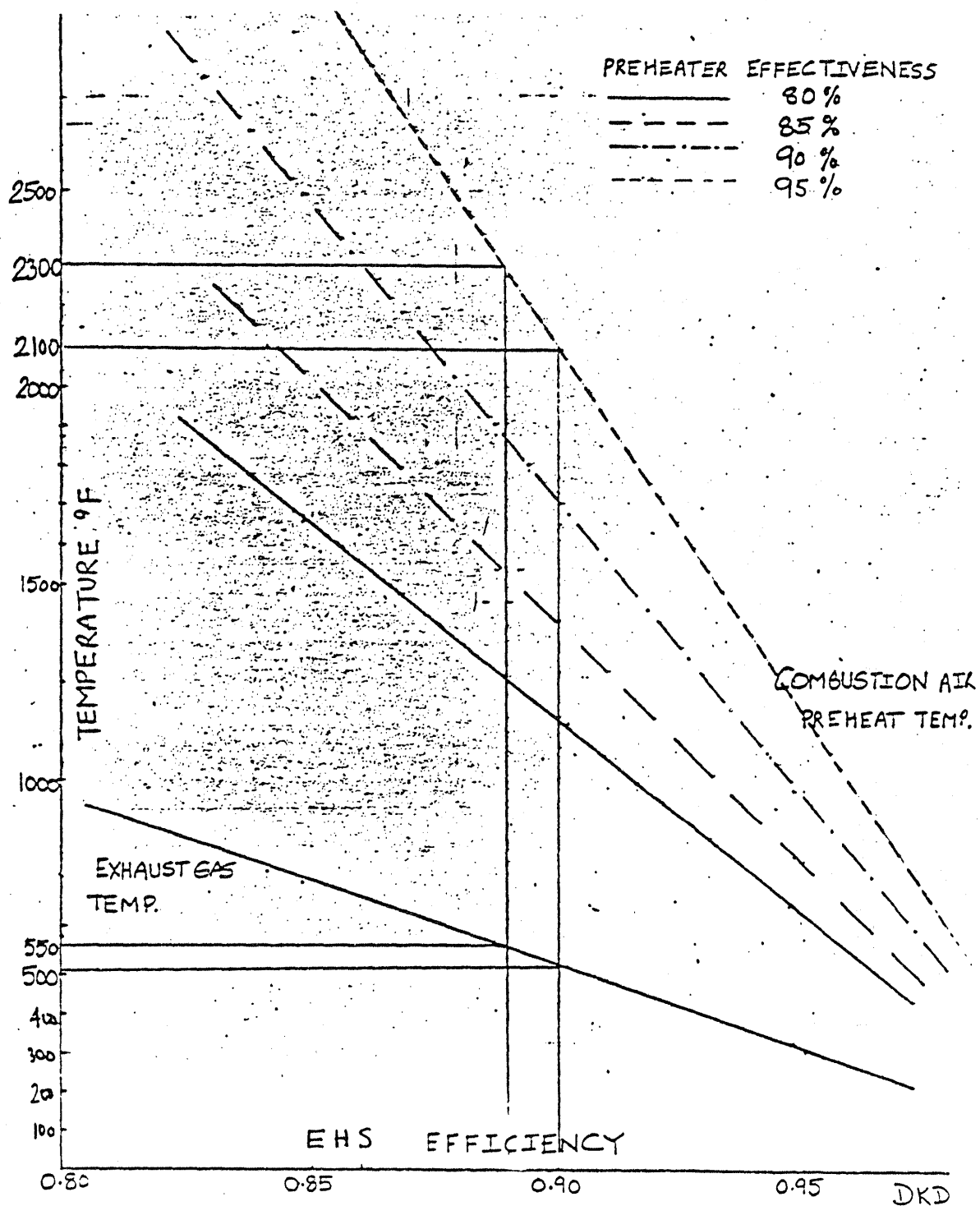


FIGURE 12.16 EXHAUST GAS TEMPERATURE AND PREHEAT TEMPERATURE AS A FUNCTION OF EHS EFFICIENCY

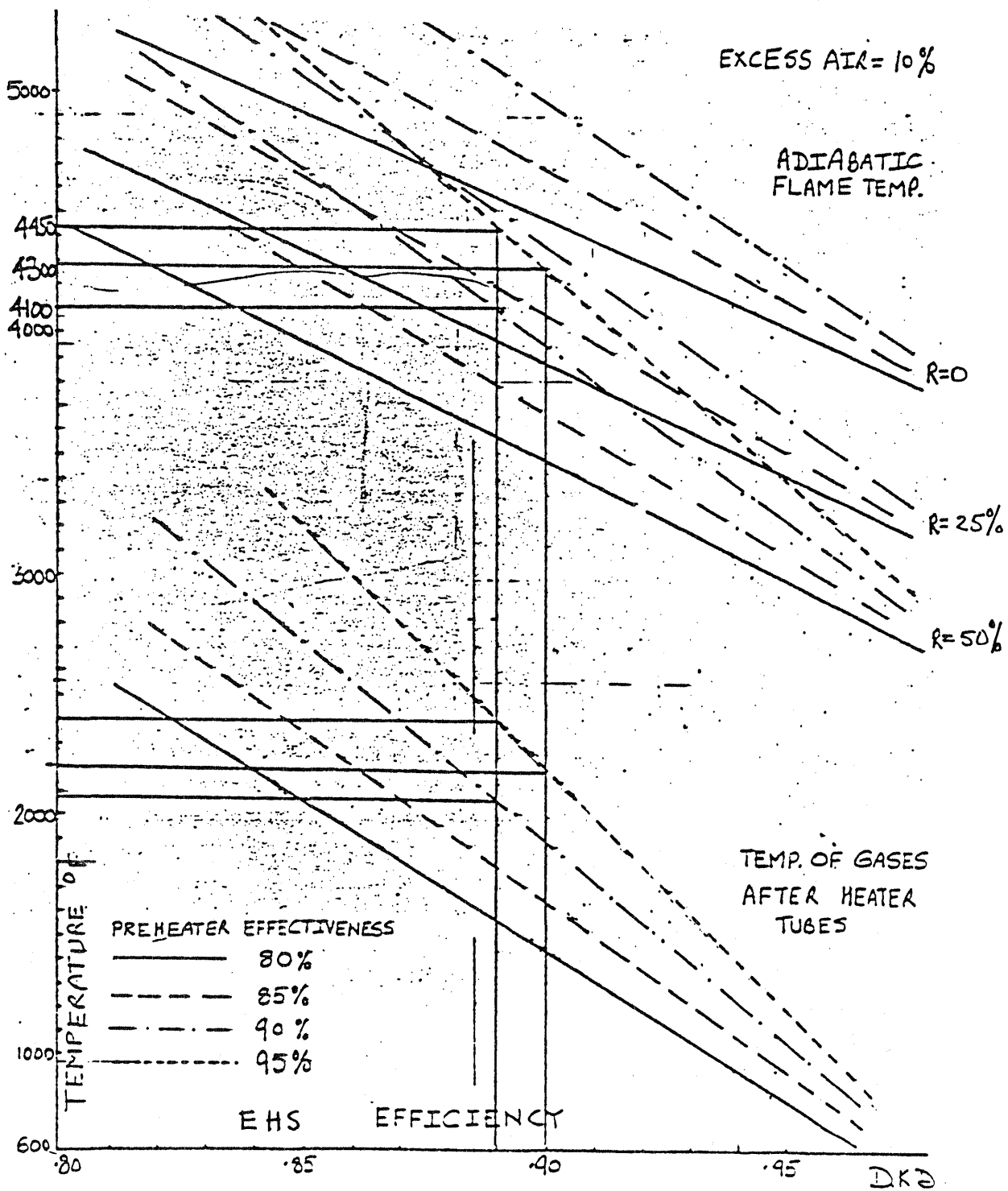


FIGURE 12.17 ADIABATIC FLAME TEMPERATURE

TABLE 12.9 COMPARISON OF STEADY STATE BURNING AND PULSATING BURNING

<u>PARAMETERS</u>	<u>UNITS</u>	<u>STEADY STATE</u>	<u>PULSATING</u>
o COMBUSTION INTENSITY	kW_t/M^3	100-1000	10,000-50,000
o EFFICIENCY OF BURNING	%	85-96	90-99
- Losses due to chemical underburning	%	0-3	0-1
- Losses due to mechanical underburning	%	0-15	0-5
o CONCENTRATION IN EXHAUST			
- CO	%	0-2	0-1
-NO _x	mg/m^3	100-7000	20-70
o COEFFICIENTS OF DEPOSITS ON HEATED SURFACE		0-0.5	0-0.05
o CONVECTIVE HEAT TRANSFER COEFFICIENT	$\text{Wt}/\text{M}^2\text{K}$	50-100	100-500
o NOISE PRODUCED BY THE BURNING ZONE	dB	85-100	100-130
o TIME OF REACTION	T sec	1-10	0.01-0.5
o EXCESS AIR LEVEL	%	10-20	0-10

12.7 PERFORMANCE

Based on the aforementioned design, the performance map of the long range ceramic automotive Stirling engine was made. The maximum and minimum mean pressure levels of the engine are 15 MPa and 3 MPa respectively. Also, the minimum and maximum limits on the operation speed of 500 and 4500 rpm respectively were maintained as in CASE 1. The engine performance curves (indicated power vs. speed) are presented in Fig.12.18 with constant indicated efficiency and constant mean pressure level lines. In order to obtain net power and net efficiency, the auxiliary power consumption and the losses associated with friction and seals is deducted. The overall system efficiency also includes the efficiency of the external heating system which is determined to be 90% and stays constant with load.

The parasitic power requirements normally include the following:

- o Combustor Blower
- o Water Pump
- o Alternator
- o Lubricating Oil Pump
- o Hydrogen Gas Compressor

In the case of the proposed concept, the external heating system is based on pulse combustion. The air is naturally aspirated into the combustion chamber during normal operation and therefore no blower is required except during startup to purge the combustion chamber. As such, the parasitic power loss in the blower is saved. The water pump power demand is assumed to be identical to that in CASE 1 and is prorated for improved indicated efficiency which means lower heat rejection requirements. The other parasitic power and the friction power are based on identical considerations as in CASE 1

Fig.12.19 shows the performance of CASE 2 as a function of speed. It is noted from the figure that whereas the load requirements under maximum efficiency and part load conditions can be met at speeds the same as ASRE design, the full load requirement can be met at a reduced speed of 3400 rpm. At the part load and the low load operation, the charge pressure was raised to 6 MPa. The performance of the CASE 2 at four load points is compared with CASE 1 and ASRE

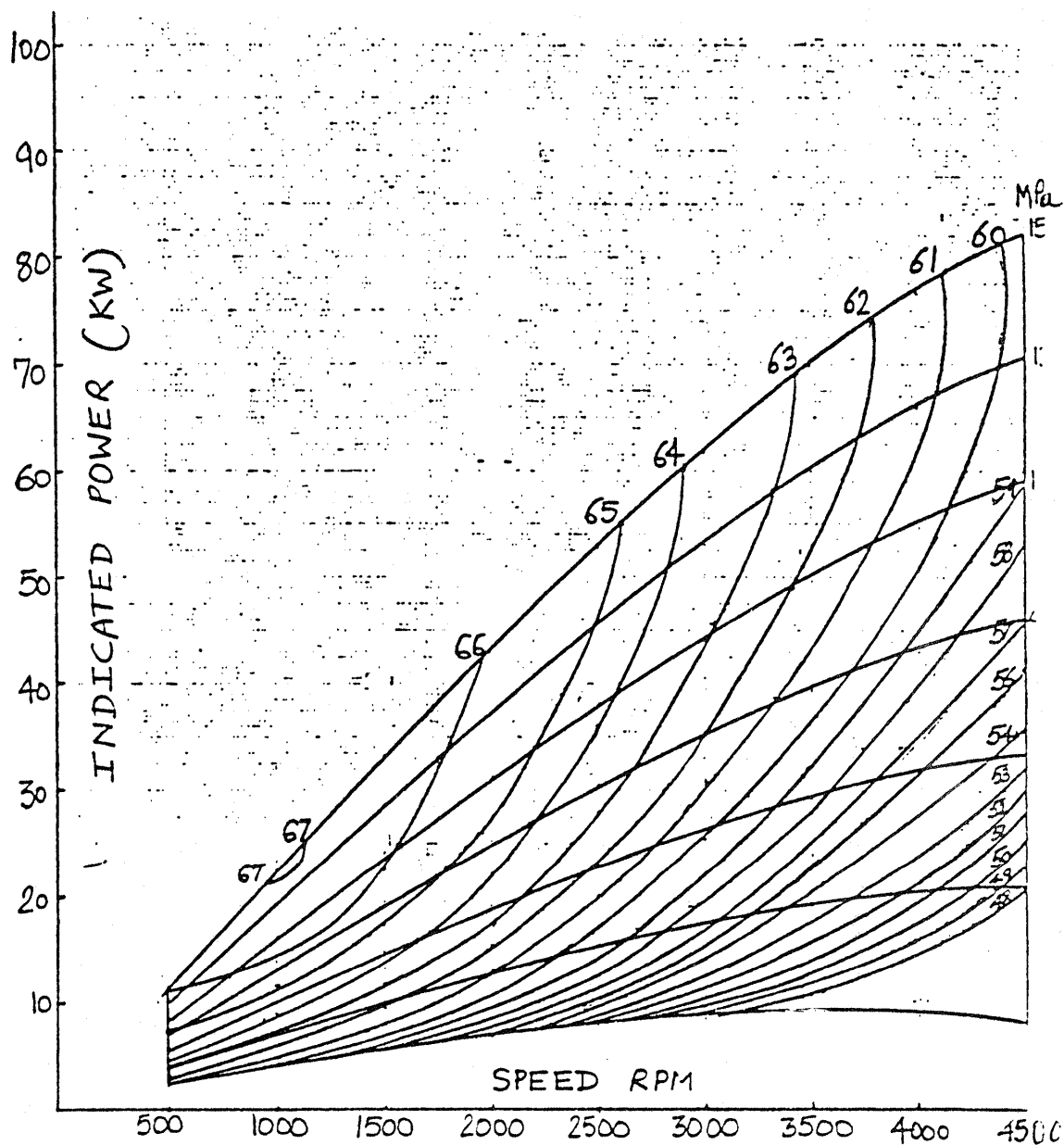


FIGURE 12.18 PERFORMANCE MAP OF CASE 2: CURVES OF CONSTANT INDICATED EFFICIENCY AND CONSTANT MEAN PRESSURE

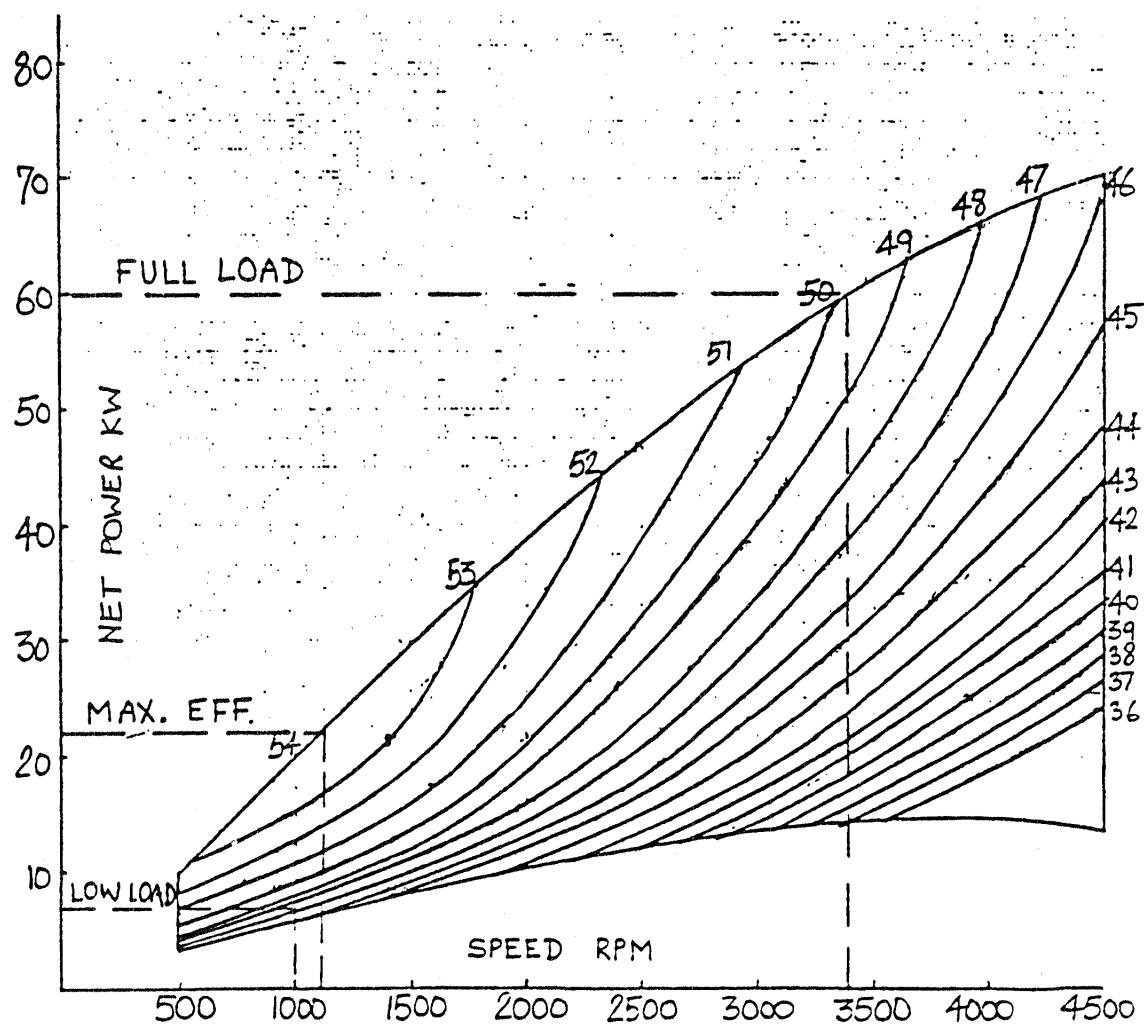


FIGURE 12.19 PERFORMANCE MAP OF CASE 2: CURVES OF CONSTANT NET EFFICIENCY (%)

design in Table 12.10. It is seen that significant gains can be achieved throughout the load conditions for CASE 2 designs. Most importantly, the significant gain in net efficiency occurs at low load condition, where it is seen that almost 34% gain over ASRE design can be achieved.

The relative thermal and dynamic losses for CASE 2 are compared with ASRE and CASE I design in Table 12.11. The greatest improvement occurs in wall conduction losses and displacer pumping and shuttling losses. The improvement in regenerator effectiveness results in additional flow losses, but considerable savings occur in reheat loss. Since the frictional heat regenerated by the flow losses is assumed to be dissipated internally, the overall effect is the net gain in efficiency.

TABLE 12.10 PERFORMANCE COMPARISON OF CASE AND ASRE DESIGN

		FULL LOAD			MAX EFFICIENCY			PART LOAD			LOW LOAD		
		CASE 2	CASE 1	ASRE	CASE 2	CASE 1	ASRE	CASE 2	CASE 1	ASRE	CASE 2	CASE 1	ASRE
ENGINE SPEED	(RPM)	3400	3300	4000	1100	1100	1100	2000	2000	2000	1000	1000	1000
CHARGE PRESSURE	(MPa)	15	15	15	15	15	15	6	5	5	6	5	5
INDICATED POWER	(KW)	68.5	69.2	73.3	24.6	25.0	24.8	16.2	14.8	15.0	8.5	7.2	7.9
FRICTION	(KW)	7.2	6.9	9.6	2.2	2.2	2.2	2.1	2.0	2.0	1.0	0.9	0.9
AUXILIARIES	(KW)	1.3	1.8	3.6	0.3	0.3	0.5	0.6	0.7	0.8	0.3	0.3	0.4
NET POWER	(KW)	60.0	60.5	60.1	22.1	22.5	22.1	13.5	12.1	12.2	7.2	6.0	6.6
EXTERNAL HEATING SYSTEM EFFICIENCY	(%)	90	89	90.5	90	89	92.4	90	89	91.7	90	89	89.8
INDICATED EFF.	(%)	63.38	55.57	46.1	67.1	60.0	52.8	62.48	58.17	50.9	63.8	55.3	48.5
NET EFFICIENCY	(%)	50.0	43.2	34.2	54.2	48.1	43.5	47.1	42.4	37.7	48.6	41.0	36.4
PERCENTAGE GAIN OVER ASRE		46.2	26.3		24.6	10.6		24.9	12.5		33.5	12.6	

TABLE 12.11 RELATIVE LOSSES IN ASRE AND CASE DESIGN

<u>THERMAL LOSSES (W)</u>	<u>ASRE</u>	<u>CASE 1</u>	<u>CASE 2</u>	<u>KEY ATTRIBUTE</u>
CORR. FOR ADIABATIC HX.	2791.55	2477.15	2146.42	REDUCED VOID VOLUME
REHEAT LOSS	1262.19	1236.46	425.97	IMPROVED REGENERATOR
SHUTTLE LOSS	763.64	554.08	29.41	RECONFIGURED DISPLACER
PUMPING LOSS	1032.44	1105.63	90.050	HOT DISP. RING
TEMP SWING	57.9	52.56	38.35	
CYL. WALL COND.	523.84	116.4	21.16	} REDUCED WALL THICKNESS
DISP. WALL COND.	315.97	25.74	6.78	
REG. WALL COND.	1071.11	200.76	151.33	
CYL. GAS COND.	27.58	19.42	15.69	
REG. MTX. COND.	94.24	105.58	127.3	
RADIATION IN DISP.	35.47	52.84	55.63	
<u>DYNAMIC LOSSES (W)</u>				
ADIABATIC CORR.	1303.26	533.52	121.33	REDUCED VOID VOLUME
HEATER FLOW LOSS	239.76	99.26	106.26	
REGENERATOR FLOW LOSS	198.88	129.61	658.46	SMALLER REG. FILAMENT SIZE
COOLER FLOW LOSS	16.01	10.01	5.46	

12.8 COLD START PENALTY

It has been recognized that, during cold start of the engine, some of the fuel that is spent in heating the engine would normally be lost through conduction and radiation. This penalty is roughly assumed to be equivalent to the heat stored in the hot parts of the engine. This, however, is not exactly true due to several effects. First, the engine, transmission, and axle oil added to the penalty due to its increased viscosity at low temperatures. Second, during the heating of the engine, much of the heat went into establishing the temperature profile that drove the conduction losses. Thus, the conduction losses are lower, which somewhat offset the energy required to heat the engine. Additionally, the thermal efficiency of the engine is somewhat higher due to the low cooling water temperature. Because of complex interaction of these various effects, the approach taken in ASRE design to quantify the cold start penalty, is to base on it the actual test data of P-40 engine. The losses due to different mechanisms are segregated and appropriately adjusted. The largest of these losses is the engine heating loss which is assumed to be proportional to the ratio of stored heat in the engine. The reheating loss is assumed to be proportional to the stored heat and it is also assumed that the run-down losses are cut in half by completely closing the air throttle after the ignition is turned off. The last item is especially true in the case of the proposed concept where pulse combustion is utilized, where, when the ignition is turned off, no air is aspirated into the burner and the engine parts remain hot.

In order to adjust the engine losses assumed for ASRE to account for the ceramic components used in CASE design, the considerations listed in Figure 12.20 were adopted.

A comparison of ASRE and CASE I material weight estimate was made as shown in Tables 12.12 and 12.13 and from this cold start penalty (CSP) was estimated.

It was determined that the cold start penalty for CASE I design can be expected to be 13% greater than ASRE design. A fundamental reason for the higher cold start penalty in CASE I is the high specific heat of the ceramic materials relative to an equal weight of metal. For example, the specific heat of iron is 0.106 cal/g compared to the mullite value of 0.210 cal/g. However, the CSP is reduced by 20% compared to ASRE in CASE II because of the substantial difference in design between CASE I and CASE II.

- o COLD AND HOT TRANSIENT CONDITIONS OF ENGINE REQUIRES ADDITIONAL FUEL CONSUMPTION.
- o COMPLEX INTERACTION OF VARIOUS EFFECTS REQUIRES USE OF ACTUAL TEST DATA.
- o ASRE COLD START PENALTY BASED ON ACTUAL TEST DATA OF P-40 ENGINE.
- o CASE 1 COLD START PENALTY PRORATED FROM ASRE DATA.*
- o THE LARGEST LOSS IS THE ENGINE HEATING LOSS - ASSUMED PROPORTIONAL TO THE RATIO OF STORED HEAT IN ENGINE HEATING SYSTEM.

* "Automotive Stirling Reference Engine Design Report,"
June 1981, NASA CR-165381.

FIGURE 12.20 COLD START PENALTY CONSIDERATIONS

TABLE 12.12 ASRE WEIGHT ESTIMATE

	LB.
o HEATER ASSEMBLY	79.38
o EXTERNAL HEAT SYSTEM	48.51
o PISTON/DOME	6.62
o REGENERATOR HOUSING	4.41
o MISCELLANEOUS	<u>6.00</u>
	144.92
o AVERAGE SP. HET OF ASRE MATERIALS AT TEMP. BTU/LB°F	0.15

TABLE 12.13 CASE 1 MATERIAL WEIGHTS HEATER SYSTEM

PT. NO.	NAME	WT. (EA.)	QTY/ENG.	WT. /ENG	
				LB.	MATERIALS
CSE 102	COMB. CHAMBER	29.05	1	29.10	Si ₃ N ₄
CSE 101-2	CYL. OUTER SLEEVE	6.18	4	24.72	Si ₃ N ₄
CSE 101-1-1	CYL. HEATER HD.	14.50	4	58.00	MULLITE
CSE 101-1-2	HTR. HD. DIST. CH.	2.53	4	10.12	SiC
CSE 101-1-6	HEATER HEAT TUBE	.15	96	14.10	SiC
CSE 109	DISPLACER	.77	4	3.08	MULLITE
CSE 109A	RADIATION SHIELD	.04	12	.48	MULLITE
CSE 101-3	INSULTAING SLEEVE	1.50	4	6.00	MULLITE
CSE 101-3	RAD. MANTLE DOME	2.15	4	8.60	SiC
CSE 101-5	MANTLE-BAFFLE	.13	4	.52	Si ₃ N ₄
CSE 105-4	CYL. LINER	1.66	4	6.64	MULLITE
CSE 104-1	PRE HEATER PLATES	.035	800	<u>28.00</u>	SiC
TOTAL				<u>189.66</u>	

WEIGHT BREAKDOWN BY MATERIAL (LB)	Si ₃ N ₄	MULLITE	SiC
	54.34	74.2	61.12
SPECIFIC HEAT BTU/16°F	0.17	0.275	.186

TIME CONSTANT $\tau = \frac{\rho C V}{h A}$ FOR MULLITE PARTS SIGNIFICANTLY LONGER THAN OTHERS.

12.9 FEDERAL DRIVING CYCLE

The results of this study were utilized by NASA Le RC to determine the performance of the Ceramic Automotive Stirling Engine considering federal driving cycle. The results of this analysis are presented in Table 12.14.

TABLE 12.14 COMPARISON BETWEEN CERAMIC AND METAL STIRLING ENGINES

	ASRE	CASE I	CASE II	
PERFORMANCE				
BSFC (BEST)	.32 lb/BHP-HR	.287 lb/BHP-HR	0.255 lb/BHP-HR	
BRAKE η	43%	48%	54%	
METRO-HWY	34.6 MPG (CITY)	34.9 MPG (CITY)	42.8 (CITY)	48.1 (CITY)
DRIVING CYCLE	66.0 MPG (HWY)	68.5 MPG (HWY)	76.8 (HWY)	86.1 (HWY)
	44.0 MPG (COMB.)	44.8 MPG (COMB.)	53.4 (COMB.)	60.0 (COMB.)
	PHOENIX WITH AUTOMATIC	PHOENIX WITH AUTOMATIC	PHOENIX WITH AUTOMATIC	PHOENIX WITH CVT
RATED POWER	80 BHP @ 4000 rpm	80 BHP @ 3300 rpm	80 BHP @ 3400 rpm	
CONFIGURATION	U-4 CYL.	V-4 CYL.	V-4 CYL.	
WEIGHT	145 LB. HOT SIDE 585 LB. TOTAL	184 LB. HOT SIDE 625 LB. TOTAL	400 LB. TOTAL	
SIZE	22" x 22" x 26"	30" x 30" x 33"	24" x 24" x 33"	
	163 gm FUEL (CSP)	184 gm FUEL (CSP)	131 gm FUEL (CSP)	

TABLE 12.15 MARTINI CODE NOMENCLATURE

C_D	Cold dead volume
C_p	Heat capacity of gas at constant pressure
DC	Diameter of compression space piston
DCY	Diameter of engine cylinder
E	Regenerator effectiveness
FR	Fraction of gas inventory in regenerator
G	Mass velocity per unit area
GR	Displacer gap thickness
H_D	Hot dead volume
K1	Thermal conductivity of displacer
K2	Thermal conductivity of cylinder wall
KG	Gas thermal conductivity
LD	Length of displacer
m	Working gas mass flow rate
n	Dimensionless parameter
NU	Engine frequency
P_{\max}	Maximum engine pressure
P_{\min}	Minimum cycle pressure
QPU	Pumping loss
QZ	Static heat conduction loss
R_D	Regenerator dead volume
RM	Gas constant
SD	Stroke of displacer
T_C	Effective cold space temperature
TCM	Heat sink temperature
T_H	Effective hot space temperature
TMH	Heater head temperature
T_R	Regenerator temperature
V_L	Swept volume
Z1	Compressibility factor

REFERENCES

1. Meijer, R.J. and Ziph, B. "Evaluation of the Potential of the Stirling Engine for Heavy Duty Application". NASA Contractor Report 165473.
2. Merrigan, M.A. and Keddy, E.S., "High-Temperature Heat Pipes for Waste-Heat Recovery", J. Energy.
3. Parker, G.H. and Hanson, J.P., "Heat Pipe Analysis".
4. Rios, P.A., "An Approximate Solution to the Shuttle Heat Transfer Losses in a Reciprocating Machine," J. Engng. Pwr 93, 1971.
5. Martini W.R., Hanser S.G. and Martini M.W., "Experimental and Computational Evaluations of Isothermalized Stirling Engines," Proceedings 12th IECE Conference, 779250.

SECTION 13
CRITICAL DEVELOPMENT AREAS

13.1 CRITICAL MATERIALS PROBLEMS

In order to realize the design presented, certain critical materials development tasks will be required:

1. The continued development of structural ceramics is needed to provide ceramics which are strong, have a high fracture toughness, and a high Weibull modulus. Fiber and whisker reinforcement and transformation toughening technology will be advanced to meet these needs. The reaction of any of these ceramics with H_2 at the temperature of operation must be investigated and possible dopants to the H_2 be defined to reduce deleterious reactions, if any. Although much R&D work has been done on SiC , Si_3N_4 and ZrO_2 very little has been conducted on mullite. Mullite should be further developed because of its unique combination of favorable properties for heat engine application, in particular its low thermal conductivity coupled with excellent mechanical properties.
2. In a number of places, the gas tight joining of SiC to mullite is required:
 - a. SiC head to mullite cylinder
 - b. SiC heater head tubes to the mullite regenerator housing

These joints not only have to be gas tight but have to withstand substantial stresses due to pressure and thermal strain loads. The development of process technology to provide such joints is a critically important task.

3. The effect of high temperature, high pressure hydrogen on the SiC and mullite, and on the joints, needs to be evaluated for long time exposure.
4. The highest temperature exposure of the ceramic components will be directly beneath the burner where the surface temperature is anticipated to reach 3800°F (2093°C). Zirconia coated Si₃N₄ is proposed for this area. A relatively thin layer of zirconia will substantially reduce the maximum temperature that the substrate will reach. (Also, an active cooling loop can be incorporated in this area, if necessary, to reduce the surface temperature.) The development of this coating process and thermal durability tests of the composite will need to be conducted.
5. In this design, a ceramic fiber regenerator core is proposed. The fabrication techniques and the ability of the core to tolerate cyclic high temperature hydrogen gas flow will have to be evaluated.
6. Development of the fabrication for a complete cylinder assembly would follow the successful solution of the above problems.

13.2 CRITICAL DESIGN ISSUES

In the area of thermal and structural designs, the following critical issues will have to be resolved.

1. The emission level, especially the NO_x emission, from the combustion exhaust may increase as the flame temperature is increased. The influence of the combustion gas recirculation level and other means to reduce NO_x emission needs to be investigated.

2. The present study does not allow a rigorous transient analysis. More in-depth transient analysis is needed to investigate the effects of thermal shock on key ceramic components and identify means to reduce the thermal shock. Start-up stresses are severe for ceramics.
3. Potential for the performance advantage of a ceramic engine over a metal engine is proven to be feasible in this study, but has not been fully explored as indicated in Figure 1.10. Additional design iteration will allow the reduction of localized stress level and permit even higher engine operating temperature.
4. A more rigorous structural analysis should include the engine cylinder and heater head as a whole so that the stress concentration at the tube-cylinder head interface can also be evaluated. The natural frequency of the tubes and their dynamic response need to be analyzed to assess potential failure modes of the engine.
5. The cumulative probability of failure as a function of the volumetric distribution of stress and flaw population needs to be analyzed. Such an analysis will require extensive statistical data on the materials selected.
6. For the CASE II design, development of reliable heat pipes which can operate in the severe thermal environments proposed for the design will be required.

A summary of critical issues is presented in Table 13.1.

Near term key follow-on efforts which are recommended if this technology is to be developed are listed in Table 13.2.

TABLE 13.1 CRITICAL CERAMIC TECHNOLOGY ISSUES (CASE I)

1. DEVELOPMENT OF LOW THERMAL CONDUCTIVITY, HIGH PERFORMANCE STRUCTURAL CERAMIC, MULLITE ($3 \text{ Al}_2\text{O}_3 \cdot 2 \text{ SiO}_2$)

TENSILE STRENGTH 600-700 MPa (90-100 KSI)
 WEIBULL MODULUS 15-20 (REQUIRES NDE AND PROOF TESTING)
 FRACTURE TOUGHNESS 5-10 M Pa

- CANDIDATE TRANSFORMATION TOUGHENED, FIBER REINFORCED MATRIX
- STRENGTH RETENTION AT ELEVATED TEMPERATURE
- CHEMICAL STABILITY IN PRESENCE OF H_2 , 1000C (POSSIBLE REQUIREMENT TO DOPE H_2 OR GO TO HE)
- IMPERMEABILITY TO HIGH TEMP H_2 .

2. COMBUSTION CHAMBER CAPABLE OF MAXIMUM TEMPERATURE 3800 F ($\sim 2100\text{C}$) NEEDS TO BE DEVELOPED. CANDIDATE SYSTEM IS ZrO_2 COATED Si_3N_4 .

ELIMINATION OF SPALLATION WILL BE CRITICAL PROBLEM. WILL REQUIRE TRANSITION LAYER BETWEEN HIGH EXPANSION ZrO_2 AND LOW EXPANSION Si_3N_4 .

SEGMENTED DESIGN WILL PROBABLY BE NEEDED TO MINIMIZE THERMAL STRESSES

3. FABRICATION TECHNOLOGY DEVELOPMENT

- THIN WALL TUBES, IMPERMEABLE TO H_2
- PRECISION ASSEMBLY OF HEATER HEAD
- RESISTANT TO VIBRATION FATIGUE FAILURE

4. GENERAL PROBLEM: FOREIGN OBJECT DAMAGE, REQUIRES MORE CARE IN ASSEMBLY, HANDLING, MAINTENANCE THAN METAL ENGINE.

5. JOINING OF SiC TO MULLITE, SiC TO SiC , SIMILAR THERMAL EXPANSION COEFFICIENTS AND PRESENCE OF Si IN EACH, INDICATES BONDING BY Si METAL, SINTERING, OR DIFFUSION WILL BE SUCCESSFUL.

6. REGENERATOR MATRIX

$3\mu\text{M}$ CERAMIC FIBER CAPABLE OF CYCLIC THERMAL SHOCK SURVIVABILITY
 ($4000 \times 2000 = 8 \times 10^6$ CYCLES).

TABLE 13.1 (CONT'D)

ADDITIONAL CRITICAL ISSUES (CASE II)

1. DEVELOP DURABLE CERAMIC HEAT PIPE COMPATIBLE WITH Li , FLAME TEMPERATURE OF 4300 F (2370C) AND COLD SIDE 2000 F (1093 C)

HIGH THERMAL CONDUCTIVITY SiC WILL REDUCE ΔT IN CERAMIC.

2. HOT RING TO OPERATE AT 1100 C IN CONTACT WITH CERAMIC WALL
3. THIN WALL CERAMIC PLATES FOR RECUPERATOR ENHANCED EFFICIENCY ($\eta=95\%$)
4. OILLESS, LOW FRICTION BEARINGS IN CRANKCASE SECTION.
5. DESIGN AND DEVELOPMENT OF PRESSURIZED CRANKCASE
6. FINE DIAMETER CERAMIC FILAMENTS ($1\mu\text{m}$) FOR REGENERATOR MATRIX WITH REQUIRED DURABILITY.

TABLE 13.2 NEAR TERM KEY FOLLOW-ON EFFORTS RECOMMENDED

1. ANALYSIS

- ITERATE THERMAL ANALYSIS AND DESIGN TO FIND HIGHER OVERALL EFFICIENCY DESIGN POINT
 - REDUCTION OF THERMAL LOSSES
 - OPERATION AT HIGHER TEMPERATURE

2. MATERIALS DEVELOPMENT

- SUPPLEMENT CURRENT NASA-LEWIS PROGRAM ON TOUGHENED HIGH TEMPERATURE MULLITE DEVELOPMENT PROGRAM (CONTRACT NO. DEN 3-339) AND CONCURRENT ORNL PROGRAM ON MULLITE COMPOSITES (CONTRACT NO. 86 x-00218C)
- ASSESS MULLITE MECHANICAL PROPERTIES IN CYCLIC FATIGUE, AND LONG TIME HYDROGEN, STRESS, ELEVATED TEMPERATURE ENVIRONMENT
- DEVELOP FINE FILAMENT (1-3 μ m) CERAMIC FOR REGENERATOR CORE

3. FABRICATION PROCESS DEVELOPMENT

- DEVELOP CURVED, THIN WALLED TUBE PROCESS
- VERIFY TUBE TO HEAD JOINING APPROACHES
- FABRICATE JOINTS BY VARIOUS APPROACHES
- VERIFY ASSEMBLY APPROACH FOR MULLITE CYLINDER HOUSING.
- FABRICATE SIMULATED COMPONENT AND PERFORM MECHANICAL TESTS

4. COMPONENT DEVELOPMENT

- DEVELOP HIGH TEMPERATURE, DURABLE COMBUSTOR HOUSING CONCEPT

ADIABATIC FLAME TEMP. CALCULATION

LIST

```
100 REM PROGRAM STORED IN FILE NUMBER 5
110 REM THIS PROGRAM CALCULATES THE ADIABATIC FLAME
120 REM TEMPERATURE FOR VARIOUS PREHEAT TEMP. AND
130 REM RECIRCULATION LEVELS.
140 E=0.1
150 O1=18500
160 PRINT "EXCESS AIR LEVEL = ";E*100,"PERCENT"
170 PRINT "CALORIFIC VALUE OF THE FUEL = ";O1;"BTU/HR/LB."
180 T1=1000
190 FOR J=1 TO 3
200 PRINT "TEMP. OF THE PREHEATED COMBUSTION AIR = ";T1;"F."
210 PRINT "RECIR.      FLAME      SP.HEAT AT"
220 PRINT "LEVEL      TEMP.F      TF.BTU/HR/LB/F"
230 T=T1+460
240 GOSUB 500
250 O2=14.31*(1+E)*C*T1
260 T2=1000
270 FOR K=1 TO 4
280 R=0
290 T=T2+460
300 PRINT "TEMP. OF THE RECIRCULATED COMBUSTION GASES";T2;"F."
310 GOSUB 500
320 FOR L=1 TO 6
330 O3=((14.31*(1+E)+1)*R*C*T2
340 C1=0.275
350 T3=(O1+O2+O3)/(((14.31*(1+E)+1)*C1*(1+R))
360 T=T3+460
370 GOSUB 500
380 IF C=C1 THEN 410
390 C1=C
400 GO TO 350
410 PRINT USING 420,R,T3,C1
420 IMAGE 40.20,11T,60.10,23T,40.30
430 R=R+0.2
440 NEXT J
450 T2=T2+200
460 NEXT K
```

```
470 T1=T1+300
480 NEXT J
490 END
500 REM CALCULATE SP. HEAT AT A GIVEN TEMP.
510 REM THIS CORRELATION IS OBTAINED FROM MARKS HB
520 REM FOR NITROGEN
530 A1=9.47
540 A2=3470/T
550 A3=1160000/T12
560 C=(A1-A2+A3)/28
570 RETURN
```

EXT. HEAT SYSTEM PERFORMANCE ANALYSIS

```
100 REM THIS PROGRAM IS STORED IN FILE NUMBER 7
110 E2=0.8
120 O1=18500
130 O=49324
140 E=0.1
150 PRINT "EXCESS AIR % = ",E*100,"PREHEATER EFFECTIVENESS % = ",E2*100
160 PRINT "REQUIRED HEAT INPUT TO ENGINE=",O,"BTU/HR"
170 R=0
180 FOR J=1 TO 3
190 PRINT
200 PRINT "RECIRCULATION LEVEL % = ",R*100
205 PRINT "FLAME RECIR.GAS PREHEAT EXH.GAS COMB. EXHAUST ADDITION"
206 PRINT "TEMP.F TEMP. F TEMP.F TEMP.F EFF. HEAT LOSS LOSS"
210 E1=0.75
215 FOR K=1 TO 4
220 T2=1200
230 T1=1000
240 O5=O/E1
250 M1=O5/O1
260 M2=M1*14.31*(1+E)
270 M=M1+M2
280 PRINT "TOTAL MASS FLOW RATE = ",M
290 T=T1+460
300 GOSUB 730
310 O2= 14.31*(1+E)*C*T1
320 T=T2+460
330 GOSUB 730
340 O3=((14.31*(1+E)+1)*R*C*T2
350 C1=0.275
360 T3=(O1+O2+O3)/((14.31*(1+E)+1)*C1*(1+R))
370 T=T3+460
380 GOSUB 730
390 IF C=C1 THEN 420
400 C1=C
410 GO TO 360
420 D2=T3-O/((14.31*(1+E)+1)*(1+R)*0.29*M1)
430 IF D2>0 THEN 460
```

```

440 PRINT "ERROR-NEGATIVE TEMP.,D2 = ",D2
450 GO TO 660
460 IF ABS(D2-T2)<1 THEN 490
470 T2=D2
480 GO TO 320
490 D1=E2*(T2-100)+100
500 IF ABS(D1-T1)<1 THEN 540
510 REM PRINT USING 690,T3,T2,T1,D1,E1,03
520 T1=D1
530 GO TO 290
540 F1=14.31*(1+E)/(14.31*(1+E)+1)*0.9
550 T4=T2-F1*(T1-100)
560 T=T4+460
570 GOSUB 730
580 O6=M*C*(T4-100)
590 O7=O6
600 REM PRINT T4,O7,O5
610 (E3=1-O7/O5)
620 REM IF ABS(E3-E1)<1.0E-3 THEN 650
650 O8=O+O6-O5
680 PRINT USING 690:T3,T2,T1,T4,E3,O6,O8
690 IMAGE 4D ,7T,4D ,18T,4D ,24T,4D ,32T,1D,3D,37T,6D,45T,6D
694 E1=E1+0.05
695 NEXT K
700 R=R+0.25
710 NEXT J
720 END
730 REM CALCULATE SP. HEAT AT A GIVEN TEMP.
740 REM THIS CORRELATION IS OBTAINED FROM MARKS HB.
750 REM FOR NITROGEN
760 A1=9.47
770 A2=3470/T
780 A3=1160000/T1.2
790 C=(A1-A2+A3)/28
800 RETURN

```

APPENDIX II

Estimate of Displacer Piston

Ring Friction Power Losses

Figure 1 shows a schematic diagram of the proposed displacer piston ring seal arrangement for the reduction of shuttle/pumping losses. Figure 2 shows a schematic of the pressure gradients on a given piston ring seal. An analysis of the friction forces and power losses resulting from the pressure forces acting on the piston ring is as follows:

Assumptions

1. Power loss due to radial friction is negligible.
2. The axial pressure gradient will be somewhere between linear and parabolic. The effective radial unit pressure acting on the ring will be $\Delta P/a$ where:

$$a = 2 \text{ for linear}$$

$$a = 3 \text{ for parabolic}$$

The axial drag force as a function of the ring dimensions and pressure differential is:

$$F_A = \pi D b \mu \left(\frac{\Delta P}{a} \right) \quad \text{Eq. \#1}$$

Where:

F_A = axial drag force, lbs.

D = piston ring outside dia., in.

b = piston ring width, in.

μ = coef. of friction of ring on cylinder

ΔP = pressure differential across ring, PSI

a = pressure gradient factor

The pressure differential was calculated to be 483 PSI, based upon a charge pressure of 2176 PSIA (15 MPa) and an engine pressure ratio of 1.57.

The average ring velocity with respect to the cylinder wall was based upon an assumed sinusoidal motion:

$$v = \text{velocity} = V_{\max} \sin \alpha$$

$$V_{\text{avg}} \times \pi = \int_0^{\pi} v d\alpha = \int_0^{\pi} V_{\max} \sin \alpha d\alpha$$

$$V_{\text{avg}} \times \pi = - \left[V_{\max} \cos \alpha \right]_0^{\pi} = 2 V_{\max}$$

$$\therefore V_{\text{avg}} = 2 V_{\max} / \pi$$

Eq. #2

Also, for simple harmonic motion:

$$V_{\max} = r\omega, \text{ in } \times \text{ rad/sec}$$

Where: r = stroke amplitude, in.

ω = angular velocity, rad/sec

If: N = engine RPM

S = displacer stroke (peak-to-peak), in.

$$V_{\max} = \frac{\pi SN}{60}$$

Eq. #3

and $V_{\text{avg}} = \frac{SN}{30}, \text{ in/sec}$

Eq. #4

Since Power = force \times velocity

$$\text{Pwr} = F_A \times V_{\text{avg}}$$

Eq. #5

Subst. Eqs. #1 thru #4 into Eq. #5 gives:

$$\text{Pwr} = \pi D b \mu \left(\frac{\Delta P}{a} \right) \left(\frac{SN}{30} \right)$$

Eq. #6

Where: Pwr = the frictional power loss of one ring

For the present application, let:

$$D = 6 \text{ cm} = 2.36 \text{ in.}$$

$$b = 0.47 \text{ cm} = 0.187 \text{ in.}$$

$$\Delta P = 3.33 \text{ MPa} = 483 \text{ PSI}$$

$$S = 3.4 \text{ cm} = 1.339 \text{ in.}$$

$$N = 1100 \text{ RPM}$$

$$a = 2 \text{ for linear pressure gradient}$$

$$a = 3 \text{ for parabolic pressure gradient}$$

$$\mu_1 = 0.2 = \text{hot side coef. of friction}$$

$$\mu_2 = 0.1 = \text{cold side coef. of friction}$$

For a linear pressure gradient across the seal ring face ($a = 2$):

$$\text{TOTAL PWR LOSS} = \text{Pwr}_{\text{HOT}} + \text{Pwr}_{\text{COLD}}$$

$$\text{PWR}_{\text{TOTAL}} = \frac{\pi D_b (P) S N}{30a} [\mu_1 + \mu_2]$$

$$\text{PWR}_{\text{TOTAL}} = \frac{\pi (2.36)(.187)(483)(1.339)(1100)}{30 (2)} [0.2 + 0.1]$$

$$\text{PWR}_{\text{TOTAL}} = 4932 \text{ in-lb/sec.} = \underline{0.56 \text{ KW/cyl.}}$$

For a parabolic pressure gradient across the seal ring face ($a = 3$):

$$\text{PWR}_{\text{TOTAL}} = 3288 \text{ in-lb/sec.} = \underline{0.37 \text{ KW/cyl.}}$$

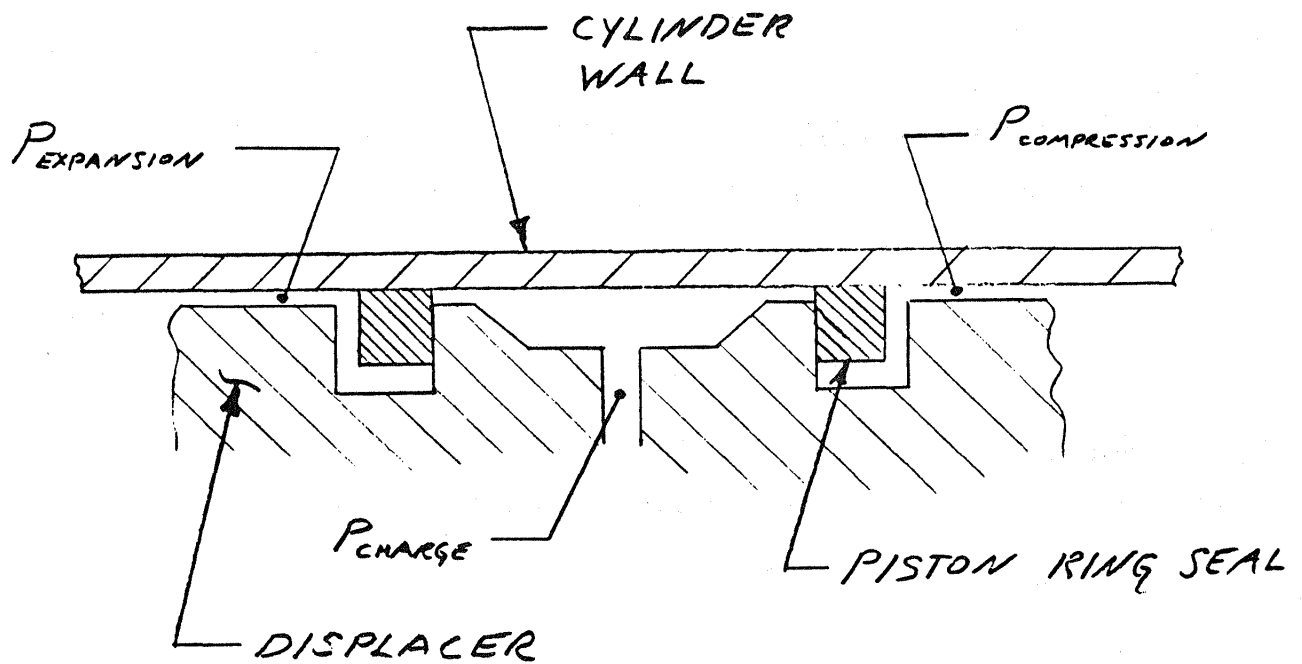


FIG. - 1 , DISPLACER PISTON RING SCHEMATIC

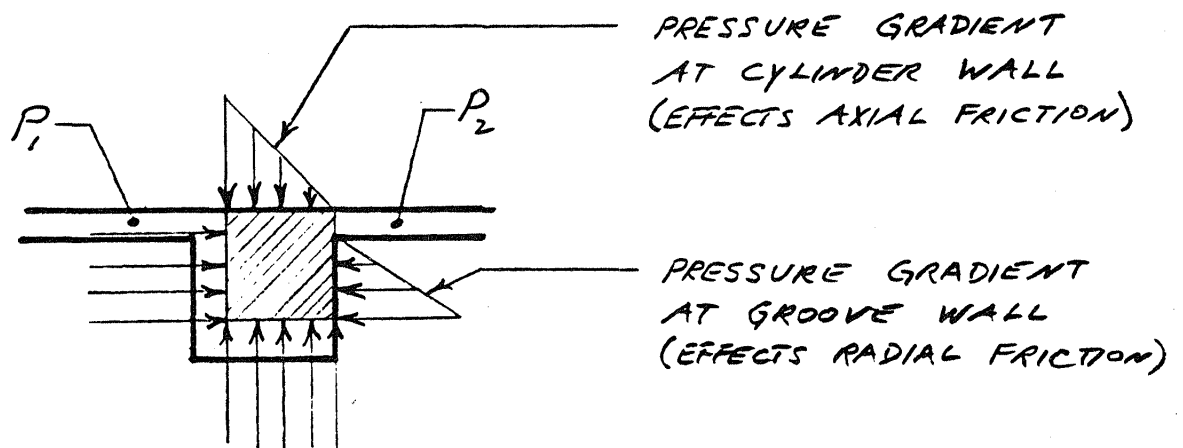


FIG. - 2 , SCHEMATIC OF PRESSURE DISTRIBUTION ON PISTON RING

APPENDIX III

SAPV.2 STRUCTURAL ANALYSIS DATA OUTPUT

SILICON CARBIDE

CERAMIC HEATER HEAD TUBE

- . TABLE 1A -- DISPLACEMENTS
- . TABLE 2A -- FORCES AND MOMENTS
- . FIGURE 1A -- TOP VIEW, UNDEFORMED SHAPE
- . FIGURE 2A -- TOP VIEW, STATIC LOAD CASE
- . FIGURE 3A -- SIDE VIEW, UNDEFORMED SHAPE
- . FIGURE 4A -- SIDE VIEW, STATIC LOAD CASE

SILICON MULLITE

CERAMIC HEATER HEAD TUBE

- . TABLE 3A -- DISPLACEMENTS
- . TABLE 4A -- FORCES AND MOMENTS
- . FIGURE 5A -- TOP VIEW, UNDEFORMED SHAPE
- . FIGURE 6A -- TOP VIEW, STATIC LOAD CASE
- . FIGURE 7A -- SIDE VIEW, UNDEFORMED SHAPE
- . FIGURE 8A -- SIDE VIEW, STATIC LOAD CASE

TABLE - 1A

STATIC ANALYSIS

TUBE MAT'L.: S.C

LOAD CASE 1

DISPLACEMENTS/ROTATIONS OF UNRESTRAINED NODES

NODE NUMBER	X- TRANSLATION	Y- TRANSLATION	Z- TRANSLATION	X- ROTATION	Y- ROTATION	Z- ROTATION
2	-2.78218E-05	2.16871E-04	2.10528E-05	2.64801E-04	-3.68036E-04	2.47831E-04
3	-1.14616E-04	4.72652E-04	1.93029E-04	5.96047E-04	-8.14868E-04	4.75826E-04
4	-2.62536E-04	6.91224E-04	4.69275E-04	9.00809E-04	-1.21926E-03	6.16060E-04
5	-4.83583E-04	8.65328E-04	8.93243E-04	1.19644E-03	-1.60184E-03	6.86273E-04
6	-7.27708E-04	1.02741E-03	1.36960E-03	1.44367E-03	-1.92356E-03	6.78519E-04
7	-1.03295E-03	1.12114E-03	2.02333E-03	1.66973E-03	-2.21055E-03	5.90585E-04
8	-1.36652E-03	1.08910E-03	2.82775E-03	1.83777E-03	-2.41408E-03	4.39449E-04
9	-1.62854E-03	1.05411E-03	3.61335E-03	1.92008E-03	-2.50904E-03	2.69454E-04
10	-1.83864E-03	9.81063E-04	4.44270E-03	1.93748E-03	-2.52059E-03	7.35489E-05
11	-1.97819E-03	8.74952E-04	5.29073E-03	1.88844E-03	-2.44811E-03	-1.34482E-04
12	-2.02283E-03	6.80819E-04	6.39999E-03	1.71878E-03	-2.22270E-03	-3.99824E-04
13	-1.89105E-03	5.18526E-04	7.37558E-03	1.45736E-03	-1.88148E-03	-6.14365E-04
14	-1.62111E-03	4.10710E-04	8.13626E-03	1.14841E-03	-1.47836E-03	-7.73245E-04
15	-1.22591E-03	3.09628E-04	8.72508E-03	7.77750E-04	-9.99975E-04	-8.94187E-04
16	-7.67003E-04	2.41391E-04	9.07101E-03	3.94172E-04	-5.03514E-04	-9.65083E-04
17	-2.61440E-04	1.96329E-04	9.18940E-03	-5.16187E-06	1.68277E-05	-9.98696E-04
18	2.51376E-04	1.24285E-04	9.06682E-03	-4.12335E-04	5.40248E-04	-9.91864E-04
19	7.16201E-04	7.33273E-05	8.72154E-03	-7.86565E-04	1.02929E-03	-9.48990E-04
20	1.12919E-03	-4.10575E-05	8.13378E-03	-1.15485E-03	1.50206E-03	-8.63604E-04
21	1.41763E-03	-1.80737E-04	7.39089E-03	-1.45853E-03	1.89141E-03	-7.37563E-04
22	1.58821E-03	-3.64655E-04	6.42601E-03	-1.71795E-03	2.22418E-03	-5.54560E-04
23	1.59585E-03	-5.81464E-04	5.33240E-03	-1.88802E-03	2.44260E-03	-3.23828E-04
24	1.49251E-03	-7.49822E-04	4.49866E-03	-1.94096E-03	2.51114E-03	-1.30848E-04
25	1.29160E-03	-8.98315E-04	3.56212E-03	-1.91739E-03	2.48314E-03	9.36929E-05
26	1.06814E-03	-9.47124E-04	2.78602E-03	-1.82468E-03	2.36608E-03	2.71738E-04
27	7.77864E-04	-9.56587E-04	1.96614E-03	-1.63739E-03	2.12871E-03	4.31942E-04
28	5.45658E-04	-8.42271E-04	1.37528E-03	-1.41549E-03	1.84050E-03	5.09875E-04
29	3.42779E-04	-7.26564E-04	8.97586E-04	-1.16686E-03	1.52141E-03	5.18267E-04
30	1.62340E-04	-5.22282E-04	4.75627E-04	-8.36198E-04	1.09164E-03	4.46906E-04
31	4.90197E-05	-3.39966E-04	1.45312E-04	-4.81251E-04	6.42197E-04	3.00389E-04
32	8.05240E-06	-1.08436E-04	5.96453E-06	-1.47601E-04	2.00383E-04	1.08824E-04

TABLE - 2 A

PIPE FORCES AND MOMENTS

TUBE MAT'L: S.C

ELEMENT NUMBER	ELEMENT TYPE	LOAD CASE	STATION	AXIAL FORCE	Y-AXIS SHEAR	Z-AXIS SHEAR	TORSIONAL MOMENT	Y-AXIS MOMENT	Z-AXIS MOMENT
1	TANGENT	1	END-I	-1.61473E 01	-3.33853E-01	-2.03379E 01	-1.76120E 01	1.51471E 01	1.44191E 01
			END-J	-1.61473E 01	-3.33853E-01	-2.03379E 01	-1.76120E 01	1.18930E 01	1.44725E 01
2	TANGENT	1	END-I	-1.75780E 01	2.80877E 00	1.89103E 01	-1.25206E 01	-2.04218E 01	-9.34160E 00
			END-J	-1.75780E 01	2.80877E 00	1.89103E 01	-1.25206E 01	-1.64910E 01	-9.92545E 00
3	TANGENT	1	END-I	-1.79662E 01	1.07344E 00	1.87226E 01	-1.03313E 01	-1.81096E 01	-9.61964E 00
			END-J	-1.79662E 01	1.07344E 00	1.87226E 01	-1.03313E 01	-1.42509E 01	-9.84088E 00
4	TANGENT	1	END-I	-1.83047E 01	-1.30714E 00	1.83768E 01	-7.57906E 00	-1.61200E 01	-9.45369E 00
			END-J	-1.83047E 01	-1.30714E 00	1.83768E 01	-7.57906E 00	-1.19821E 01	-9.15937E 00
5	TANGENT	1	END-I	-1.87542E 01	1.64719E-01	1.79645E 01	-7.86636E 00	-1.20093E 01	-8.87726E 00
			END-J	-1.87542E 01	1.64719E-01	1.79645E 01	-7.86636E 00	-8.06507E 00	-8.91342E 00
6	TANGENT	1	END-I	-1.91524E 01	-2.25583E 00	1.73945E 01	-6.05975E 00	-9.66938E 00	-8.72678E 00
			END-J	-1.91524E 01	-2.25583E 00	1.73945E 01	-6.05975E 00	-5.36379E 00	-8.16841E 00
7	TANGENT	1	END-I	-1.91248E 01	-5.80233E 00	1.65845E 01	-4.21169E 00	-6.95546E 00	-8.13001E 00
			END-J	-1.91248E 01	-5.80233E 00	1.65845E 01	-4.21169E 00	-2.54807E 00	-6.58802E 00
8	TANGENT	1	END-I	-2.02561E 01	-4.60376E 00	1.55875E 01	-3.84442E 00	-2.78997E 00	-6.71340E 00
			END-J	-2.02561E 01	-4.60376E 00	1.55875E 01	-3.84442E 00	9.89933E-01	-5.59700E 00
9	TANGENT	1	END-I	-2.09125E 01	-5.19231E 00	1.44973E 01	-3.52285E 00	4.85691E-01	-5.86852E 00
			END-J	-2.09125E 01	-5.19231E 00	1.44973E 01	-3.52285E 00	4.06064E 00	-4.58813E 00
10	TANGENT	1	END-I	-2.15263E 01	-5.83819E 00	1.33041E 01	-3.42676E 00	3.64584E 00	-4.99153E 00
			END-J	-2.15263E 01	-5.83819E 00	1.33041E 01	-3.42676E 00	6.98379E 00	-3.52674E 00
11	TANGENT	1	END-I	-2.21161E 01	-7.17665E 00	1.15686E 01	-3.67008E 00	6.46092E 00	-4.21197E 00
			END-J	-2.21161E 01	-7.17665E 00	1.15686E 01	-3.67008E 00	1.04187E 01	-1.75676E 00
12	TANGENT	1	END-I	-2.33320E 01	-6.29831E 00	9.50889E 00	-3.28741E 00	1.03510E 01	-2.67476E 00
			END-J	-2.33320E 01	-6.29831E 00	9.50889E 00	-3.28741E 00	1.35126E 01	-5.80646E-01
13	TANGENT	1	END-I	-2.44131E 01	-4.90881E 00	7.37435E 00	-2.64647E 00	1.35689E 01	-1.61706E 00
			END-J	-2.44131E 01	-4.90881E 00	7.37435E 00	-2.64647E 00	1.58466E 01	-1.00848E-01
14	TANGENT	1	END-I	-2.49399E 01	-4.98241E 00	5.25714E 00	-2.84353E 00	1.57676E 01	-1.19478E 00
			END-J	-2.49399E 01	-4.98241E 00	5.25714E 00	-2.84353E 00	1.74410E 01	3.91232E-01
15	TANGENT	1	END-I	-2.54622E 01	-4.09247E 00	3.06509E 00	-2.36102E 00	1.74993E 01	-7.90478E-01
			END-J	-2.54622E 01	-4.09247E 00	3.06509E 00	-2.36102E 00	1.84293E 01	4.51075E-01
16	TANGENT	1	END-I	-2.57622E 01	-3.12814E 00	9.94581E-01	-1.73164E 00	1.84915E 01	-6.91972E-01
			END-J	-2.57622E 01	-3.12814E 00	9.94581E-01	-1.73164E 00	1.87957E 01	2.64486E-01
17	TANGENT	1	END-I	-2.55921E 01	-4.26146E 00	-1.16073E 00	-2.52484E 00	1.86842E 01	-9.33848E-01
			END-J	-2.55921E 01	-4.26146E 00	-1.16073E 00	-2.52484E 00	1.83255E 01	3.83220E-01

TABLE - 2A (CONT.)

PIPE FORCES AND MOMENTS

TUBE MAT'L: S.C

ELEMENT NUMBER	ELEMENT TYPE	LOAD CASE	STATION	AXIAL FORCE	Y-AXIS SHEAR	Z-AXIS SHEAR	TORSIONAL MOMENT	Y-AXIS MOMENT	Z-AXIS MOMENT
18	TANGENT	1	END-I	-2.55945E 01	-2.90660E 00	-3.30700E 00	-1.44606E 00	1.84288E 01	-7.95879E-01
			END-J	-2.55945E 01	-2.90660E 00	-3.30700E 00	-1.44606E 00	1.74397E 01	7.35256E-02
19	TANGENT	1	END-I	-2.49129E 01	-4.93577E 00	-5.42641E 00	-2.63353E 00	1.72684E 01	-1.05093E 00
			END-J	-2.49129E 01	-4.93577E 00	-5.42641E 00	-2.63353E 00	1.55499E 01	5.12244E-01
20	TANGENT	1	END-I	-2.42272E 01	-5.54270E 00	-7.53543E 00	-2.80505E 00	1.55186E 01	-5.48884E-01
			END-J	-2.42272E 01	-5.54270E 00	-7.53543E 00	-2.80505E 00	1.32439E 01	1.12429E 00
21	TANGENT	1	END-I	-2.33187E 01	-6.18765E 00	-9.61315E 00	-2.98004E 00	1.32526E 01	1.46629E-01
			END-J	-2.33187E 01	-6.18765E 00	-9.61315E 00	-2.98004E 00	1.00925E 01	2.18063E 00
22	TANGENT	1	END-I	-2.21423E 01	-7.01107E 00	-1.16199E 01	-3.28100E 00	1.01473E 01	1.32748E 00
			END-J	-2.21423E 01	-7.01107E 00	-1.16199E 01	-3.28100E 00	6.23731E 00	3.68662E 00
23	TANGENT	1	END-I	-2.09204E 01	-7.65843E 00	-1.33468E 01	-3.62050E 00	6.39093E 00	3.05091E 00
			END-J	-2.09204E 01	-7.65843E 00	-1.33468E 01	-3.62050E 00	3.08242E 00	4.94935E 00
24	TANGENT	1	END-I	-2.03037E 01	-6.88221E 00	-1.46579E 01	-3.77302E 00	3.52707E 00	4.51989E 00
			END-J	-2.03037E 01	-6.88221E 00	-1.46579E 01	-3.77302E 00	-5.59867E-01	6.43880E 00
25	TANGENT	1	END-I	-2.00032E 01	-4.70519E 00	-1.58806E 01	-4.26288E 00	3.55699E-01	6.14073E 00
			END-J	-2.00032E 01	-4.70519E 00	-1.58806E 01	-4.26288E 00	-3.46639E 00	7.27316E 00
26	TANGENT	1	END-I	-1.92725E 01	-4.64837E 00	-1.67754E 01	-4.80835E 00	-2.93344E 00	7.16669E 00
			END-J	-1.92725E 01	-4.64837E 00	-1.67754E 01	-4.80835E 00	-7.53863E 00	8.44276E 00
27	TANGENT	1	END-I	-1.91238E 01	-9.38702E-01	-1.75458E 01	-6.80429E 00	-5.69549E 00	8.51436E 00
			END-J	-1.91238E 01	-9.38702E-01	-1.75458E 01	-6.80429E 00	-9.78124E 00	8.73295E 00
28	TANGENT	1	END-I	-1.85075E 01	-2.20848E 00	-1.80846E 01	-6.84482E 00	-9.56149E 00	8.94215E 00
			END-J	-1.85075E 01	-2.20848E 00	-1.80846E 01	-6.84482E 00	-1.33997E 01	9.41087E 00
29	TANGENT	1	END-I	-1.82504E 01	-3.15446E-01	-1.84738E 01	-8.84092E 00	-1.19532E 01	9.69153E 00
			END-J	-1.82504E 01	-3.15446E-01	-1.84738E 01	-8.84092E 00	-1.63799E 01	9.76711E 00
30	TANGENT	1	END-I	-1.74898E 01	-3.36115E 00	-1.89015E 01	-7.07740E 00	-1.69071E 01	1.02917E 01
			END-J	-1.74898E 01	-3.36115E 00	-1.89015E 01	-7.07740E 00	-2.11039E 01	1.10380E 01
31	TANGENT	1	END-I	-1.74641E 01	1.70535E 00	-1.91457E 01	-1.34819E 01	-1.74338E 01	1.14718E 01
			END-J	-1.74641E 01	1.70535E 00	-1.91457E 01	-1.34819E 01	-2.10467E 01	1.11500E 01
32	TANGENT	1	END-I	-1.61467E 01	-3.32568E-01	-2.03380E 01	-1.91782E 01	-1.10600E 01	1.60910E 01
			END-J	-1.61467E 01	-3.32568E-01	-2.03380E 01	-1.91782E 01	-1.26870E 01	1.61176E 01

STATIC SOLUTION TIME LOG

EQUATION SOLUTION = 0.23
 DISPLACEMENT OUTPUT = 0.08
 STRESS RECOVERY = 0.43

CERAMIC HEATER HEAD UBE
 ND FO MED SHAPE
 05/10/63
 IAXIS- 2 -LPHA- 90.00 B.TA- 0.00

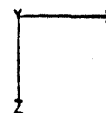
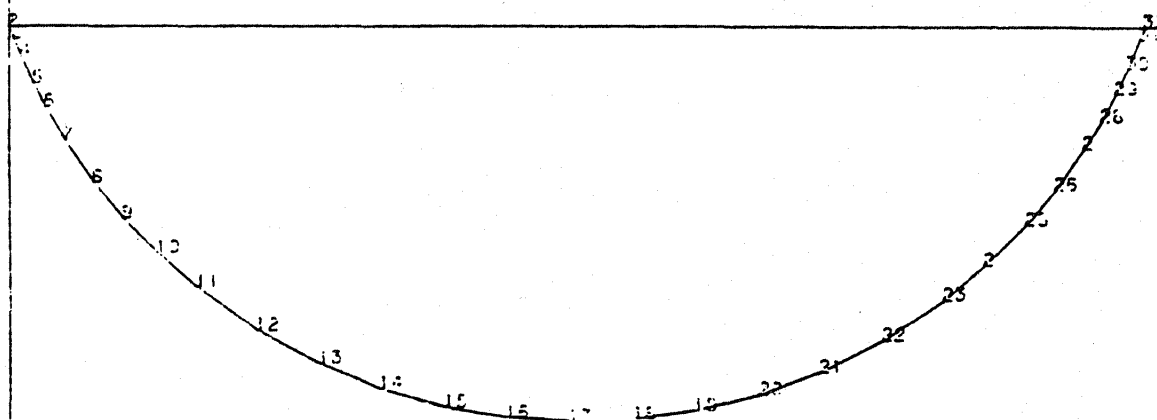


FIGURE - 1A
 (TUBE MAT'L. : SiC)



CERAMIC HEATER CAD TUB.

ST-TIC LOAD CASE 1

05/10/83

AXIS= 2 ALPHA= 90.00 BETA= 0.00
FLECTION SCALE FACTOR = 100.07

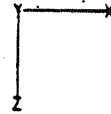
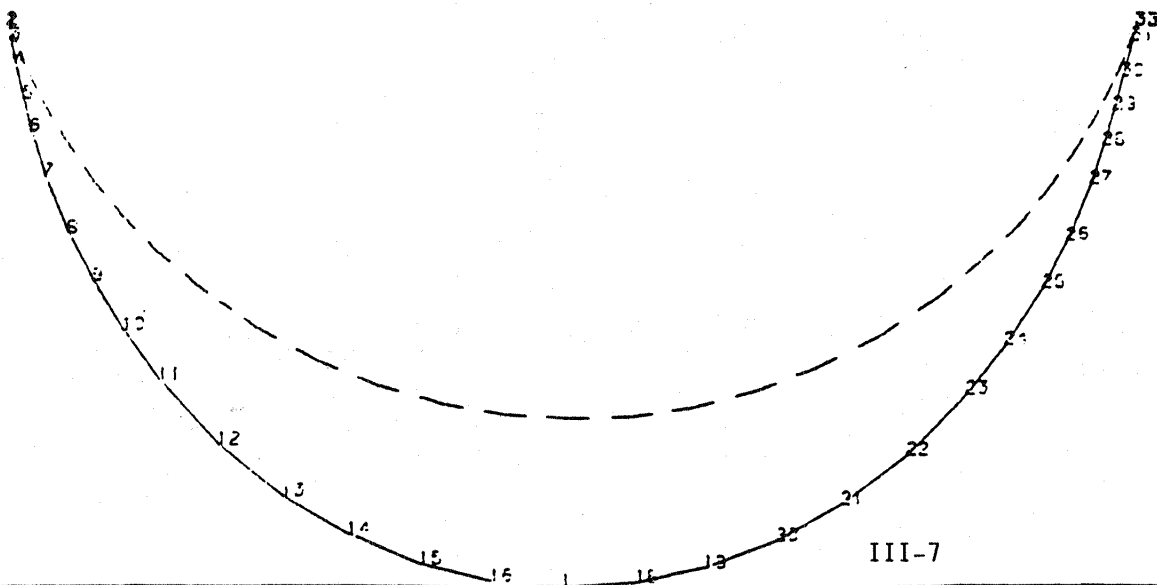


FIGURE - 2A

(TUBE MAT'L: SiC)

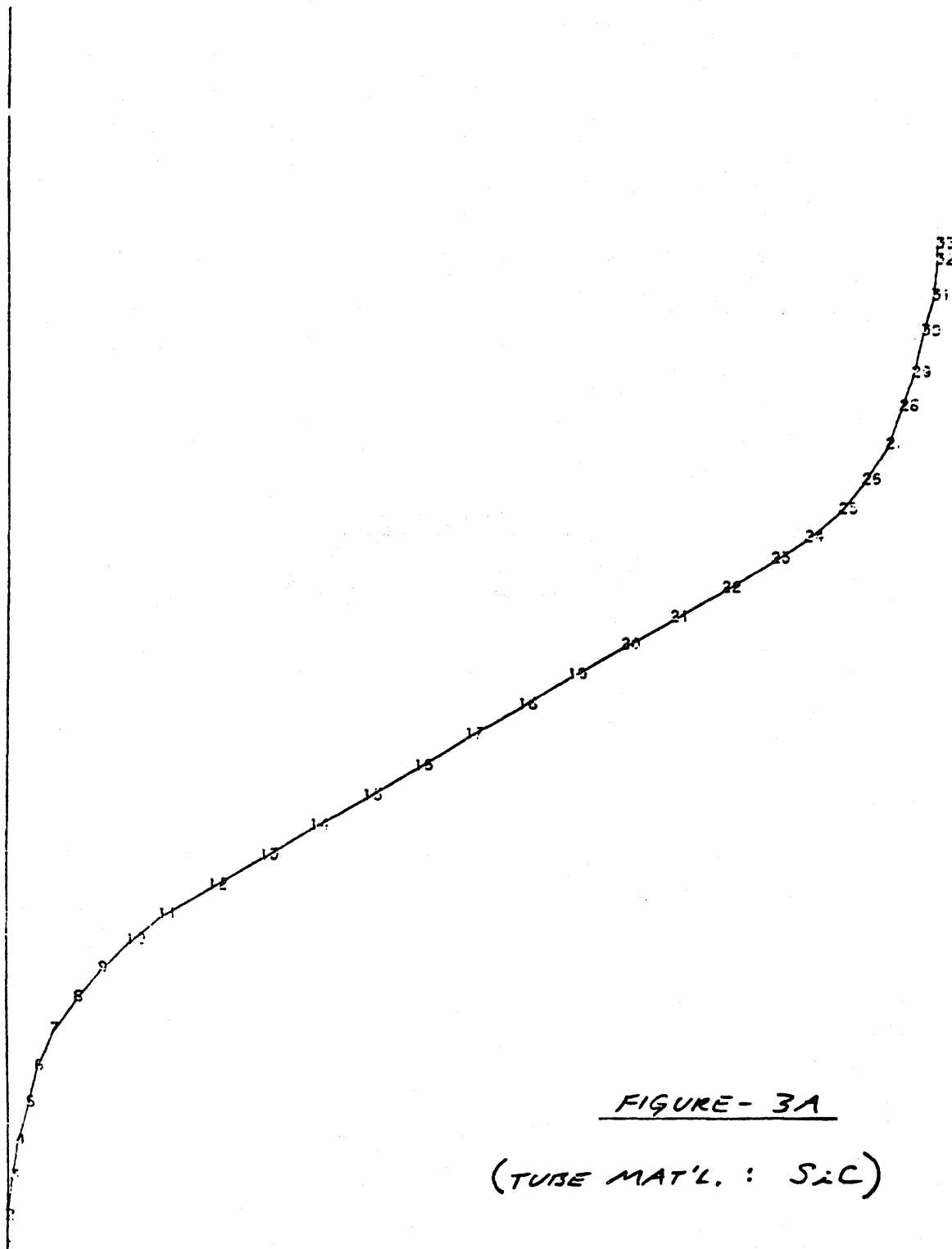


CERAMIC HEATER HEAD TUBE

INDEFORMED SHAPE

JS/10/60

AXIS = 2 ALPHA = 0.00 BETA = 0.00



CERAMIC HEATER HEAD JOB
 STATIC LOAD CASE
 05/10/63
 IAXIS= 2 ALPHA= 0.00 BETA= 0.00
 REFLECTION SCALE FACTOR= 25.33

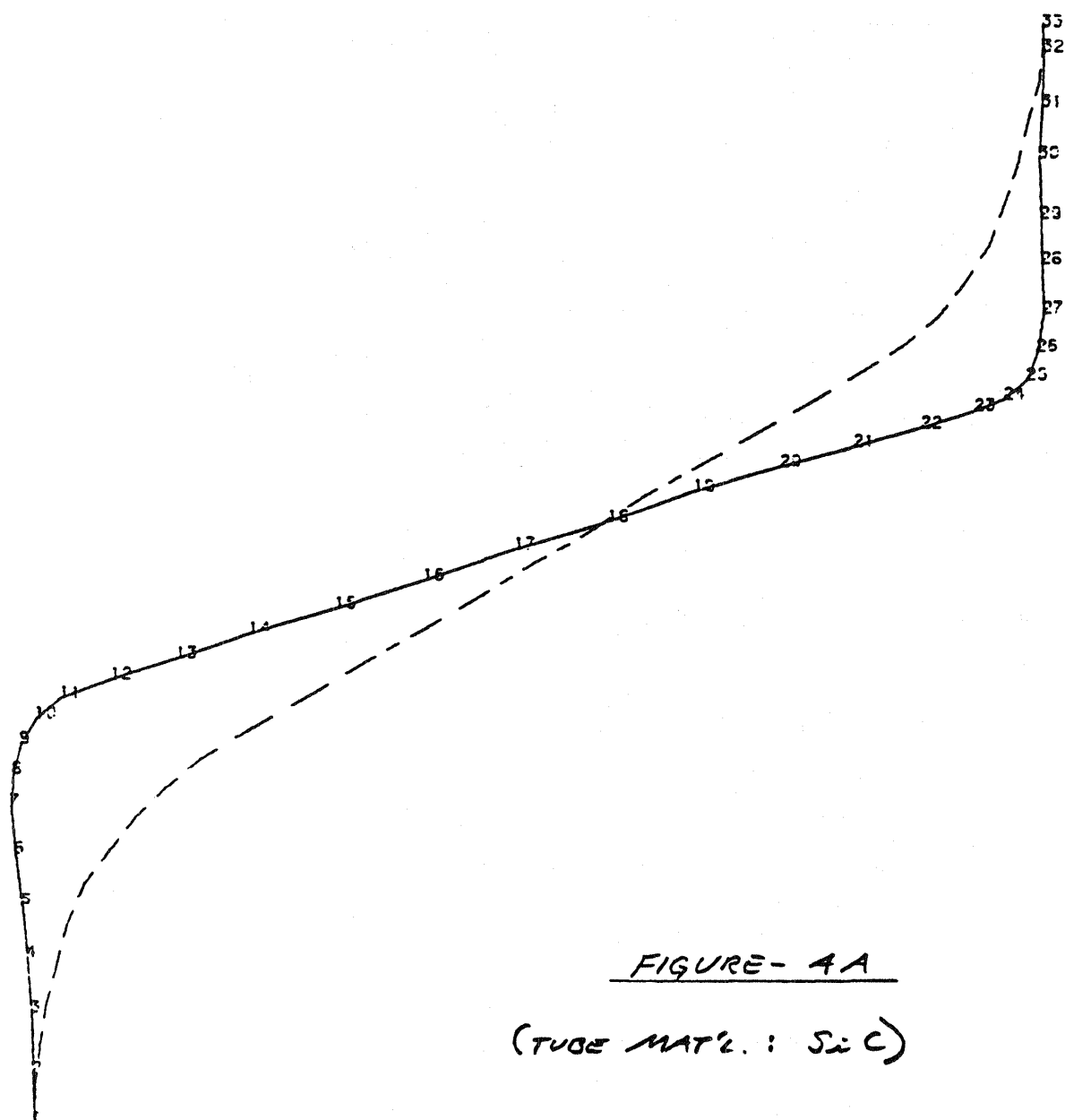


FIGURE- 4A

(TUBE MAT'L: SiC)

TABLE - 3A

STATIC ANALYSIS

LOAD CASE 1

DISPLACEMENTS/ROTATIONS OF UNRESTRAINED NODES

NODE NUMBER	X- TRANSLATION	Y- TRANSLATION	Z- TRANSLATION	X- ROTATION	Y- ROTATION	Z- ROTATION
2	-2.97663E-05	2.27675E-04	2.18644E-05	2.75203E-04	-4.08696E-04	2.59723E-04
3	-1.22340E-04	5.96470E-04	2.01943E-04	6.16597E-04	-8.92058E-04	4.91909E-04
4	-2.79192E-04	7.26540E-04	4.91027E-04	9.30100E-04	-1.32463E-03	6.32187E-04
5	-5.13529E-04	9.10504E-04	9.35106E-04	1.23392E-03	-1.72701E-03	6.99893E-04
6	-7.70712E-04	1.08199E-03	1.43308E-03	1.48770E-03	-2.06739E-03	6.87412E-04
7	-1.09318E-03	1.18245E-03	2.11770E-03	1.71940E-03	-2.36623E-03	5.92079E-04
8	-1.44673E-03	1.15148E-03	2.96206E-03	1.89186E-03	-2.57225E-03	4.33003E-04
9	-1.72326E-03	1.11699E-03	3.78572E-03	1.97631E-03	-2.66584E-03	2.55628E-04
10	-1.94477E-03	1.04233E-03	4.65536E-03	1.99384E-03	-2.67208E-03	5.18373E-05
11	-2.09175E-03	9.32592E-04	5.54467E-03	1.94255E-03	-2.59079E-03	-1.64502E-04
12	-2.13874E-03	7.30004E-04	6.70836E-03	1.76485E-03	-2.34874E-03	-4.41318E-04
13	-1.99936E-03	5.59490E-04	7.73085E-03	1.49355E-03	-1.98663E-03	-6.64410E-04
14	-1.71430E-03	4.44997E-04	8.52729E-03	1.17544E-03	-1.56028E-03	-8.28691E-04
15	-1.29754E-03	3.36439E-04	9.14368E-03	7.92857E-04	-1.05617E-03	-9.54028E-04
16	-8.13745E-04	2.61715E-04	9.50551E-03	3.98713E-04	-5.33113E-04	-1.02727E-03
17	-2.80775E-04	2.10903E-04	9.62916E-03	-9.33785E-06	1.57989E-05	-1.06200E-03
18	2.59750E-04	1.31438E-04	9.50080E-03	-4.28314E-04	5.66464E-04	-1.05520E-03
19	7.50085E-04	7.45839E-05	9.13956E-03	-8.09453E-04	1.08315E-03	-1.01179E-03
20	1.18588E-03	-4.86802E-05	8.52426E-03	-1.18852E-03	1.58132E-03	-9.23872E-04
21	1.49069E-03	-1.97542E-04	7.74629E-03	-1.50142E-03	1.99243E-03	-7.93721E-04
22	1.67161E-03	-3.91952E-04	6.73537E-03	-1.76903E-03	2.34538E-03	-6.04340E-04
23	1.68074E-03	-6.19722E-04	5.58878E-03	-1.94517E-03	2.57964E-03	-3.64831E-04
24	1.57227E-03	-7.95802E-04	4.71404E-03	-2.00071E-03	2.65614E-03	-1.63815E-04
25	1.36085E-03	-9.50345E-04	3.73144E-03	-1.97708E-03	2.63259E-03	7.02435E-05
26	1.12602E-03	-1.00008E-03	2.91802E-03	-1.88182E-03	2.51416E-03	2.56382E-04
27	8.20288E-04	-1.00820E-03	2.05852E-03	-1.68925E-03	2.26995E-03	4.25386E-04
28	5.76980E-04	-8.86920E-04	1.44059E-03	-1.46114E-03	1.96613E-03	5.10084E-04
29	3.63548E-04	-7.64369E-04	9.40499E-04	-1.20517E-03	1.63100E-03	5.22980E-04
30	1.73927E-04	-5.49072E-04	4.99110E-04	-8.64627E-04	1.17384E-03	4.54775E-04
31	5.28627E-05	-3.57067E-04	1.52371E-04	-4.98264E-04	7.02903E-04	3.08007E-04
32	8.76036E-06	-1.13838E-04	6.22203E-06	-1.53790E-04	2.23456E-04	1.14363E-04

TUBE MAT'L.: Si MULLITE

TABLE - 4A

PIPE FORCES AND MOMENTS

TUBE MAT'L: Si MULLITE

ELEMENT NUMBER	ELEMENT TYPE	LOAD CASE	STATION	AXIAL FORCE	Y-AXIS SHEAR	Z-AXIS SHEAR	TORSIONAL MOMENT	Y-AXIS MOMENT	Z-AXIS MOMENT
1	TANGENT	1	END-I	-8.00252E 00	-1.71099E-01	-1.01286E 01	-8.58802E 00	7.63231E 00	7.21495E 00
			END-J	-8.00252E 00	-1.71099E-01	-1.01286E 01	-8.58802E 00	6.01173E 00	7.24233E 00
2	TANGENT	1	END-I	-8.71777E 00	1.41382E 00	9.41596E 00	-6.03333E 00	-1.02123E 01	-4.65345E 00
			END-J	-8.71777E 00	1.41382E 00	9.41596E 00	-6.03333E 00	-8.25500E 00	-4.94734E 00
3	TANGENT	1	END-I	-8.91321E 00	5.53867E-01	9.32233E 00	-4.93941E 00	-9.03629E 00	-4.79271E 00
			END-J	-8.91321E 00	5.53867E-01	9.32233E 00	-4.93941E 00	-7.11498E 00	-4.90686E 00
4	TANGENT	1	END-I	-9.08538E 00	-6.26265E-01	9.14998E 00	-3.56857E 00	-8.01117E 00	-4.71004E 00
			END-J	-9.08538E 00	-6.26265E-01	9.14998E 00	-3.56857E 00	-5.95090E 00	-4.56903E 00
5	TANGENT	1	END-I	-9.30821E 00	1.05356E-01	8.94443E 00	-3.71103E 00	-5.97319E 00	-4.42416E 00
			END-J	-9.30821E 00	1.05356E-01	8.94443E 00	-3.71103E 00	-4.00940E 00	-4.44730E 00
6	TANGENT	1	END-I	-9.51084E 00	-1.09517E 00	8.66036E 00	-2.81532E 00	-4.77360E 00	-4.34881E 00
			END-J	-9.51084E 00	-1.09517E 00	8.66036E 00	-2.81532E 00	-2.62994E 00	-4.07773E 00
7	TANGENT	1	END-I	-9.50412E 00	-2.85601E 00	8.25667E 00	-1.90927E 00	-3.37798E 00	-4.05147E 00
			END-J	-9.50412E 00	-2.85601E 00	8.25667E 00	-1.90927E 00	-1.18374E 00	-3.29247E 00
8	TANGENT	1	END-I	-1.00666E 01	-2.25967E 00	7.75981E 00	-1.72415E 00	-1.30853E 00	-3.34693E 00
			END-J	-1.00666E 01	-2.25967E 00	7.75981E 00	-1.72415E 00	5.73183E-01	-2.79898E 00
9	TANGENT	1	END-I	-1.03954E 01	-2.55161E 00	7.21661E 00	-1.56895E 00	3.33572E-01	-2.92619E 00
			END-J	-1.03954E 01	-2.55161E 00	7.21661E 00	-1.56895E 00	2.11316E 00	-2.29698E 00
10	TANGENT	1	END-I	-1.07031E 01	-2.87244E 00	6.62216E 00	-1.52623E 00	1.91704E 00	-2.48972E 00
			END-J	-1.07031E 01	-2.87244E 00	6.62216E 00	-1.52623E 00	3.57852E 00	-1.76904E 00
11	TANGENT	1	END-I	-1.09998E 01	-3.53786E 00	5.75756E 00	-1.65658E 00	3.33371E 00	-2.09921E 00
			END-J	-1.09998E 01	-3.53786E 00	5.75756E 00	-1.65658E 00	5.30345E 00	-8.88861E-01
12	TANGENT	1	END-I	-1.16042E 01	-3.10078E 00	4.73150E 00	-1.46357E 00	5.26688E 00	-1.33370E 00
			END-J	-1.16042E 01	-3.10078E 00	4.73150E 00	-1.46357E 00	6.84005E 00	-3.02720E-01
13	TANGENT	1	END-I	-1.21409E 01	-2.40973E 00	3.66809E 00	-1.13942E 00	6.86081E 00	-8.06675E-01
			END-J	-1.21409E 01	-2.40973E 00	3.66809E 00	-1.13942E 00	7.99380E 00	-6.23707E-02
14	TANGENT	1	END-I	-1.24034E 01	-2.44629E 00	2.61351E 00	-1.23864E 00	7.95702E 00	-5.95439E-01
			END-J	-1.24034E 01	-2.44629E 00	2.61351E 00	-1.23864E 00	8.78897E 00	1.83267E-01
15	TANGENT	1	END-I	-1.26621E 01	-2.00384E 00	1.52164E 00	-9.95129E-01	8.81299E 00	-3.93301E-01
			END-J	-1.26621E 01	-2.00384E 00	1.52164E 00	-9.95129E-01	9.27462E 00	2.14611E-01
16	TANGENT	1	END-I	-1.28099E 01	-1.52451E 00	4.90381E-01	-6.78171E-01	9.29930E 00	-3.43423E-01
			END-J	-1.28099E 01	-1.52451E 00	4.90381E-01	-6.78171E-01	9.44925E 00	1.22711E-01
17	TANGENT	1	END-I	-1.27263E 01	-2.08831E 00	-5.82955E-01	-1.07699E 00	9.40157E 00	-4.62332E-01
			END-J	-1.27263E 01	-2.08831E 00	-5.82955E-01	-1.07699E 00	9.22139E 00	1.83091E-01

TABLE - 4A (CONT.)

PIPE FORCES AND MOMENTS

TUBE MAT'L.: Si MULLITE

ELEMENT NUMBER	ELEMENT TYPE	LOAD CASE	STATION	AXIAL FORCE	Y-AXIS SHEAR	Z-AXIS SHEAR	TORSIONAL MOMENT	Y-AXIS MOMENT	Z-AXIS MOMENT
18	TANGENT	1	END-I	-1.27251E 01	-1.41501E 00	-1.65181E 00	-5.34410E-01	9.26218E 00	-3.92240E-01
			END-J	-1.27251E 01	-1.41501E 00	-1.65181E 00	-5.34410E-01	8.76811E 00	3.10101E-02
19	TANGENT	1	END-I	-1.23875E 01	-2.42442E 00	-2.70719E 00	-1.13218E 00	8.69581E 00	-5.16952E-01
			END-J	-1.23875E 01	-2.42442E 00	-2.70719E 00	-1.13218E 00	7.83843E 00	2.50865E-01
20	TANGENT	1	END-I	-1.20459E 01	-2.72676E 00	-3.75749E 00	-1.21886E 00	7.82496E 00	-2.65192E-01
			END-J	-1.20459E 01	-2.72676E 00	-3.75749E 00	-1.21886E 00	6.69068E 00	5.57934E-01
21	TANGENT	1	END-I	-1.15934E 01	-3.04793E 00	-4.79197E 00	-1.30725E 00	6.69672E 00	8.38453E-02
			END-J	-1.15934E 01	-3.04793E 00	-4.79197E 00	-1.30725E 00	5.12152E 00	1.08575E 00
22	TANGENT	1	END-I	-1.10075E 01	-3.45803E 00	-5.79111E 00	-1.45894E 00	5.15119E 00	6.74040E-01
			END-J	-1.10075E 01	-3.45803E 00	-5.79111E 00	-1.45894E 00	3.20257E 00	1.83763E 00
23	TANGENT	1	END-I	-1.03989E 01	-3.78050E 00	-6.65075E 00	-1.62898E 00	3.27983E 00	1.53325E 00
			END-J	-1.03989E 01	-3.78050E 00	-6.65075E 00	-1.62898E 00	1.63118E 00	2.47040E 00
24	TANGENT	1	END-I	-1.00891E 01	-3.39554E 00	-7.30346E 00	-1.69976E 00	1.84138E 00	2.26658E 00
			END-J	-1.00891E 01	-3.39554E 00	-7.30346E 00	-1.69976E 00	-1.94984E-01	3.21333E 00
25	TANGENT	1	END-I	-9.93463E 00	-2.31519E 00	-7.91203E 00	-1.93423E 00	2.34518E-01	3.07513E 00
			END-J	-9.93463E 00	-2.31519E 00	-7.91203E 00	-1.93423E 00	-1.66971E 00	3.63234E 00
26	TANGENT	1	END-I	-9.56952E 00	-2.28807E 00	-8.35739E 00	-2.20446E 00	-1.41162E 00	3.58759E 00
			END-J	-9.56952E 00	-2.28807E 00	-8.35739E 00	-2.20446E 00	-3.70589E 00	4.21571E 00
27	TANGENT	1	END-I	-9.48990E 00	-4.48328E-01	-8.74070E 00	-3.19301E 00	-2.83356E 00	4.25923E 00
			END-J	-9.48990E 00	-4.48328E-01	-8.74070E 00	-3.19301E 00	-4.86894E 00	4.36363E 00
28	TANGENT	1	END-I	-9.18335E 00	-1.07990E 00	-9.00886E 00	-3.21389E 00	-4.75376E 00	4.47390E 00
			END-J	-9.18335E 00	-1.07990E 00	-9.00886E 00	-3.21389E 00	-6.66577E 00	4.70310E 00
29	TANGENT	1	END-I	-9.05276E 00	-1.42102E-01	-9.20250E 00	-4.20922E 00	-5.97185E 00	4.84769E 00
			END-J	-9.05276E 00	-1.42102E-01	-9.20250E 00	-4.20922E 00	-8.17692E 00	4.88174E 00
30	TANGENT	1	END-I	-8.67611E 00	-1.65467E 00	-9.41525E 00	-3.33067E 00	-8.41468E 00	5.14886E 00
			END-J	-8.67611E 00	-1.65467E 00	-9.41525E 00	-3.33067E 00	-1.05052E 01	5.51626E 00
31	TANGENT	1	END-I	-8.65892E 00	8.56728E-01	-9.53673E 00	-6.52877E 00	-8.73816E 00	5.73599E 00
			END-J	-8.65892E 00	8.56728E-01	-9.53673E 00	-6.52877E 00	-1.05378E 01	5.57432E 00
32	TANGENT	1	END-I	-8.00235E 00	-1.70451E-01	-1.01288E 01	-9.39104E 00	-5.60268E 00	8.07222E 00
			END-J	-8.00235E 00	-1.70451E-01	-1.01288E 01	-9.39104E 00	-6.41298E 00	8.08586E 00

STATIC SOLUTION TIME LOG

EQUATION SOLUTION = 0.23
DISPLACEMENT OUTPUT = 0.08

CERAMIC HEATER HEAD TUBE
UNDEFORMED SHAPE

05/18/83

1AXIS= 2 ALPHA= 90.00 BETA= 0.00

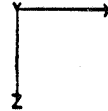
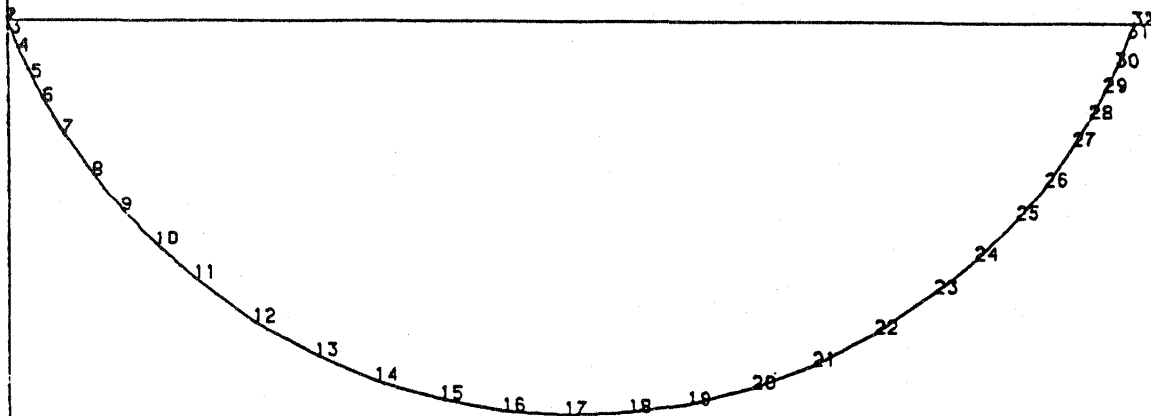


FIGURE - 5A

(TUBE MATL. : Si MULLITE)



CERAMIC HEATER HEAD TUBE
STATIC LOAD CASE 1
05/18/83
JAXIS= 2 ALPHA= 90.00 BETA= 0.00
DEFLECTION SCALE FACTOR= 95.503

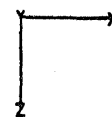
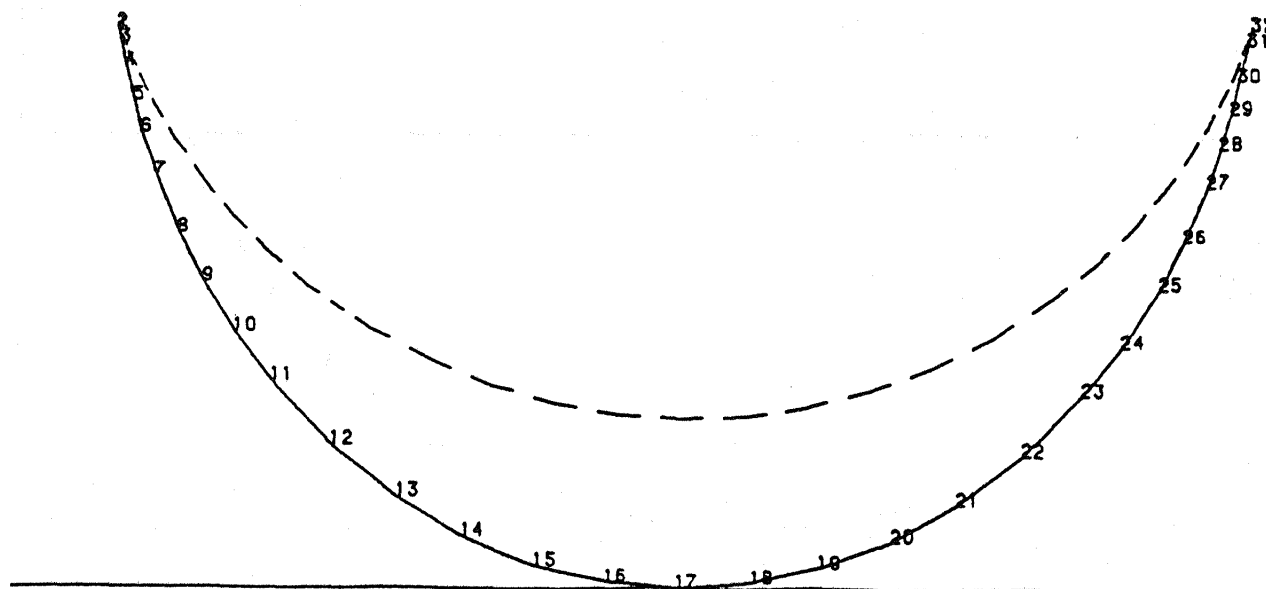


FIGURE - 6A

(TUBE MAT'L. : S_i MULLITE)



CERAMIC HEATER HEAD TUBE
UNDEFORMED SHAPE

05/18/83

1 AXIS= 2 ALPHA= 0.00 BETA= 0.00

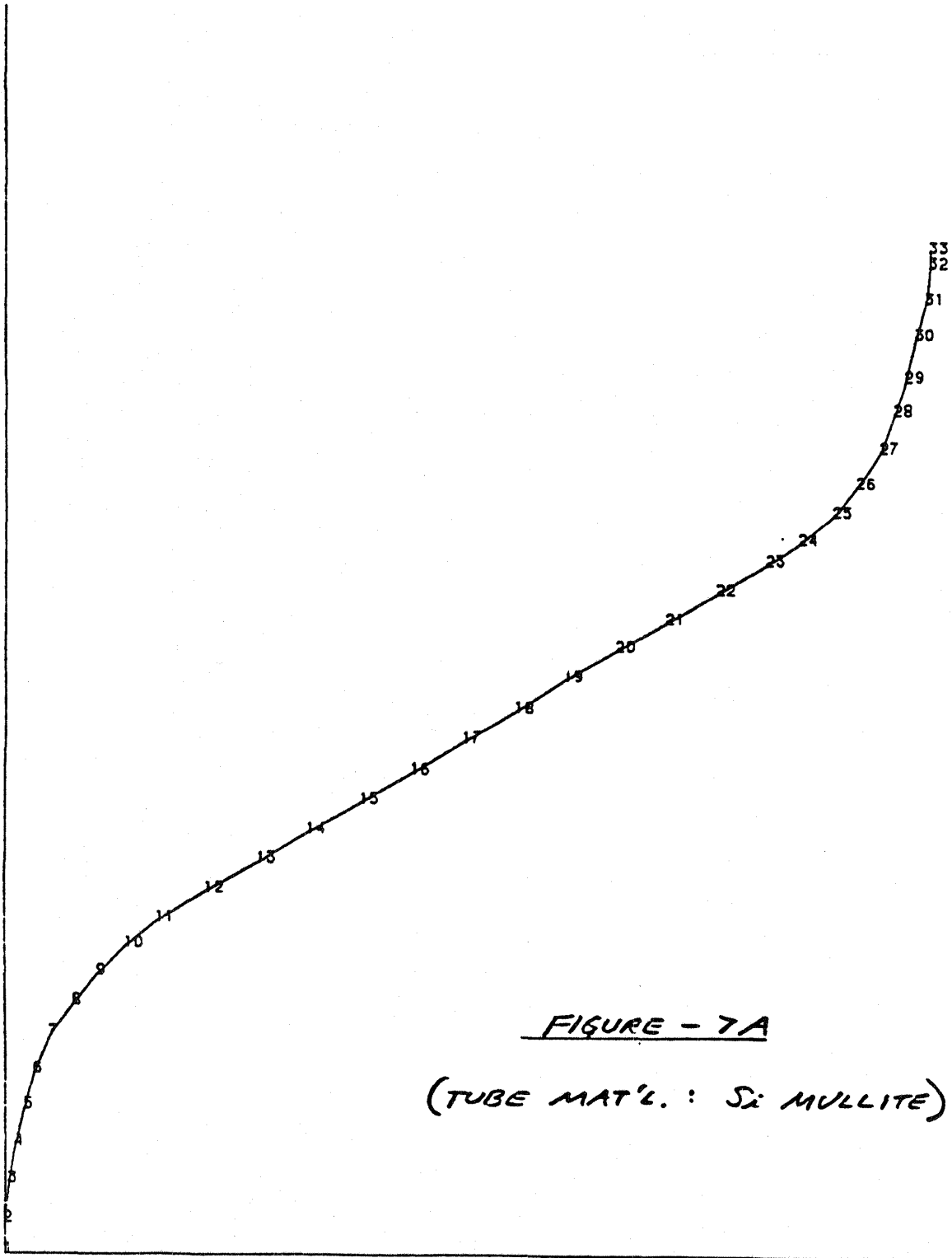
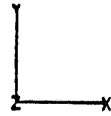


FIGURE - 7A

(TUBE MAT'L. : Si MULLITE)

ERAMIC HEATER HEAD TUBE
STATIC LOAD CASE 1
05/18/83
1 AXIS= 2 ALPHA= 0.00 BETA= 0.00
DEFLECTION SCALE FACTOR= 401.71

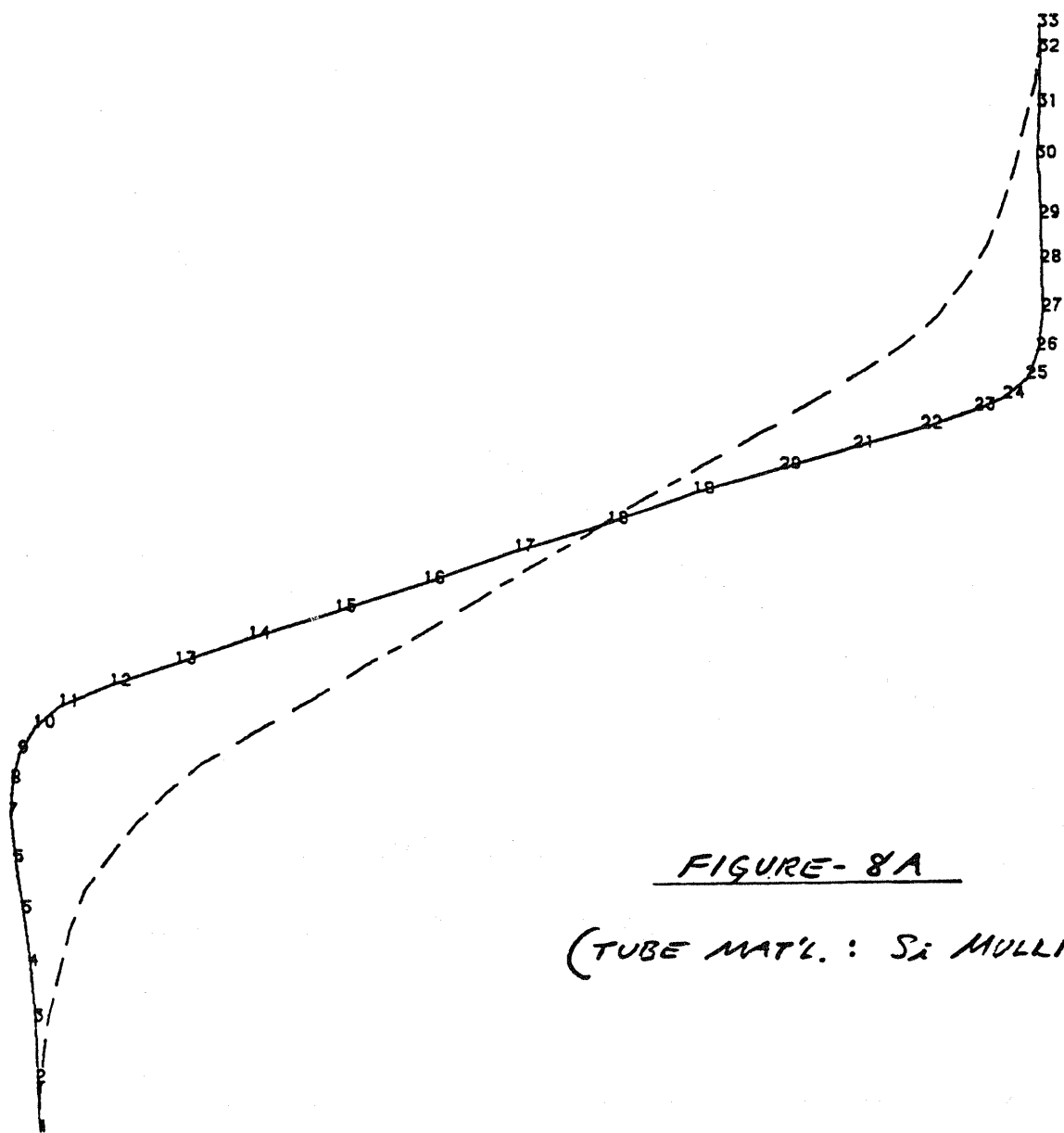
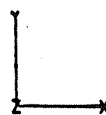


FIGURE- 8A

(TUBE MAT'L. : Si MULLITE)

APPENDIX IV

MANUFACTURING AND COST DATA

GENERAL ELECTRIC
ADVANCED ENERGY
PROGRAMS DEPT.

PROGRAM INFORMATION REQUEST / RELEASE

		*CLASS. LTR.	OPERATION	PROGRAM	SEQUENCE NO. 008	REV. LTR.												
PIR NO.																		
*USE "C" FOR CLASSIFIED AND "U" FOR UNCLASSIFIED																		
FROM D. M. Mullings <i>D.M. Mullings</i>		TO Dr. S. Musikan																
DATE SENT 12/8/83	DATE INFO. REQUIRED N.A.	PROJECT AND REQ. NO.			REFERENCE DIR. NO.													
SUBJECT CERAMIC AUTOMOTIVE STIRLING ENGINE STUDY - COST EVALUATION																		
INFORMATION REQUESTED/RELEASED																		
<p><u>Preface</u></p> <p>We have concentrated on the detailed study of manufacturing, planning and cost estimation for the ceramic parts of this engine design. The metal parts are presumed to be the same or very similar to those previously detailed in the metal engine designs done before. Our emphasis, therefore, is on the ceramic parts and the unique processes needed to produce these parts in the volumes of 1,000 engines per day, or 300,000 per year.</p> <p>Data for this analysis is given on pages IV- 7 ff.</p> <p><u>Estimating Methods</u></p> <p>I. <u>Material Processing</u></p> <p>All three basic ceramic materials, (mullite, silicon carbide, and silicon nitride) are purchased in a raw state (at the cost levels of Section 11.1) and must be further refined for use in the various processes to which they will be applied. Because all powder preparation is similar, it seems reasonable to prepare it at a common central facility, perhaps divided by the three types of materials being used.</p> <p>The preparation method is as follows:</p> <p>a. <u>Ball Milling</u> - The unrefined powder is mixed in a wet slurry and poured into a ball-mill. The balls in the mill are made of ceramic to reduce contamination and provide longer wear. A ball milling machine large enough to handle about 1,200 lb/hr. will cost about \$400,000, complete with services and controls.</p>																		
DISTRIBUTION: W. Chiu D. Darooka R. Drummond C.A. Johnson (Sch.)		R. Meier H. Rauch J. Ortoleva R. Emmer IV-1		PAGE NO. 1 OF 4 RETENTION REQUIREMENTS <table border="1"> <tr> <th>COPIES FOR</th> <th>MASTERS FOR</th> </tr> <tr> <td><input type="checkbox"/> 1 MO.</td> <td><input type="checkbox"/> 3 MOS.</td> </tr> <tr> <td><input type="checkbox"/> 3 MOS.</td> <td><input type="checkbox"/> 6 MOS.</td> </tr> <tr> <td><input type="checkbox"/> 6 MOS.</td> <td><input type="checkbox"/> 12 MOS.</td> </tr> <tr> <td><input type="checkbox"/> MOS.</td> <td><input type="checkbox"/> MOS.</td> </tr> <tr> <td><input type="checkbox"/></td> <td><input type="checkbox"/> DO NOT DESTROY</td> </tr> </table>			COPIES FOR	MASTERS FOR	<input type="checkbox"/> 1 MO.	<input type="checkbox"/> 3 MOS.	<input type="checkbox"/> 3 MOS.	<input type="checkbox"/> 6 MOS.	<input type="checkbox"/> 6 MOS.	<input type="checkbox"/> 12 MOS.	<input type="checkbox"/> MOS.	<input type="checkbox"/> MOS.	<input type="checkbox"/>	<input type="checkbox"/> DO NOT DESTROY
COPIES FOR	MASTERS FOR																	
<input type="checkbox"/> 1 MO.	<input type="checkbox"/> 3 MOS.																	
<input type="checkbox"/> 3 MOS.	<input type="checkbox"/> 6 MOS.																	
<input type="checkbox"/> 6 MOS.	<input type="checkbox"/> 12 MOS.																	
<input type="checkbox"/> MOS.	<input type="checkbox"/> MOS.																	
<input type="checkbox"/>	<input type="checkbox"/> DO NOT DESTROY																	

PROGRAM INFORMATION REQUEST / RELEASE

CLASS. LTR.	OPERATION	PROGRAM	SEQUENCE NO.	REV. LTR.
PIR NO. — — — — —				
*USE "C" FOR CLASSIFIED AND "U" FOR UNCLASSIFIED				

FROM		TO	
DATE SENT	DATE INFO. REQUIRED	PROJECT AND REQ. NO.	REFERENCE DIR. NO.
SUBJECT			

INFORMATION REQUESTED/RELEASED

- b. Spray Drying - After the powder has been ground sufficiently, it must be separated from the liquid and dried.

The liquid slurry is pumped at high pressure through nozzles and dried in the resulting spray. The liquid evaporates and the powder falls out as fine dust. This is generally done within a conical chamber where whirling air is forced at high volume to a collecting point in the apparatus, and the relatively pure dust is removed.

Each spray dry facility of 1,200 lb/hr. capacity will cost about 1.0 million dollars.

Based on the production weights of various materials, we will need to generate about 2,400 lb/hr. of silicon nitride, and about 3,600 lb/hr. each of silicon carbide and silicon nitride.

II Proof Testing and Inspection

The nature of ceramic material dictates either the use of proof-testing on 100% basis or simple visual checks. The use of X-raying equipment is ineffective, because flaws will usually not be exposed, or the machine may reject usable material due to harmless inclusions.

Two types of proof tests will be applied to critical pieces:

1. Flame testing - Apply a flame to the part long enough to generate a full-cycle thermal stress equal to or greater than the stress that the part will see in service.
2. Pressure testing - If the part is subject to pressurization in service, it may be more likely to fail from this than from thermal causes. The part is capped off, then pressurized to a value greater than that seen in actual use.

IV-2	PAGE NO. 2 of 4	RETENTION REQUIREMENTS	
		COPIES FOR	MASTERS FOR
		<input type="checkbox"/> 1 MO.	<input type="checkbox"/> 3 MOS.
		<input type="checkbox"/> 3 MOS.	<input type="checkbox"/> 6 MOS.
		<input type="checkbox"/> 6 MOS.	<input type="checkbox"/> 12 MOS.
		<input type="checkbox"/> MOS.	<input type="checkbox"/> MOS.
		<input type="checkbox"/>	<input type="checkbox"/> DO NOT DESTROY

PROGRAM INFORMATION REQUEST / RELEASE

CLASS. LTR.	OPERATION	PROGRAM	SEQUENCE NO.	REV. LTR.
PIR NO.				
*USE "C" FOR CLASSIFIED AND "U" FOR UNCLASSIFIED				

FROM		TO	
DATE SENT	DATE INFO. REQUIRED	PROJECT AND REQ. NO.	REFERENCE DIR. NO.
SUBJECT			

INFORMATION REQUESTED/RELEASED

The nature of the part and the type of stress it will see in service will determine the test to be applied. An element of labor time and equipment costs are included in the estimate for each part, where appropriate.

III Parts Costing

- a. Materials - The raw materials cost basis is explained in PIR 007. The economic feasibility of the engine will depend largely on how far the price of ceramic powders can be driven down. Because we cannot accurately forecast the future cost of ceramics, as explained in PIR 008, three projections were used in this analysis. The cost comparison of Table I uses the lowest projected prices in the foreseeable future. (Level III from the material costs summary, Table II)
- b. Labor - The nature of nearly all the processes in ceramics manufacturing demands nearly continuous operation. The production estimates are based on 20 hours of output per day, with 4 hours being allocated to maintenance, set up, cleaning and other servicing activity. The labor was calculated by multiplying the numbers of people required for a given operation times the 20 hour day, then adjusted by a factor of 1.2 to account for the above service activity. Table III shows the labor cost summary for each ceramic part, plus the sub-assembly and final assembly of the upper end of the engine.

Labor rates were calculated at a base rate of \$18.00/hr., with a 10% second shift and 15% third shift differential, making an average cost rate of \$19.50/hr.

IV-3	PAGE NO. 3 OF 4	RETENTION REQUIREMENTS	
		COPIES FOR	MASTERS FOR
		<input type="checkbox"/> 1 MO. <input type="checkbox"/> 3 MOS. <input type="checkbox"/> 6 MOS. <input type="checkbox"/> MOS. <input type="checkbox"/>	<input type="checkbox"/> 3 MOS. <input type="checkbox"/> 6 MOS. <input type="checkbox"/> 12 MOS. <input type="checkbox"/> MOS. <input type="checkbox"/> DO NOT DESTROY

PROGRAM INFORMATION REQUEST / RELEASE

CLASS. LTR.	OPERATION	PROGRAM	SEQUENCE NO.	REV. LTR.
PIR NO. _____				
*USE "C" FOR CLASSIFIED AND "U" FOR UNCLASSIFIED				

FROM		TO	
DATE SENT	DATE INFO. REQUIRED	PROJECT AND REQ. NO.	REFERENCE DIR. NO.
SUBJECT			

INFORMATION REQUESTED/RELEASED

IV Equipment and Tooling

The estimates for these items are tabulated in Table IV. Equipment cost was developed for each part in detail on the Manufacturing Summary Sheets. Estimates are in 1983 dollars, and in some cases are derived from scaled-up versions of smaller equipment in existence today. Tooling estimates are possibly low due to difficulty in discriminating between tools and equipment costs on some of the more specialized automated machinery. However, this is balanced by possibly high equipment estimates that include features which could be identified as tooling.

V Factory Floor Space and Plant

The major parts processes were estimated from roughly 2-3 times actual machine floor space, to allow for access to the equipment. These figures were totalled to yield basic floor space needs. Service and staging access area is estimated by a factor of 0.667. This would include aisles, conveyor space, supervision offices, and other service area. The cost of building is calculated at \$80.00/ft.² for a fully-equipped modern factory in 1983.

IV-4	PAGE NO. 4 OF 4	RETENTION REQUIREMENTS	
		COPIES FOR	MASTERS FOR
		<input type="checkbox"/> 1 MO.	<input type="checkbox"/> 3 MOS.
		<input type="checkbox"/> 3 MOS.	<input type="checkbox"/> 6 MOS.
<input type="checkbox"/> 6 MOS.	<input type="checkbox"/> 12 MOS.		
<input type="checkbox"/> MOS.	<input type="checkbox"/> MOS.		
<input type="checkbox"/>	<input type="checkbox"/> DO NOT DESTROY		

GENERAL ELECTRIC

ADVANCED ENERGY
PROGRAMS DEPT.

PROGRAM INFORMATION REQUEST / RELEASE

*CLASS. LTR.	OPERATION	PROGRAM	SEQUENCE NO.	REV. LTR.
PIR NO. — — —				
*USE "C" FOR CLASSIFIED AND "U" FOR UNCLASSIFIED				

FROM		TO	
DATE SENT	DATE INFO. REQUIRED	PROJECT AND REQ. NO.	REFERENCE DIR. NO.
SUBJECT			

INFORMATION REQUESTED/RELEASED

VI Furnace Power Costs - This cost factor may be considered, but as we will see, it is not a significant number compared to other processing cost factors such as raw material and factory equipment costs. A simplified calculation is as follows:

Total mass of parts + conveyor setters per hour x heat capacity:

$23.4 \text{ LB/Part} \times (2) \times 454 \text{ GM/LB} \times 50 \text{ Parts/Hr.} \times .25 \text{ Cal/GM}^\circ\text{C} = 265,590 \text{ Cal/Hr}^\circ\text{C}$
 $265,590 \text{ Cal/Hr}^\circ\text{C} \times .0039682 \text{ BTU/Cal} \times 1900^\circ\text{C} \times 1/3413 \text{ KW/BTU} = \underline{586 \text{ KW}}$
 $586 \text{ KW} \times 24 \text{ Hr./Day} \times \$.06/\text{KWH} = \$845/\text{Day cost of operation}$
 $\$845/1000 \text{ engines} = \underline{\$.84 \text{ each}}$

*Weight factor for setters and conveyor material.

As can be seen, the raw material cost for this part so far outweighs the power cost as to be lost in the accuracy of the calculation process. This will prove to be true in the case of all the operating costs of similar sintering furnaces which are to be used in making other ceramic parts.

IV-5

PAGE NO.

4 OF 4

RETENTION REQUIREMENTS

COPIES FOR

<input type="checkbox"/> 1 MO.
<input type="checkbox"/> 3 MOS.
<input type="checkbox"/> 6 MOS.
<input type="checkbox"/> 12 MOS.
<input type="checkbox"/> MOS.
<input type="checkbox"/>

MASTERS FOR

<input type="checkbox"/> 3 MOS.
<input type="checkbox"/> 6 MOS.
<input type="checkbox"/> 12 MOS.
<input type="checkbox"/> MOS.
<input type="checkbox"/> DO NOT DESTROY

CERAMIC AUTOMOTIVE ENGINE STUDY

1. Table I - Cost Comparison based on MOD-1 report of 12/9/81 by Mechanical Technology Inc.
2. Table II - Material Cost Estimates by part.
3. Table III - Labor Cost Summary, parts and final assembly elements.
4. Table IV - Equipment and tooling cost, including powder processing.
5. Table V - Factory Floor Space and Plant Cost totals.
6. Direct labor estimate details for assembly costs.
7. Direct labor estimate details for each ceramic part. Includes powder processing/mixing time.

TABLE I

CASES ENGINE COST - 1983
EXTRAPOLATED FROM MOD-1 ENGINE COST DATA

	(1) Est. Basic Engine Cost (Mod 1 Design)	(2) Est. Cost ¹ Equivalent Top Side Components	(3) Est. Cost ¹ Lower Engine Block Components	(4) Cost Equivalent ² Ceramic Engine Top Side Components (Level III) ⁴	(5) CASES Est. Basic Cost (Col 3 + Col 4)
Matl.	887.91			629.54	
Labor	155.50			114.87	
Burden	445.34			328.98	
Scrap ³	8.98			36.05	
	<u>1,497.73</u>	<u>664.82</u>	<u>832.91</u>	<u>1,109.44</u>	<u>1,942.35</u>

NOTES:

1. From Report dated 12/9/81, By Mechanical Technology Inc. Under Contract DEN3-32
2. Lowest material cost level predicted.
3. For ceramic parts, 5 percent of material is considered normal loss factor.
4. Level III refers to material cost projections of \$5.00/lb. for silicon carbide and silicon nitride, \$1.00/lb. for mullite and \$2.00/lb. for zirconia. See PIR 007.

TABLE II

MATERIAL COSTS: ALL CERAMIC PARTS

<u>PT.NO.</u>	<u>NAME</u>	<u>WT.(EA.)</u>	<u>QTY./ENG.</u>	<u>WT./ENG. LB.</u>	<u>RAW MAT.* \$</u>		
					<u>I</u>	<u>II</u>	<u>III</u>
CSE 102	Comb. Chamber	29.05	1	29.10	529.00	264.50	129.20
CSE 101-2	Cyl. Outer Sleeve	6.18	4	24.72	470.40	233.20	116.40
CSE 101-1-1	Cyl. Heater Hd.	14.50	4	58.00	290.00	174.00	58.00
CSE 101-1-2	Htr. Hd. Dist. Ch.	2.53	4	10.12	202.90	101.20	50.60
CSE 101-1-6	Htr. Hd. Tube	.15	96	14.40	294.00	147.00	73.50
CSE 109	Displacer	.77	4	3.08	15.40	9.24	3.08
CSE 109A	Radiation Shield	.04	12	.48	2.40	1.44	.48
CSE 101-3	Insulating Sleeve	1.50	4	6.00	30.00	18.00	6.00
CSE 101-3	Rad. Mantle Dome	2.15	4	8.60	172.00	86.00	43.00
CSE 101-5	Mantle-Baffle	.13	4	.52	10.40	5.20	2.60
CSE 105-4	Cyl. Liner	1.66	4	6.64	33.20	20.00	6.68
CSE 104-1	Pre Heater Plates	.035	800	28.00	560.00	280.00	140.00
TOTAL				189.66	\$2,609.20	1,339.78	629.54

COST IN \$/LB

<u>SiC</u>	<u>Si₃N₄</u>	<u>Mull.</u>	<u>Zr.</u>
Level I	20	5	10
Level II	10	3	5
Level III	5	1	2

*Three cost levels are projected:

TABLE III
LABOR COST - CERAMIC PARTS

CSE 102	Comb. Chamber	89.7	17.50	1	17.50
CSE 101-2	Cyl. Outer Slv.	9.6	1.87	4	7.48
CSE 101-1-1	Cyl. Htr. Hd.	14.0	2.80	4	11.20
CSE 101-1-2	Htr. Hd. Dist. Ch.	10.2	1.99	4	7.96
CSE 101-1-6	Htr. Hd. Tube	.48	0.095	96	9.12
CSE 109	Displacer	7.5	1.46	4	5.84
CSE 109A	Radiation Shield	1.32	.257	12	3.08
CSE 101-1-3	Insul. Sleeve	3.6	.70	4	2.80
CSE 101-3	Rad. Mantle Dome	12.6	2.46	4	9.84
CSE 101-5	Mantle-Baffle	2.2	.42	4	1.68
CSE 105-4	Cyl. Liner	7.8	1.52	4	6.08
CSE 104-1	Pre-Heater Plates	.057	.011	800	<u>8.80</u>
Sub-Total - Parts					<u>\$91.38</u>
	Sub-Assembly Htr. Head	10.0	1.95	4	7.80
	Sub-Assembly Cold Side	8.0	1.56	4	6.24
	Final Assembly	98.46	9.45	1	<u>9.45</u>
Sub-Total - Assembly					<u>23.49</u>
TOTAL LABOR UPPER ENGINE					<u>\$ 114.87</u>

TABLE IV
EQUIPMENT & TOOLING COST

<u>PT. NO.</u>	<u>NAME</u>	<u>\$ EQUIP. (THOUS.)</u>	<u>\$ TOOLING (THOUS.)</u>
CSE 102	Comb. Chamber	15,050	1,170
CSE 101-2	Cyl. Outer Sleeve	6,100	530
CSE 101-1-1	Cyl. Heater Hd.	12,100	980
CSE 101-1-2	Htr. Hd. Dist. Ch.	10,000	570
CSE 101-1-6	Htr. Hd. Tube	9,275	730
CSE 109	Displacer	8,800	420
CSE 109A	Radiation Shield	1100	80
CSE 101-1-3	Insulating Sleeve	800	100
CSE 101-3	Rad. Mantle Dome	8,400	1,240
CSE 101-5	Mantle-Baffle	800	90
CSE 105-4	Cyl. Liner	3,700	530
CSE 103-1	Pre Heater Plates	<u>4,500</u>	<u>500</u>
Sub-Totals (Parts)		<u>79,905</u>	<u>6,940</u>
	Powder Processing	<u>10,200</u>	<u>NA</u>
TOTALS - Equipment & Tooling		\$90,105,000	\$6,940,000

TABLE V

FACTORY FLOOR SPACE REQUIREMENTS
AND PLANT COSTS

<u>PT.NO.</u>	<u>NAME</u>	<u>BASIC FLR. (FT² SPACE)</u>	<u>SERV & STAGING</u>	<u>TOTAL FT²</u>	<u>COST @ \$80/FT²</u>
CSE 102	Comb. Chamber	28828	19195	48023	3,841,840
CSE 101-2	Cyl. Outer Slv.	9700	6466	16166	1,293,359
CSE 101-1-1	Cyl. Htr. Hd.	10700	7133	17833	1,426,666
CSE 101-1-2	Htr. Hd. Dist.Ch.	19240	9620	28860	2,308,800
CSE 101-1-6	Htr. Hd. Tube	13320	8880	22200	1,775,999
CSE 109	Displacer	7200	4800	12000	959,996
CSE 109A	Radiation Shield	1390	427	2317	185,326
CSE 101-1-3	Insul.Sleeve	1000	667	1667	133,360
CSE 101-3	Rad. Mantle Dome	9780	6520	16300	1,304,000
CSE 101-5	Mantle-Baffle	950	633	1583	126,660
CSE 105-4	Cyl. Liner	3800	2533	6333	506,646
CSE 104-1	Pre Heater Plates	<u>9920</u>	<u>6944</u>	<u>16864</u>	<u>1,349,120</u>
	Sub-Total			190146	\$15,211,772
	(Powder Process Common Facility)	<u>5000</u>	<u>3300</u>	<u>8300</u>	<u>664,000</u>
	TOTALS			<u>198446</u>	<u>\$15,875,772</u>

DIRECT LABOR ESTIMATE

ASSEMBLY LABOR

Sub-Assembly - Cylinder Heater Head CSE 101-1

<u>Activity</u>	<u>Hrs./Each</u>
Wrap Outer Cylinder	.005
Slide Insulator Sleeve over Cylinder	.010
Assemble 24 Spiral Tubes to Head & Fixture	.033
Drop Baffle Support in Place	.002
Place Heater Dist. Chamber on Head	.080
Joining Operation Load/Unload	.020
TOTAL HOURS	.100
COST	<u>\$1.95</u>

Sub-Assembly - Cold Side Components and Cylinder Liner CSE 105/6

<u>Activity</u>	<u>Hrs./Each</u>
Assemble 50 Tubes into Manifold	.040
Apply Collector Ring to Fixtured Tubes	.003
Load/Unload Furnace Tray Assy.	.020
Slide Liner Backup With Seal in Place	.008
Slide Cylinder Liner in Place	.002
Insert Connector and Seal	.007
TOTAL HOURS	.080
COST	<u>\$1.56</u>

FINAL ASSEMBLY LABOR

Upper End of CSE Engine

<u>Activity</u>	<u>Hrs./Each</u>
Assemble Displacers onto Seal Assy.	.020
Add Lower Housing to Crankcase	.007
Assemble Cold Side Components	.007
Add Cooling Water Connector Parts	.040
Cylinder and Clamp Assy.	.070
Apply Inner Insulation	.010
Assemble Combustion Chamber	.020
Attach Fuel Atomizer Assy.	.005
Add Preheater Components	.160
Assemble Outer Insul. and Covers	.146
TOTAL	.485
TOTAL COST	<u>\$9.45</u> each

DIRECT LABOR ESTIMATE

PT. NO. CSE 102

NAME COMBUSTION CHAMBER

ACTIVITY	Men	Mhr/d
Mixing 1170 lb/hr. 20 lb/min.	2.0	40
Pouring 15 min./PC	2.5	250
Drying Load/Unload	1.0	20
Mold Making	0.4	8
Mold Handling Split Mold/Load/Unload	2	240
Sinter Furnace Load/Unload	2.0	40
Grinding Machine	2.0	40
Plasma Coat Load/Unload	4.0	80
Flame Testing, Inspection	2	40

TOTAL

748

Prod. Rate PCS/Day	1,000
Man Hr./PC	.748
1.2 Adj. Factor	.897
BASE LABOR COST \$/ea.	17.50

DIRECT LABOR ESTIMATE

PT. NO. CSE 101-2

NAME CYLINDER OUTER SLEEVE

ACTIVITY	Men	Mhr/d
Power Processing 1156 lb/hr.	2.0	40
Press Operation	2.0	40
Machine Green Parts	2.0	40
Sinter Furnace Load/Unload	2.0	40
Dense Grind Machining	2.0	40
Plasma Coating	2.0	40
Flame Testing Inspection	4.0	80

TOTAL

320

Prod. Rate PCS/Day	4,000
Man Hr./PC	.08
1.2 Adj. Factor	.096
BASE LABOR COST \$/ea.	1.87

DIRECT LABOR ESTIMATE

PT. NO. CSE 101-1-1

NAME CYL. HEATER HEAD

ACTIVITY	Men	Mhr/d
Powder Processing 2900 lb/hr.	4.0	80
Press Operation	4.0	80
Machine Green Parts	4.0	80
Drill/Index	2.0	90
Sintering Furnace Load/Unload	2.0	40
Dense Grind Machining I.D.	2.0	40
Dense Grind Machining O.D.	2.0	40
Dense Grind Machining Ream	2.0	40
Pressure Test	2.0	40
		480

TOTAL

Prod. Rate PCS/Day	4,000
Man Hr./PC	.12
1.2 Adj. Factor	.14
BASE LABOR COST \$/ea.	2.80

DIRECT LABOR ESTIMATE

PT. NO. CSE 101-1-2

NAME CYL. HEAD DISTRIB. CHAMBER

ACTIVITY	Men	Mhr/d
Powder Processing/Mixing	2.0	40
Injection Mold Core (Plastic)	1.0	20
Injection Mold Part	4.0	80
Oven Dry/Core Removal (Load/Unload)	2.0	40
Sintering Furnace Load/Unload	2.0	40
Dense Grind/Ream 24 Holes	4.0	80
Pressure Test	2.0	40
		340

TOTAL

Prod. Rate PCS/Day	4,000
Man Hr./PC	.085
1.2 Adj. Factor	.102
BASE LABOR COST \$/ea.	1.99

DIRECT LABOR ESTIMATE

7. 10. CSE 101-1-6

WAVE SPIRAL TUBES!

ACTIVITY	Men	Mhr/d
Injection Mold Core	2.0	40
Ultrasonic Weld Core Rings	1.0	20
Carbon Coat Core	1.0	20
Carbon Removal	1.0	20
Powder Preparation	1.0	20
Electroph. Bath Maint.	0.5	10
Drying/Unload Conveyor	1.0	20
Sintering Furnace Load/Unload	1.0	20
Cutoff/End Machining	2.0	40
Final Grind	8.0	160
Press. Test	1.0	20
TOTAL		390

Prod. Rate PCS/Day	96,000
Man Hr./PC	.0048
1.2 Adj. Factor	.0048
BASE LABOR COST \$/ea.	.095

DIRECT LABOR ESTIMATE

PT. NO. CSE 109

NAME DISPLACER

ACTIVITY	Men	Mhr/d
Powder Preparation 160 lb/hr.	0.5	10
Isostatic Press Operation	4.0	80
Trim/Cutoff End	2.0	40
Sintering Furnace Load/Unload	1.0	20
Dense Grind Machining	4.0	80
Pressure Test	1.0	20
TOTAL		250

Prod. Rate PCS/Day	4.000
Man Hr./PC	.0625
1.2 Adj. Factor	.075
BASE LABOR COST \$/ea.	1.46

SECRET LABOR PRIVATE

3. 12. CSE 109A

NAME

RADIATION SHIELD

ACTIVITY	Men	Mhr/d
Powder Preparation 24 lb/hr	0.10	2
Premixing	0.5	10
Injection Molding	1.0	20
Oven Dry Load/Unload	2.0	40
Sintering Furnace Load/Unload	1.0	20
Flame Test/Mechanical Test	2.0	40
TOTAL		132

Prod. Rate PCS/Day	<u>12,000</u>
Man Hr./PC	<u>.011</u>
1.2 Adj. Factor	<u>.0132</u>
BASE LABOR COST \$/ea.	<u>.257</u>

DIRECT LABOR ESTIMATE

PT. NO. CSE 101-1-3

NAME _____

BUR ESTIMATE
CYLINDER INSULATION SLEEVE

ACTIVITY	Men	Mhr/d
Powder Preparation 300 lb/hr.	1.0	20
Isostatic Press Operation	2.0	40
Cutoff/Trim Ends	1.0	20
Sintering Furnace Load/Unload	2.0	40
TOTAL		120

Prod. Rate PCS/Day	4,000
Man Hr./PC	.03
1.2 Adj. Factor	.036
BASE LABOR COST \$/ea.	.70

DIRECT LABOR ESTIMATE

File No. CSE 101-3

NAME RADIATION MANTLE-DOME

ACTIVITY	Men	Mhr/d
Powder Preparation 500 lb/hr.	1.0	20
Green-State Machining	4.0	80
Sintering Furnace Load/Unload	2.0	40
Dense Machining	8.0	160
Flame Testing	2.0	40
TOTAL		420

Prod. Rate PCS/Day	4,000
Man Hr./PC	.105
1.2 Adj. Factor	.126
BASE LABOR COST \$/ea.	2.46

DIRECT LABOR ESTIMATE

PT. NO. CSE 101-1-5

NAME MANTLE BAFFLE

ACTIVITY	Men	Mhr/d
Powder Preparation 26 lb/hr.	0.1	2
Uniaxial Press Operation	1	20
Sintering Furnace Load/Unload	1	20
Dense Grind	1	10
Flame Testing	1	20
TOTAL		72

Prod. Rate PCS/Day	4,000
Man Hr./PC	.018
1.2 Adj. Factor	.022
BASE LABOR COST \$/ea.	.42

DIRECT LABOR ESTIMATE
NAME CYLINDER LINER

PT. NO. CSE 105-4

ACTIVITY	Men	Mhr/d
Powder Preparation 330 lb/hr.	1.0	20
Isostatic Press. Operation	2.0	40
Green Machine	2.0	40
Sintering Furnace Load/Unload	1.0	20
Dense Grinding	5.0	100
Pressure Test	2.0	40
TOTAL		260

Prod. Rate PCS/Day 4,000
 Man Hr./PC .065
 1.2 Adj. Factor .078
 BASE LABOR COST \$/ea. 1.52

DIRECT LABOR ESTIMATE
NAME PREHEATER PLATE

PT. NO. CSE 104-1

ACTIVITY	Men	Mhr/d
Powder Preparation 1400 lb/hr.	2.0	40
Slurry Mixing	2.0	40
Doctor Blade Load/Maintain	5.0	100
Dry/Sinter Unload	10.0	200
TOTAL		380

Prod. Rate PCS/Day 800,000
 Man Hr./PC .000475
 1.2 Adj. Factor .00057
 BASE LABOR COST \$/ea. .011

GENERAL ELECTRIC

ADVANCED ENERGY
PROGRAMS DEPT.

PROGRAM INFORMATION REQUEST / RELEASE

*CLASS. LTR.	OPERATION	PROGRAM	SEQUENCE NO.	REV. LTR.
PIR NO. _____				
*USE "C" FOR CLASSIFIED AND "U" FOR UNCLASSIFIED				

FROM		TO	
DATE SENT	DATE INFO. REQUIRED	PROJECT AND REQ. NO.	REFERENCE DIR. NO.

SUBJECT

INFORMATION REQUESTED/RELEASED

SUMMARY OF MANUFACTURING DATA

Attached is an Appendix of all ceramic parts that follows this general format:

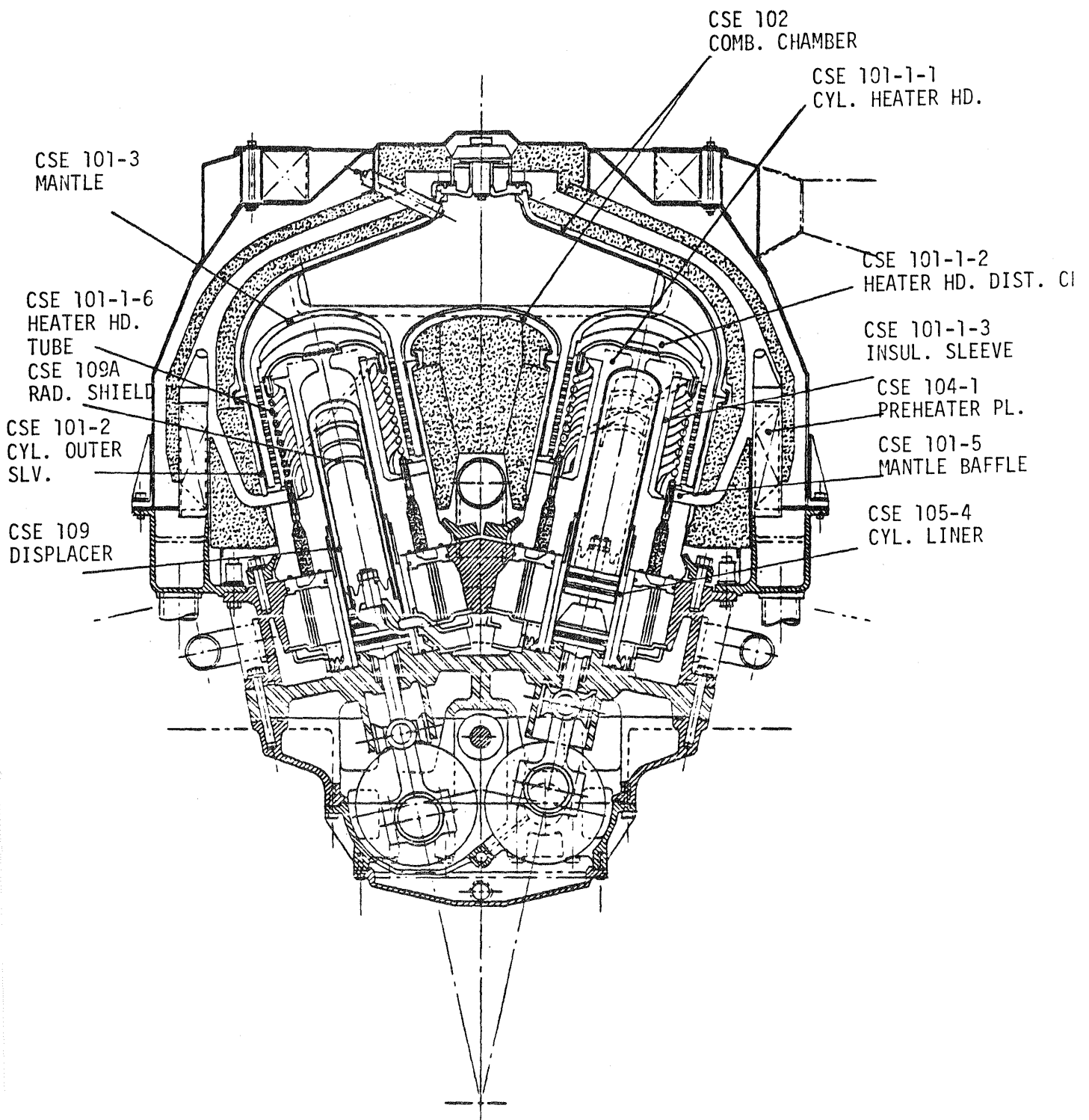
1. Sketch of the part being considered with dimensions, material and weight estimate given.
2. A process-flow summary for the part from raw material to end piece ready for assembly.
3. A cost-estimate sheet that shows capital equipment, major tool expense, size and cost of plant space and an estimated labor cost.
4. Finally, some statistics that were accrued from these data are summed up to show totals for all ceramic parts.

IV-19	PAGE NO. ____ OF ____	RETENTION REQUIREMENTS	
		COPIES FOR	MASTERS FOR
		<input type="checkbox"/> 1 MO.	<input type="checkbox"/> 3 MOS.
		<input type="checkbox"/> 3 MOS.	<input type="checkbox"/> 6 MOS.
		<input type="checkbox"/> 6 MOS.	<input type="checkbox"/> 12 MOS.
		<input type="checkbox"/> MOS.	<input type="checkbox"/> MOS.
		<input type="checkbox"/>	<input type="checkbox"/> DO NOT DESTROY

TABLE 10.1

Ceramic Automotive Stirling Engine - Ceramic Components

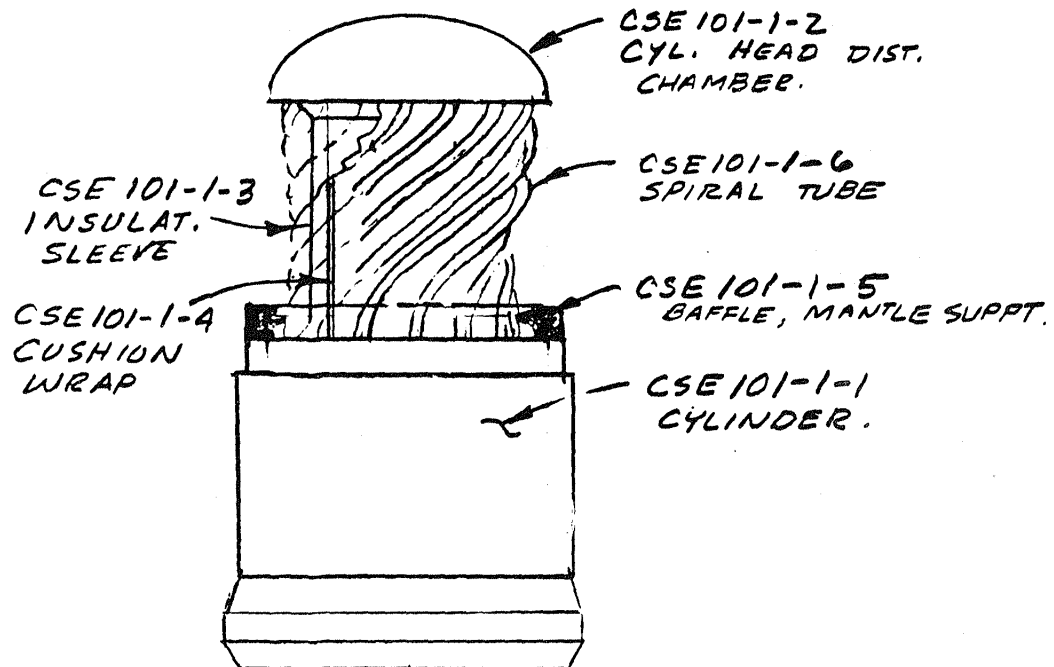
<u>Sketch No.</u>	<u>Item</u>	<u>Quan. Per Engine</u>	<u>Material</u>	<u>Vol in³</u>	<u>Weight lb.</u>
CSE 102	Combustion Chamber	1	Zirconia Coated Si ₃ N ₄	188	23.4
CSE 101-2	Cylinder Outer Sleeve	4	Si ₃ N ₄	46.5	5.78
CSE 101-1-1	Cylinder Heater Head	4	Mullite	134.5	15.4
CSE 101-1-2	Cylinder Heater Head Distribution Chamber	4	SiC	21.8	2.53
CSE 101-1-6	Heater Head Tube	96	SiC	1.27	.15
CSE-109	Displacer	4	Mullite	6.70	.77
CSE-109A	Radiation Shield	12	Mullite	0.333	.04
CSE 101-1-3	Cylinder Insulating Sleeve	4	Mullite	18.7	1.50
CSE 101-3	Radiation Mantle- Dome	4	SiC	18.5	2.15
CSE 101-1-5	Mantle Baffle	4	Si ₃ N ₄	1.06	.13
CSE 105-4	Cylinder Liner	4	Mullite	14.6	1.66
CSE 104-1	Preheater Plate	800	SiC	.30	.035

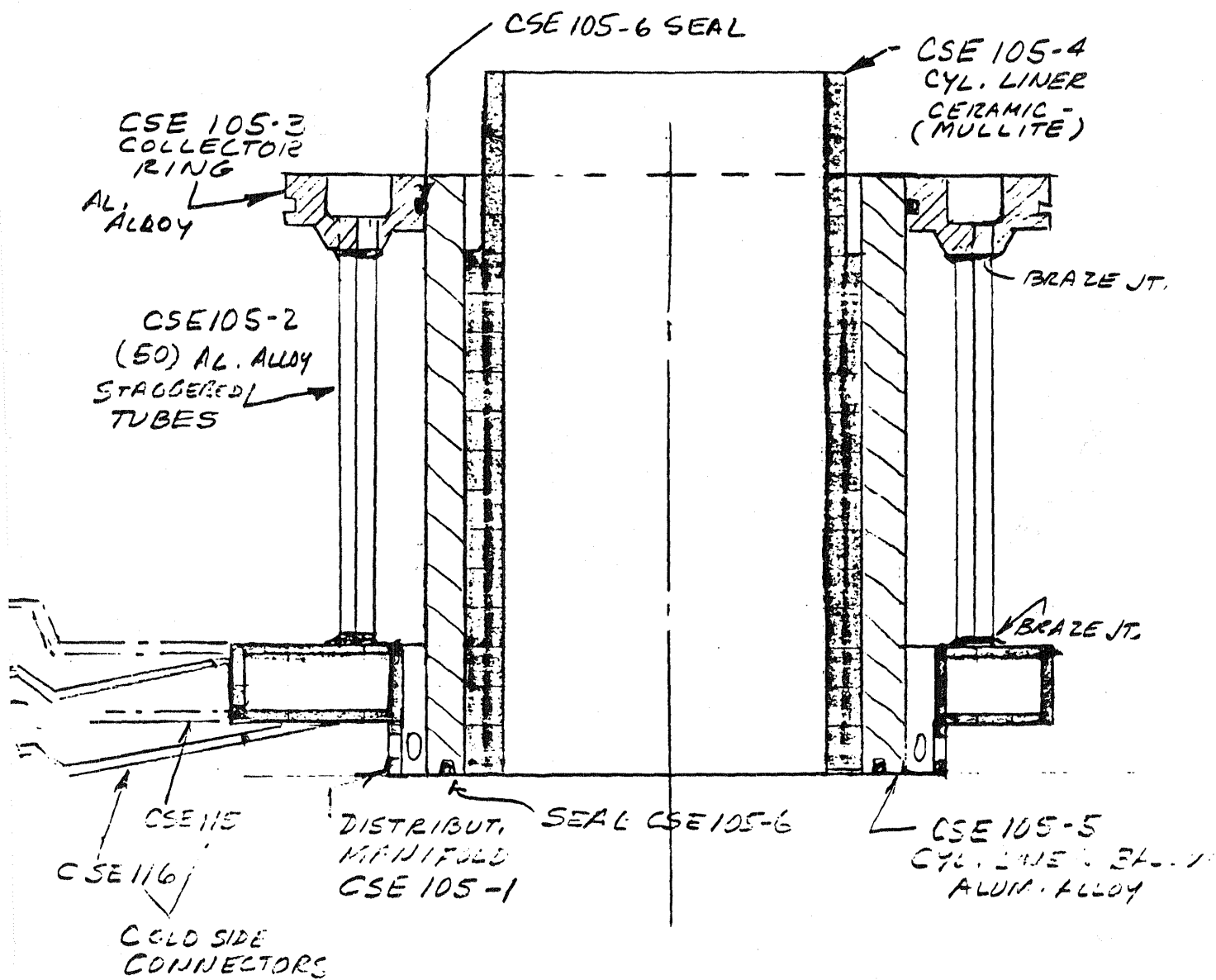


LOCATION OF
CERAMIC PARTS
C.A.S.E

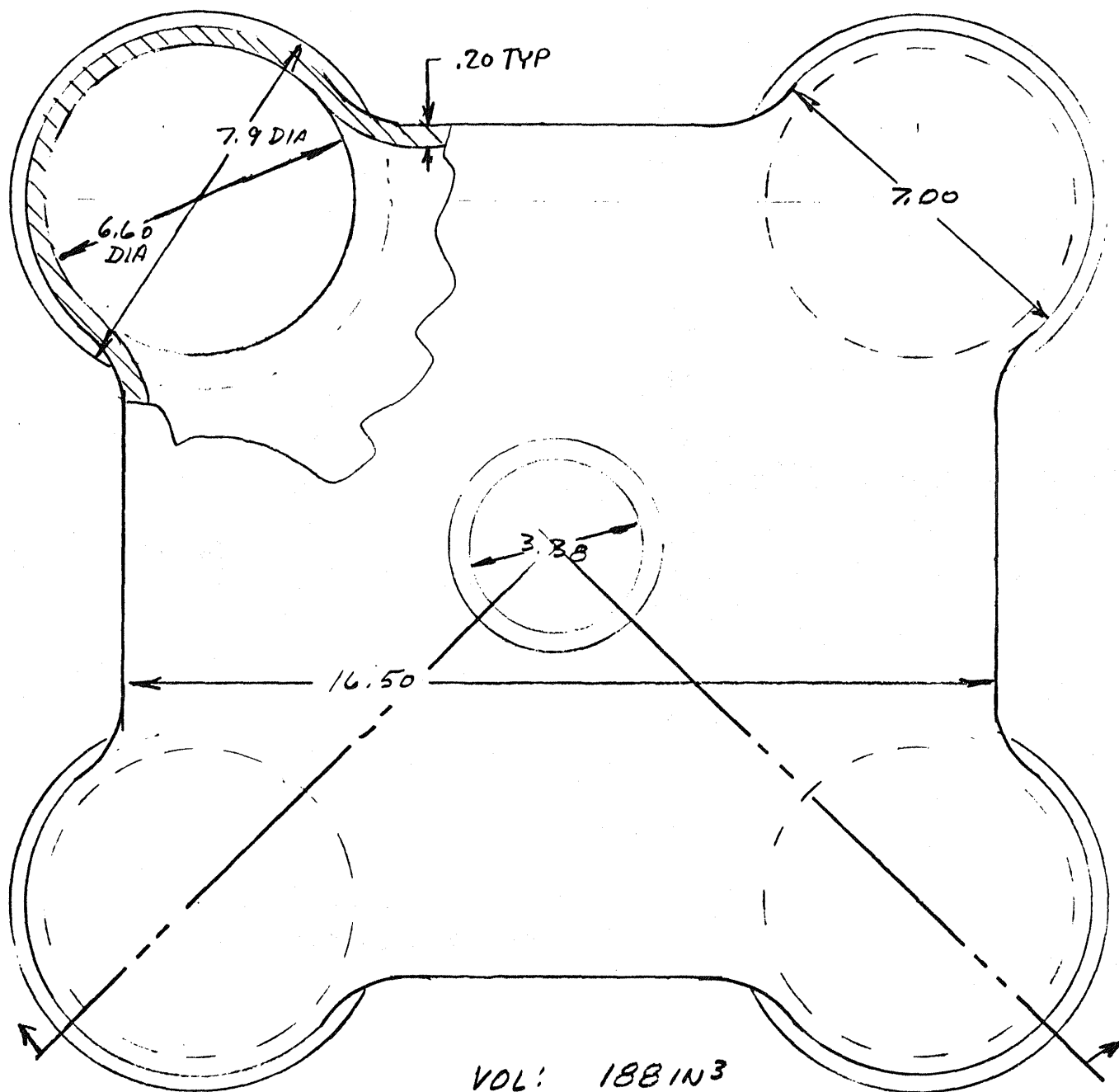
CSE 101-1

CYLINDER HEATER HEAD
ASSEMBLY.

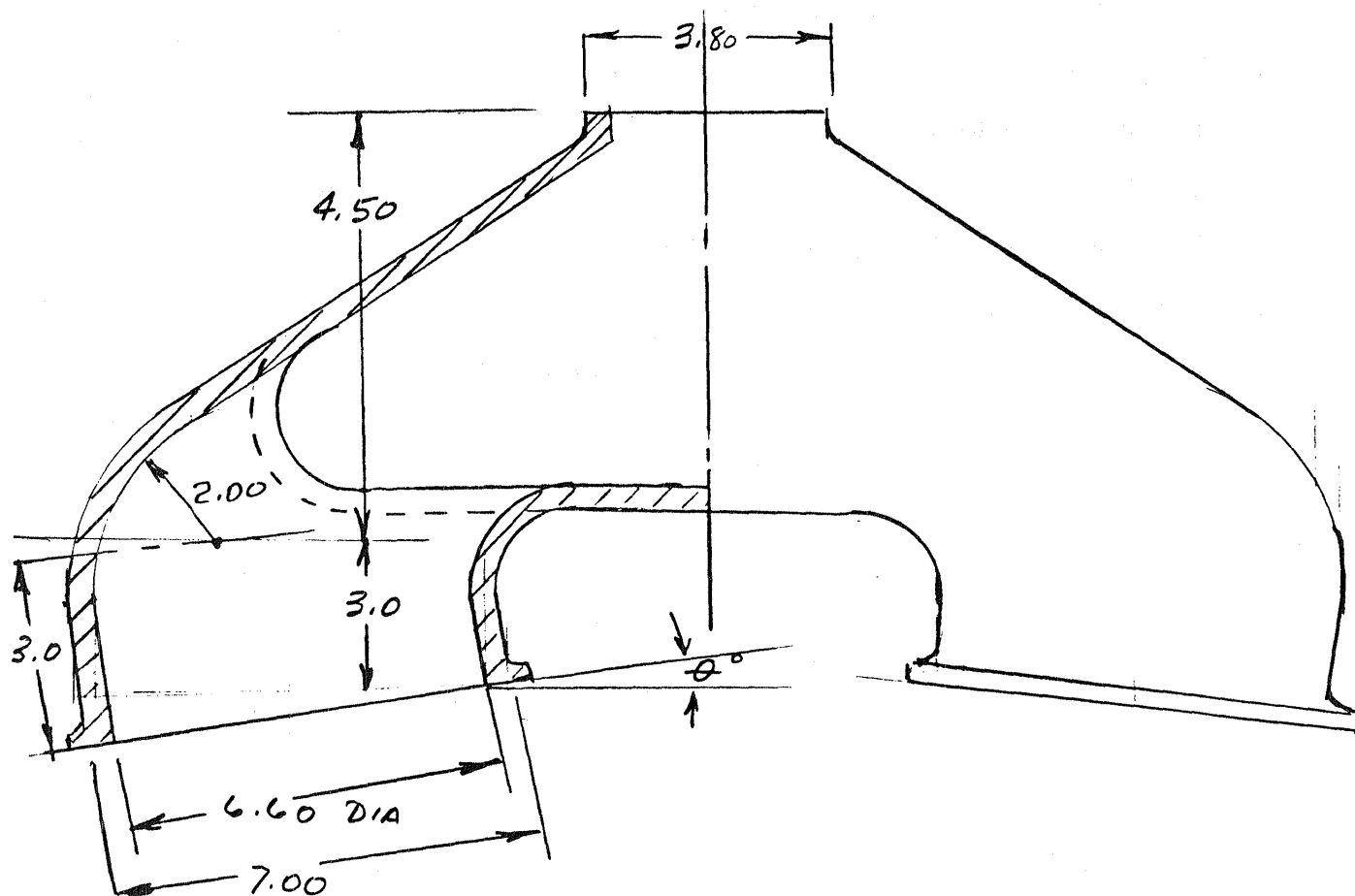




COLD SIDE COMPONENTS
ASSEMBLY.

COMBUSTION CHAMBERPROCESS: SLIP CAST / PLASM.
SPRAYMATL: Si_3N_4 / ZIRCONIAVOL: 188 IN³WT: 23.4 LB

CSE 102
COMB. CHAMBER



PROCESS FLOW CHART

CSE 102

COMBUSTION CHAMBER (Silicon Nitride)

A. Part Process Flow:

1. Slurry preparation - powder, water, additives - ball milling operation.
2. Pour mixture in plaster mold - 5 min. "cure". Pour off excess slip, then 10 min. dry.
3. Remove mold.
4. Controlled humidity. Dry cycle - 24 hrs.
5. Furnace cycle (N_2) - 4-5 hrs.
6. Diamond grind 5 surfaces (auto. machine).
7. Non-destructive test and inspection.

B. Mold Process Flow:

1. Mold assembly.
2. Mold Removal.
3. 1 hr. dry cycle in $150^{\circ}C$ ($300^{\circ}F$) oven.

C. Zirconia Plasma Coating

1. (8) machines) automatically controlled 5 head machine - 4 min. per part.

CSE 101-2

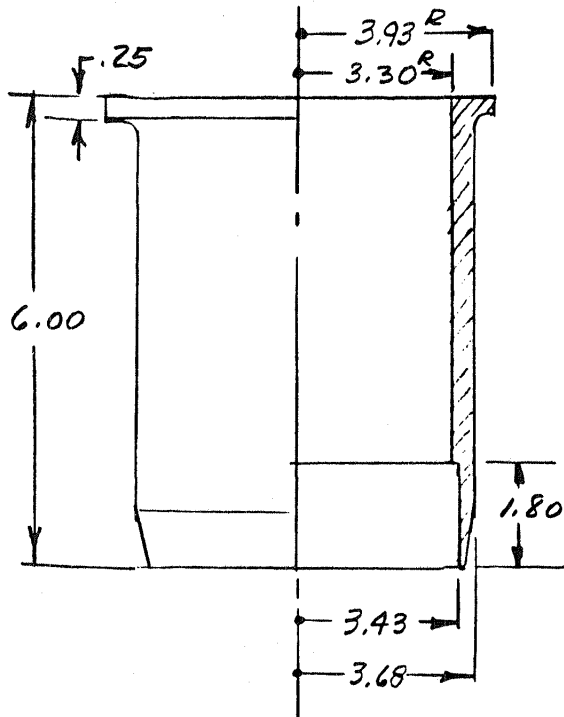
CYLINDER OUTER SLEEVE (4/ENGINE)

PROCESS: ISOSTATIC
PRESS.

MATL. Si_3N_4

VOLUME 46.5 IN³

WT. 5.78 LB



PROCESS FLOW CHART

CSE 101-2

CYLINDER OUTER SLEEVE (Silicon Nitride)

A. Process Flow:

1. Powder preparation (ball mill, etc.).
2. Isostatic press cycle (1 min./cycle - 2 pcs./each.).
3. (a) Green cut off ends and part at center.
(b) Grind step at each end.
4. Furnace sinter (N_2 ATM).
5. Dense grind-finish length and step.
6. Non-destructive test and inspection.

B. Process Flow: Zirconia Coating

1. plasma spray station (10) - rotating head or ware (2.5 min./sleeve).

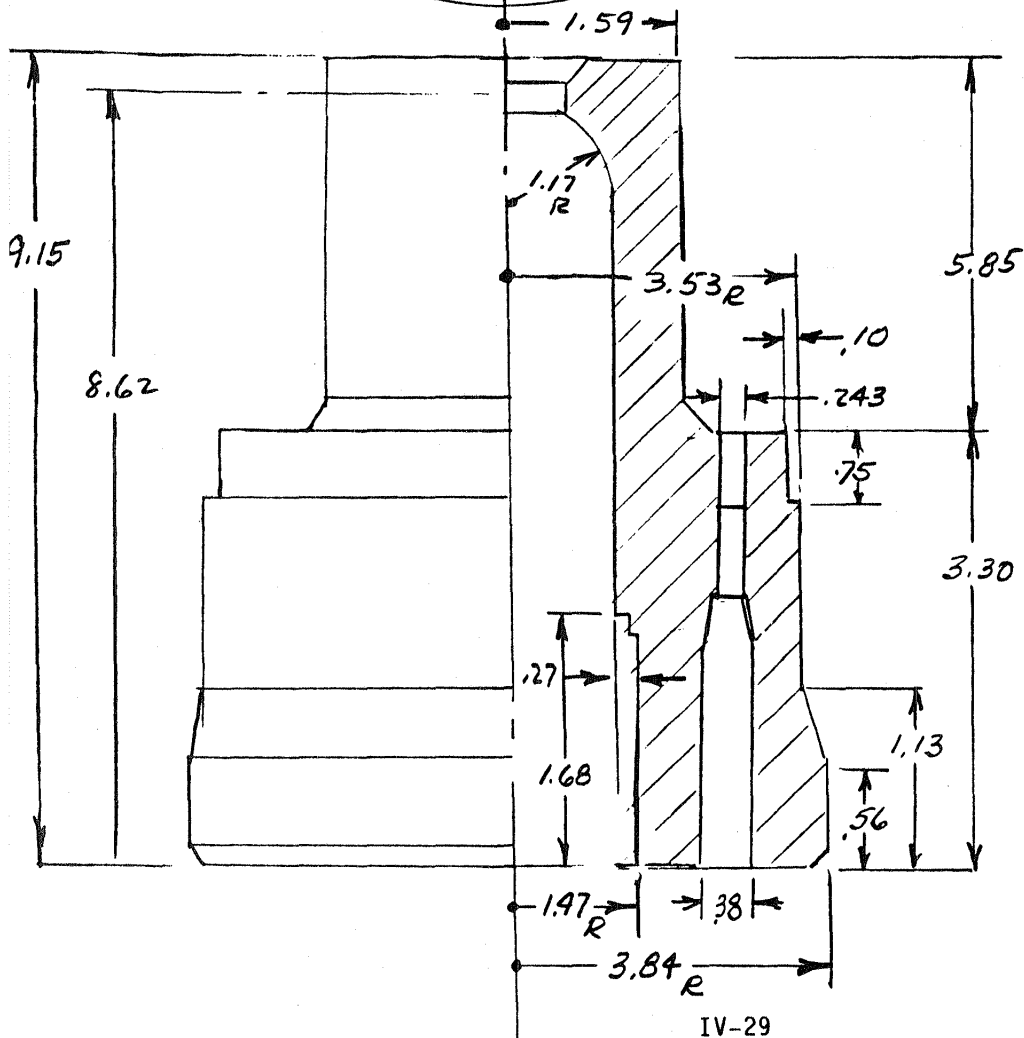
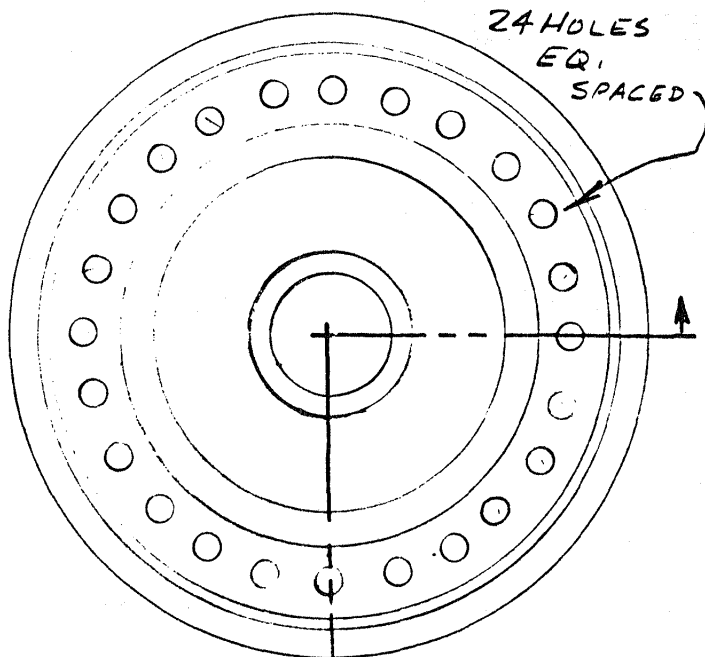
CSE 101-1-1 CYL. HEATER HEAD

PROCESS: ISOSTATIC
 PRESS

MATL: MULLITE

VOLUME: 134.47 IN³

WT: 15.4 LB.



PROCESS FLOW CHART

CSE 101-1-1

Cylinder Heater Head (Mullite)

1. Powder preparation
2. Isostatic dry bag press cycle - 1 min./cycle
3. Green-state machine operations
 - (a) Step-drill 24 holes - drill, index 1 min/cyc.
 - (b) Machine outside shape
 - (c) Cut inner features
4. Bake out/sinter (air atmosphere oven/furnace) 5 hr./total cycle.
5. Dense grind operations.
 - (a) Grind O.D.(head area).
 - (b) Grind I.D.(sleeve area).
 - (c) Ream 24 holes (for tube seat).
6. Non-destructive test & inspection.

CSE101-1-2

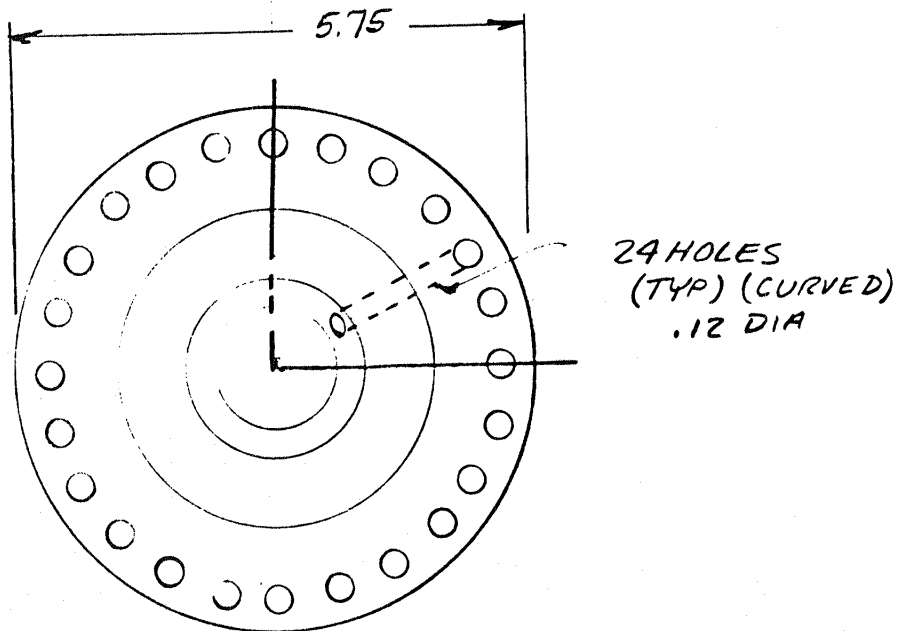
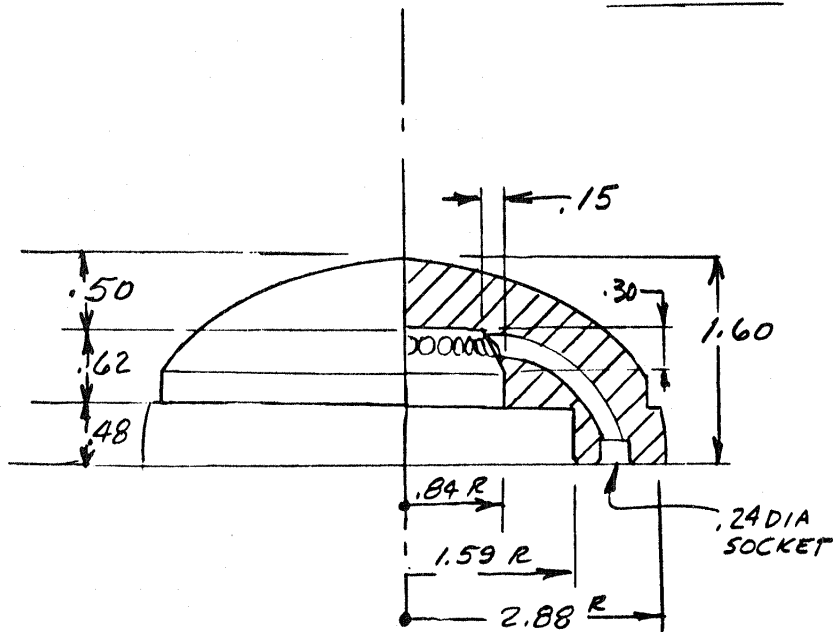
CYL. HEATER HD. DISTRIBUTION CHAMBER

PROCESS: INJECT. MOLD
FUGITIVE CORE

MATL: SIC

VOLUME: 21.78 IN³

WT: 2.53 LB



PROCESS FLOW CHART

CSE 101-1-2

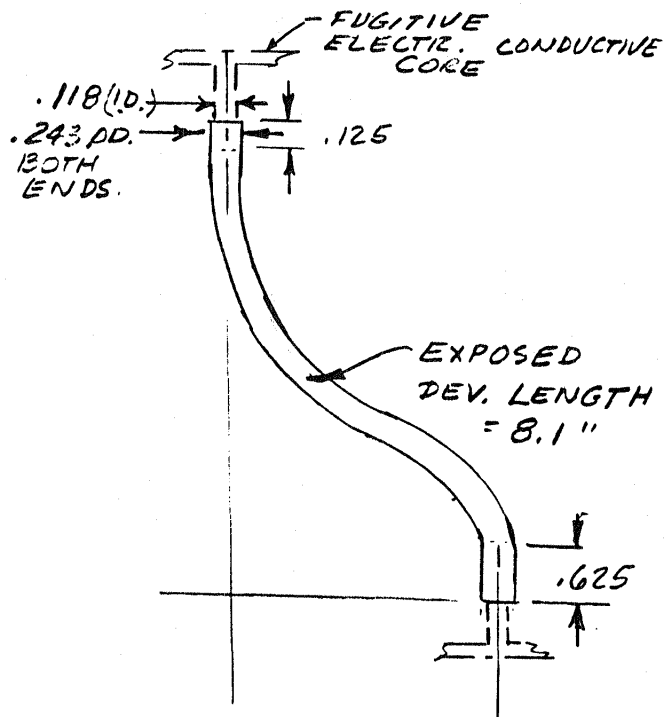
Cyl. Heater Head Distribution Chamber - (Silicon Carbide)

A. PROCESS FLOW: (Part)

1. Powder preparation
2. Mixing powder/vehicle in twin screw extruder.
3. Injection mold part around core.
4. Bakeout cycle (7 days).
5. Dense grinding.
 - (a) I.D. to fit cyl. heater head.
 - (b) Ream 24 holes to required tol.
6. Non-destructive test & inspection.

CSE 101-1-6

HEATER HEAD TUBE - 24/CYL, 96/ENGINE.



TOTAL DEV. LENGTH 8.98"

PROCESS: ELECTRO -
PHORESIS
DEPOSITION

MATL: SiC.

VOLUME: 1.27 IN³
WT: .15 LB

PROCESS FLOW CHART

CSE 101-1-6

Cylinder Heater Head Tube (Silicon Carbide)

A. PROCESS FLOW: (Part)

1. Dry powder preparation.
2. Slurry preparation/mixing/replenishing.
3. Electro-phoresis dip process (1 minute).
4. Humidity controlled dry cycle.
5. Oven core melt/sintering.
6. (a) Cut/separate tubes from end rings.
(b) Grind tube ends to tolerance.
7. Non-destructive test & inspection.

B. PROCESS FLOW (Core)

1. Pelletized material preparation.
2. Injection mold 24 tube cores.
3. Re-join (ultrasonic weld) rings.
4. Carbon-coat core (dip process) and dry.
5. Remove coating (scrape off end-ring supports).

CSE-109

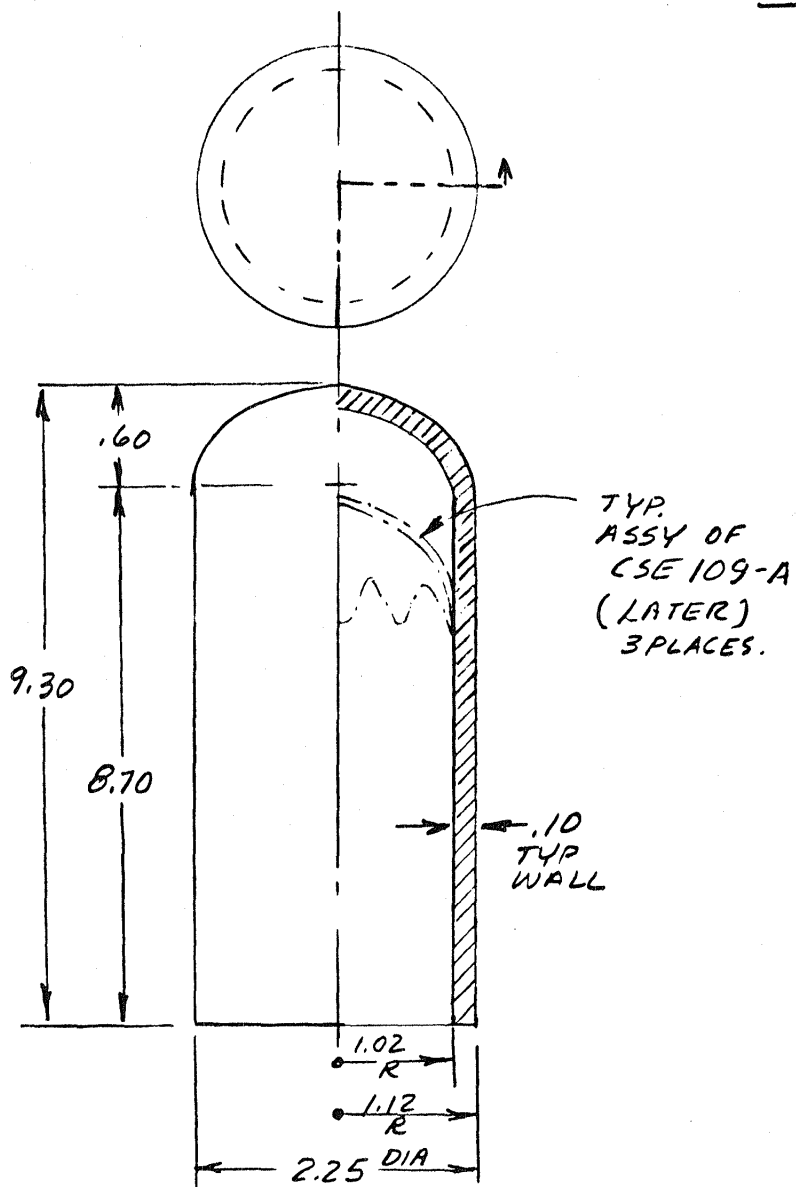
DISPLACER

PROCESS: ISOSTATIC
PRESSING

MATL: MULLITE

VOL: 6.70 IN³

WT: .77 LB



PROCESS FLOW CHART

CSE-109

Displacer (Mullite)

PROCESS FLOW:

1. Dry powder processing.
2. Isostatic (drybag) press 1 min/cycle.
3. Green machine:
 - (a) Cut off end.
 - (b) Grind O.D. to within .002 tol.
4. Furnace bake/sinter (4 hr. cycle).
5. Dense grind end.
6. Non-destructive test & inspection.

CSE 109 A

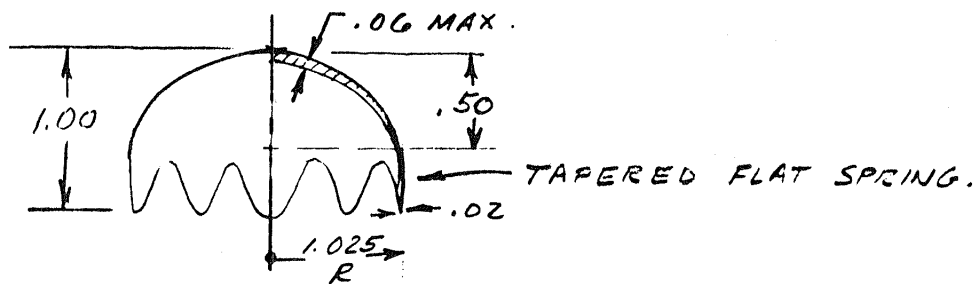
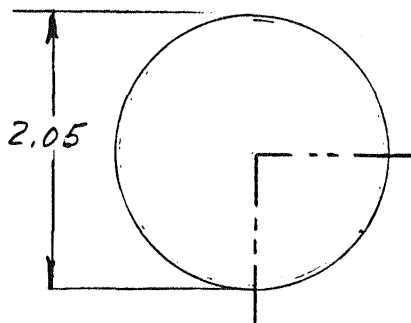
RADIATION SHIELD (3/CYL, 12/ENGINE)

PROCESS: INJECTION
MOLD

MATL: MULLITE

VOL: .333 IN³

WT: .04



PROCESS FLOW CHART

CSE 109A

Radiation Shield (Mullite)

PROCESS FLOW

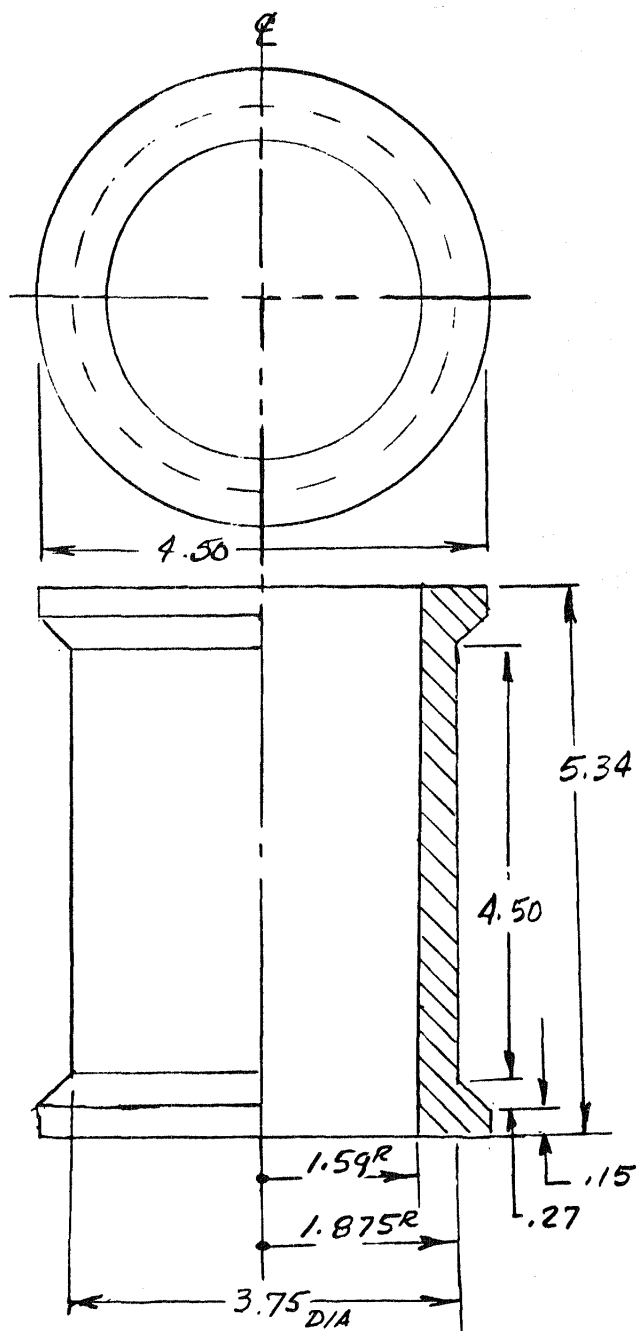
1. Dry powder processing.
2. Mixing powder/vehicle
3. Injection mold.
4. Bakeout cycle 20 hr.
5. Furnace firing (share CSE 109)
 - (a) Fire on domed setters to pre-form part to shape.
6. Non-destructive test & inspection.

CSE 101-1-3
CYL. INSULATING SLEEVE

PROCESS : ISOSTATIC PRESS

MATL : MULLITE
(70% DENSE)

VOL. 18.69 IN³
WT : 1.50 LB



PROCESS FLOW CHART

CSE 101-1-3

Cylinder Insulating Sleeve (Mullite - 70% dense)

PROCESS FLOW:

1. Dry powder processing.
2. Isostatic press (2 pcs./cycle) (1 cy./min).
3. Green cut off/trim ends-center.
4. Furnace firing - (share CSE 109)
5. Complete (no final sizing).
6. Non-destructive test & inspection.

CSE 101-3

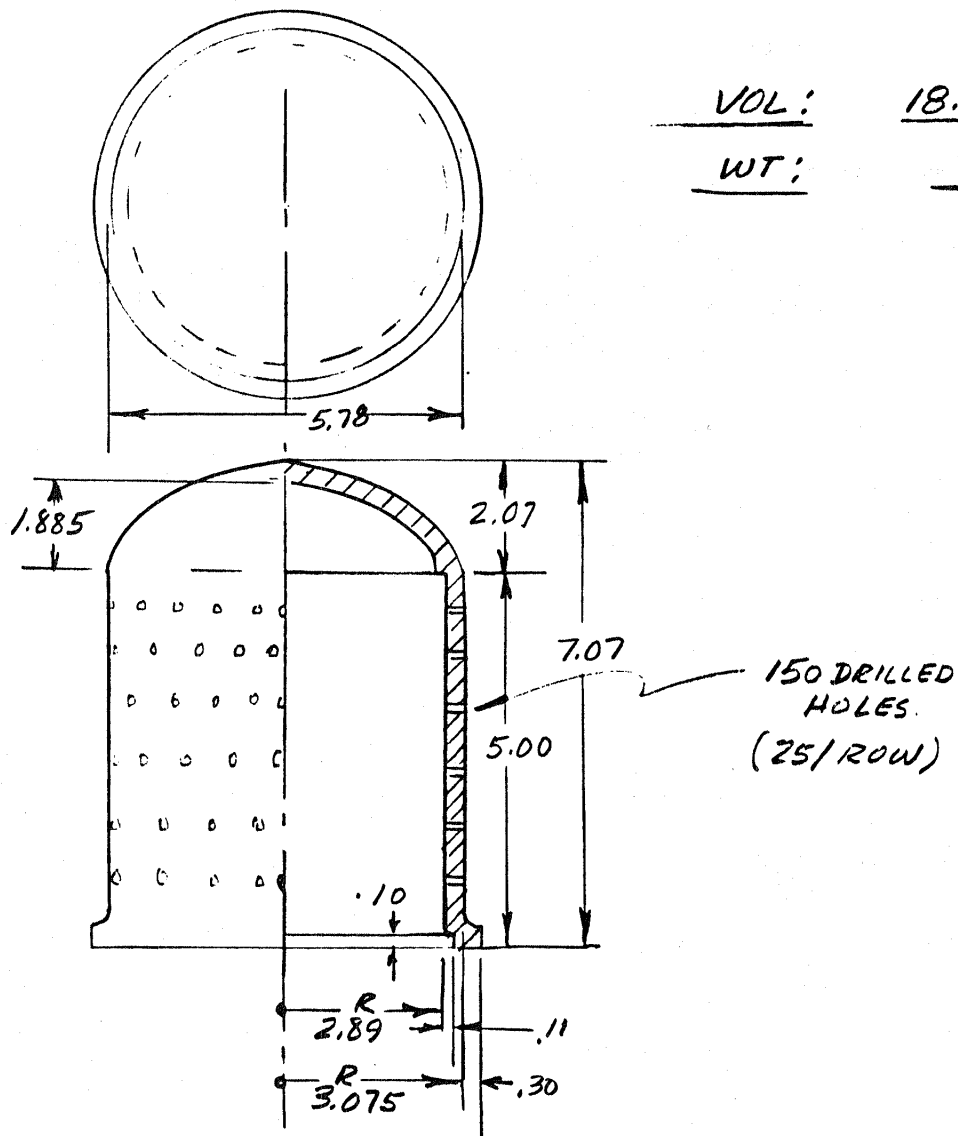
RADIATION MANTLE - DOME

PROCESS: ISOSTATIC PRESS

MATERIAL SIC

VOL: 18.51 IN³

WT: 2.15 LB



PROCESS FLOW CHART

CSE 101-3

Radiation Mantle Dome (Silicon Carbide)

PROCESS FLOW:

1. Dry powder processing.
2. Isostatic (drybag) press.
3. Green machining:
 - (a) Turn foot to shape & tol. (incl. O.D.).
 - (b) Trim length, establish perpendicularity.
 - (c) Drill/index 150 holes (25 x 6).
 - (d) Turn I.D. notch, clean holes.
4. Furnace sinter (N_2 ATM).
5. Dense grind.
 - (a) Length.
 - (b) Foot, notch.
 - (c) I.D. step.
6. Non-destructive test & inspection.

CSE 101-1-5

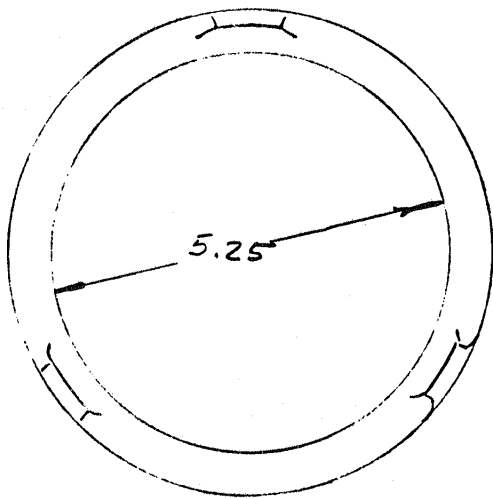
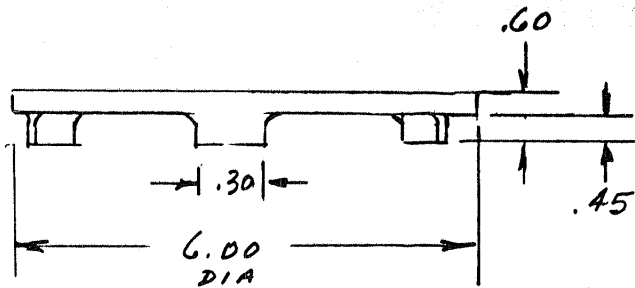
MANTLE BAFFLE

PROCESS: UNIAXIAL PRESS

MATL: Si₃N₄

VOL: 1.06 IN³

WT: .13 LB



PROCESS FLOW CHART

CSE 101-1-5

Mantle Baffle (Silicon Nitride)

1. Dry powder preparation.
2. Uniaxial die pressing (15 sec/cycle).
3. Furnace sinter (share with CSE 101-2).
4. Dense grind to thickness/dia.
5. Non-destructive test & inspection.

CSE 105-4

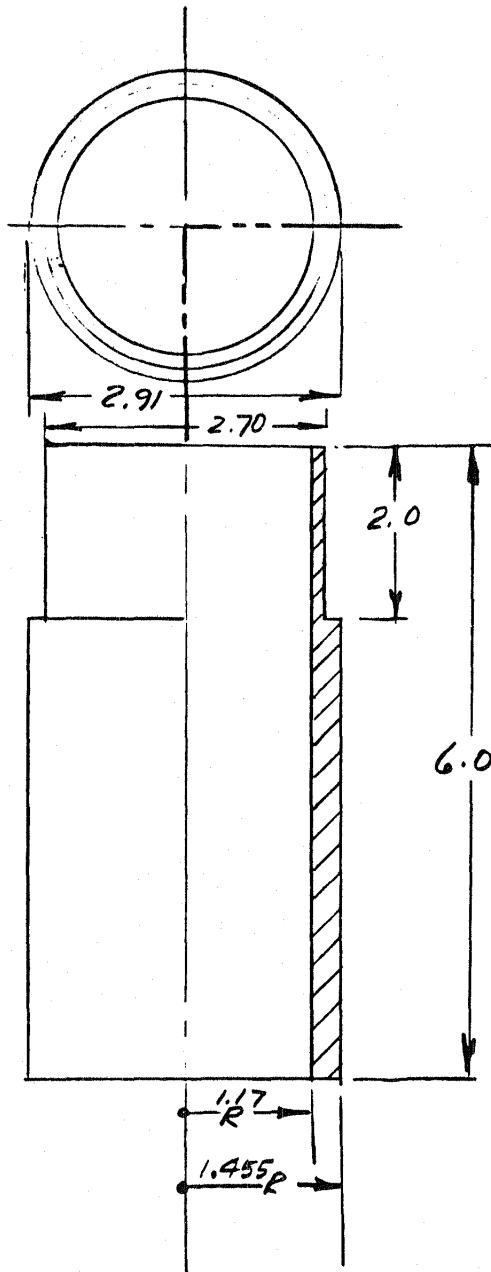
CYLINDER LINER

PROCESS: ISOSTATIC PRESS

MATL: MULLITE

VOL: 14.55 IN³

WT: 1.66 LB



PROCESS FLOW CHART

CSE 105-4

Cylinder Liner (Mullite)

1. Dry powder preparation.
2. Isostatic (drybag) press (2 pcs./cycle, 1 min.)
3. Green machine
 - (a) Rough grind O.D. and step.
 - (b) Saw cut-off - 3 places.
4. Furnace sinter (N_2 ATM) (share CSE 109).
5. Dense grind
 - (a) O.D. and step to .015.
 - (b) I.D. grind to tolerance.
6. Non-destructive test & inspection.

CSE 104-1
PREHEATER PLATE (800 PLATES/ENGINE)

PROCESS:

TAPECAST, DOCTOR BLADE.
(RIB REMOVAL AUTOMATIC
IN GREEN STATE)

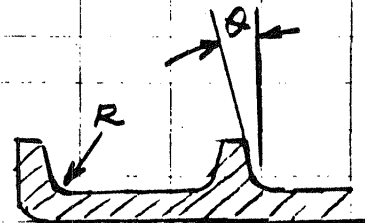
LOCALIZED
RIB REMOVAL

MATL: SiC.

VOLUME = .30 IN³

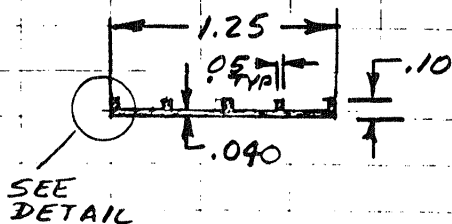
WT = .035 LB

5.0



TYPICAL RIB
DETAIL -

R & Ø ARE GENEROUS
AND NOT CRITICAL.



PROCESS FLOW CHART

CSE 104-1

Preheater Plate (Silicon Carbide)

PROCESS FLOW:

1. Powder preparation.
2. Mixing operations - (twin screw extr.).
3. Tape cast - doctor blade.
4. Auto. scrape/skim rib removal.
5. Loading setters (5 high, 8 wide).
6. Furnace sinter (N_2 ATM).
7. Non-destructive test & inspection.

MANUFACTURING SUMMARY SHEET

C.A.S.E.S

Part No. CSE 102 Title Combustion Chamber

Material Sl₃ N₄ Basic Process Slip Cast

Volume 188 (IN³) Weight 23.4 (lb)

Over Dimensions: Green 29 X 32 X 9.2 IN.
(Inches) 20.00 Fired 24 X 26 X 7.5 IN.
10.00
Material Cost 5.00 \$/lb \$468
\$234
Raw Material Cost/Piece \$117

Production Rates 1000 /Day 50 /Hr. 1 /Min.

EQUIPMENT REQUIREMENTS:

DESCRIPTION	QTY.	EST. COST \$ (1000's)	SQ. FT. PLANT SPACE	TOOL \$ & DIE (1000's)
Conveyor Systems	1	1000		
Mixers	2	200	1500	
Slip Cast Operations	1		2500	
Mold Assembly	1		1600	
Controlled HU Room	1	350	9600	
Mold Recycle	1		1600	120
Oven, Mold Bakeout	1	300	4800	
Furnace (N ₂ ATM)	1	3000	4480	
Grinding System	2	2000	500	200
TOTAL EQUIPMENT COST \$1000's		\$6850		
TOTAL PLANT SPACE FT ²			26580	
TOOLING COSTS				320

Estimated Plant Cost (1984 \$) \$ 2,126,400/3,543,998

Labor Hours Required .754 HR

Labor Cost at 1984 Rates \$ 14.70

Estimate By D. Mullings

Date 11/9/83 IV-49

MANUFACTURING SUMMARY SHEET

C.A.S.E.S

Part No. CSE 102 Title Combustion ChamberMaterial Zirconia - 30mil Thk. Basic Process Plasma CoatingVolume 28.2 (IN³) Weight 6.1 (lb)

Over Dimensions: Green NA X X IN.
 (Inches) 10.00 Fired NA X X IN.
 5.00

Material Cost 2.00 \$/lb \$61.00

Raw Material Cost/Piece \$30.50

Production Rates 1000 /Day 50 /Hr. 1 /Min. \$12.20

EQUIPMENT REQUIREMENTS:

DESCRIPTION	QTY.	EST. COST \$ (1000's)	SQ. FT. PLANT SPACE	\$ TOOL & DIE (1000's)
Five-Head Plasma Spray	8	8000	2048	800
Proof Test System-Flame	1	200	200	50
TOTAL EQUIPMENT COST		8200		
TOTAL PLANT SPACE			2248	
TOOLING COSTS				850

Estimated Plant Cost (1984 \$)

\$ 179,840/299,721

Labor Hours Required

.144 HR

Labor Cost at 1984 Rates

\$ 2.80Estimate By D. MullingsDate 11/9/83

IV-50

MANUFACTURING SUMMARY SHEET

C.A.S.E.S

Part No. CSE 101-2 Title Cylinder Outer Sleeve

Material Si₃N₄ Basic Process Isostatic Press

Volume 46.5 (IN³) Weight 5.78 (lb)

Over Dimensions: Green 7.3 X 7.3 X 9.75 IN.
(Inches) 20.00 Fired 6 X 6 X 8.0 IN.
10.00

Material Cost 5.00 \$/lb \$115.60
\$ 57.80

Raw Material Cost/Piece \$ 28.90

Production Rates 4000 /Day 200 /Hr. 4 /Min.

EQUIPMENT REQUIREMENTS:

DESCRIPTION	QTY.	EST. COST \$ (1000's)	SQ. FT. PLANT SPACE	\$ TOOL & DIE (1000's)
Isostatic Press (1 min/cy	2	400	500	100
Green Grind/Cut Machine	2	600	500	100
Furnace (N ₂ Atm.)	1	3000	4480	
Finish Grinder	2	800	1000	80
Conveyor	1	100	--	
TOTAL EQUIPMENT COST		4900		
TOTAL PLANT SPACE			6490	
TOOLING COSTS				280

Estimated Plant Cost (1984 \$) \$ 518,400/864,000

Labor Hours Required .06 HR

Labor Cost at 1984 Rates \$ 1.17

Estimate By D. Mullings

Date 11/9/83 IV-51

MANUFACTURING SUMMARY SHEET

C.A.S.E.S

Part No. CSE 101-2 Title Cylinder Outer Sleeve
 Material Zirconia (30 mil thk) Basic Process Plasma Spray
 Volume 1.86 (IN³) Weight .40 (lb)
 Over Dimensions: Green NA X X IN. 8-101b/hr nozzle
 (Inches) 10.00 Fired X X X IN. Power 60kw/NO₂ =
 5.00 60 x 10 = 600kw
 Material Cost 2.00 \$/lb \$4.00
 Raw Material Cost/Piece (.4 lb of Zr/piece) \$2.00
 \$.80
 Production Rates 4000 /Day 200 /Hr. 4 /Min.

EQUIPMENT REQUIREMENTS:

DESCRIPTION	QTY.	EST. COST \$ (1000's)	SQ. FT. PLANT SPACE	\$ TOOL & DIE (1000's)
Plasma Spray Stations	10	1000	2560	200
Proof Test System-Flame	1	200	200	50
TOTAL EQUIPMENT COST		1200		
TOTAL PLANT SPACE			2760	
TOOLING COSTS				250

Estimated Plant Cost (1984 \$) \$ 220,800 / 368,000
 Labor Hours Required .036 HR
 Labor Cost at 1984 Rates \$.70

Estimate By D. Mullings

Date 11/9/83 IV-52

MANUFACTURING SUMMARY SHEET

C.A.S.E.S

Part No. CSE 101-1-1 Title Cylinder Heater Head

Material Mullite Basic Process Isostatic Dry B. Press

Volume 134.5 (IN³) Weight 14.5 (lb)

Over Dimensions: Green 4.68 X 4.68 X 11.16 IN.
(Inches) 5.00 Fired 3.84 X 3.84 X 9.15 IN.
3.00

Material Cost 1.00 \$/lb \$72.50
\$43.50
Raw Material Cost/Piece \$14.50

Production Rates 4000 /Day 200 /Hr. 4 /Min.

EQUIPMENT REQUIREMENTS:

DESCRIPTION	QTY.	EST. COST \$ (1000's)	SQ. FT. PLANT SPACE	\$ TOOL & DIE (1000's)
Isostatic Press (1 min/cy.)	4	800	1000	200
Grinding Machine (green)	4	1200	1000	120
Drill Station	4	00	600	300
Furnace (air atm.)	1	6000	4500	--
Grinding Machines: I.D.	4	800	1000	120
O.D.	4	800	1000	120
(Hole) Ream	4	800	600	120
Pressure Test	1	500	400	
TOTAL EQUIPMENT COST		12,100		
TOTAL PLANT SPACE			10,700	
TOOLING COSTS				980

Estimated Plant Cost (1984 \$) \$ 856,000 / 1,426,666

Labor Hours Required .14 HR

Labor Cost at 1984 Rates \$ 2.80

Estimate By D. Mullings IV-53

Date 11/9/83

MANUFACTURING SUMMARY SHEET

C.A.S.E.S

Part No. CSE 101-1-2 Title Cyl. Hd. Distribution Chamber

Material SiC Basic Process Injection Mold (with fugitive core)

Volume 21.8 (IN³) Weight 2.53 (lb)

Over Dimensions: Green 7.0 X 7.0 X 1.95 IN.
(Inches) Fired 5.75 X 5.75 X 1.60 IN.
10.00

Material Cost 5.00 \$/lb \$50.00
\$25.30
Raw Material Cost/Piece \$12.65

Production Rates 4000 /Day 200 /Hr. 4 /Min.

EQUIPMENT REQUIREMENTS:

DESCRIPTION	QTY.	EST. COST \$ (1000's)	SQ. FT. PLANT SPACE	TOOL \$ & DIE (1000's)
Extruder, Twin Scr.(mix)	2	1000	640	--
Inject. Mold Mach (core)	1	200	240	50
Inject. Mold Mach (part)	4	1200	960	300
Extruder/Chopper	1	500	320	
Bake Out Ovens (7 day cycle)	20	2000	10600	
Sintering Furnace (N ₂)	1	3000	4480	
Dense Grind Equip. ID/OD	4	1100	1000	220
TOTAL EQUIPMENT COST		10,000		
TOTAL PLANT SPACE			19,240	
TOOLING COSTS				570

Estimated Plant Cost (1984 \$) \$ 1,539,200/2,308,800

Labor Hours Required .102 HR

Labor Cost at 1984 Rates \$ 1.99

Estimate By D. Mullings

IV-54

Date 11/9/83

MANUFACTURING SUMMARY SHEET

C.A.S.E.S

Part No. CSE 101-1-6 Title Heater Head Tube

Material SiC Basic Process Electrophoresis

Volume 1.27 (IN³) Weight .15 (lb)

Over Dimensions: (Group of Green 7.0 x 7.0 x 7.7 IN.
(Inches) 24 Fired 5.7 x 5.7 x 6.3 IN.
20.00

Material Cost 10.00 \$/lb \$3.00
5.00 \$1.50

Raw Material Cost/Piece \$.75

Production Rates 100,000 /Day 5,000 /Hr. 100 /Min.

EQUIPMENT REQUIREMENTS:

DESCRIPTION	QTY.	EST. COST \$ (1000's)	SQ. FT. PLANT SPACE	\$ TOOL & DIE (1000's)
Inject. Mold Press (core)	2	200	800	150
Carbon Coating Eq.	1	50	150	
Electroph. Vat & Dryer	1	125	450	
Core Removal Oven	1	200	2240	
Sintering Furnace	1	3000	4480	
Grind & Cutoff Eq.	4	400	1000	100
Final Grind Ends	16	4800	4000	480
Pressure Test	1	500	200	
TOTAL EQUIPMENT COST		9275		
TOTAL PLANT SPACE			13320	
TOOLING COSTS				730

Estimated Plant Cost (1984 \$) \$ 1,065,600 / 1,775,992

Labor Hours Required .0048 HR

Labor Cost at 1984 Rates \$.095

Estimate By D. Mullings

Date 11/9/83

IV-55

MANUFACTURING SUMMARY SHEET

C.A.S.E.S

Part No. CSE-109 Title Displacer

Material Mullite Basic Process Isostatic Press

Volume 6.70 (IN³) Weight .77 (lb)

Over Dimensions: Green 2.75 x 2.75 x 11.3 IN.
(Inches) Fired 2.25 x 2.25 x 9.30 IN.
5.00
3.00
Material Cost 1.00 \$/lb \$3.85
\$2.31
Raw Material Cost/Piece \$0.77

Production Rates 4000 /Day 200 /Hr. 4 /Min.

EQUIPMENT REQUIREMENTS:

DESCRIPTION	QTY.	EST. COST \$ (1000's)	SQ. FT. PLANT SPACE	\$ TOOL & DIE (1000's)
Isostatic Press	4	800	1000	120
Cut Off/Trim End	2	400	500	80
Furnace* (Air ATM)	1	6000	4500	
Finish Grinders	4	1100	1000	220
Proof Pressure Test	1	500	200	
*Share with CSE 109 and CSE 101-1-3)				
TOTAL EQUIPMENT COST		8800		
TOTAL PLANT SPACE			7200	
TOOLING COSTS				420

Estimated Plant Cost (1984 \$) \$ 576,000 / 959,996

Labor Hours Required .075 HR

Labor Cost at 1984 Rates \$ 1.46

Estimate By D. Mullings

Date 11/9/83

IV-56

MANUFACTURING SUMMARY SHEET

C.A.S.E.S

Part No. CSE 109A Title Radiation Shield

Material Mullite Basic Process Injection Mold

Volume .33 (IN³) Weight .04 (lb)

Over Dimensions: Green 2.5 X 2.5 X 1.25 IN.
(Inches) 5.00 Fired 2.04 X 2.04 X 1.0 IN.
3.00

Material Cost 1.00 \$/lb \$.20
\$.12
Raw Material Cost/Piece \$.04

Production Rates 12000 /Day 600 /Hr. 12 /Min.

EQUIPMENT REQUIREMENTS:

DESCRIPTION	QTY.	EST. COST \$ (1000's)	SQ. FT. PLANT SPACE	TOOL & DIE \$ (1000's)
Twin Screw Extruder	1	500	320	
Inject. Mold Mach	1	300	240	50
Oven, Bakeout	1	100	530	
Sintering Furnace*				
Proof Mech. Stress Test	1	200	300	30
*Share with CSE 109				
TOTAL EQUIPMENT COST		1,100		
TOTAL PLANT SPACE			1390	
TOOLING COSTS				80

Estimated Plant Cost (1984 \$) \$ 111,200 /185,326

Labor Hours Required .0132 HR

Labor Cost at 1984 Rates \$.257

Estimate By D. Mullings

Date 11/9/83

IV-57

C.A.S.E.S

EQUIPMENT REQUIREMENTS:

Estimated Plant Cost (1984 \$)	\$ 80,000 / 133,360
Labor Hours Required	<u>.036</u> HR
Labor Cost at 1984 Rates	\$.70

Estimate By D. Mullings IV-58
Date 11/9/83

MANUFACTURING SUMMARY SHEET

C.A.S.E.S

Part No. CSE 101-3 Title Radiation Mantle-Dome

Material SiC Basic Process Isostatic Press

Volume 18.51 (IN³) Weight 2.15 (lb)

Over Dimensions: Green 8 X 8 X 8.7 IN.
(Inches) 20.00 Fired 6.5 X 6.5 X 7.07 IN.
10.00

Material Cost 5.00 \$/lb \$43.00
\$21.50
Raw Material Cost/Piece \$ 10.75

Production Rates 4000 /Day 200 /Hr. 4 /Min.

EQUIPMENT REQUIREMENTS:

DESCRIPTION	QTY.	EST. COST \$ (1000's)	SQ. FT. PLANT SPACE	\$ TOOL & DIE (1000's)
Isostatic Press (1 min/cy)	4	800	1000	120
Grinder (OD & Foot)	4	3000	2000	800
Trim Length Grind				
Drill Machine				
Furnace (N ₂ ATM)	1	3000	4480	
Grinders - OD	4	800	1000	160
ID/Step	4	800	1000	160
Proof Test-Flame	1	200	300	
TOTAL EQUIPMENT COST		8400		
TOTAL PLANT SPACE			9780	
TOOLING COSTS				1240

Estimated Plant Cost (1984 \$) \$ 782,400 / 1,304,000

Labor Hours Required .126 HR

Labor Cost at 1984 Rates \$ 2.46

Estimate By D. Mullings IV-59

MANUFACTURING SUMMARY SHEET

C.A.S.E.S

Part No. CSE 101-5 Title Mantle-Baffle

Material Si₃N₄ Basic Process Uni-Axial Press

Volume 5.49 (IN³) Weight .13 (lb)

Over Dimensions: Green 7.3 X 7.3 X 0.70 IN. 15 sec/cyc. (4/min)
 (Inches) 20.00 Fired 6.0 X 6.0 X 0.60 IN.
 10.00

Material Cost 5.00 \$/lb \$ 2.60
 \$ 1.30
 Raw Material Cost/Piece \$.65

Production Rates 4000 /Day 200 /Hr. 4 /Min.

EQUIPMENT REQUIREMENTS:

DESCRIPTION	QTY.	EST. COST \$ (1000's)	SQ. FT. PLANT SPACE	TOOL & DIE \$ (1000's)
Uniaxial Press	1	200	250	50
Furnace" Sinter				
Dense Grinder	2	400	500	40
Proof Test-Flame	1	200	200	
*Share with CSE 101-2				
TOTAL EQUIPMENT COST		800		
TOTAL PLANT SPACE			950	
TOOLING COSTS				90

Estimated Plant Cost (1984 \$) \$ 76,000/126,660

Labor Hours Required .022 HR

Labor Cost at 1984 Rates \$.42

Estimate By D. MullingsDate 11/9/83 IV-60

MANUFACTURING SUMMARY SHEET

C.A.S.E.S

Part No. CSE 105-4 Title Cylinder Liner

Material Mullite Basic Process Isostatic Press

Volume 14.55 (IN³) Weight 1.66 (lb)

Over Dimensions: Green 3.5 X 3.5 X 7.3 IN.
(Inches) Fired 2.9 X 2.9 X 6.0 IN.
5.00
3.00
Material Cost 1.00 \$/lb \$8.30
\$5.00
Raw Material Cost/Piece \$1.67

Production Rates 4000 /Day 200 /Hr. 4 /Min.

EQUIPMENT REQUIREMENTS:

DESCRIPTION	QTY.	EST. COST \$ (1000's)	SQ. FT. PLANT SPACE	\$ TOOL & DIE (1000's)
Isostatic Press	2	400	500	80
Rough Grind & Cutoff	2	600	500	120
Furnace* Sinter		--	--	
Dense Grinder - OD	4	1000	1000	150
- ID	4	1000	1000	150
Trim/CO Ends	2	200	500	30
Proof Test Press.	1	500	300	
CSE 101-1-3 and *Share with CSE 109				
TOTAL EQUIPMENT COST		3700		
TOTAL PLANT SPACE			3800	
TOOLING COSTS				530

Estimated Plant Cost (1984 \$) \$ 304,000 / 506,646

Labor Hours Required .078 HR

Labor Cost at 1984 Rates \$ 1.52

Estimate By D. Mullings IV-61
Date 11/9/83

MANUFACTURING SUMMARY SHEET

C.A.S.E.S

Part No. CSE 104-1 Title Preheater Plate

Material SiC Basic Process Tapecast - Dr. Blade

Volume 319 (IN³) Weight .035 (lb)

Over Dimensions: Green .12 X 1.5 X 6.0 IN.
(Inches) 20.00 Fired .10 X 1.2 X 5.0 IN.
10.00

Material Cost 5.00 \$/lb

Raw Material Cost/Piece \$.70 (560.00/Eng)
\$.35 (280.00/Eng)

Production Rates 800,000 /Day 40000 /Hr. 800 /Min \$.17 (140.00/Eng)

EQUIPMENT REQUIREMENTS:

DESCRIPTION	QTY.	EST. COST \$ (1000's)	SQ. FT. PLANT SPACE	\$ TOOL & DIE (1000's)
Twin Screw Extruder	2	1000	640	
Tapecast Machine*	10	2500	3200	500
Furnace (N ₂ ATM)	1	3000	4480	
Loading Setters		--	1600	
*Includes Rib-Relief				
Operation				
TOTAL EQUIPMENT COST		4500		
TOTAL PLANT SPACE			9920	
TOOLING COSTS				500

Estimated Plant Cost (1984 \$) \$ 793,600/1,349,120

Labor Hours Required .00057 HR

Labor Cost at 1984 Rates \$.011

Estimate By D. Mullings
Date 11/9/83 IV-62

MANUFACTURING SUMMARY SHEET

C.A.S.E.S

Part No. Common Title Ball Mill/Powder Dry FacilityMaterial SiC, Si₃N₄ Mullite Basic Process _____Volume NA (IN³) Weight NA (lb)Over Dimensions: Green NA X NA X NA IN.
(Inches) Fired NA X NA X NA IN.Material Cost NA \$/lbRaw Material Cost/Piece NA \$ NA

Production Rates _____/Day _____/Hr. _____/Min.

EQUIPMENT REQUIREMENTS:

DESCRIPTION	QTY.	EST. COST \$ (1000's)	SQ. FT. PLANT SPACE	
Ball Mill Machines	3	1,200	675	SiC
Powder Drying Facility	3	3,000	1,200	SiC
Ball Mill Machine	2	800	450	Si ₃ N ₄
Powder Drying Mill	2	2,000	800	Si ₃ N ₄
Ball Mill Machine	3	1,200	675	Mull.
Powder Drying Mill	3	3,000	1,200	Mull.
TOTAL EQUIPMENT COST		10,200		
TOTAL PLANT SPACE			5,000	
TOOLING COSTS				

Estimated Plant Cost (1984 \$)

\$ 400,000/664,000

Labor Hours Required

REF. LABOR EST. HR
FOR EACH PART

Labor Cost at 1984 Rates

\$ _____

Estimate By D. MullingsDate 12/9/83

IV-63

1. Report No. NASA CR-174907		2. Government Accession No.		3. Recipient's Catalog No.	
4. Title and Subtitle Ceramic Automotive Stirling Engine Study				5. Report Date January 1985	
				6. Performing Organization Code	
7. Author(s) S. Musikant, W.S. Chiu, D.K. Darooka D.M. Mullings, and C.A. Johnson				8. Performing Organization Report No.	
				10. Work Unit No.	
9. Performing Organization Name and Address General Electric Company Space Systems Division Valley Forge Space Center Philadelphia, Pennsylvania 19101				11. Contract or Grant No. DEN 3-312	
				13. Type of Report and Period Covered Contractor Report	
12. Sponsoring Agency Name and Address U.S. Department of Energy Office of Vehicle and Engine R&D Washington, D.C. 20546				14. Sponsoring Agency Code Report No. DOE/NASA/0312-1	
15. Supplementary Notes Final Report. Prepared under Interagency Agreement DE-AI01-85CE50112. Project Manager, W. Tomacic, Power Technology Division, NASA Lewis Research Center, Cleveland, Ohio 44135.					
16. Abstract A conceptual design study for a Ceramic Automotive Stirling Engine (CASE) was performed. Year 1990 structural ceramic technology was assumed. Structural and performance analyses of the conceptual design were performed as well as manufacturing and cost analysis. The general conclusions from this study are that an engine using ceramic hot parts would be 10-26% more efficient over its performance map than the current metal Automotive Stirling Reference Engine (ASRE). Cost of such a ceramic engine is likely to be somewhat higher than that of the ASRE but engine cost is very sensitive to the ultimate cost of the high purity, ceramic powder raw materials required to fabricate high performance parts. When the design study was projected to the year 2000 technology, substantial net efficiency improvements, on the order of 25 to 46% over the ASRE, were computed. This design employed advanced heat pipe technology in addition to year 2000 ceramic technology.					
17. Key Words (Suggested by Author(s)) Stirling engine; Ceramics; Mullite; Silicon carbide; Heat pipes; Pulse combustion; Ceramic heat exchanger			18. Distribution Statement Unclassified - unlimited STAR Category 85 DOE Category UC-96		
19. Security Classif. (of this report) Unclassified	20. Security Classif. (of this page) Unclassified		21. No. of pages 363	22. Price* A16	

End of Document